

A Tracer Study of the Hydrolysis of Methyl Methacrylate and Methyl Acrylate Units in Homopolymers and Copolymers

F. C. BAINES and J. C. BEVINGTON, *Department of Chemistry, The University, Lancaster, England*

Synopsis

Homopolymers and copolymers were prepared from methyl methacrylate, methyl acrylate, and styrene by radical reactions at 60°. Monomers suitably labeled with carbon-14 were used so that it was possible to monitor the hydrolysis of ester groups in the polymers during treatment under alkaline conditions. It was found that methyl acrylate units were hydrolyzed completely whatever their environment in a polymer chain. Under the same conditions only about 9% of the ester groups in a homopolymer of methyl methacrylate reacted; the proportion was increased by the introduction of comonomer units into the polymer chain. For copolymers of methyl methacrylate with methyl acrylate the extent of reaction may be correlated with the lengths of the sequences of methyl methacrylate units.

Some of the studies of reactions of high polymers have revealed significant differences between the reactivities of functional groups in macromolecules and those of the same groups in small molecules. In certain cases the effects of neighboring groups are quite pronounced;¹ in other cases the reactivity is strongly dependent upon the tacticity of the polymer chain.²⁻⁴ There have been reports that the extent of hydrolysis of pendant ester groups in a particular polymer varies to some extent with the molecular weight of the polymer.⁵

Polymethyl acrylate, prepared by a radical process at 60°, can be hydrolyzed rapidly and completely under alkaline conditions;⁶ on the other hand, the monomer units in polymethyl methacrylate prepared and treated similarly are resistant to hydrolysis,⁶ although benzoate endgroups react readily.⁷ This marked difference between the esters of polyacrylic and polymethacrylic acids has now been studied further by using tracer methods for examination of the hydrolysis of the monomer units in copolymers of methyl methacrylate with methyl acrylate and in copolymers of these monomers with styrene.

Experimental

Polymers were prepared in vacuum dilatometers at 60° with benzoyl peroxide as initiator; conversions were restricted to 5%, and the reactions

2511

showed the expected kinetic characteristics. Polymers were purified by precipitation and subjected to prolonged drying in vacuum. Labeled monomers were prepared by exchange reactions involving the unlabeled materials and ^{14}C -methanol.⁸ Monomer reactivity ratios for copolymerizations were determined by the procedure due to Fineman and Ross;⁹ the probable error in the quoted results is believed not to exceed 5%.

For hydrolysis a solution of polymer (about 50 mg.) in benzene (25 ml.) was mixed with a solution of caustic soda (1 g.) in methanol (7 ml.); the mixture was kept at 80° under reflux. The hydrolyzed polymers were recovered and then purified by reprecipitation; various solvents and precipitants were required according to the natures of the polymers.

Materials were assayed by gas counting.¹⁰ This procedure gives counting rates that are directly proportional to the specific activities of the specimens in units such as microcuries per gram of carbon. In considerations of the results of the assays of polymers it is necessary to consider only the carbon contents of the various units in the polymer molecules. The compositions of copolymers and the degrees of hydrolysis can be calculated from the counting rates of polymers before and after treatment (see Table I). In the derivation of the formulae isotope effects during polymerization and the effects of endgroups upon compositions of polymers are ignored.

Results

Homopolymers of methyl methacrylate and methyl acrylate were hydrolyzed for various periods; the products were isolated and assayed. It was confirmed that only about 9% of the ester groups in polymethyl methacrylate reacted even during prolonged treatment; hydrolysis of polymethyl acrylate was complete in 0.5 hr.

Copolymers were prepared from ^{14}C -methyl methacrylate and styrene. The monomer reactivity ratios r_1 and r_2 were 0.46 and 0.52 (methyl methacrylate taken as monomer 1). Samples of the copolymers were recovered after various periods of hydrolysis and assayed; the fractions of ester groups hydrolyzed were calculated (by means of formulas in Table I), and the results are presented in Figure 1.

Copolymers were prepared from ^{14}C -methyl acrylate and styrene; the mole fractions of the former in the products were 0.12, 0.26, 0.34, 0.41, and 0.56. The monomer reactivity ratios r_1 and r_2 were 0.21 and 0.74 (methyl acrylate taken as monomer 1). The copolymers were hydrolyzed and assayed; the fractions of ester groups hydrolyzed during treatment for 0.5 hr. were 0.54, 0.63, 0.89, 0.97, and 0.98; in all cases hydrolysis was complete after treatment for 4 hr.

One set of copolymers of methyl methacrylate and methyl acrylate was prepared with the use of a labeled sample of the first monomer; for another set the conditions were identical, except that the labeling was in the methyl acrylate. The compositions of the pairs of copolymers agreed to within 5%, and the mean values are quoted in Table II. The monomer reactivity

TABLE I
Formulae for Counting Rates of Polymers and Copolymers^a

| Polymer | Monomer units | | Ratios of counting rates | |
|--|---|--|----------------------------|---|
| | Before hydroly. | After hydroly. | B/M | A/M |
| ¹⁴ C-MMA | C ₅ [*] | (C ₅ [*]) _{1-x} | 1 | $\frac{5(1-x)}{5(1-x)+4x}$ |
| | | (C ₄) _x | | $\frac{4(1-y)}{4(1-y)+3y}$ |
| ¹⁴ C-MA | C ₄ [*] | (C ₄ [*]) _{1-y} | 1 | |
| | | (C ₃) _y | | |
| Copolymer of ¹⁴ C-MMA and S | (C ₅ [*]) _a (C ₃) _{1-a} | (C ₅ [*]) _{a(1-x)} | | $\frac{5a(1-x)}{5a(1-x)+4ax+8(1-a)}$ |
| | | (C ₄) _{ax} | $\frac{5a}{5a+8(1-a)}$ | $\frac{4a(1-y)}{4a(1-y)+3ay+8(1-a)}$ |
| | | (C ₈) _{1-a} | | |
| | | (C ₃ [*]) _{a(1-y)} | $\frac{4a}{4a+8(1-a)}$ | $\frac{5a(1-x)}{5a(1-x)+4ax+8(1-a)}$ |
| Copolymer of ¹⁴ C-MA and S | (C ₄ [*]) _a (C ₈) _{1-a} | (C ₈) _{1-a} | | $\frac{5a(1-x)}{5a(1-x)+4ax+8(1-a)}$ |
| | | (C ₃ [*]) _{a(1-x)} | $\frac{5a}{5a+4(1-a)}$ | $\frac{4(1-a)(1-y)}{4(1-a)(1-y)+3(1-a)y}$ |
| | | (C ₄) _{ax} | | |
| | | (C ₄) _{(1-a)(1-y)} | | |
| Copolymer of ¹⁴ C-MMA and MA | (C ₅ [*]) _a (C ₄) _{1-a} | (C ₅) _{(1-a)y} | | $\frac{4(1-a)(1-y)}{4(1-a)(1-y)+3(1-a)y}$ |
| | | (C ₅) _{a(1-x)} | $\frac{4(1-a)}{5a+4(1-a)}$ | $\frac{4(1-a)(1-y)}{4(1-a)(1-y)+3(1-a)y}$ |
| | | (C ₄) _{ax} | | |
| | | (C ₄ [*]) _{(1-a)(1-y)} | | |

^a M = counting rate for labeled monomer, B = counting rate for polymer before treatment, A = counting rate for polymer after treatment, a = mole fraction of monomer in copolymer, x = fraction of methyl methacrylate units hydrolyzed, y = fraction of methyl acrylate units hydrolyzed, * signifies labeled unit, and MA, MMA, and S represent methyl acrylate, methyl methacrylate, and styrene, respectively.

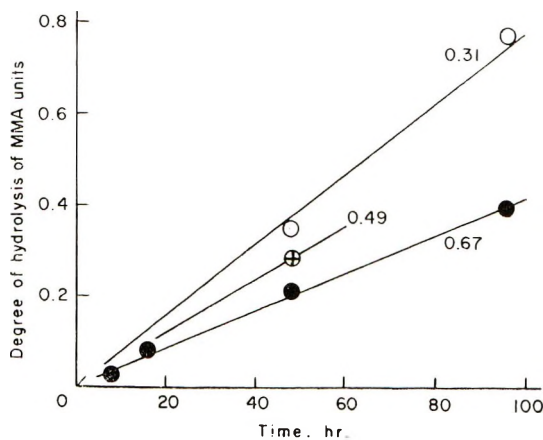


Fig. 1. Hydrolysis of MMA units in copolymers with styrene. The numbers refer to mole fractions of MMA in polymer.

ratios r_1 and r_2 were 2.00 and 0.43 (methyl methacrylate taken as monomer 1); these values are close to those given by Grassie and his co-workers.¹¹ Samples of the copolymers were assayed after various periods of hydrolysis; the degrees of hydrolysis are shown in Table II and Figure 2.

A sample of unlabeled polymethyl methacrylate was hydrolyzed under the standard conditions for 16 hr. with the use of a mixture containing

TABLE II
Hydrolysis of Copolymers of Methyl Methacrylate and Methyl Acrylate^a

| Mole fract. of MMA in feed | Mole fract. of MMA in orig. copol. | Time of hydrolysis, hr. | Ratio counting rates A/M | | Fraction of ester groups hydrolyzed | |
|----------------------------|------------------------------------|-------------------------|--------------------------|------|-------------------------------------|----------|
| | | | MMA* | MA* | <i>x</i> | <i>y</i> |
| 0.75 | 0.86 | 0.5 | 0.87 | 0.05 | 0.04 | 0.56 |
| | | 4 | 0.83 | 0.01 | 0.11 | 0.94 |
| | | 8 | 0.66 | 0 | 0.32 | 1.00 |
| | | 16 | 0.57 | 0 | 0.43 | 1.00 |
| | | 48 | 0.59 | 0 | 0.41 | 1.00 |
| | | 96 | 0.60 | 0 | 0.40 | 1.00 |
| 0.50 | 0.65 | 0.5 | 0.67 | 0.08 | 0.11 | 0.76 |
| | | 4 | 0.53 | 0.01 | 0.34 | 0.97 |
| | | 8 | 0.43 | 0.01 | 0.48 | 0.98 |
| | | 16 | 0.30 | 0 | 0.65 | 1.00 |
| | | 48 | 0.26 | 0 | 0.70 | 1.00 |
| | | 96 | 0.24 | 0 | 0.71 | 1.00 |
| 0.25 | 0.44 | 0.5 | 0.33 | 0.04 | 0.45 | 0.93 |
| | | 4 | 0.19 | 0.01 | 0.70 | 0.99 |
| | | 8 | 0.13 | 0.01 | 0.80 | 0.99 |
| | | 16 | 0.12 | 0.01 | 0.81 | 0.99 |
| | | 48 | 0.07 | 0 | 0.89 | 1.00 |
| | | 96 | 0.07 | 0 | 0.89 | 1.00 |

^a See footnotes to Table I.

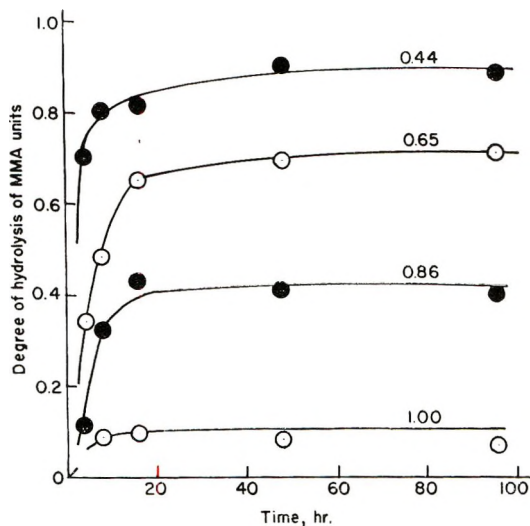


Fig. 2. Hydrolysis of MMA units in copolymers with methyl acrylate. The numbers refer to mole fractions of MMA in polymer.

^{14}C -methanol; there was no detectable radioactivity in the recovered polymer. The specific activity of the methanol was such that the polymer would have acquired a counting rate of about 25 counts/min. if 1% of the ester groups in the polymer had exchanged with the methanol.

Discussion

It is thought that those monomer units in polymethyl methacrylate which are susceptible to hydrolysis are the center units of isotactic triads. The conclusion of Glavis,³ that in polymers prepared by radical reaction at 60° about 9% of the monomer units are of this type, has been confirmed.

Hydrolysis of methyl acrylate was rapid and complete for the homopolymer and for the copolymers containing styrene or methyl methacrylate, although the rate was reduced by the presence of the comonomer. The effect of composition upon rate of reaction may have been associated with differences between the solubilities of the various materials in the mixture used for hydrolysis.

The introduction of methyl acrylate or styrene units into the methyl methacrylate chain clearly affected the hydrolysis of the monomer units (see Figs. 1 and 2). Hydrolysis in the copolymers with styrene was slow and obviously not complete even after 96 hr. The reactions involving the methyl methacrylate units in the copolymers with methyl acrylate were more rapid; the limiting degree of hydrolysis increased markedly as more methyl acrylate units were introduced into the polymer chain (see Figure 2).

The resistance to hydrolysis of the methyl methacrylate units is reduced when the sequences of those units are shortened by the presence of the comonomer. The relative numbers of the various sequences of particular monomer units in copolymers can be calculated from a knowledge of the

monomer reactivity ratios for the copolymerization and the composition of the monomer feed. In the following discussion it is assumed that (a) a methyl methacrylate unit attached to a styrene or to a methyl acrylate unit can be hydrolyzed, and that (b) only 99% of the methyl methacrylate units inside a sequence of such units can be hydrolyzed.

The probability that a methyl methacrylate sequence chosen at random contains n members is equal to $P^{n-1}(1 - P)$, where

$$P = r_1C/(r_1C + 1)$$

Here r_1 is the appropriate monomer reactivity ratio (methyl methacrylate taken as monomer 1), and C is the concentration of methyl methacrylate per the concentration of methyl acrylate in the feed.¹² The relative numbers of the sequences of methyl methacrylate units are shown in Table III, which includes also the relative numbers of all monomer units, terminal monomer units, and nonterminal monomer units in these sequences.

TABLE III
Sequences of MMA Units in Copolymers

| Seq. length | Rel. no. of seq. | Rel. no. of monomer units in seq. | | |
|-------------|------------------|-----------------------------------|-------------------|-------------------------|
| | | Total | Terminal | Nonterm. |
| 1 | $(1 - P)$ | $(1 - P)$ | $(1 - P)$ | 0 |
| 2 | $P(1 - P)$ | $2P(1 - P)$ | $2P(1 - P)$ | 0 |
| 3 | $P^2(1 - P)$ | $3P^2(1 - P)$ | $2P^2(1 - P)$ | $P^2(1 - P)$ |
| 4 | $P^3(1 - P)$ | $4P^3(1 - P)$ | $2P^3(1 - P)$ | $2P^3(1 - P)$ |
| n | $P^{n-1}(1 - P)$ | $nP^{n-1}(1 - P)$ | $2P^{n-1}(1 - P)$ | $(n - 2)P^{n-1}(1 - P)$ |

The sums to infinity of the series in the third, fourth, and fifth columns in Table III are respectively $(1 - P)^{-1}$, $(1 + P)$, and $P^2(1 - P)^{-1}$. According to assumptions (a) and (b) above, the fractional number of hydrolyzable methyl methacrylate units is given by

$$[(1 + P) + 0.09P^2(1 - P)^{-1}]/(1 - P)^{-1} \quad \text{or} \quad 1 - 0.91P^2$$

The values of this quantity have been calculated for the copolymers referred to in Table II with r_1 as 2.00. Figure 3 shows that the agreement between the observed and calculated degrees of hydrolysis is quite good, although the calculated values are lower than the observed values.

The calculated and observed degrees of hydrolysis cannot be made to coincide by variations of up to 10% in the monomer reactivity ratios. The values quoted here for those quantities agree closely with those found by Grassie et al.,¹¹ and it is unlikely, therefore, that the discrepancies can be attributed to errors in monomer reactivity ratios. Discrepancies, such as those found, would occur if part of the reduction in the specific activities of the copolymers had resulted, not from hydrolysis, but from exchange of methyl groups between the copolymers and the unlabeled methanol used in the hydrolysis medium. The direct test reported in this paper indicates that such an exchange is unlikely.

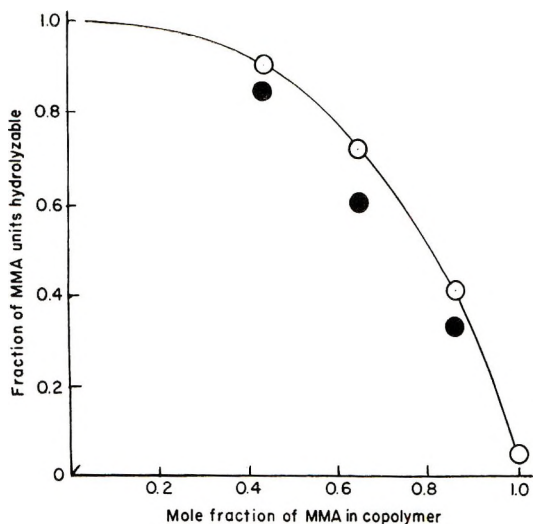


Fig. 3. Degrees of hydrolysis of MMA units in copolymers with methyl acrylate: (○) observed; (●) calculated.

The difference between the observed and calculated degrees of hydrolysis would be found if there were effectively two distinct types of hydrolysis for the methyl methacrylate units in the copolymers; the calculated values might refer solely to a fairly rapid process, whereas the observed values might include also small contributions from a very slow reaction of the units which, in the calculations, are assumed to be completely unreactive. The results presented in Figure 2 are not accurate enough for this hypothesis to be tested.

The assumptions could be modified to allow for the possibility that the chance of hydrolysis for an internal monomer unit depends to some extent upon its position in a sequence. It would be possible to adjust the calculations to give better agreement between the observed and calculated degrees of hydrolysis by supposing that there is more than a 9% chance for hydrolysis of an internal unit in the short sequences of methyl methacrylate units. The same result would be achieved if the proportions of atactic and syndiotactic methyl methacrylate units were made a little smaller by the presence of monomeric methyl acrylate in the feed.

The discrepancies revealed in Figure 3 are, however, not large. It is considered that there is reasonable agreement between the observed degrees of hydrolysis and the values calculated on the basis of assumptions (a) and (b). A similar procedure can be followed for the copolymers of methyl methacrylate with styrene; the calculated degrees of hydrolysis are 0.69, 0.91, and 0.98 in order of increasing styrene content. The results shown in Figure 1 show that reaction was not complete in 96 hr. for any of the copolymers but that the calculated degrees of hydrolysis were not exceeded.

It is concluded that the sensitivity of a methyl methacrylate unit to

alkaline hydrolysis can be correlated with its environment in a polymer chain. The sensitivity to alkaline hydrolysis of a methyl acrylate unit in a polymer chain is, however, very little affected by the natures of the neighboring groups. Morawetz¹³ has already commented on differences of this type and has pointed out that in some reactions of polymers there are steric restraints that cannot be simulated in simple molecular analogues.

The authors thank Messrs. Turner and Newall Ltd. for the award of a Research Scholarship to F.C.B.

References

1. H. Morawetz and P. E. Zimmering, *J. Phys. Chem.*, **58**, 752 (1954).
2. H. Morawetz and E. Gaetjens, *J. Am. Chem. Soc.*, **83**, 1738 (1961).
3. F. J. Glavis, *J. Polymer Sci.*, **36**, 547 (1959).
4. G. Smets and W. de Loecker, *J. Polymer Sci.*, **41**, 375 (1959).
5. A. D. Yakovlev and Z. S. Sokolov, *Zh. Priklad. Khim.*, **34**, 461 (1961).
6. J. C. Bevington, D. E. Eaves, and R. L. Vale, *J. Polymer Sci.*, **32**, 317 (1958).
7. J. C. Bevington, *Trans. Faraday Soc.*, **56**, 1762 (1960).
8. D. E. Blackley and H. W. Melville, *Makromol. Chem.*, **18**, 16 (1955).
9. M. Fineman and S. D. Ross, *J. Polymer Sci.*, **5**, 259 (1950).
10. J. C. Bevington, H. W. Melville, and R. P. Taylor, *J. Polymer Sci.*, **14**, 463 (1954).
11. N. Grassie, J. Thomson, and A. Walton, *European Polymer J.*, **4**, 139 (1968).
12. T. Alfrey, J. J. Bohrer, and H. Mark, *Copolymerization*, Interscience, New York, 1952.
13. H. Morawetz, *Macromolecules in Solution*, Interscience, New York, 1965, p. 425.

Received November 17, 1967

Studies on the Charge Transfer Complex and Polymerization. XIV. Spontaneous Copolymerization of 1-Methylcyclopropene and Sulfur Dioxide

SHOUJI IWATSUKI, TAKASHI KOKUBO,
and YUYA YAMASHITA, *Department of Synthetic Chemistry,
Faculty of Engineering, Nagoya University, Nagoya, Japan*

Synopsis

Copolymerization between 1-methylcyclopropene (MCP) and sulfur dioxide (SO_2) was studied. It took place spontaneously even at a low temperature, and was found to be consistent with polymerization by a "living" radical, as suggested by the increase of reduced viscosity with conversion and by the formation of block polymers in the presence of acrylates. The rate of copolymerization was proportional to $[\text{MCP}]^3$ and $[\text{SO}_2]^2$, and the overall activation energy of copolymerization was about 15.1 kcal/mole. A tentative mechanism to explain the experimental results is discussed.

INTRODUCTION

Sulfur dioxide (SO_2) reacts with a number of olefins in the liquid phase under the influence of radicals to form 1:1 copolymers known as olefin polysulfones¹ over a wide range of feed compositions, except for some cases, such as styrene- SO_2 ² and vinyl chloride- SO_2 ,^{3,4} which can produce 2:1 copolymers. The polysulfone reaction was first discovered by Solonina⁵ in 1898, and since then, many investigations have been reported. The polymers are now believed to have ordinary head-to-tail structures⁶ rather than the structures proposed⁷ by Marvel.

Many monomer pairs giving alternating copolymers form complexes in solution which are highly dissociated. Dainton and Ivin⁸ and Barb⁹ have invoked a complex participation to interpret the kinetics of olefin- SO_2 copolymerization. But Walling's¹⁰ treatment of the styrene- SO_2 system is in good agreement with a scheme in which styrene- SO_2 complexes are not involved. Recently Zutty et al.¹¹ found a spontaneous copolymerization of bicyclo[2,2,1]hept-2-ene with SO_2 , and proposed a mechanism in which the charge transfer complex between the monomers rearranged to biradicals which combined each other to give a polysulfone.

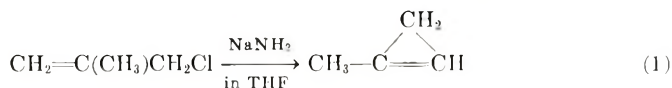
We expected a system of 1-methylcyclopropene (MCP) and SO_2 to copolymerize in a similar pattern, since the electron-donor character of MCP may be large due to the three-membered ring. We carried out this study

on their copolymerization in order to elucidate the copolymerization mechanism, especially the copolymerization kinetics and the role of the MCP-SO₂ complex.

EXPERIMENTAL

Preparation of Monomers and Reagents

MCP was prepared from methallyl chloride through the γ -elimination of hydrogen chloride by use of sodium amide as catalyst [eq. (1)]. Its purity and structure were examined by NMR,¹² where the τ values of CH₃, CH₂, and CH were respectively 7.29 (doublet, $J = 1$ cps), 9.20 (doublet, $J = 2$ cps), and 3.73 (multiplet) and another absorption was not observed.



The yield of MCP with the use of commercial or freshly prepared¹³ sodium amide was poor ($\sim 25\%$) compared to that of Fisher et al. (50%).¹¹ Since MCP was too unstable to be stored, it was used immediately after preparation, and physical properties of this monomer were not well determined. Peroxides which would yield radical species even at low temperature may be considered absent in the monomer, as monomer preparation was carried out under nitrogen.

Benzoquinone, chloranil, etc., which are the conventional inhibitors or retarders of radical and ionic polymerizations, were purified by the usual methods (recrystallization, distillation, etc.) before use. Ethyl, and methyl acrylate and methyl methacrylate used for terpolymerizations were distilled and stored in the dark at low temperature.

Copolymerization of MCP with SO₂

Bulk copolymerization of MCP with SO₂ took place spontaneously and very rapidly even at -78°C to give a polysulfone. Dilution with toluene permitted control and determination of the polymerization rate. A glass ampule was charged with necessary amounts of monomers and toluene at Dry Ice-methanol temperature, flushed with nitrogen, and sealed. It was placed in a bath at the desired temperature. At the initial stage of copolymerization, the system was homogeneous, but became heterogeneous with conversion. After a given copolymerization time, saturated hydroquinone-toluene solution was added to stop polymerization and excess ethyl ether was added to precipitate copolymer, which was repeatedly washed with ethyl ether. The copolymer obtained was dried under vacuum at room temperature.

Measurement of Solution Viscosity of MCP-SO₂ Copolymer

The viscosity was measured in DMF solution, of 0.1 g/100 ml concentration, by using an Ostwald viscometer at 30°C .

Determination of Copolymer Composition

Composition was determined from the elemental analysis for sulfur by the Schöniger method.¹⁴ About 2–5 mg of copolymer was burned on a Pt wire in oxygen, and SO₃ (or SO₂) produced was absorbed into the water containing H₂O₂ and titrated with 0.01*N* NaOH.

RESULTS AND DISCUSSION

The polysulfone obtained was soluble in concentrated sulfuric acid, *N,N*-dimethylformamide, and formic acid, slightly soluble in tetralin, but insoluble in many ordinary organic solvents.

As shown in Table I, the compositions of the polysulfones obtained were found to be always 1 : 1, regardless of the monomer feed.

TABLE I
Polymer Composition

| Feed SO ₂ /MCP | Conversion, % | S, wt-% | MCP in product, mole-% |
|------------------------------|------------------|---------|---------------------------|
| 0.27 | 62.2 | 28.0 | 48.5 |
| 0.83 | 9.4 | 27.2 | 50.1 |
| 1.00 | 7.9 | 26.5 | 51.3 |
| 2.13 | 6.8 | 27.8 | 48.8 |
| 2.14 | 12.1 | 26.7 | 51.0 |
| 3.37 | 29.9 | 25.8 | 52.8 |

The structure of the copolymer was not clear, although NMR and infrared spectra were measured. NMR spectra showed two main peaks at 6.99 and 8.11 τ , indicating the ratio of areas to be 1:2. Assignments of peaks were not clear. The peak at 6.99 τ may be assignable to methylene protons and that at 8.11 τ methyl and methyne protons. Peaks due to olefinic protons were not observed, however, so we think that vinyl polymerization occurs and the cyclopropane ring remains. No clear facts could be obtained from the infrared spectrum, except for absorptions due to SO₂ (1100 and 1310 cm⁻¹).

The effects of known inhibitors of radical or ionic polymerization on the copolymerization are shown in Table II. Addition of conventional radical inhibitors resulted in the decrease of the rate of polymerization, indicating that the copolymerization proceeds through radical intermediates. In the case of ionic inhibitors, a consistent tendency was not observed. However, amines, such as triethylamine and pyridine, were observed to develop a yellow color due to interactions with SO₂, and the viscosities of the resulting copolymers were generally low compared with those in the presence of the other inhibitors.

In Figure 1 are shown the relations between polymerization time and conversion. Actually polymerization proceeded to violent explosion in bulk, and an acceleration phenomenon was observed from the sigmoidal

TABLE II
 Inhibition or Retardation Effect^a

| Additive | Amt additive, wt-% | Rate, mg./min | Conversion, % | η_{sp}/c of product |
|---------------------------------|--------------------------|------------------|------------------|-----------------------------|
| Benzoquinone | 0.15 | 0.260 | 3.8 | 0.091 |
| | 0.4 | 0.200 | 2.9 | 0.102 |
| Chloranil | 0.2 | 0.154 | 2.3 | 0.030 |
| | 1.2 | 0.015 | 0. | — |
| 2,5-Dichloro- <i>p</i> -quinone | 0.2 | 0.237 | 5.8 | 0.077 |
| | 0.8 | 0.151 | 3.9 | 0.075 |
| 2,6-Dichloro- <i>p</i> -quinone | 0.15 | 0.138 | 4.3 | 0.089 |
| | 0.7 | 0.054 | 1.7 | 0.074 |
| DPPH | 0.3 | 0.102 | 3.9 | 0.074 |
| | 1.4 | 0.086 | 3.3 | 0.062 |
| Hydroquinone | 0.15 | 0.254 | 5.0 | 0.102 |
| Phenothiazine | 1.2 | 0.160 | 4.9 | — |
| Triethylamine | 58 | 1.11 | 32.6 | 0.049 |
| Pyridine | 58 | 0.152 | 5.1 | — |
| | — | 0.304 | — | — |

^a [MCP] = 2.07 mole/l, [SO₂] = 2.21 mole/l, -40°C.

curve in Figure 1. This is believed to come from the increase of the radical concentration without termination. The initial rates were determined from the initial slope of the time conversion curves. From the initial rates at various temperatures an overall activation energy of the copolymerization was calculated to be 15.1 kcal/mole.

In Figure 2 is shown the log-log relation between the monomer concentration and the initial rate of polymerization. In each run, the concentration of the comonomer was kept constant. From the gradient of these lines the following experimental relation was obtained:

$$-d[\text{MCP}]/dt = k[\text{MCP}]^3[\text{SO}_2]^2$$

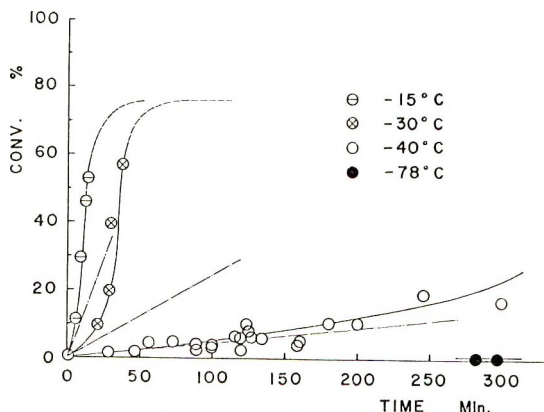


Fig. 1. Copolymerization of MCP and SO₂ at various temperatures. [MCP] = 2.07 mole/l, [SO₂] = 2.21 mole/l.

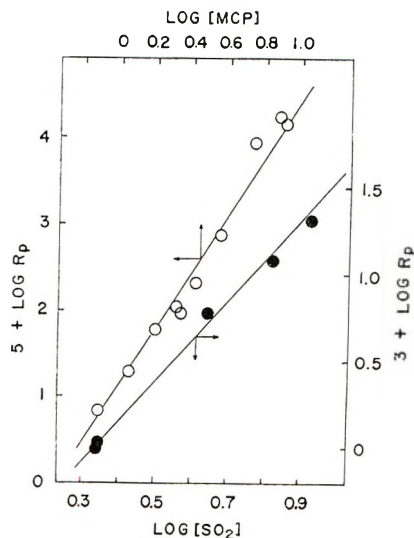


Fig. 2. Effect of monomer concentration on the initial rate of MCP-SO₂ copolymerization reaction at -40°C.

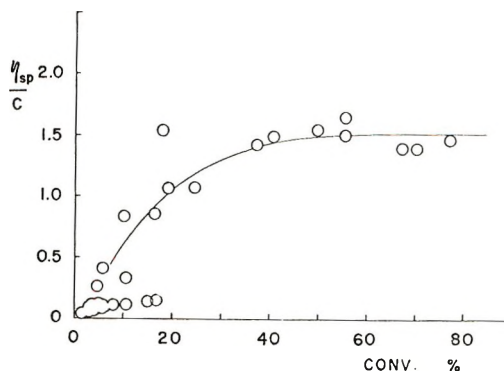


Fig. 3. Relation between reduced viscosity and conversion in MCP-SO₂ copolymerization system. Polymerization temperature; -40°C. Reduced viscosity: 100 ml/g, measured as DMF solution.

The reduced viscosity of the copolymer was found, as shown in Figure 3, to increase with conversion similarly to both the condensation polymerization and polymerization in the system bicycloheptene-SO₂ (in which the increase of the reduced viscosity with reaction time was observed even at a constant conversion). The increase of molecular weights is not due to the Trommsdorff effect alone, because we did not observe the same phenomenon for the spontaneous copolymerization system, cyclopentene-SO₂,¹⁵ which became heterogeneous as copolymerization proceeded. This fact might indicate the propagating radical to have the character of a long-lived "living" radical.

Some particular terpolymerizations with ethyl acrylate, (EA), methyl

acrylate (MA), or methyl methacrylate (MMA) were attempted to examine the propagating mode of this MCP-SO₂ copolymerization. After MCP and SO₂ were copolymerized to the desired conversion, EA, MA, or MMA was added, and the temperature was raised to promote the subsequent polymerization. These results are shown in Table III. The terpolymers obtained were extracted with acetone (which dissolves poly-EA and poly-MMA but do not polysulfone) with a Soxhlet extractor for 20 hr. The results are shown in Table IV. Both the extract and the residue contained all three monomer units of each system. If these polymerization were to take place through the usual radical mechanism, a fraction containing only MCP-SO₂ units should be obtained as a residue. In practice, the residue contained considerable amounts of EA or MMA units, though only qualitatively estimated from infrared measurements. We therefore assumed the polysulfone chain to have some living radical character capable of adding EA or MMA monomers.

The ESR spectrum of the MCP-SO₂ system is shown in Figure 4. The doublet signal characteristic of the SO₂ radical¹⁶ was not observed, and the *g* values were different from those of SO₂ radical (2.0030 and 2.0124) as given by Zutty et al.¹¹ Therefore, we considered that the alkyl radical might be present in this MCP-SO₂ system in place of the SO₂ radical.

The experimental results are summarized as follows. The alkyl radical

TABLE III
Addition of Acrylate to MCP-SO₂ System

| Run | Acrylate | Before addition | | After addition | | Overall conversion, % | D_{CO}/D_{SO}^a |
|-----|----------|-----------------|----------|----------------|----------|-----------------------|-------------------|
| | | Time, min | Temp, °C | Time, hr | Temp, °C | | |
| 1 | EA | 180 | -40 | 2 min | 21 | 13 | 0.15 |
| 2 | MA | 164 | -40 | 4 min | 21 | 8.5 | 0.14 |
| 3 | EA | 33 | -30 | 40 | 0 | 21 | 0.39 |
| 4 | EA | 22 | -30 | 89 | 0 | 33 | 0.39 |
| 5 | MMA | 17 | -30 | 89 | 0 | 41 | 1.02 |

$$^a D_{CO} = D_{1730cm^{-1}}, D_{SO} = D_{1320cm^{-1}}.$$

TABLE IV
Extraction of Terpolymer (Runs 4 and 5) by Acetone (Soxhlet, 20 hr)

| Acrylate | | Am't, wt-% | D_{CO}/D_{SO} | MCP, mole fraction (by NMR) ^a |
|----------|---------|------------|-----------------|--|
| EA | Extract | 46.9 | 1.00 | 0.26 |
| | Residue | 83.1 | 0.41 | — |
| MMA | Extract | 56.1 | 1.45 | 0.27 |
| | Residue | 43.9 | 0.24 | — |

^a (MCP mole fraction) + (acrylate mole fraction) = 1. Calculated as (SO₂ mole fraction) = 0.

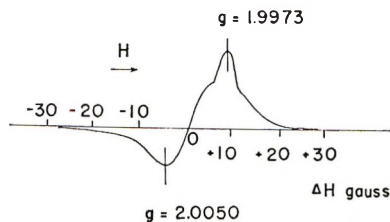
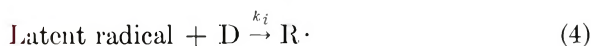


Fig. 4. ESR spectrum of MCP-SO₂ copolymerization system.

detected by ESR was considered to be the MCP radical. The rate of copolymerization was proportional to [MCP]³ and [SO₂]². Block polymerizations with EA, MA, or MMA were successful, indicating the existence of a living radical.

Tentative Mechanisms

Although Walling¹⁰ denied the contribution of a complex to polymerization, it was difficult in the MCP-SO₂ system to interpret the polymerization results without this contribution, because of the unusually high order of monomer concentration affecting the rate of the copolymerization. Therefore, we considered tentatively the mechanism shown in eqs. (2)–(6), which involves a complex between MCP and SO₂ and by which the experimental results were explained well.

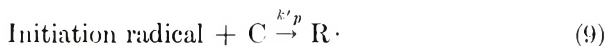
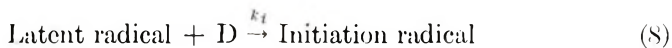
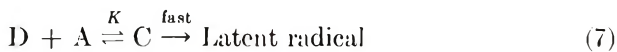


Here D, A, C, and R· refer to the electron donor, electron acceptor, complex, and propagating alkyl radical, respectively. Equation (2) is an equilibrium reaction between free monomers and a complex, and the value of *K* would be assumed to be much less than unity, than 1 so that the concentration of the complex, [C], was approximately equal to *K*[D][A]. With the assumption of the stationary state, typical rate equations were calculated as in Table V. Even if these rate equations should partially explain the experimental results, there would be some questions on the use of the stationary-state assumption, because this MCP-SO₂ system showed the behavior of a living radical polymerization. Therefore, we assumed that the termination reaction would be negligible and did not assume a stationary state. With no termination, the high order of monomer con-

TABLE V
Typical Rate Equations Assuming the Stationary State

| Equation (3) Equation (6) (termination) | C → Latent radical | | 2C → Latent radical | |
|---|--|---|---|---|
| | Uni-molecular | Bi-molecular | Uni-molecular | Bi-molecular |
| Rate R_p | $k_p \left(\frac{k_0 k_i}{k_t} \right) [D]^3 [A]^{5/2}$ | $k_p \left(\frac{k_0 k_i}{k_t} \right)^{1/2} [D]^2 \times [A]^{2/2}$ | $k_p \left(\frac{k_0 k_i}{k_t} \right) [D]^4 \times [A]^3$ | $k_p \left(\frac{k_0 k_i}{k_t} \right)^{1/2} [D]^{5/2} \times [A]^2$ |

centrations on the rate of copolymerization could be interpreted by the scheme shown in eqs. (7)–(10).



Here $R \cdot$ radical, which might be so long-lived as to attack acrylates when they were added into the MCP-SO₂ copolymerization system after a while, might attack the complex on the SO₂ side to form a new $R \cdot$. The rates of initiation and propagation might be considered to be given by eqs. (11) and (12), respectively.

$$R_i = k_i [D] [C] \quad (11)$$

$$R_p = k_p [C] [R \cdot] \quad (12)$$

When $k'_p = k_p$, the rate of the copolymerization is given by eq. (13):

$$R_p = k_i k_p K^2 [D]^3 [A]^2 \quad (13)$$

This scheme seems to explain the above experimental results well.

Although Zutty et al.¹¹ had assumed propagation by biradical coupling in the bicycloheptene-SO₂ system, in the MCP-SO₂ system such a propagation would be ruled out for the following reasons. The first reason is the experimental fact that the molecular weight of the copolymer at a constant conversion did not change with the copolymerization time, which result differs from the results of Zutty et al.¹¹ The second reason is that the resulting copolymer should be different from the observed 1:1 composition if the propagation occurred through the biradical couplings, because the biradical produced by the above scheme should be $\cdot D(A-D)_n A-D \cdot$ as suggested from the absence of SO₂ radical.

To discuss the copolymerization behavior of the MCP-SO₂ system more exactly, it is necessary to pay attention to the initiation step as well as the propagation step, and we have made some attempt to do.

References

1. E. M. Fettes and F. O. Davis, in *Polyethers, Part 3, Polyalkylene Sulfides and other Polythioethers*, N. G. Gaylord, Ed., Interscience, New York, 1962, p. 225.
2. W. G. Barb, *Proc. Roy. Soc. (London)*, **A212**, 66 (1952).
3. C. S. Marvel and F. J. Glavis, *J. Amer. Chem. Soc.*, **60**, 2622 (1938).
4. C. S. Marvel and L. H. Dunlap, *J. Amer. Chem. Soc.*, **61**, 2709 (1939).
5. V. Solonina, *J. Russ. Phys. Chem. Soc.*, **30**, 839 (1898).
6. M. Iino, A. Hara, and N. Tokura, *Makromol. Chem.*, **98**, 81 (1966).
7. C. S. Marvel and E. D. Weil, *J. Amer. Chem. Soc.*, **76**, 61 (1954).
8. F. S. Dainton and K. J. Ivin, *Proc. Roy. Soc. (London)*, **A212**, 96 (1952); *ibid.*, **A212**, 207 (1952).
9. W. G. Barb, *Proc. Roy. Soc. (London)*, **A212**, 177 (1952).
10. C. Walling, *J. Polym. Sci.*, **16**, 315 (1955).
11. N. L. Zutty, C. W. Wilson, G. H. Potter, D. C. Priest, and C. J. Witworth, *J. Polym. Sci. A*, **3**, 2781 (1965).
12. F. Fisher and D. E. Applequist, *J. Org. Chem.*, **30**, 2089 (1965).
13. K. N. Campbell and B. K. Campbell, *Org. Syn.*, **30**, 72 (1950).
14. W. Schöniger, *Mikrochim. Acta*, **1955**, 123.
15. S. Iwatsuki, T. Okada, and Y. Yamashita, *J. Polym. Sci. A-1*, **6**, 2451 (1968).
16. Z. Kuri, "ESR, its Application to Chemistry," Y. Deguchi et al., Eds., Kagakudojin, Kyoto, 1964, p. 193.

Received October 4, 1967

Revised January 10, 1968

Studies on the Charge Transfer Complex and Polymerization. XVI. Spontaneous Copolymerization of Cyclopentene and Sulfur Dioxide*

SHOUJI IWATSUKI, TSUNEYOSHI OKADA, AND YUYA YAMASHITA, *Department of Synthetic Chemistry, Faculty of Engineering, Nagoya University, Nagoya, Japan*

Synopsis

The alternating copolymerization of cyclopentene and sulfur dioxide was studied. It takes place spontaneously at -15°C . The rate of copolymerization in toluene was found to be proportional to $[\text{CPT}]^3$ and $[\text{SO}_2]^2$ with the overall activation energy of 16.5 kcal/mole. Terpolymerizations with eight different third monomers were carried out to examine the character and behavior of the copolymerization system of CPT and SO_2 . However, the polymerizations with styrene and methyl methacrylate as the third monomers were found to be extraordinary, in that all the three components are not incorporated into the polymer chain.

INTRODUCTION

It is well known that SO_2 and a variety of cycloolefins may be copolymerized by conventional radical initiators to give alternating copolymers. Recently Zutty² reported a spontaneous, alternating copolymerization of SO_2 with the strained monomer, bicyclo[2,2,1]hept-2-ene and proposed, from the abnormal polymerization behavior, that a complex between bicycloheptene and SO_2 might rearrange to a biradical which could combine to give an alternating copolymer.

We investigated the role of ring strain of cycloolefins on their copolymerization with SO_2 ³ by studying the copolymerization of SO_2 with 1-methylcyclopropene⁴ which was considered to be extremely strained. This alternating copolymerization takes place spontaneously in bulk even at -78°C . Dilution with toluene enabled the rate of copolymerization to be controlled. The dependence of the rate of copolymerization on monomer concentrations was of abnormally high order, the rate being equal to $k_p \cdot [\text{MCP}]^3 [\text{SO}_2]^2$. An attempt to produce a block terpolymer by using acrylates as the third monomers added subsequently to the copolymerization system was successful. Therefore, we supposed that an active intermediate of the system might be a long-lived radical and that a complex

* For Part XV see Iwatsuki et al.¹

formed between SO_2 and methylcyclopropene might play an important role in the copolymerization.

In this work, we intended to study the copolymerization between SO_2 and cyclopentene (CPT) which was considered to be less strained than the three- and four-membered cyclic olefins. We found that SO_2 and CPT copolymerize spontaneously at a temperature higher than do SO_2 and methylcyclopropene, and that the rate of copolymerization depends upon a high order of monomer concentrations similar to that of SO_2 and methylcyclopropene. In addition, terpolymerizations with several vinyl monomers differing in e value as the third monomers were carried out to examine the properties of the active intermediate and the behavior of the copolymerization of SO_2 and CPT.

EXPERIMENTAL

Materials

Cyclopentene was prepared by dehydration of commercial cyclopentanol with 85% phosphoric acid (85% yield, bp 44.0–44.5°C) and its purity was checked by gas chromatography.

Commercial sulfur dioxide (SO_2) was used without further purification.

Commercial crystalline acrylamide (AAm) and methacrylamide (MAAm) were used without further purification. Commercial acrylonitrile (AN) was washed with dilute sulfuric acid and water, dried over calcium hydride, and fractionally distilled. Commercial methyl acrylate (MA) and methyl methacrylate (MMA) were washed with aqueous alkaline solution and water, dried over calcium hydride, and fractionally distilled. Commercial vinylidene chloride (VDC) was washed with aqueous sodium carbonate solution, dried over calcium chloride, and fractionally distilled. Commercial styrene (St) was dried over calcium hydride and fractionally distilled.

Toluene was washed repeatedly with concentrated sulfuric acid until the coloration of the acid disappeared and twice with water, dried over calcium hydride and fractionally distilled. *N,N*-Dimethylformamide (DMF) was dried over phosphorus pentoxide and distilled carefully.

Polymerization Procedure

The necessary amount of each monomer and toluene in a 30 ml ampule was cooled in a bath of Dry Ice–methanol, flushed with nitrogen, and after sealing, set without stirring in a bath at the required temperature. After a given time of polymerization, excess methanol was added to precipitate the copolymer, which was washed repeatedly with methanol and dried under reduced pressure to a constant weight.

Characterization of the Copolymer

The SO_2 content in the copolymer was calculated from the sulfur content determined by the Schöniger method.⁵ About 2–5 mg of the copolymer

was burned on a Pt wire in oxygen, and the SO_3 (or SO_2) produced was absorbed in water containing hydroperoxide. This aqueous solution was then titrated with 0.01*N* NaOH solution.

The reduced viscosity of the copolymer was determined at 30°C with an Ostwald viscometer, DMF containing 0.1% LiCl being used as solvent.

RESULTS AND DISCUSSION

Bulk copolymerization of CPT and SO_2 takes place spontaneously at a remarkable rate even at -15°C . The spontaneous, bulk copolymerization of methylcyclopropene and SO_2 takes place explosively at a lower temperature, while cyclohexene or cyclooctene and SO_2 do not copolymerize without radical initiators. Therefore, it was concluded that a ring strain plays an important role.

Dilution with toluene enabled the rate of the copolymerization to be controlled and therefore most experiments were carried out in toluene solution.

The time-conversion curve of the copolymerization at 0 and 10°C at a concentration of each monomer of 3.65 mole/l are shown in Figure 1. Copolymers produced during the reaction precipitated as white powders. The copolymers obtained were soluble in DMF, chloroform, and liquid SO_2 , but insoluble in cyclopentene. On heating, they decomposed at 220–230°C without melting. The initial rate at 10°C was greater than that at 0°C, and during polymerization the surface of the copolymer precipitated was colored; the conversion did not proceed to over 25%; the reason for this is not very clear at present.

The relationship between conversion and reduced viscosity is shown in Figure 2, from which the reduced viscosity of the copolymer was found to be independent of the conversion in the range investigated. The relationship was different from those for the bicycloheptene- SO_2 and methylcyclopropene- SO_2 systems, in which the reduced viscosity increased with conversion.

Table I shows the dependence of the initial rate upon the temperature of polymerization, and from the Arrhenius plot in Figure 3 the overall activation energy of the spontaneous copolymerization of CPT and SO_2 was calculated to be 16.5 kcal/mole.

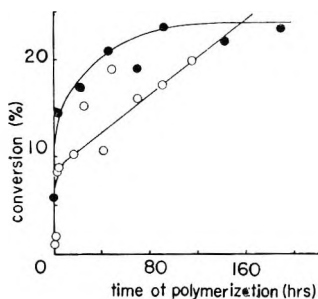


Fig. 1. Time-conversion curves of copolymerization (○) at 0°C; (●) at 10°C.

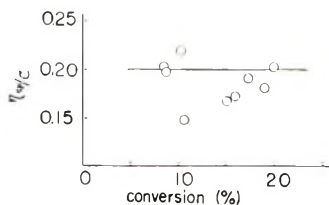


Fig. 2. Relationship between conversion and reduced viscosity; copolymer concentration, 0.2 g/100 ml; solvent, DMF + 0.1 wt-% LiCl.

TABLE I
Dependence of the Initial Rate of Copolymerization upon
Temperature of Polymerization*

| Expt | Temperature T , °K | $10^3/T$ | R_p , mg./min |
|------|-------------------------|----------|-----------------|
| 411 | 273 | 3.66 | 2.30 |
| 412 | 273 | 3.66 | 2.02 |
| 413 | 283 | 3.54 | 4.19 |
| 414 | 283 | 3.54 | 2.79 |
| 415 | 293 | 3.41 | 4.96 |
| 416 | 304 | 3.29 | 8.84 |
| 417 | 263 | 3.80 | 2.59 |

* Concentration of each monomer, 3.65 mole/l; total amount of monomers (CPT + SO₂), 0.02 mole; solvent, toluene; time of polymerization, 20 min.

Dependence of the initial rate of the polymerization upon monomer concentration was checked by varying one monomer concentration while the comonomer concentration was kept constant. In Table II and Figures 4 and 5 are shown the results of the copolymerization at varying CPT concentrations and a constant SO₂ concentration at 0 and 10°C. The plots of the rate of the copolymerization and [CPT]³ were found to be linear and independent of copolymerization temperature or SO₂ concentration. Table III and Figures 6 and 7 show the results of the copolymerization at varying SO₂ concentrations and a constant CPT concentration. The rate of copolymerization was linear with [SO₂].² Therefore, the rate of the

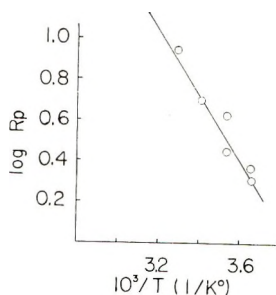


Fig. 3. Arrhenius plot of the rate of the copolymerization.

TABLE II
Results of Copolymerization at Varying CPT Concentration and Constant
SO₂ Concentration^a

| Expt | Temp, °C | Total vol, ml | Polym- eri- zation time, min | Monomer feed | | Polymer yield, mg | <i>R_p</i> , mg/ min |
|------|-------------|---------------------|--|---------------|-------------------------|-------------------------|--------------------------------------|
| | | | | CPT, mmole | CPT/ SO ₂ | | |
| 106 | 0 | 3.5 | 60 | 22.31 | 1.757 | 564.9 | 9.415 |
| 107 | 0 | 3.5 | 60 | 16.74 | 1.291 | 257.2 | 4.287 |
| 108 | 0 | 3.5 | 60 | 10.97 | 0.833 | 226.9 | 3.781 |
| 109 | 0 | 3.5 | 60 | 5.46 | 0.437 | 7.4 | 0.123 |
| 119 | 0 | 5.5 | 30 | 45.59 | 3.531 | 302.9 | 10.10 |
| 120 | 0 | 5.5 | 30 | 37.89 | 3.168 | 237.8 | 7.927 |
| 121 | 0 | 5.5 | 30 | 34.32 | 2.696 | 156.6 | 5.220 |
| 122 | 0 | 5.5 | 30 | 28.57 | 2.213 | 137.2 | 4.573 |
| 123 | 0 | 5.5 | 30 | 22.81 | 1.783 | 64.0 | 1.800 |
| 124 | 0 | 5.5 | 30 | 16.92 | 1.352 | 31.8 | 1.060 |
| 153 | 10 | 3.5 | 20 | 17.12 | 1.377 | 439.6 | 21.98 |
| 154 | 10 | 3.5 | 20 | 11.35 | 0.913 | 282.7 | 14.24 |
| 155 | 10 | 3.5 | 20 | 9.24 | 0.743 | 135.7 | 6.79 |
| 156 | 10 | 3.5 | 20 | 6.98 | 0.562 | 60.4 | 3.02 |
| 157 | 10 | 3.5 | 60 | 5.14 | 0.414 | 44.9 | 0.75 |

^a SO₂, 11.59 mmole; solvent, toluene.

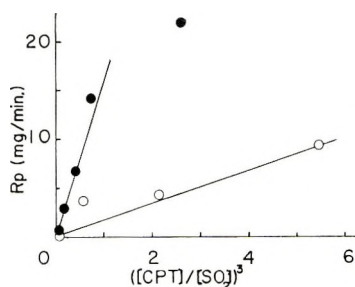


Fig. 4. Dependence of the rate of the copolymerization on CPT concentration at constant SO₂ concentration (3.65 mole/l); (O) at 0°C; (●) at 10°C.

copolymerization was considered to depend upon an extraordinarily high order of monomer concentration according to eq. (1):

$$R_p = k_p [\text{CPT}]^3 [\text{SO}_2]^2 \quad (1)$$

This relationship is similar to that obtained for the copolymerization of methylcyclopropene and SO₂. From eq. (1), the maximum rate of copolymerization is expected to be at 0.4 of SO₂ mole fraction in the monomer feed. In Figure 8 is shown the dependence of the rate of copolymerization upon SO₂ mole fraction in the monomer feed at a constant total monomer concentration. The maximum rate was found to be between 0.4 and 0.5 mole fraction of SO₂. This is considered verify eq. (1).

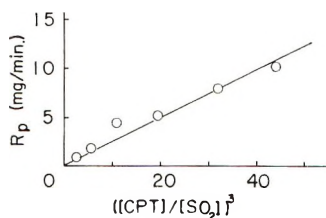


Fig. 5. Dependence of the rate of the copolymerization on CPT concentration at constant SO_2 concentration (2.07 mole/l) at 0°C .

TABLE III
Results of Copolymerization at Varying SO_2 Concentration and Constant CPT Concentration^a

| Expt | Temp, $^\circ\text{C}$ | Total vol, ml | Polymerization time, min | Monomer feed | | | Polymer yield, mg | R_p , mg/min |
|------|------------------------|---------------|--------------------------|--------------|-----------------------|--------------------------|-------------------|----------------|
| | | | | CPT, mmole | SO_2 , mmole | SO_2/CPT | | |
| 114 | 0 | 3.5 | 60 | 11.39 | 30.85 | 2.706 | 633.4 | 5.28 |
| 115 | 0 | 3.5 | 60 | 11.39 | 23.98 | 2.041 | 438.5 | 3.66 |
| 116 | 0 | 3.5 | 60 | 11.39 | 18.50 | 1.630 | 171.3 | 1.46 |
| 117 | 0 | 3.5 | 60 | 11.39 | 12.60 | 1.127 | 122.4 | 1.02 |
| 118 | 0 | 3.5 | 60 | 11.39 | 6.46 | 0.573 | 37.7 | 0.31 |
| 140 | 0 | 3.0 | 45 | 11.39 | 24.99 | 2.206 | 376.2 | 8.227 |
| 141 | 0 | 3.0 | 45 | 11.39 | 18.64 | 1.645 | 184.7 | 4.104 |
| 142 | 0 | 3.0 | 45 | 11.39 | 12.46 | 1.100 | 238.9 | 5.309 |
| 143 | 0 | 3.0 | 60 | 11.39 | 10.19 | 0.899 | 130.8 | 2.180 |
| 144 | 0 | 3.0 | 124 | 11.39 | 8.29 | 0.732 | 64.2 | 0.518 |
| 145 | 0 | 3.0 | 124 | 11.39 | 4.19 | 0.370 | 28.0 | 0.226 |
| 180 | 10 | 3.5 | 7 | 11.24 | 18.87 | 1.679 | 428.4 | 61.65 |
| 181 | 10 | 3.5 | 7 | 11.24 | 12.69 | 1.129 | 299.1 | 42.65 |
| 182 | 10 | 3.5 | 7 | 11.24 | 10.37 | 0.973 | 187.2 | 26.74 |
| 183 | 10 | 3.5 | 15 | 11.24 | 7.75 | 0.690 | 80.4 | 5.36 |
| 184 | 10 | 3.5 | 15 | 11.24 | 6.47 | 0.576 | 85.0 | 5.66 |
| 185 | 10 | 3.5 | 15 | 11.24 | 4.30 | 0.383 | 50.0 | 3.33 |

^a Solvent, toluene.

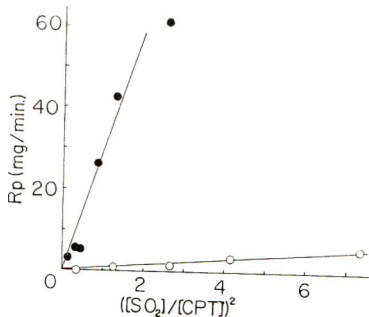


Fig. 6. Dependence of the rate of the copolymerization on SO_2 concentration at constant CPT concentration (3.65 mole/l): (O) at 0°C ; (●) at 10°C .

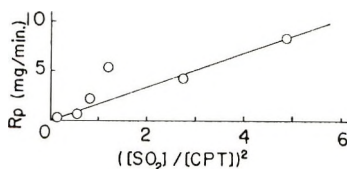


Fig. 7. Dependence of the rate of the copolymerization on SO_2 concentration at constant CPT concentration (3.78 mole/l) at $0^\circ C$.

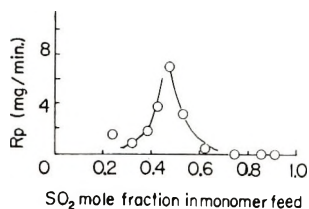


Fig. 8. Dependence of the rate of the copolymerization on SO_2 mole fraction in monomer feed at constant total monomer concentration (7.30 mole/l) at $0^\circ C$.

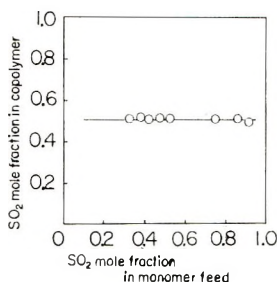


Fig. 9. Composition diagram of the copolymerization.

Figure 9 shows that the SO_2 content in copolymer was about 50 mole-% regardless of monomer feed ratios.

Development of a yellow color in mixing CPT and SO_2 , extraordinarily high order dependence of the rate of copolymerization upon monomer concentration, and alternating tendency of the copolymerization might suggest an important participation of a molecular complex between CPT and SO_2 in the initiation and propagation steps in the copolymerization, similar to that proposed for the copolymerization of methylenecyclopropane and SO_2 .

In addition, terpolymerizations were carried out to examine the property of the propagating species and the behavior of the copolymerization. Vinyl compounds and olefins are classified into two groups with regard to their copolymerizability with SO_2 ; one group of compounds forms a molecular complex with SO_2 and copolymerizes with SO_2 by radical initiators to give a polysulfone (group I), and the other group consists of compounds which do not form a complex but either polymerize to give a homopolymer or it does not polymerize at all (group II). In general, group I consists of elec-

tron donor-type monomers with low or negative e values, such as ethylene, butene, butadiene, styrene, allyl chloride, etc., while group II consists of electron-acceptor type monomers with high or positive e values, such as AAm, MAAm, AN, MA, MMA, VDC, etc. Therefore, terpolymerizations containing these monomers and SO_2 are considered to be divided into the following three cases: (a) group I-group I- SO_2 ; (b) group I-group II- SO_2 ; and (c) group II-group II- SO_2 . In the case *a*, Ito et al.⁶ reported that terpolymerization of allyl chloride, butene-1, and SO_2 yielded terpolymer containing 50 mole-% of SO_2 unit regardless of monomer feed ratios and could be regarded as a copolymerization of a complex between allyl chloride and SO_2 and a complex between butene-1 and SO_2 . Terpolymerization systems belonging to case *b* are those of acrylic ester-butene-1- SO_2 ,⁷ AN-allyl alcohol- SO_2 ,⁸ AN-St- SO_2 ,⁹ AN-butene-1- SO_2 ,¹⁰ MA-allyl chloride- SO_2 ,¹¹ and MA-vinyl chloride- SO_2 .¹¹ The AN-butene-1- SO_2 system was regarded as the copolymerization of a complex of butene-1 and SO_2 with free AN.¹⁰ In case *c* no terpolymerization is known to take place.

The third monomers used in this experiment were (in order of decreasing e value) AAm, MAAm, AN, MA, MMA, VDC, and St. Most terpolymerization systems in this experiment are considered to belong to case *b* except for the CPT-St- SO_2 system which would be the case *a*. For comparison, copolymerizations of the third monomer and SO_2 were also carried out. The concentration of each monomer in the feed was always equimolar, and terpolymerization and copolymerization were carried out in bulk at 30 and 60°C without radical initiator. The monomer components incorporated into the polymers were checked qualitatively by means of infrared and NMR spectra and the presence of VDC was checked also by the Beilstein test.

In Table IV are shown the results. Most terpolymerization systems investigated gave polymers containing the three monomers as expected, except for the systems CPT-MMA- SO_2 and CPT-St- SO_2 . It is quite ordinary that the binary systems of monomer of group II and SO_2 did not give copolymers but that the group I- SO_2 systems gave copolymer.

The CPT-MMA- SO_2 system gives only a homopolymer of MMA. Considering the spontaneous copolymerization of CPT and SO_2 , this fact is very extraordinary, so that MMA must be supposed to behave in an unusual fashion in the presence of SO_2 . Recently, O'Driscoll et al.¹² reported the polymerization of MMA and copolymerization of MMA and St induced by SO_2 , and inferred from the abnormal behaviors that the propagating species might be a complex radical. Thus the propagating species in MMA polymerization in the presence of SO_2 might be different from those in CPT- SO_2 copolymerization.

The CPT-St- SO_2 system gave a copolymer containing only St and SO_2 . Since the CPT- SO_2 system is more reactive than the St- SO_2 system in the spontaneous copolymerization, this fact might be explained by the CPT- SO_2 system being more reactive in initiation but less in propagation than St- SO_2 system. This situation is considered to be similar to the alternating

TABLE IV
 Terpolymerization with a Third Monomer and Copolymerization of SO₂
 and Third Monomer

| Components in monomer feed | Price-Alfrey values for third monomer | | Components in polymer | Polymeri- zation time, hr | Conversion, % | |
|--|---|----------|---------------------------------|---------------------------------|---------------|-------|
| | <i>e</i> | <i>Q</i> | | | 60°C | 30°C |
| CPT + SO ₂ + AAM | 1.39 | 1.18 | CPT + SO ₂ + AAM | 24 | 5.68 | 8.17 |
| SO ₂ + AAM | | | b | 24 | b | b |
| CPT + SO ₂ + MAAM | 1.24 | 1.46 | CPT + SO ₂ + MAAM | 24 | 15.03 | 16.45 |
| SO ₂ + MAAM | | | b | 24 | b | b |
| CPT + SO ₂ + AN | 1.20 | 0.60 | CPT + SO ₂ + AN | 24 | 49.70 | 36.38 |
| SO ₂ + AN | | | b | 45 | b | b |
| CPT + SO ₂ + MA | 0.60 | 0.42 | CPT + SO ₂ + MA | | | |
| SO ₂ + MA | | | b | | | |
| CPT + SO ₂ + MMA | 0.40 | 0.74 | MMA | | | |
| SO ₂ + MMA | | | MMA | | | |
| CPT + SO ₂ + VDC | 0.36 | 0.20 | CPT + SO ₂ + VDC | 24 | 7.39 | 16.98 |
| SO ₂ + VDC | | | VDC | 24 | 14.40 | 0.07 |
| CPT + SO ₂ + St | -0.80 | 1.0 | SO ₂ + St | 37.5 | 17.82 | 10.02 |
| SO ₂ + St | | | SO ₂ + St | 37.5 | | 10.93 |
| CPT + SO ₂ + St + MMA | | | SO ₂ + St + MMA | 37.5 | 14.78 | 17.54 |
| SO ₂ + St + MMA | | | SO ₂ + St + MMA | 45 | 45.17 | 9.34 |

^a No radical initiator; in bulk; equal molar concentrations of each monomer.

^b No polymer obtained.

copolymerizations of vinyl ether with maleic anhydride and of *p*-dioxene with maleic anhydride.¹³ The former system develops a yellow color in the monomeric state and copolymerization takes place spontaneously at a remarkable rate at room temperature but the latter neither develops a color nor copolymerizes spontaneously, while the rate of copolymerization by a radical initiator is larger in the latter than in the former system. However, the behavior of the CPT–St–SO₂ system is too extraordinary to be explained well at present.

In quarternary polymerization of CPT, St, MMA, and SO₂, the obtained polymer contains St, MMA, and SO₂ but no CPT (Table IV). It might be assumed from this fact that the nature of propagation of the St–SO₂ and the MMA–SO₂ systems is different from that of the CPT–SO₂ system. Thus in the present systems, a propagating radical might not be necessarily of a single species, although a free radical in conventional vinyl polymerizations is commonly considered to be of a single species.

To permit the copolymerization of CPT and SO₂ to be discussed more exactly, we intend to examine the initiation and the propagation steps separately in the future.

References

1. S. Iwatsuki, S. Amano, and Y. Yamashita, *Kogyo Kagaku Zasshi*, **90**, 2027 (1967); part XV.
2. N. L. Zutty, C. W. Wilson, G. H. Potter, D. C. Priest, and C. J. Witworth, *J. Polymer Sci. A*, **3**, 2781 (1965).
3. S. Iwatsuki, T. Kokubo, and Y. Yamashita, *J. Polymer Sci. A-1*, **6**, 2441 (1968).
4. F. Fisher and D. E. Applequist, *J. Org. Chem.*, **30**, 2089 (1965).
5. W. Schöniger, *Mikrochim. Acta*, **1955**, 123.
6. I. Ito, H. Hayashi, T. Saegusa and J. Furukawa, *Kogyo Kagaku Zasshi*, **65**, 703 (1962).
7. Phillips Petroleum Co. U.S. Pat. 2,779,749 (1957).
8. Badische Aniline U. Sodafabrik, German Pat. 1,068,894 (1959).
9. N. Tokura, M. Matsuda, and M. Iino, paper presented at 14th Meeting, Chemical Society of Japan, Tokyo, 1961, paper 2M50.
10. H. Hayashi, I. Ito, T. Saegusa, and J. Furukawa, *Kogyo Kagaku Zasshi*, **65**, 1634 (1962).
11. I. Ito, T. Saegusa, and J. Furukawa, *Kogyo Kagaku Zasshi*, **65**, 1878 (1962).
12. P. Ghosh and K. F. O'Driscoll, *J. Polymer Sci. B*, **4**, 519 (1966).
13. S. Iwatsuki, Y. Tanaka, and Y. Yamashita, *Kogyo Kagaku Zasshi*, **67**, 1467, 1470 (1964).

Received September 20, 1967

Revised November 28, 1967

Synthesis and Polymerization Studies of Several Chloro and Cyano Epoxides

PETER E. WEI and PETER F. BUTLER, *Esso Research and Engineering Company, Linden, New Jersey 07036*

Synopsis

The polar epoxides, glycidonitrile, dimethyl glycidonitrile, tetracyanoethylene oxide, epicyanohydrin, 4,4,4-trichlorobutylene-1,2-epoxide, and 1,1-dichloro-3,4-epoxy-1-butene were prepared, characterized by their infrared and nuclear magnetic resonance spectra and their polymerizations studied. Epicyanohydrin was found to be an unpolymerizable dimer, and those epoxides with a cyano group attached directly to the epoxide ring could not be polymerized. The halogenated epoxides, 4,4,4-trichlorobutylene-1,2-epoxide and its dehydrochlorination product, 1,1-dichloro-3,4-epoxy-1-butene were polymerized to high polymers with a complex catalyst from aluminum alkyl, acetyl acetone, and water. The polymerization of these monomers gave low conversions and required large amounts of catalyst. Higher conversions were obtained by copolymerization with propylene oxide or terpolymerization with propylene oxide and allyl glycidyl ether. The polymerizability of the substituted epoxide in $X-\overline{\text{CH}-\text{CH}_2-\text{O}}$ (where X is CH_3- , ClCH_2- , Cl_2CCH_2- , and $\text{Cl}_2\text{C}=\text{CH}-$) was found to follow the order: $\text{CH}_3- > \text{ClCH}_2- > \text{Cl}_2\text{C}-\text{CH}_2- > \text{Cl}_2\text{C}=\text{CH}-$. The polymers of 4,4,4-trichlorobutylene-1,2-epoxide and its dehydrochlorination product were not vulcanizable through the chlorine functionality or the olefinic unsaturation of the type $\text{Cl}_2\text{C}=\text{CH}-$. The presence of an active third monomer such as allyl glycidyl ether was necessary to facilitate vulcanization. Properties of such vulcanizates are reported.

INTRODUCTION

Due to the combination of their many superior properties, high molecular weight polyethers, such as polypropylene oxide and polyepichlorohydrin, have attracted considerable commercial interest as specialty elastomers. The main objective of this paper is to report the effect of polar substitution on both the polymerizability of such epoxides and the properties of the resulting polymers. The instrumental characterization of the monomers is also discussed.

EXPERIMENTAL

Monomer Preparation

4,4,4-Trichlorobutylene-1,2-epoxide, $\text{CCl}_3\text{CH}_2\overline{\text{CH}-\text{CH}_2-\text{O}}$ and 1,1-dichloro-3,4-epoxy-1-butene, $\text{CCl}_2=\text{CH}-\overline{\text{CH}-\text{CH}_2-\text{O}}$ were prepared according to the method of Dowbenko.¹

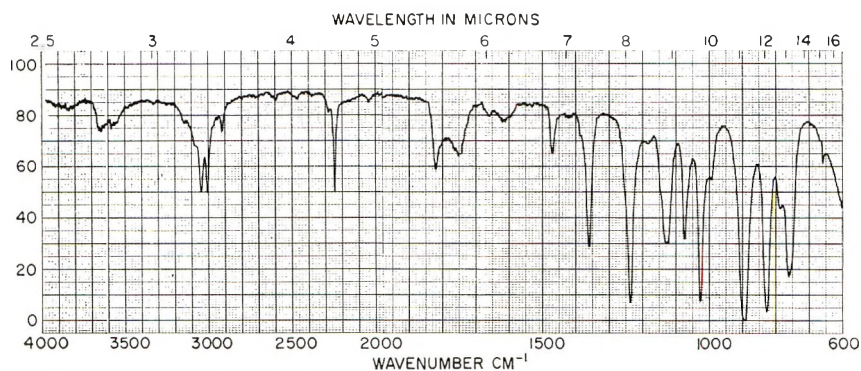


Fig. 1. Infrared spectrum of 4,4,4-trichlorobutylene-1,2-epoxide.

The overall yield of the trichlorobutylene oxide from allyl alcohol was 27.4 mole-%. This yield was improved to 47.2 mole-% by eliminating the isolation of the intermediate and recovering the unreacted materials before the removal of FeCl_3 .

In this synthesis a small amount of 1,1-dichloro-3,4-epoxy-1-butene was formed and was difficult to remove. By repeated fractionation we managed to obtain 40 g of a sample (bp, $60^\circ\text{C}/20$ mm Hg; n_D^{20} , 1.4920; d^{25} , 1.3495) containing 73.9% of 1,1-dichloro-3,4-epoxy-1-butene and 21.9% trichlorobutylene oxide as determined from a gas chromatogram.

The infrared spectrum (Fig. 1) of 4,4,4-trichlorobutylene-1,2-epoxide was characterized by prominent bands for the epoxide group at 2950 cm^{-1} (epoxide C—H stretching) and 1270 cm^{-1} (epoxide C—O stretching). Prominent C—Cl stretching bands were present in the $700\text{--}800\text{ cm}^{-1}$ region.

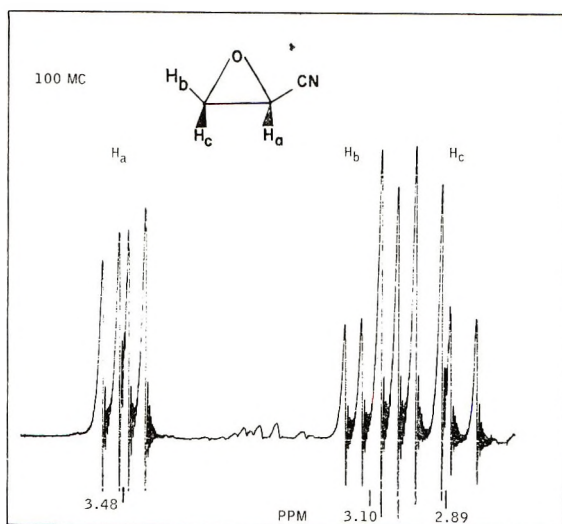
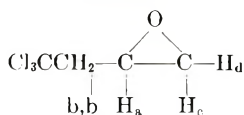


Fig. 2. NMR spectrum of 4,4,4-trichlorobutylene-1,2-epoxide.

TABLE I



| H | δ , ppm | J , cps |
|---|----------------|-----------------------------------|
| a | 3.26 | $J_{ab} = 5.08$; $J_{ad} = 5.30$ |
| b | 3.04 | $J_{b,b} = 14.5$ |
| b | 2.75 | $J_{c,d} = 5.00$ |
| c | 2.81 | $J_{ac} = 3.81$ |
| d | 2.60 | $J_{ad} = 2.33$ |

The 100 Mcps NMR spectrum (Fig. 2, Table I) is quite complex due to the overlapping of the two ABX type systems (both the exo methylene and ring methylene protons are nonequivalent, due to proximity to the asymmetric center; in addition, the ring methylene protons are nonequivalent due to their geometric relationship to the ring substituent) and long-range coupling between both sets of methylene protons. The ring methine proton is at lowest field position, 3.25 ppm, and appears as a doublet of a double, doublet (16 lines) due to coupling with each nonequivalent methylene proton. Each of these protons is in turn a double doublet reflecting both geminal and vicinal coupling. The *cis* vicinal coupling is larger than the *trans* coupling.

The infrared spectrum (Fig. 3) of 1,1-dichloro-3,4-epoxy-1-butene has characteristic bands for the epoxide group at 2930 cm^{-1} (epoxide C—H stretching) and 1248 cm^{-1} (epoxide C—O stretching) and for the olefin group at 1630 cm^{-1} (C=C stretching). Prominent C—Cl bands are in the $700\text{--}800 \text{ cm}^{-1}$ region.

The 60 Mcps NMR spectrum (Fig. 4) is fully in agreement with the assigned structure. It has peaks at 5.61 (doublet), 3.61 (doublet of a doublet), 2.97 (double doublet) and 2.69 (double doublet) ppm in a

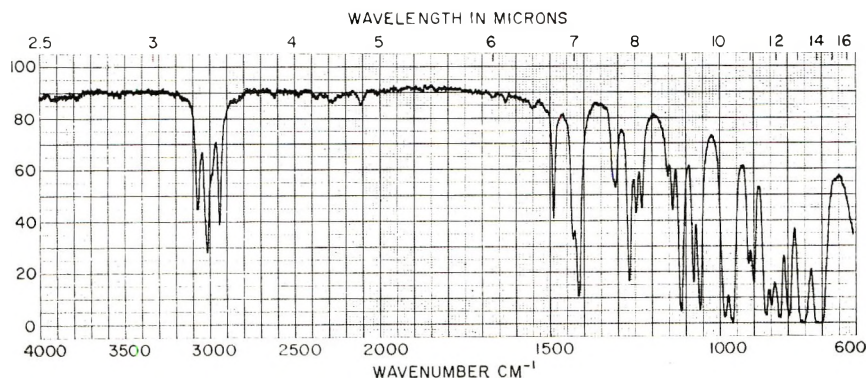


Fig. 3. Infrared spectrum of a mixture of 1,1-dichloro-3,4-epoxy-1-butene (73.9%) and 4,4,4-trichlorobutylene-1,2-epoxide (21.9%).

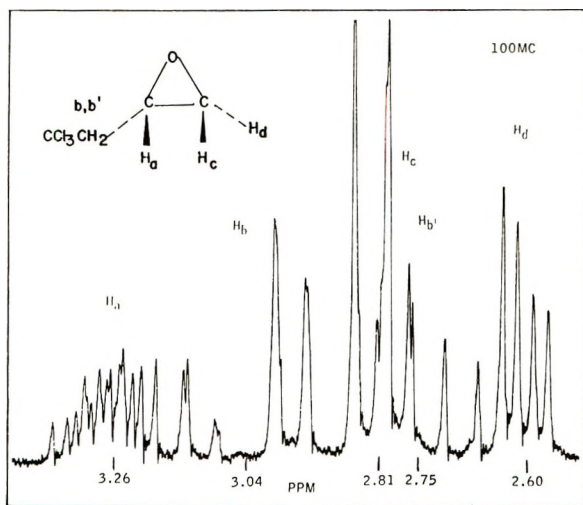


Fig. 4. NMR spectrum of a mixture of 1,1-dichloro-3,4-epoxy-1-butene (73.9%) and 4,4,4-trichlorobutylene-1,2-epoxide (21.9%).

1 : 1 : 1 : 1 ratio for the olefin, ring methine, and nonequivalent ring methylene protons, respectively.

Glycidonitrile, $\text{O}-\text{CH}_2-\text{CHCN}$, was synthesized according to Payne's method.²

The infrared spectrum of this material (Fig. 5) has characteristic bands at 2255 cm^{-1} ($-\text{C}\equiv\text{N}$ stretching), 2920 cm^{-1} (epoxide $\text{C}-\text{H}$ stretching), and 1237 cm^{-1} (epoxide $\text{C}-\text{O}$ stretching). The spectrum contains trace amounts of the anhydride. The glycidonitrile structure was confirmed by an analysis of the 100 Mcps NMR spectrum (Fig. 6) which displayed a typical ABX type pattern for the ring methylene and methine protons (the NMR spectra were run in CCl_4 on the JEOLCO 4H-100

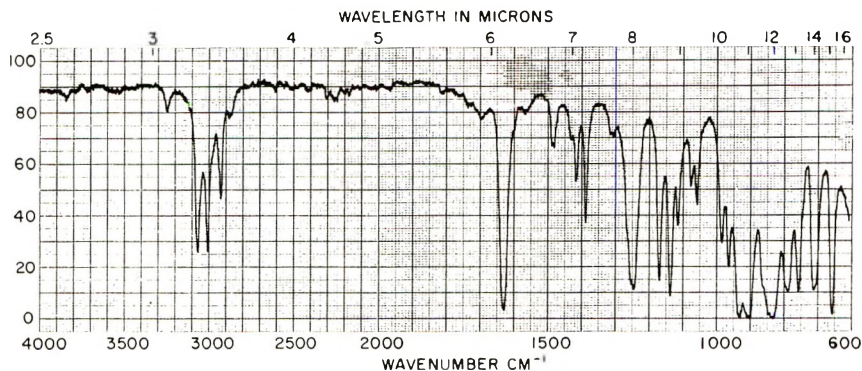


Fig. 5. Infrared spectrum of glycidonitrile.

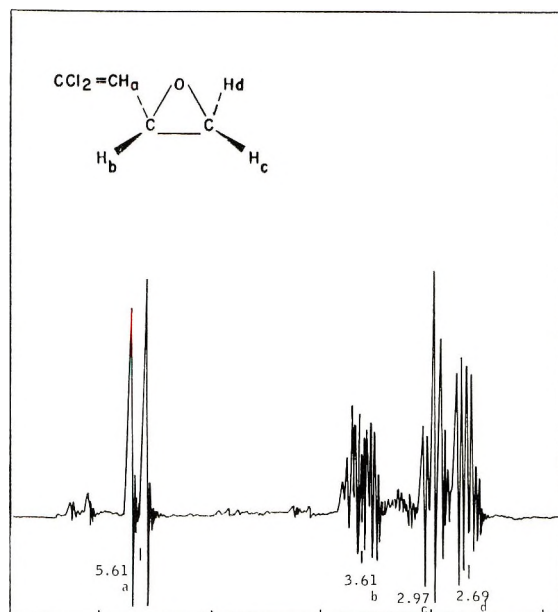


Fig. 6. NMR spectrum of glycidonitrile.

spectrometer). The methine proton at 3.49 ppm is deshielded relative to the two methylene protons by the additional contribution of the cyano group and appears as a double doublet due to *cis* (4.08 cps) and *trans* (2.60 cps) vicinal coupling. In line with literature data², J_{cis} is larger than J_{trans} . The upfield methylene proton at 2.99 ppm is a double doublet reflecting the larger *cis* vicinal coupling and the geminal coupling of 5.50 cps. The methylene proton *cis* to the cyano group is deshielded by the anisotropy of the $C\equiv N$ bond and appears as a double doublet at 3.10 ppm.

Dimethyl glycidonitrile, $(CH_3)_2C-CHCN-O$, was prepared according to Martynov and Shchelkunov³ from the reaction of acetone and chloroacetonitrile in the presence of $NaOCH_3$.

Tetracyanoethylene oxide, $(CN)_2C-C(CN)_2$, was prepared from tetracyanoethylene by epoxidation with hydrogen peroxide.⁴

Pazschke⁵ and Hartenstein⁶ reported the synthesis of epicyanohydrin, $O-CH_2-CH-CH_2-CN$, by condensation of potassium cyanide and epichlorohydrin. The compound we prepared by their method had a melting point of $166^\circ C$, corresponding to the literature value, and had elemental analyses close to the suggested composition of epicyanohydrin, but the molecular weight was found to be 195, which was about twice the value, 83, of epicyanohydrin. The compound synthesized may be its dimer. No molecular weight was reported in the literature.

Polymerization Studies

Polymerization studies were carried out in 8-oz screw-capped bottles, which were placed in a chain-driven rotator in a water bath at constant temperatures. Solvents and commercial monomers were freshly distilled under N_2 over CaH_2 before use. Bottles were charged up in a dry nitrogen box, first the solvent, then the monomer (or monomers), and lastly the catalyst. Unless mentioned otherwise, polymers were isolated by pouring the entire reaction mixture into boiling water with continued heating until the mixture was completely free from solvent and unreacted monomers. The resultant solid polymers were dried *in vacuo* at $60^\circ C$. Polymer viscosities were determined in α -chloronaphthalene at $135^\circ C$ unless indicated otherwise.

Vulcanization and Vulcanizate Evaluation

The polymers were mixed with vulcanization ingredients on a two-roll mill and the mixtures were heated in a mold under pressure. The prepared sample pads of 20-mil thickness were tested with a Scott tester for tensile properties and swelled in ASTM No. 3 oil or other solvents for evaluating their oil and solvent resistant properties.

RESULTS AND DISCUSSION

Propylene oxide may be polymerized⁷⁻⁹ to a high polymer by using a variety of catalyst systems including $FeCl_3$ ·propylene oxide; $ZnEt_2$ · H_2O ; and AlR_3 ·acetylacetonate· H_2O . The substitution of one hydrogen atom by a chlorine atom (propylene oxide \rightarrow epichlorohydrin) changes not only the polymerizability of the monomer but also the resultant polymer properties such as solvent resistance and air permeability. Epicyanohydrin is closely related to epichlorohydrin and was also expected to afford polymers of interesting properties. Unfortunately, we found that the reported epicyanohydrin^{5,6} is actually a dimer, probably of a dioxane structure, and could not be polymerized. Other epoxides with cyano groups directly attached

TABLE II

| TCBO, mmole | Al- AcAc, mmole | Al- (iBu) ₃ , mmole | Ac- (iBu) ₃ - AcAc, (1:1), mmole | Total Sol- vent, cc ^a | Catalyst/ mono- mer, mole-% | H ₂ O, mmole | Condi- tions, °C/hr | Polymer yield, mole-% ^b | [η] |
|-------------|--------------------|-----------------------------------|---|-------------------------------------|-----------------------------------|-------------------------|------------------------|------------------------------------|------------|
| 200 | 10 | 10 | — | 20 | 5 | 5 | 54/43 | 13.4 | 1.60 |
| 200 | — | — | 10 | 20 | 5 | 5 | 50/22 | 4.3 | 1.65 |
| 80 | — | — | 10 | 20 | 12.5 | 5 | 50/22 | 13.2 | 1.05 |
| 24 | — | — | 10 | 20 | 41.7 | 5 | 50/22 | 26.2 | 0.33 |

^a *n*-Heptane was dried by distilling over Li dispersion.

^b Polymer was isolated by precipitation with methanol followed by deashing with dilute HCl.

to the ring, such as glycidonitrile, dimethyl glycidonitrile, and tetracyanoethylene, although monomeric in structure, also could not be polymerized. The negative data from the polymerization studies are omitted because these polymerizations were attempted with the use of conditions identical to those used throughout our study with ferric chloride, diethylzinc, and triisobutylaluminum catalyst systems. For brevity, the following abbreviations are used: PO = propylene oxide, ECH = epichlorohydrin, AGE = allyl glycidyl ether, TCBO = 4,4,4-trichlorobutylene-1,2-epoxide, DCB = 1,1-dichloro-3, 4-epoxy-1-butene. Catalysts such as $\text{FeCl}_3 \cdot \text{PO}$ or $\text{ZnEt}_2 \cdot \text{H}_2\text{O}$ complexes did not polymerize any of these polar epoxides and are omitted in this report.

TCBO Homopolymerizations

TCBO was polymerized with a catalyst system consisting of triisobutylaluminum, acetyl acetone (AcAc), and water in a mole ratio of 1:1:0.5. The conversion of TCBO to homopolymer was dependent on the catalyst concentrations as shown in Table II. The conversion of TCBO to polymer is dependent on the amount of catalyst (increasing with increased catalyst). However, the molecular weight of the resultant polymer was decreased as indicated by decreasing viscosities. This result is not surprising.

The TCBO homopolymers were tough but flexible. One of the typical infrared spectra is shown in Figure 7. It has two C—Cl absorptions at 700 and 770 cm^{-1} and one C=C absorption at 1615 cm^{-1} due to the presence of some DCB in the monomer which was copolymerized with TCBO. One of these polymers was extracted with hot acetone; the following obtained are shown in Table III.

TCBO Copolymerizations

TCBO copolymerizes better than it homopolymerizes, and the resulting products are all rubbery. Table IV shows the copolymerization of TCBO with propylene oxide (PO). An overall monomer conversion of 40–60% was obtained at a catalyst level of 1.76–5 mole-%. Based on chlorine

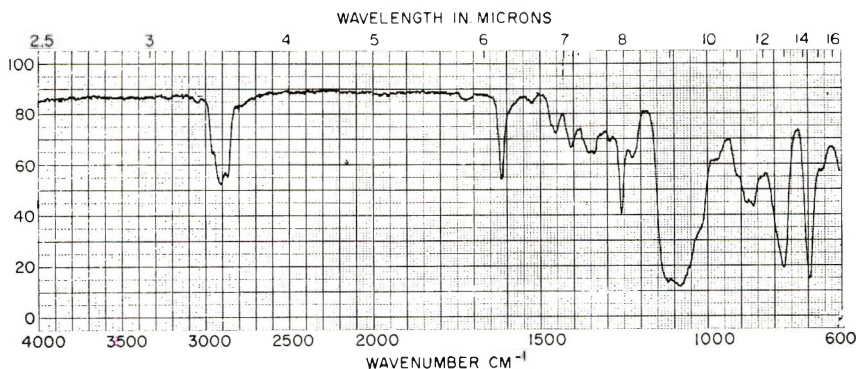


Fig. 7. Infrared spectrum of homopolymer of 4,4,4-trichlorobutylene-1,2-epoxide.

TABLE III
 Polymer Fractions^a

| | Acetone-soluble fraction | Acetone-insoluble fraction |
|-------------------------------|--------------------------|----------------------------|
| Fraction wt, g | 2.1 | 2.6 |
| Appearance | Rubbery | Tough, flexible |
| Cl, wt-% | 53.3 | 59.6 |
| [η] | 0.4 ^b | 2.64 ^c |
| Crystallinity (x-ray and DTA) | 0 | |
| Glass temperature, °C | -70 | -2 |

^a Original polymer: wt, 4.7 g; [η] in α -chloronaphthalone at 135°C, 1.6.

^b In benzene at 25°C.

^c In α -chloronaphthalene at 135°C.

analysis, TCBO monomer conversions were calculated. Comparison of Tables II and IV indicates that the conversion of TCBO monomer to polymer is much greater in the presence of propylene oxide (PO) than in the absence of it at an equal catalyst concentration. For instance, at a catalyst concentration of 5 mole-%, a conversion of 32.8 mole-% TCBO monomer to copolymer was obtained compared with only 13.4 mole-% TCBO to the homopolymer.

Table V shows the copolymerization of TCBO with allyl glycidyl ether (AGE). A higher TCBO monomer conversion was also observed, though the inherent viscosities of the TCBO-AGE copolymers were all low.

TCBO Terpolymerizations

Table VI shows the terpolymerizations of TCBO, PO, and AGE. With increased propylene oxide in the monomer mixture both overall conversions and TCBO conversions increase; this is depicted in Figure 8. The top curve represents the amount of total monomer converted to the polymer

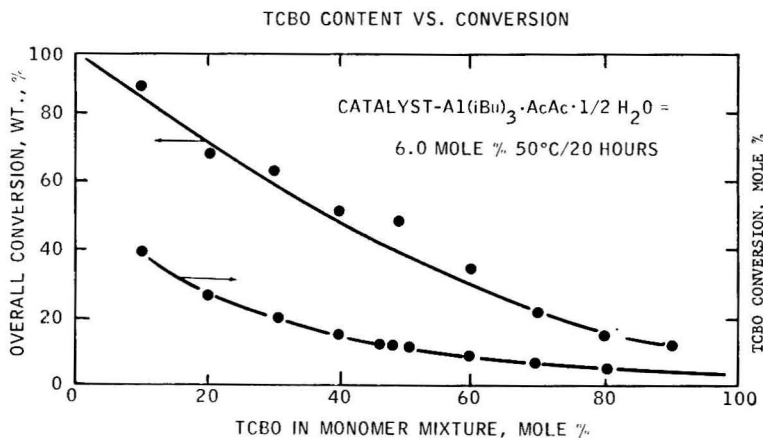


Fig. 8. TCBO content vs. conversion.

TABLE IV
TCBO-PO Copolymerizations

| PO, mmole | TCBO, mmole | <i>n</i> -Heptane, cc | Al(<i>i</i> Bu) ₃ - AcAc(1:1), mmole | H ₂ O, mmole | Conditions, °C/hr | Polymer yield, g | Cl, wt-% | [η] ^a | Al(<i>i</i> Bu) ₃ / monomer, mole-% | Overall con- version, wt-% | TCBO conversion, mole-% |
|--------------|----------------|--------------------------|--|----------------------------|----------------------|------------------------|-------------|-------------------------|---|-------------------------------------|-------------------------------|
| 190 | 97 | 50 | 5 | 2.5 | 80/16 | 11.3 | 7.10 | 4.1 | 1.76 | 40 | 7.8 |
| 72 | 40 | 20 | 10 | 5 | 50/20 | 6.1 | 15.90 | 1.9 | 4.50 | 54 | 22.8 |
| 143 | 120 | 13 | 13 | 6.5 | 54/43 | 17.3 | 24.20 | 1.8 | 5.00 | 60 | 32.8 |

^a In benzene at 25°C.TABLE V
TCBO-AGE Copolymerizations

| AGE, mmole | TCBO, mmole | <i>n</i> -Heptane, cc | Al(<i>i</i> Bu) ₃ - AcAc(1:1), mmole | H ₂ O, mmole | Conditions, °C/hr | Polymer yield, g | Cl, wt-% | [η] ^a | Al(<i>i</i> Bu) ₃ / monomer, mole-% | Overall con- version, wt-% | TCBO conversion, mole-% |
|---------------|----------------|--------------------------|--|----------------------------|----------------------|------------------------|-------------|-------------------------|---|-------------------------------------|-------------------------------|
| 67.5 | 16.2 | 20 | 10 | 5 | 50/20 | 8.7 | 6.63 | 0.6 | 11.9 | 82.8 | 33.4 |
| 16.5 | 64.0 | 20 | 10 | 5 | 50/20 | 2.0 | 24.3 | 0.5 | 12.4 | 15.1 | 7.2 |
| 8.0 | 195.0 | 20 | 10 | 5 | 50/91 | 3.66 | 35.2 | 1.1 | 4.9 | 10.3 | 6.2 |

^a In benzene at 25°C, 62% gel.

TABLE VI
 TCBO-PO-AGE Terpolymerizations

| TCBO content Mole-% | TCBO content cc | PO, cc | AGE, cc | Ben- zene, cc | Al(iBu) ₃ - AcAc(1:1), mmole | H ₂ O, mmole | Conditions, °C/hr | Polymer yield, g | Cl, wt-% | [η] | Al(iBu) ₃ / monomer, mole-% | Over- all con- version, wt-% | TCBO con- version, mole-% |
|------------------------|--------------------|-----------|------------|---------------------|---|----------------------------|----------------------|------------------------|-------------|-----|--|--|------------------------------------|
| | | | | | | | | | | | | | |
| 0 | 0 | 24.00 | 1.0 | 20 | 10 | 5 | 50/20 | 21.0 | 0 | 2.7 | 2.8 | 100 | — |
| 10 | 3.88 | 19.60 | 1.53 | 25 | 19.5 | 9.8 | 50/20 | 20.3 | 6.1 | 3.2 | 6.0 | 88.5 | 38.8 |
| 20 | 7.55 | 16.03 | 1.42 | 25 | 18.1 | 9.1 | 50/20 | 17.7 | 8.6 | 2.3 | 6.0 | 69.5 | 23.4 |
| 30 | 10.62 | 13.04 | 1.34 | 25 | 17.0 | 8.5 | 50/20 | 18.0 | 10.5 | 2.6 | 6.0 | 66.5 | 20.6 |
| 40 | 13.40 | 10.40 | 1.30 | 25 | 16.3 | 8.2 | 50/20 | 15.0 | 12.1 | 1.9 | 6.0 | 52.1 | 15.5 |
| 46.5 | 15.73 | 8.08 | 3.37 | 25 | 16.3 | 8.2 | 50/20 | 16.0 | 11.8 | 1.6 | 6.0 | 49.3 | 13.1 |
| 48.7 | 15.73 | 8.08 | 2.38 | 25 | 15.7 | 7.9 | 50/20 | 13.9 | 12.7 | 1.5 | 6.0 | 44.6 | 12.3 |
| 50.0 | 15.73 | 8.08 | 1.19 | 25 | 15.1 | 7.6 | 50/20 | 11.8 | 13.6 | 1.7 | 6.0 | 49.2 | 11.2 |

 TABLE VII
 Comparison at TCBO and ECH Reactivities

| Epoxide | Epoxide content | | PO, mmole | AGE, mmole | Condi- tions, °C/hr | Polymer yield, g | Cl, wt-% | [η] | Al(iBu) ₃ / monomer, mole-% | Overall con- version, wt-% | Epoxide con- version, mole-% |
|---------|-----------------|-------|--------------|---------------|---------------------------|---------------------|-------------|-----|--|-------------------------------------|---------------------------------------|
| | mole-% | mmole | | | | | | | | | |
| TCBO | 73 | 383 | 143 | — | 50/20 | 13.0 | 26.7 | 1.2 | 4.95 | 17.3 | 8.5 |
| TCBO | 46 | 240 | 286 | — | 50/20 | 27.9 | 13.0 | 2.1 | 4.95 | 47.5 | 14.5 |
| TCBO | 46 | 120 | 143 | — | 50/20 | 22.0 | 15.0 | 2.2 | 9.9 | 75.1 | 25.9 |
| ECH | 69 | 383 | 143 | 31.6 | 50/20 | 25.8 | 23.5 | 3.2 | 4.68 | 53.5 | 42.0 |
| ECH | 45 | 240 | 286 | 31.6 | 50/20 | 25.2 | 22.0 | 2.8 | 4.68 | 49.0 | 67.5 |
| ECH | 45 | 120 | 143 | 15.8 | 50/20 | 20.7 | 18.8 | 3.5 | 9.35 | 95.0 | 90.0 |

in weight per cent. As the amount of TCBO is increased in the monomer feed, the overall conversion decreases because TCBO is less reactive than PO and AGE; the bottom curve represents the amount of TCBO converted to the polymer with respect to the TCBO monomer in the feed in mole per cent. It seems that the TCBO molecule at the polymer chain end preferentially joins a PO or AGE monomer molecule giving a random structure. We found that this is also true for epichlorohydrin. The infrared spectrum of the product has two absorption peaks (1615 and 1640 cm^{-1}) for C=C stretching vibrations. The peak at 1615 cm^{-1} is due to the presence of some DCB; the other one at 1640 cm^{-1} is due to the presence of AGE as compared with the PO-AGE copolymer infrared spectrum.

TCBO and ECH Reactivities

TCBO is less reactive than epichlorohydrin with the aluminum alkyl type catalyst as shown in Table VII. At identical polymerization conditions ($50^\circ\text{C}/20\text{ hr}$) and comparable monomer ratios and catalyst concentrations, both overall conversions and TCBO monomer conversions are lower than those of ECH. For instance, at a monomer mole ratio of TCBO (or ECH): PO of about 45:55 and at a catalyst concentration of about 5 mole-% the TCBO monomer conversion is only 14.5 mole-% as compared with 67.5 mole-% for ECH, although the overall conversion is 47.5 wt-% for TCBO and 49.0 wt-% for ECH.

DCB-TCBO-PO Terpolymerizations

DCB and TCBO were obtained in two mixtures (with concentrations of DCB in 78 mole-% and 61 mole-%) as determined by gas chromatography [$2\text{ ft} \times \frac{1}{4}\text{ in.}$ column, 275°C silicone gum rubber (SE 30)]. The gas chromatography (GC) data (Table VIII) correlated well with infrared absorbancies at 1620 cm^{-1} (with a 0.030-mm cell against air as reference) for DCB in DCB-TCBO mixtures.

TABLE VIII
Analysis of DCB in DCB-TCBO Mixtures

| GC data, mole-% | IR at 1620 cm^{-1} (absorbance) |
|--------------------|---|
| 1.3 | 0.027 |
| 4.8 | 0.124 |
| 11.4 | 0.334 |
| 17.4 | 0.470 |

The polymerization studies of these mixtures with PO are shown in Table IX. The overall conversions and the conversion of DCB-TCBO monomer mixtures to the polymers were much lower than those in pure TCBO systems. In other words, DCB is even less reactive than TCBO in the polymerizations.

TABLE IX
 DCB-TCBO-PO Terpolymerizations

| DCB, mmole | TCBO mmole ^a | PO, mmole | Ben- zene, cc | Al(<i>i</i> Bu) ₃ - AcAc(1:1), mmole | H ₂ O, mmole | Condi- tions, °C/hr | Polymer yield, g | Cl, wt-% | [η] | Al(<i>i</i> Bu) ₃ / monomer, mole-% | Overall con- version, wt-% | TCBO + DCB con- version, wt-% |
|---------------|----------------------------|--------------|---------------------|--|----------------------------|---------------------------|------------------------|-------------|------------|---|-------------------------------------|---|
| 72 | 20 | 145 | 24 | 10 | 5 | 50/18 | 4.0 | 15.0 | 1.93 | 4.20 | 18.5 | 6.1 |
| 40 | 26 | 74 | 25 | 7.2 | 3.6 | 50/20 | 2.8 | 21.2 | 1.10 | 5.18 | 24.1 | 2.5 |

Vulcanization

Unlike polyepichlorhydrins, TCBO homopolymers and TCBO-PO copolymers were not successfully vulcanized through the chlorine atoms. The DCB-TCBO-PO terpolymers did not afford a testable vulcanizate despite the presence of both chlorine atoms and unsaturation of the type, $\text{Cl}_2\text{C}=\text{CH}-$. Apparently the types of chlorine atoms and unsaturation in these elastomers were not reactive enough. It was found necessary to incorporate some AGE into these polymers to facilitate vulcanization. Even in the presence of AGE no suitable vulcanization system was developed for these elastomers. The formulations used were arbitrarily adapted from those developed for ECH-PO-AGE terpolymers.

Vulcanizate Properties

The vulcanizate properties of TCBO elastomers are shown in Table X. The tensile strengths of these elastomers were in the range of 900-1400 psi. The swelling data in ASTM No. 3 oil at 212°F and in cyclohexane at room temperature are shown to depend on the chlorine content of the elastomers and the modulus of the vulcanizates. Samples with chlorine content of 6-10 wt-% and with 300% modulus of 250-340 psi give 103-109% swelling in ASTM No. 3 oil at 212°F and 162-206% swelling in cyclohexane at room temperature; other samples with chlorine content of 12-14 wt-% and with 300% modulus of 520-620 psi give 60-83% swelling in ASTM No.3 oil and 106-110% swelling in cyclohexane at the said temperatures.

TABLE X
Vulcanizate Properties of TCBO Elastomers^a

| Raw elastomer | | Vulcanizate ^b | | | | | |
|------------------------|------------|--------------------------|------------------|-------------------------|-----------------------------------|--|-------------------|
| | | Tensile, psi | Elongation, % | 300% Modulus, psi | Swelling in ASTM #3 oil, | Swelling in cyclo-hexane ^c | |
| Cl content, wt-% | $[\eta]^c$ | | | | wt-% increase ^d | wt-% increase | wt-% extracted |
| 6.1 | 3.2 | 965 | 930 | 250 | 103 | 206 | 8 |
| 8.6 | 2.3 | 1100 | 895 | 330 | 109 | 181 | 8 |
| 10.5 | 2.6 | 1050 | 880 | 335 | 103 | 162 | 8 |
| 12.1 | 1.9 | 890 | 865 | 300 | 88 | 146 | 10 |
| 13.6 | 1.7 | 1250 | 765 | 515 | 83 | 107 | 9 |
| 12.7 | 1.5 | 1120 | 635 | 520 | 60 | 106 | 11 |
| 11.8 | 1.6 | 1400 | 615 | 620 | 67 | 110 | 8 |

^a TCBO elastomers are TCBO-PO-AGE terpolymers.

^b Formulation: elastomer, 100 parts; FEF carbon black, 30 phr; stearic acid, 1 phr; PBN, 0.5 phr; ZnO , 5 phr; sulfur, 2 phr; TMTDS, 0.2 phr; MBTS, 0.2 phr. Cured at 307°F for 40 min.

^c In α -chloronaphthalene at 135°C.

^d At 212°F for 70 hr.

^e At room temperature for 24 hr.

TABLE XI
 Comparison of TCBO and ECH Vulcanizate Properties

| Elastomer | | Vulcanizate ^a | | | | | | | | | |
|-------------|----------|--------------------------|--------------|---------------|----------------------|---|---------------|--|---------------|------------------------------|---------------|
| Type | Cl, wt-% | [η] | Tensile, psi | Elongation, % | Modulus, 200% psi | Swelling in ASTM #3 oil, wt-% increase ^b | | Swelling in benzene-cyclohexane ^c | | Swelling in MEK ^c | |
| | | | | | | wt-% increase | wt-% increase | wt-% increase | wt-% increase | wt-% increase | wt-% increase |
| TCBO-PO-AGE | 20.6 | 2.0 | 1250 | 360 | 750 | 58 | 100 | 5.8 | 90 | 7.4 | |
| | 13.4 | 2.6 | 1400 | 290 | 980 | 64 | 134 | 3.2 | 120 | 1.5 | |
| | 13.4 | 2.2 | 1360 | 250 | 1220 | 60 | 121 | 4.1 | 105 | 1.4 | |
| ECH-PO-AGE | 22.0 | 2.8 | 2360 | 310 | 1860 | 17 | 73 | 2.3 | 99 | 1.1 | |
| | 18.8 | 3.5 | 2270 | 280 | 1800 | 23 | 75 | 2.1 | 85 | 0.9 | |
| | 23.1 | 3.2 | 2650 | 320 | 1420 | 16 | 69 | 3.0 | 103 | 0.9 | |

^a Formulation: elastomer, 100 parts; PBX, 0.66 phr; stearic acid, 1 phr; sulfur, 2 phr; ZnO, 5 phr; Neotex carbon black, 50 phr; Tellurac, 1.5 phr; red lead, 2 phr; NA-22, 1 phr; MgO, 2 phr. Cured at 310°F for 30 min.

^b At 212°F for 48 hr.

^c At room temperature for 24 hr.

Comparison of TCBO and ECH Vulcanizates

At comparable chlorine levels, ECH-PO-AGE terpolymers afford better overall properties than TCBO elastomers without taking into account the difference in the state of vulcanization, as shown in Table XI. The swelling in ASTM No. 3 oil at 212°C is in a range of 16–23% for ECH vulcanizates and 58–64% for TCBO vulcanizates. The swelling in a 50:50 mixture of benzene and cyclohexane at room temperature is 69–75% for ECH vulcanizates and 100–134% for TCBO vulcanizates. The swelling in MEK at room temperature is practically the same for both ECH and TCBO vulcanizates in the range of 85 and 120%. The differences in oil resistance between TCBO and ECH vulcanizates may be smaller than the values reported here if a better vulcanizing system is found for the TCBO elastomers.

Apparently, the even distribution of chlorine atoms throughout the macromolecules in polyepichlorohydrin elastomers gives better oil resistance than the CCl_3 group in the TCBO elastomers.

References

1. R. Dowbenko, *Tetrahedron*, **21**, 1647 (1965).
2. G. B. Payne, *J. Amer. Chem. Soc.*, **81**, 4901 (1959).
3. V. F. Martynov and A. V. Shchekunov, *J. Gen. Chem. (USSR)*, **27**, 1271 (1957).
4. W. J. Linn, O. W. Webster, and R. E. Benson, *J. Amer. Chem. Soc.*, **87**, 3651 (1965).
5. F. O. Pazschke, *J. Prakt. Chem.*, [2] **1**, 97 (1870).
6. W. Hartenstein, *J. Prakt. Chem.*, [2] **7**, 297 (1873).
7. M. E. Pruitt and J. M. Baggett (to the Dow Chemical Co.), U.S. Pat. 2,706,182 (April 12, 1965).
8. J. Furukawa, T. Tsuruta, R. Sakata, T. Saegusa, and A. Kawasaki, *Makromol. Chem.*, **20**, 90 (1959).
9. E. J. Vandenberg (to the Hercules Powder Co.), U.S. Pat. 3,135,705 (June 2, 1964).

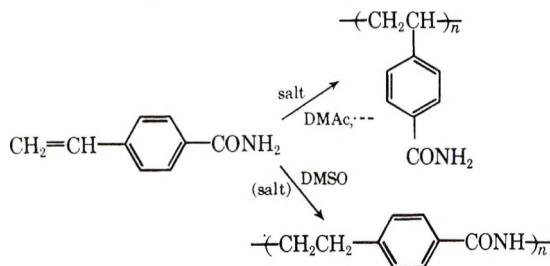
Received December 21, 1967

Salt Effect in the Base-Catalyzed Polymerization of Unsaturated Amide Compounds. II. Polymerization of *p*-Vinylbenzamide and Acrylamide*

TOMOHIKO ASAHARA and NAOYA YODA, *Basic Research
Laboratories, Toyo Rayon Company Ltd., Tebiro, Kamakura, Japan*

Synopsis

In the presence of a variety of inorganic salts, *p*-vinylbenzamide underwent vinyl-type polymerization by anionic initiators to form the polystyrene derivative, whereas in dimethyl sulfoxide as solvent the aromatic polyamide was always obtained through a proton-transfer mechanism regardless of the presence of the salts.



In the presence of of the salts, acrylamide is generally polymerized to the polyamide through a proton transfer reaction.

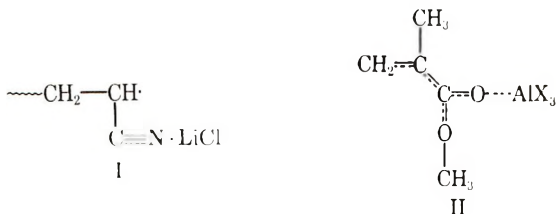
INTRODUCTION

Inorganic salts have widely played significant parts in radical²⁻⁴ or anionic⁵ polymerization of vinyl monomers, and also in polycondensation reactions.⁶

An attempt to elucidate the behavior of inorganic salts in these systems encountered the characteristic complexities of polymerization reactions, i.e., the very low concentration of active species or the small size of active sites as compared with the total length of a polymer chain. A thorough clarification of these systems will provide the precise mechanism of the interaction between polymerizing species and inorganic compounds, where the latter may act as "acceptor" as in the organic reactions involving transition metals.

* Presented at the Annual Meeting of Japan High Polymer Society, Tokyo, May 1967. For Part I see Asahara and Yoda.¹

Literature reveals that the coordination interaction takes place at the cyano group² or the ester group^{3,4} in the radical polymerization of vinyl monomers in the presence of metal halides.



No reaction occurs at the coordination site in these polymerizations. In anionic polymerizations of unsaturated amide monomers, however, the coordination of the inorganic salt occurs at the amide group where the proton is released in the proton-transfer reaction.



It is presumed therefore that the participation of the coordination plays a more important role between the monomer and the additive than in the ordinary catalytic vinyl polymerizations. Solvent may be another factor which should be taken into account. Organic polar solvents usually have active sites capable of coordination. Thus an ether oxygen atom of tetrahydrofuran acts as a Lewis base. In the coordination reaction, the monomer, solvent, and inorganic additive should be taken into consideration to interpret the orientation effect of the polymerization system. In this case either vinyl or proton transfer polymerization may occur.

In this paper, the authors wish to report the effect of inorganic additives on the proton transfer polymerization of vinyl amide monomers, which would shed light on the complex coordination involved in most of the catalytic polymerization systems.

RESULTS AND DISCUSSION

Base-Catalyzed Polymerization of *p*-Vinylbenzamide in the Absence of Inorganic Salts

Polymerization of *p*-vinylbenzamide (VBA) initiated by anionic catalysts has previously been reported to give aromatic polyamide.^{7,8} Extensive study of VBA polymerization in various solvents gave the results shown in Table I.

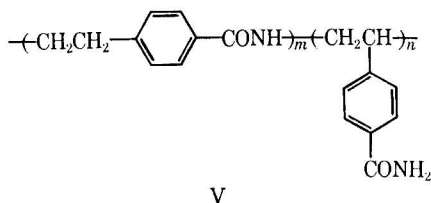
It was found that the reaction systems of an alkali alkoxide in a polar solvent are effective for the proton-transfer polymerization of VBA, and that pyridine as a solvent was not suitable for the polymerization of VBA contrary to the polymerization of acrylamide.⁹

TABLE I
Proton-Transfer Polymerization of *p*-Vinylbenzamide in Various Solvents in the Absence of Inorganic Salts

| Solvent | Solvent vol, ml | Monomer, mole $\times 10^3$ | Initiator | | Polymerization conditions, $^{\circ}\text{C}/\text{hr}$ | Polymer yield, % | η_{inh}^a |
|------------------------------------|-----------------------|-----------------------------------|--------------------|--------------------------------|---|------------------------|-----------------------|
| | | | Type | Concn, $\times 10^4$, mole | | | |
| <i>N</i> -Methylpyrrolidone | 8.0 | 8.23 | <i>n</i> -BuLi | 6.50 | 135/17 | 17.8 | 0.148 |
| <i>N,N</i> -Dimethyl- acetamide | 7.0 | 8.02 | <i>tert</i> -BuOCs | 1.88 | 130/21 | 91.5 | 0.126 |
| Hexamethylphos- phoramide | 8.0 | 5.98 | <i>tert</i> -BuOK | 3.62 | 135/16 | 86.3 | 0.157 |
| Dimethyl sulfoxide | 7.0 | 5.49 | <i>tert</i> -BuOCs | 2.17 | 135/15.5 | 81.2 | 0.158 |
| Pyridine | 5.0 | 3.24 | <i>n</i> -BuLi | 3.34 | 100/22 | trace | — |

^a In *m*-cresol, $c = 0.0050$ g/ml, 25.0°C .

By Kjeldahl analysis, the resulting polymer was determined to have about 90% polyamide structure with 10% polystyrene moiety as shown in structure V.¹



The existence of about 10% of the polystyrene type structure was also determined by infrared absorption of the resulting polymer at 1620 and 1565 cm^{-1} (shoulders) as shown in Figure 1.¹ These characteristic absorption bands appeared in the vinyl polymerization product as shown in Figure 2.

The polymerization systems were heterogeneous at the end of the polymerization as a result of precipitation of the insoluble proton-transfer polymer. However, the proton-transfer polymer is soluble in the presence of lithium chloride in these polar solvents except in pyridine. The polymer is also soluble in *m*-cresol and concentrated sulfuric acid without the lithium salt. The increase of solubility by the addition of the salt is presumably due to the bridged coordination to the metal cation both of the polymer chain and the solvent molecule.

Base-Catalyzed Polymerization of VBA in the Presence of Lithium Chloride

The addition of anhydrous lithium chloride to the VBA polymerization system caused the inhibition of the proton-transfer reaction and the con-



Fig. 1. Infrared spectrum of the proton transfer polymer of *p*-vinylbenzamide.

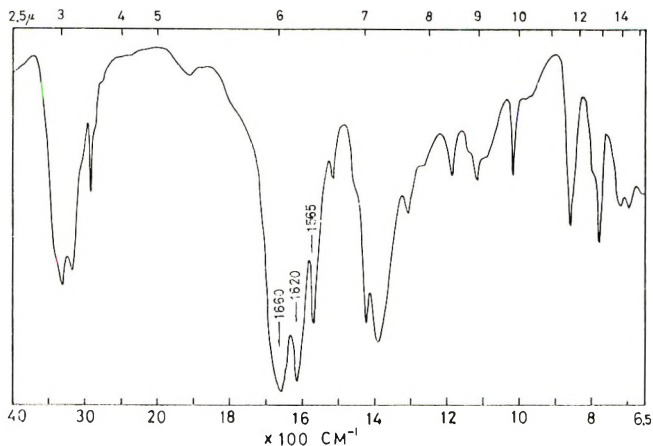


Fig. 2. Infrared spectrum of the VBA polymer obtained in the presence of lithium chloride.

siderable decreases of the polymer yield with any of basic initiators in *N*-methylpyrrolidone or *N,N*-dimethylacetamide as shown in Table II. The polymer structure was determined by the infrared spectra (Fig. 2) in comparison with those of the radical-initiated polymer.

The solvent effect of dimethyl sulfoxide in the presence of salt was remarkable in affording the proton-transfer polymer, as shown in Table III. It was reasonably presumed that the metal salt formed a coordination complex only with the dimethyl sulfoxide molecule without the formation of a complex with the monomer. The inhibition was probably caused by the coordination formation between the monomer and the salt, and at the same time the steric effect of the bulky phenyl group of the monomer may interfere the proton transfer reaction. A detailed discussion will be presented in a following paper.¹⁰

The effect of the amount of lithium chloride on the polymerization is shown in Figure 3. The polymer yield increased with the increase of the salt added, where the square root plots of the salt added versus polymer yield gave a linear relationship,² and the total amount of active species of the polymerization was shown to increase with the increase of the salt added. This effect is similar to the relation between the amount of an initiator and the yield of the polymer in radical-initiated polymerization. The linear relationship in this anionic polymerization shown in Figure 3 suggests the formation of some kinds of coordination complex with the propagating species.

The characteristic anionic feature of the polymerization was shown by the kinetic aspect of the salt-added polymerization (Fig. 4). The anionic mechanism was also supported by the data of the anionic copolymerization of VBA with *p*-styrenesulfonamide (SSA).¹¹ The copolymerization proceeded in two different fashions, depending on the conditions: poly(amide sulfonamide) was formed when the amount of basic catalyst was

TABLE II
 Polymerization of *p*-Vinylbenzamide in the Presence of LiCl and Various Initiators^a

| Initiator | | Monomer | | LiCl × 10 ³ , mole | Solvent ^b | Solvent vol, ml | Polymer yield, % | η_{inh}^c | Polymerization type |
|--------------------|--------------------------------------|-----------------------------|-----------------------------|-------------------------------------|----------------------|-----------------------|------------------------|----------------|------------------------|
| Type | Concn × 10 ⁴ , mole | × 10 ³ , mole | × 10 ³ , mole | | | | | | |
| <i>tert</i> -BuOLi | 2.36 | 7.24 | 7.36 | DMAc | 7.0 | 27.2 | 0.861 | vinyl | |
| <i>tert</i> -BuOK | 1.17 | 7.22 | 7.36 | DMAc | 7.0 | 32.9 | 0.583 | vinyl | |
| <i>tert</i> -BuOCs | 1.66 | 7.41 | 7.36 | DMAc | 7.0 | 63.2 | 0.618 | vinyl | |
| <i>n</i> -BuLi | 2.23 | 9.58 | 11.8 | NMP | 7.0 | 32.1 | 0.588 | vinyl | |

^a Polymerization conditions: 130°C/21 hr (130°C/24 hr for the last row).

^b DMAc; *N,N*-dimethylacetamide, NMP; *N*-methylpyrrolidone.

^c In *m*-cresol, *c* = 0.0050 g/ml, 25°C.

TABLE III
 Polymerization of VBA in Various Solvents in the Presence of LiCl and Basic Initiators

| Solvent ^a | Solvent vol, ml | Monomer × 10 ⁻³ , mole | Initiator | | LiCl × 10 ⁻³ , mole | Polymerization conditions °C/hr | Polymer yield, % | η_{inh}^b | Polymerization type |
|----------------------|-----------------------|---|--------------------|---------------------------------------|--------------------------------------|---------------------------------------|------------------------|----------------|-------------------------|
| | | | Type | Concn × 10 ⁻⁴ , mole | | | | | |
| NMP | 7.0 | 9.60 | <i>n</i> -BuLi | 2.23 | 11.76 | 130/24 | 32.1 | 0.588 | vinyl |
| HMPA | 3.0 | 2.36 | <i>tert</i> -BuONa | 2.15 | 1.92 | 120/20 | 18.2 | 0.784 | vinyl |
| DMAc | 7.0 | 7.06 | <i>tert</i> -BuOLi | 2.76 | 2.07 | 130/21 | 41.6 | 0.632 | vinyl |
| DMSO | 3.0 | 2.44 | <i>tert</i> -BuONa | 3.84 | 2.27 | 120/20 | 44.0 | 0.10 | H ⁺ transfer |
| Py ^c | 3.0 | 2.38 | <i>tert</i> -BuONa | 1.21 | 3.06 | 120/20 | 10.0 | — | vinyl |

^a HMPA; hexamethylphosphoramide, DMSO; dimethyl sulfoxide, Py; pyridine.

^b In concentrated H₂SO₄, *c* = 0.0050 g/ml, 25°C.

^c Polymer is insoluble in this solvent.

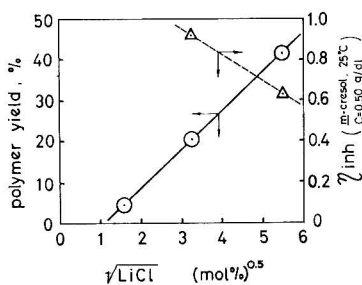


Fig. 3. Effect of the amount of added lithium chloride on (○) polymerization yield and (△) η_{inh} of polymer. Polymerization conditions: 7.0×10^{-3} mole monomer, 3.0×10^{-4} mole *tert*-BuOLi in *N,N*-dimethylacetamide (7.0 ml) at 130°C for 21 hr.

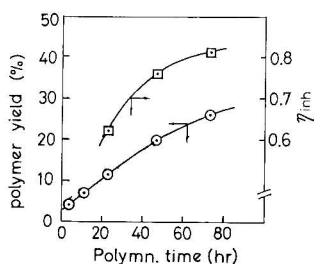
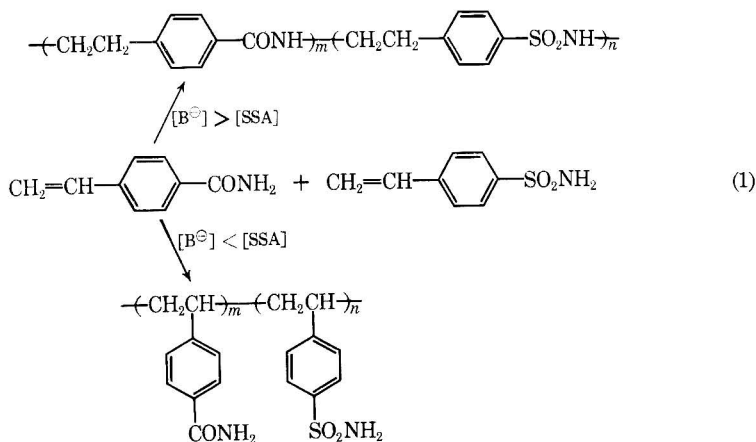


Fig. 4. Plots of (○) polymer yield and (□) η_{inh} as a function of the reaction time. Polymerization conditions: 6.0×10^{-3} mole monomer, 1.92×10^{-4} mole *n*-BuLi in *N,N*-dimethylacetamide at 135°C.

above that of SSA, whereas the copolymerization gave the polystyrene derivatives with a smaller amount of the basic catalyst than SSA, as shown in eq. (1).



Effect of Other Inorganic Salts

The addition of different metal salts led to similar results, as shown in Table IV.

TABLE IV
 Base-Catalyzed Polymerization^a of VBA in the Presence of Various Metal Salts

| Type | Salt | | Monomer, × 10 ³ , mole | System ^b | Polymer yield, % | η_{inh}^c | Polymer- ization type |
|-------------------|------|--------|---|---------------------|------------------------|----------------|-----------------------------|
| | Type | Mole-% | | | | | |
| CaCl ₂ | 29.2 | 2.27 | Heterogeneous | 12.3 | — | Vinyl | |
| CuCl ₂ | 29.0 | 2.40 | Homogeneous | 15.3 | — | Vinyl | |
| ZnCl ₂ | 29.6 | 2.33 | Heterogeneous | 14.0 | — | Vinyl | |
| CoCl ₂ | 30.4 | 2.27 | Heterogeneous | 21.6 | — | Vinyl | |
| HgCl ₂ | 29.9 | 3.35 | Homogeneous | 83.0 | 0.229 | Vinyl | |

^a Solvent, *N*-methylpyrrolidone, 3.0 ml; initiator, *n*-BuLi, 5.20×10^{-4} mole, polymerization conditions, 120°C/17 hr.

^b At the end of the polymerization

^c In concentrated H₂SO₄, *c* = 0.0050 g/ml, 25°C.

Since the salts are soluble in *N*-methylpyrrolidone, the systems at the initial stage were homogeneous. However, some of them became heterogeneous by precipitation of polymer by the interaction of the salt with polymer at the end of the polymerization. The inhibition of the proton-transfer reaction by these salts is presumably due to the formation of coordination complex as in the case of lithium chloride.

Polymerization of Acrylamide in the Presence of Lithium Chloride

The effect of lithium chloride on the polymerization of acrylamide is summarized in Table V.

The proton-transfer polymerization was not inhibited by the addition of the salt, and acrylamide–lithium chloride (1:1) complex was similarly polymerized by an anionic initiator. Decrease of the polymer yield in the polymerization of the 1:1 complex was presumably due to the moisture absorbed by the complex. The proportion of proton-transfer reaction was calculated to be about 90% by the infrared method reported by Nakayama et al.¹²

 TABLE V
 Polymerization of and Coordinated Acrylamide in Presence of
 Lithium Chloride^a

| Monomer | Monomer concn, mole | LiCl concn, mole | Polymer yield, % | η_{inh}^b | H ⁺ transfer, % ^c |
|-----------------------------|---------------------------|------------------------|------------------------|----------------|---|
| Acrylamide | 0.0197 | 0.0190 | 35.5 | 0.251 | 95 |
| Acrylamide– LiCl complex | 0.0202 | — | 8.6 | — | 86 |
| Acrylamide | 0.0191 | — | 100 | 0.622 | 90 |

^a Solvent, pyridine, 9.0 cc; initiator, *n*-BuLi, 5.52×10^{-4} mole; polymerization conditions, 116°C/19 hr.

^b In concentrated H₂SO₄, *c* = 0.0050 g/ml, 25°C.

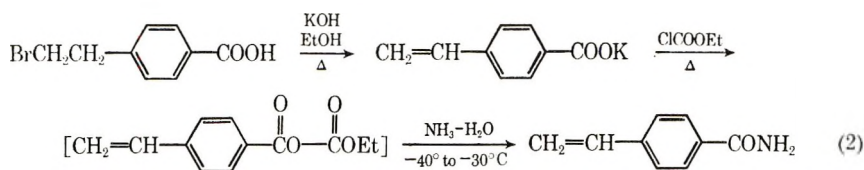
^c Calculation from the infrared spectra.¹²

It was concluded therefore that the salt effect was not observed in the base-catalyzed polymerization of acrylamide with lithium chloride. The ineffectiveness of lithium chloride suggests a poor interaction of the salt with the monomer, and some other mechanism of initiation and propagation steps should be considered for acrylamide polymerization than that of VBA polymerization.

EXPERIMENTAL

Materials

***p*-Vinylbenzamide.** The monomer was prepared by the route shown in eq. (2), starting from *p*-(2-bromoethyl)benzoic acid.¹³



A portion of 16.0 g (0.070 mole) of *p*-(2-bromoethyl)benzoic acid was added with stirring to the ice-cooled solution of 16.0 g (0.286 mole) of potassium hydroxide and a trace of hydroquinone in 200 ml of absolute ethanol. The resulting mixture was gradually heated to the gentle reflux and stirring was continued for 3 hr. The precipitated powder was filtered and washed twice with 50 ml of cold ethanol and dried *in vacuo*, yielding 20.3 g of product. About two thirds of the mixture was potassium *p*-vinylbenzoate and the rest was potassium bromide. The infrared spectrum (KBr pellet) of the product showed the existence of the vinyl (895, 985 cm^{-1}) and the carboxylate anion (1540, 1590 cm^{-1}) groups.

To a mixture of 60 g of the above product, a few drops of dry pyridine, and 150 ml of chloroform, was added at -40 to -30°C a solution of 37 g (0.34 mole) of ethyl chloroformate in 75 ml of chloroform; stirring was continued for an additional $\frac{1}{2}$ hr with cooling. The resulting precipitate was filtered off, and the filtrate was cooled to -70°C . It is then added dropwise to well-chilled 28% aqueous ammonia with satisfactory agitation. The product was filtered, washed twice with water, and dried. The yield was 16.5 g (55%); recrystallization from acetone gave colorless crystals, mp 170°C .

ANAL. Calcd: C, 73.43%; H, 6.18%; N, 9.52%; MW = 147.2. Found: C, 73.49%; H, 6.19%; N, 9.48%; MW, 149.5.

Acrylamide. Commercially available product was recrystallized from benzene, mp $83\text{--}84^\circ\text{C}$.

Lithium Chloride. Commercially available analytical grade reagent was dried under high vacuum at 200°C .

Other Inorganic Salts. Commercially available reagents were used without further purification.

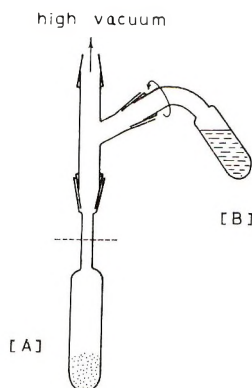


Fig. 5. Polymerization apparatus.

Butyllithium. A 15% hexane solution was obtained from Foote Chemicals Co. and the concentration was corrected by titration in each experiment.

Alkali Alkoxides. All were synthesized from the corresponding alkali metals and an excess of *tert*-butanol in the usual manner.

Monomer-Lithium Chloride Complex. The preparation methods are described in a following paper.¹⁰

Infrared Measurements

The spectra were obtained with KBr pellet in all cases.

Polymerization

Apparatus and Procedure. The apparatus shown in Figure 5 was used. The monomer, salt, and catalyst alkoxide were weighed in argon-filled ampule (A) in a dry nitrogen box. The solvent and the catalyst (in the case of *n*-BuLi catalyst) were introduced in the same manner in ampule B. The apparatus was connected to a high vacuum line, and the solvent was introduced into ampule A by inverting ampule B; liquid nitrogen cooling was used. Ampule A was sealed at the dotted line and allowed to stand at the polymerization temperature. After the polymerization, the mixture was poured into an excess of methanol and the precipitated polymer was filtered and dried under vacuum.

Determination of the Extent of Vinyl Type Polymerization. The proton transfer polymers were treated according to the analytical method reported by Nakayama et al.¹²

A 0.0779 g portion (5.30×10^{-4} mole) of proton-transfer polymer was hydrolyzed in 5 ml of 20% aqueous sodium hydroxide at 120–140°C. Liberated ammonia was absorbed in 1*N* hydrochloric acid. The resulting solution was diluted and titrated with 0.1*N* sodium hydroxide. The titration gave 5.30×10^{-5} mole ammonia liberation, which indicates that the polymer consists of 10% of the vinyl type and 90% of the proton trans-

fer structure. A 0.3590 g portion (24.4×10^{-4} mole) of the same sample was treated in the same manner and 21.1×10^{-3} mole (9.1%) of ammonia was formed. The value indicates the existence of 9.1% of the vinyl type polymer units.

The authors are deeply grateful to Dr. T. Hoshino for encouragement in the course of this work and permission for publication.

References

1. T. Asahara and N. Yoda, *J. Polymer Sci. B*, **4**, 921 (1966).
2. C. H. Bamford, A. D. Jenkins, and R. Johnston, *Proc. Roy. Soc. (London)*, **A241**, 365 (1957).
3. M. Imoto, Y. Otsu, and Y. Harada, *Makromol. Chem.*, **65**, 180 (1964).
4. V. F. Kulikova, I. V. Savinova, V. P. Zubov, V. A. Kabanov, L. S. Palak, and V. A. Kargin, *Vysokomol. Soedin.*, **A9**, 299 (1967).
5. W. E. Goode, F. H. Owens, R. P. Fellmann, W. H. Snyder, and J. E. Moore, *J. Polymer Sci.*, **46**, 317 (1960).
6. J. Preston, *J. Polymer Sci. A-1*, **4**, 529 (1966).
7. K. Kojima, N. Yoda, and C. S. Marvel, *J. Polymer Sci. A-1*, **4**, 1121 (1966).
8. S. Negishi and J. Tamura, *J. Polymer Sci. A-1*, **5**, 2911 (1967).
9. N. Ogata, *Bull. Chem. Soc. Japan*, **33**, 906 (1960).
10. T. Asahara, K. Ikeda, and N. Yoda, *J. Polymer Sci. A-1*, **6**, 2489 (1968).
11. T. Asahara, N. Yoda, H. Saito, and K. Nukada, *Kogyo Kagaku Zasshi*, **70**, 1974 (1967).
12. H. Nakayama, T. Higashimura, and S. Okamura, *Kobunshi Kagaku*, **23**, 433 (1966).
13. E. L. Foremann and S. M. McElvain, *J. Amer. Chem. Soc.*, **62**, 1435 (1940).

Received December 6, 1967

Revised January 16, 1968

Salt Effect in the Base-Catalyzed Polymerization of Unsaturated Amide Compounds. III. Nature of the Polymerization System*

TOMOHIKO ASAHARA, KOJURO IKEDA, and NAOYA YODA,
*Basic Research Laboratories, Toyo Rayon Company Ltd., Tebira,
Kaniakura, Japan*

Synopsis

Coordination complexes of lithium chloride with polar solvents and monomers were isolated, and their physical properties were studied. The parallel between stabilities of isolated complexes and coordination function in the polymerization system is discussed. The increase of the Q and e values of *p*-vinylbenzamide (VBA) supports the mechanism of vinyl-type polymerization of VBA in the presence of the salt. The specific solvent effect of dimethyl sulfoxide was determined by measurement of electrical conductivity of a model system.

INTRODUCTION

Addition of some metal halides to the polymerization system of *p*-vinylbenzamide or acrylamide in a basic medium was found to produce a variety of interesting effects on the orientation of polymerization reactions. It was reported in the preceding paper¹ that, when dimethyl sulfoxide was employed as solvent, the effect of the added salt disappeared in the base-catalyzed polymerization of *p*-vinylbenzamide. In these polymerization systems, both the solvent and the monomer are electron donors and only the metal cation is an acceptor. Therefore the both solvent-salt and monomer-salt coordination complexes should be taken into consideration.

In this paper, we wish to report the successful isolation of coordination complexes which are presumably formed in the polymerization system and to describe the characterization of those complexes by physical measurements. The increased Q and e values of the salt-coordinated VBA were consistent with the increase of the vinyl type of polymerizability of the monomer in the presence of inorganic salts. The electrical conductivity data for the model systems explain the specific effect of dimethyl sulfoxide as solvent in these polymerization. The complex of dimethyl sulfoxide with lithium cation was found to be the strongest among a variety of polar solvents. Inhibition of proton transfer polymerization was observed

*Presented at the Symposium on High Polymers, Japan, Fukuoka, Oct. 19-21, 1967.

when VBA-metal salt coordination occurred with considerable infrared shift of the corresponding stretching absorptions.

RESULTS AND DISCUSSION

Stability of the Coordination Complex of Lithium Chloride with the Solvent

As reported in the preceding paper,¹ a marked solvent effect of dimethyl sulfoxide was observed in the polymerization of VBA in the presence of lithium chloride where the polymerization proceeded through the proton-transfer mechanism even in the presence of the inorganic salt. This fact suggests that the action of lithium chloride on VBA was obstructed by the "trapping" of the metal cation by the solvent. On the contrary, in the base-catalyzed polymerization of acrylamide, the orientation of the polymerization reaction was not affected by the addition of the salts. It was therefore reasonably presumed that some type of coordination complex was formed in the course of the polymerization, which selectively determined the orientation of the reaction.

The stability of the coordination complex in the polymerization system should certainly parallel that of the isolated coordination complex of the same components. In other words, the most stable coordination is formed preferentially, or the concentration of the most stable one may be the highest in the reaction system; this is fully supported by the following experimental data.

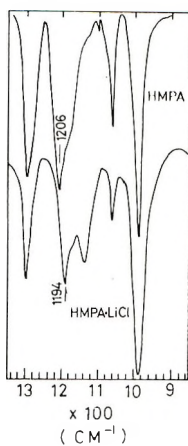
TABLE I
Solvent-Lithium Chloride Coordination Complexes

| Coordination Complex | mp, °C | Infrared data | | | |
|----------------------|---------|---|-----------------------------------|-----------------------------|--|
| | | $\nu_{C=O}$, $\nu_{S \rightarrow O}$, $\nu_{P \rightarrow O}$, cm ^{-1,a} | $\Delta\nu$, cm ⁻¹ | -100 ($\Delta\nu/\nu$) | ν_{blank} , ¹ cm ^{-1b} |
| DMSO-LiCl | 189 | 1013 | -42 | 3.98 | 1055 |
| NMP-LiCl | 123-124 | 1642 | -43 | 2.55 | 1685 |
| DMAc-LiCl | 116-117 | 1610 | -37 | 2.24 | 1647 |
| HMPA-LiCl | 56-57 | 1194 | -12 | 1.00 | 1206 |

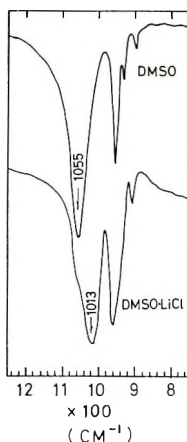
^a Measured as KBr disk.

^b Measured as liquid film.

A variety of coordination complexes of lithium chloride with various solvents were isolated as crystals, and their physical properties were characterized as shown in Table I. Infrared spectra of the solvent-LiCl complexes are shown in Figure 1. The considerable shift of carbonyl, sulfoxide, and phosphine oxide stretching absorptions suggests that coordination of the solvent with the inorganic salt takes place on the lone pair electrons in the same fashion as in the cases of the dimethylformamide (DMF)-LiCl and



(a)



(b)

Fig. 1. Infrared spectra of the solvent-LiCl complexes: (a) HMPA-LiCl complex; (b) DMSO-LiCl complex.

dimethyl sulfoxide (DMSO)-CoCl₂ systems reported in the literature.^{2,3}

The stability of compounds may generally be discussed in terms of the melting temperature. The melting point (189°C) of DMSO-LiCl was the highest in these complexes (Table I), and therefore it was concluded that DMSO-LiCl is the most stable coordination in the polymerization system. It is noteworthy to point out that solvents such as hexamethyl phosphoramide (HMPA), dimethylacetamide (DMAc), and *N*-methylpyrrolidone (NMP) in which the proton transfer polymerization of VBA was inhibited by the addition of lithium salt gave the complexes of considerable low melting point. The fact informs that stabilities of these solvent (HMPA, DMAc, NMP)-lithium chloride complexes are also low in the polymerization system.

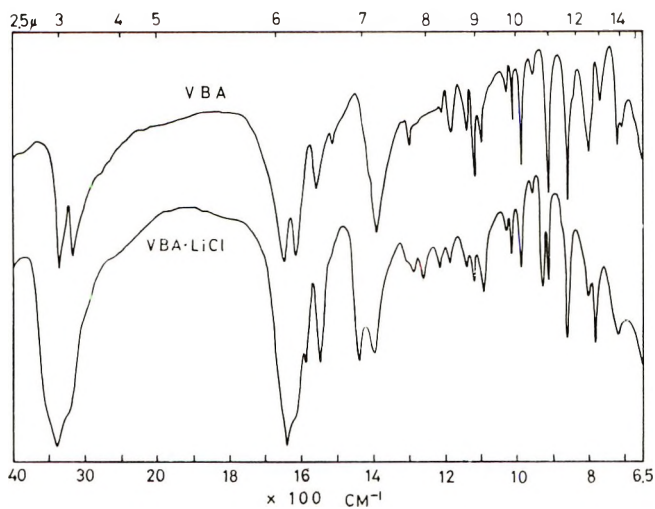


Fig. 2. Infrared spectra of VBA-LiCl complex and free VBA.

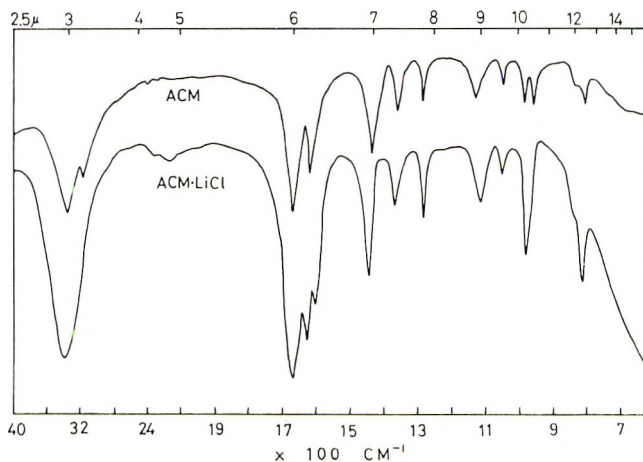


Fig. 3. Infrared spectra of ACM-LiCl complex and free ACM.

Coordination Complexes of LiCl with the Monomer

In order to compare the stabilities of coordination complexes between components in the polymerization system, coordination complexes were prepared with *p*-vinylbenzamide and acrylamide (ACM), and the melting point and the infrared spectrum were measured (Figs. 2 and 3 and Table II). Notable changes in infrared spectrum are observed for the VBA-LiCl complexes; the carbonyl stretching frequency shifted downward and some bands disappeared at 3150 and 1620 cm^{-1} . However, none of the change was observed in the absorptions of the vinyl hydrogens at 912 and 987

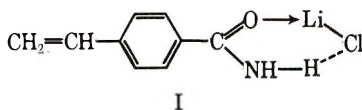
TABLE II
Physical Properties and Infrared Spectra of Coordination Complexes of Monomer-Lithium Chloride

| Coordination complex | mp, °C | Infrared data | | | Reference ν_{blank} , cm ⁻¹ |
|----------------------|-----------|--|-----------------------------------|------------------------|---|
| | | $\nu_{\text{C=O}}$, cm ⁻¹ | $\Delta\nu$, cm ⁻¹ | $-100 (\Delta\nu/\nu)$ | |
| VBA-LiCl | 320-325 | 1639 ^a | -11 | 0.67 | 1650 ^a |
| ACM-LiCl | 285-290 | 1666 ^a | 0 | 0 | 1666 ^a |
| CPL-LiCl | 81.5-82.5 | 1629 ^a | -31 | 1.87 | 1660 ^b |

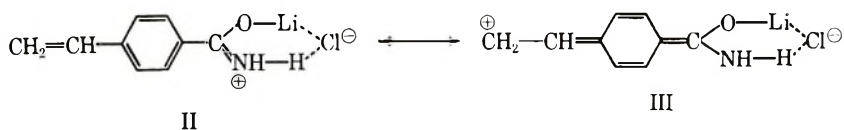
^a Measured as KBr disk.

^b Measured as Nujol mull.

cm⁻¹. These data indicated that the coordination occurs at the carbonyl oxygen by the nonbonding electrons as shown in I.



The disappearance of absorption bands at both 3150 and 1620 cm⁻¹ should be related to the amide hydrogen atoms: the former was ascribed to the inhibition of the symmetrical stretching vibration and the latter to the restriction of the deformation. Consequently, the two hydrogen atoms of the amide group are thoroughly stabilized by the formation of the hydrogen bonding of the six-membered ring, while the hydrogen atoms of the free amide group are reactive to basic species by the static repulsion; at the same time the conjugation increases to give the following structural contribution in II and III:



The acrylamide-lithium chloride complex showed no detectable change at the carbonyl-stretching frequency. Although the carbonyl frequency is not shifted in this case, nonetheless the infrared spectrum of acrylamide-LiCl is different from that of acrylamide, indicating complex formation. Such a weak interaction between the monomer and the salt possibly has no apparent effect on the orientation of the polymerization except for a decrease of the polymer yield.

Relative Stability of the Coordination Complexes of the Solvent and the Monomer with Lithium Chloride

In addition to the stability of the solvent-salt complexes mentioned above, a general treatment of the relative stabilities on the solvent-salt and the monomer-salt coordination will be discussed in this section.

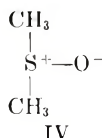
The melting point of the complex is not always a satisfactory clue for comparing the above two coordinations, because of differences in physical properties and structure of the components.

It was established that the infrared stretching shifts have a good correlation with the melting points in these solvent-salt complexes as shown in Table I. Also the polymerizability of the two monomers reported in the preceding paper¹ showed close correlations with the infrared shift in the monomer-salt complex. Therefore the infrared stretching shift of the nearest bond from the coordination site, as determined by $-100\Delta\nu/\nu$, may reasonably be applied for the stability of the complex as a general index. The following order of the stabilities was obtained for the coordination by using the infrared indexes in Tables I and II:



In this case a slight modification is necessary to interpret the experimental results according to the phase of the sample of infrared measurement. Infrared spectra of free VBA and ACM monomer were obtained as the KBr disks. When infrared measurements were made on liquid monomers, the absorption appeared at higher frequencies, so the magnitude of the shift would be larger. Hence the stability of VBA complex with the salt would be close to those of the NMP or DMAc complexes, because it is reasonable to assume that the polarities of primary and tertiary amide groups are almost similar.

The strongest coordination of DMSO to the salt is supported by the high polarity of the sulfoxide group (IV).



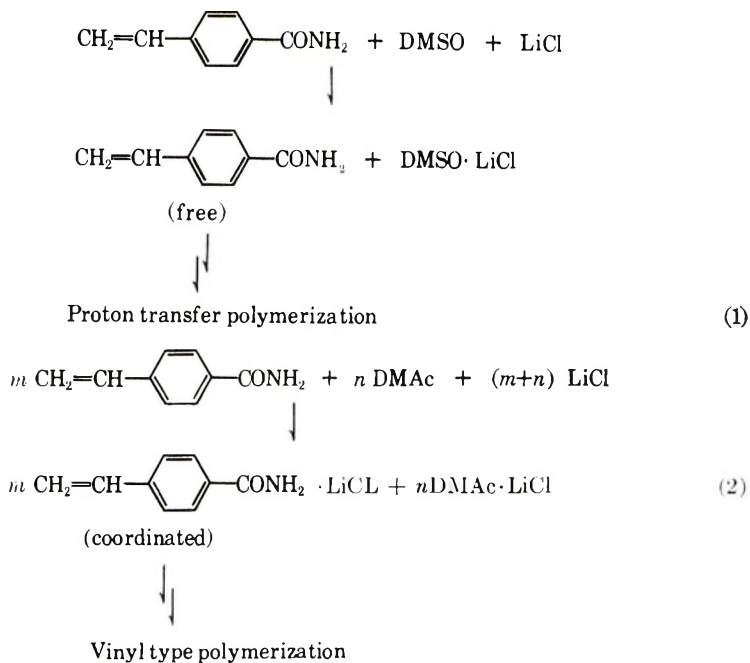
Based on these results, the coordination relations in the polymerization system are illustrated as shown in eqs. (1) and (2) where lithium chloride is coordinated with the strongest donor involved in the polymerization system.

TABLE III
Relative Conductivities of Solvent-LiCl Systems
in the Presence of Benzamide, $\text{C}_6\text{H}_5\text{CONH}_2$

| Solvent | Conductivity $\times 10^3$, $\text{ohm}^{-1} \text{cm}^{-1}$ | |
|---------|---|-------------------------------------|
| | Solvent-LiCl ^a | Solvent-LiCl-benzamide ^b |
| DMSO | 3.78 | 3.78 |
| DMAc | 2.75 | 2.50 |
| NMP | 1.56 | 1.44 |
| HMPA | 1.44 | 1.25 |

^a $[\text{LiCl}] = 0.353 \text{ mole/l.}$

^b $[\text{LiCl}] = 0.353 \text{ mole/l.}, [\text{benzamide}] = 0.331 \text{ mole/l.}$



Electrical Conductivity of a Model System

The formation of the strongest coordination of DMSO was also determined by the electrical conductivity measurement as shown in Table III, where the specific conductances of the systems with DMAc, NMP, and HMPA as solvents decreased with the addition of equimolar amounts of the monomer model compound. On the contrary, the conductance was found to be constant in the system with DMSO. The decrease was effected by the partial transfer of lithium chloride from the solvent molecule to benzamide which is a little weaker ligand; in the DMSO system, however, lithium salt transfer to form a weaker coordination by the addition of benzamide should not occur [eq. (3)].



Consequently, the coordination complex between DMSO and lithium salt is so strong that it does not easily dissociate in the polymerization system.

Q and e Values of VBA in the Presence of the Salt

The polarity of the vinyl group in VBA probably increases with the addition of the coordinating salt by the contribution of III. At the same time, the increase of conjugation may result in a change in *Q* value of the monomer. It was reasonably expected, therefore, that the copolymerization data of VBA with styrene in the absence and presence of lithium

chloride manifested the increase of Q and e values in the presence of the salt.⁴

The Q and e values in the absence of the salt were obtained by a Fineman-Ross plot of the radical copolymerization experiment (Table IV). Table V shows the result of copolymerization of VBA with styrene in the presence an equimolar amount of lithium chloride. The Q and e values were obtained as described in Table VI by the copolymerization data, where the great increase of Q and e values demonstrated the effect represented by structure III.

Spectroscopic studies by Ellul and Moodie⁵ also favored the contribution of the structure III to the complexes of substituted benzamide with boron trifluoride.

TABLE IV
Radical Copolymerization of Styrene (M_1) and
VBA (M_2) in the Absence of the Salt^a

| Polymerization time, hr | $[M_1]$ $\times 10^{-3}$, mole/l | $[M_2]$ $\times 10^{-3}$, mole/l | $[M_1]/$ $[M_2]$ | N in co- copolymer % | $d[M_1]/$ $d[M_2]$ |
|----------------------------|---|---|---------------------|----------------------------|-----------------------|
| 100 | 3.31 | 2.10 | 1.58 | 4.3 ₁ | 1.73 |
| 50 | 3.65 | 1.83 | 1.99 | 4.3 ₂ | 0.79 |
| 50 | 3.92 | 1.54 | 2.55 | 4.2 ₁ | 1.76 |
| 1170 | 4.67 | 0.79 | 5.91 | 2.2 ₃ | 4.48 |
| 1170 | 4.91 | 0.55 | 8.91 | 1.9 ₂ | 5.66 |

^a Initiator, azobisisobutyronitrile 0.0160 g; solvent, tetrahydrofuran 5.0 ml; 100°C.

TABLE V
Anionic Copolymerization of Styrene(M_1) and
VBA(M_2) in the Presence of Lithium Chloride^a

| $[M_1]$ $\times 10^{-3}$, mole/l | $[M_2]$ $\times 10^{-3}$, mole/l | $[LiCl]$ $\times 10^{-3}$, mole/l | $[Cat]$ $\times 10^{-4}$, mole/l | $[M_1]/$ $[M_2]$ | N in co- polymer, % | $d[M_1]/$ $d[M_2]$ |
|---|---|--|---|---------------------|---------------------------|-----------------------|
| 0.46 | 2.58 | 2.59 | 3.60 | 0.177 | 8.8 ₂ | 0.115 |
| 0.93 | 2.12 | 2.10 | 3.60 | 0.438 | 8.3 ₅ | 0.212 |
| 1.34 | 1.67 | 1.68 | 3.60 | 0.800 | 7.7 | 0.343 |
| 1.55 | 1.47 | 1.55 | 9.70 | 1.04 | 7.2 | 0.460 |

^a Catalyst, *n*-BuLi; solvent, DMAc, 3.0 ml; 100°C for 16 hr.

TABLE VI
 Q and e Values in the Free and Coordinated Monomer^a

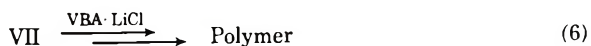
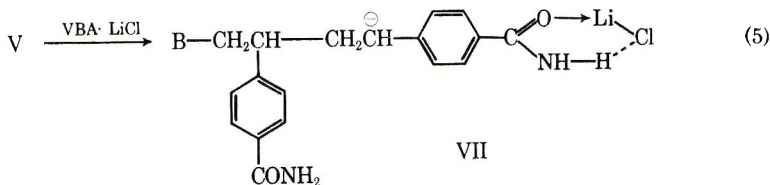
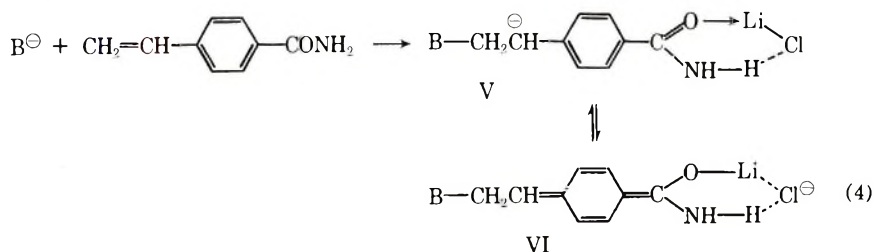
| Monomer ^b | r_1 | r_2 | Q_2 | e_2 |
|-------------------------------|-------|-------|-------|-------|
| <i>p</i> -Vinylbenzamide | 0.47 | 1.0 | 1.0 | +0.1 |
| <i>p</i> -Vinylbenzamide-LiCl | 0.10 | 1.6 | 3.4 | +0.6 |

^a Assuming $Q_1 = 1.0$, $e_2 = -0.8$ in styrene.

^b $M_1 =$ styrene, $M_2 =$ *p*-vinylbenzamide.

Proposed Polymerization Mechanism

The catalyst activity is decreased by tight coordination of the salt to a basic site, as in the formation of a complex between lithium chloride and an ether oxygen.⁶ Therefore the proton abstraction from the amide group by the initiator to form the amide anion leading to proton transfer polymerization is presumably impossible. The polymerization is forced to start with the nucleophilic addition of the catalyst species to the vinyl group of the coordinated monomer as shown in eq. (4), since the polarity of the vinyl group is enhanced by the coordination of lithium chloride. The anion V is stabilized by the contribution of the resonance forms V and VI which can not abstract the amide proton either by an intramolecular or intermolecular mechanism (for the transfer polymerization) because of the decrease of basicity of the carbanion $-\text{CH}_2\text{CH}-\text{C}_6\text{H}_4-$. At the same time, the amide hydrogen atom is stabilized by hydrogen bonding with chlorine to form a six-membered ring system. Therefore the carbanion V is forced to add to another monomer at the vinyl group [eq. (5)] in which the polarity increased, to afford the anion VII. Each active end is similarly stabilized as in V and can hardly proceed to the proton transfer polymerization. About 10% of the proton transfer structure does occur in the polymerization. A more detailed investigation is necessary to clarify the complete mechanism.



EXPERIMENTAL

Materials

Monomers. *p*-Vinylbenzamide, acrylamide, and lithium chloride were from the same sources as in the preceding paper.¹

Commercially available styrene was distilled in a high vacuum system just before use.

TABLE VII
Solvent-Salt Complexes

| | Cl, % | |
|-----------|-------|---------------------|
| | Found | Calcd. ^a |
| DMSO-LiCl | 27.2 | 29.4 |
| NMP-LiCl | 25.7 | 25.1 |
| DMAc-LiCl | 26.7 | 27.1 |
| HMPA-LiCl | 16.0 | 16.0 |

^a As 1:1 components.

Lithium Chloride Complexes with Polar Solvents. Complexes with dimethyl sulfoxide, *N*-methylpyrrolidone, and *N,N*-dimethylacetamide were prepared by slow cooling of the corresponding concentrated solution of the salt in the dry solvent. Being extremely hygroscopic, the precipitated crystals were filtered under dry nitrogen in a glove box, washed twice with dry benzene or ether, and dried in vacuum.

The coordination complex with hexamethylphosphoramide (HMPA) was obtained by the treatment of a 1:2 molar mixture of lithium chloride and HMPA with strong heating. Excess solvent was filtered, and the resulting crystals was washed twice with dry ether. Analytical data are given in Table VII.

Monomer-lithium chloride complexes. A mixture of 0.020 g (4.71×10^{-4} mole) of anhydrous lithium chloride and 0.069 g (4.70×10^{-4} mole) of *p*-vinylbenzamide in 6 ml of tetrahydrofuran was moderately heated. The excess solvent was gradually evaporated under vacuum to leave a crystalline substance. The product was dried at 80°C for 1 hr under vacuum.

Acrylamide-lithium chloride complex was isolated by slow cooling of a solution of ca. 7% lithium chloride and 30% monomer in acetone. The product was washed several times with cold acetone. An ϵ -caprolactam (CPL)-LiCl complex was synthesized similarly by using an equimolar amount of ϵ -caprolactam. Analyses of the complexes are summarized in Table VIII.

Copolymerizations

Copolymerization in the Absence of the Salt. The same apparatus was used as in Part II.¹

TABLE VIII
Monomer-Salt Complexes

| | Cl, % | |
|----------|-------|-------|
| | Found | Calcd |
| VBA-LiCl | 16.7 | 18.7 |
| ACM-LiCl | 31.0 | 31.3 |
| CPL-LiCl | 22.8 | 22.8 |

p-Vinylbenzamide, styrene, and azobisisobutyronitrile were weighed into an argon-filled ampule (see Part II) in a dry nitrogen box. The ampule was connected to a high vacuum line and evacuated with liquid nitrogen cooling, and tetrahydrofuran was introduced. The sealed ampule was kept at the prescribed temperature. The copolymer was obtained by filtering after pouring the mixture into methanol. The polymer composition was calculated by nitrogen analysis of the polymer.

Copolymerization in the Presence of Lithium Chloride. Two monomers and the salt were weighed similarly. A solution of *n*-BuLi in dimethylacetamide was prepared and introduced into the polymerization ampoule as in the previous run. The copolymer was obtained by a similar method, washed with dry benzene, and dried in vacuum.

Electrical Conductivity Measurements

This measurement was carried out with the usual apparatus with the use of a 1000 cps sine wave, where the cell constant was determined by using standard aqueous sodium chloride solutions of different concentrations.

Infrared Spectroscopy

The spectra were obtained on Hitachi EPI-S2 and Shimadzu IR-27 spectrometers. All of the absorption frequencies were corrected against the absorption of polystyrene.

The authors wish to thank Drs. T. Hoshino and R. Nakanishi for their encouragement during the course of the work and for the permission to publish the results. The authors are deeply indebted to Mr. Y. Ebata, Mr. T. Midzushima, and collaborators for their analytical work.

References

1. T. Asahara and N. Yoda, *J. Polym. Sci. A-1*, in **6**, 2477 (1968).
2. F. Madaule-Auby, *Bull. Soc. Chim. France*, **1966**, 1456.
3. F. A. Cotton and R. Francis, *J. Amer. Chem. Soc.*, **82**, 2986 (1960).
4. M. Imoto, T. Otsu, and Y. Harada, *Makromol. Chem.*, **65**, 180 (1964).
5. B. M. J. Ellul and R. B. Moodie, *J. Chem. Soc.*, **1967**, 253.
6. F. Durant, Y. Gobillon, P. Piret, and M. Van Merssche, *Bull. Soc. Chim. Belg.*, **75**, 52 (1966).

Received December 16, 1967

Revised February 2, 1968

Grafting of Monosaccharide Derivatives to Cellulose Acetate*

ROY L. WHISTLER, GUGLIELMO RUFFINI, and RICHARD E. PYLER, *Department of Biochemistry, Purdue Agricultural Experiment Station, Purdue University, Lafayette, Indiana 47907*

We are pleased to dedicate this paper to Dr. E. Husemann on her 60th Anniversary. This paper with those from others will show in small part the high esteem we have regarded Dr. Husemann the scientist and Dr. Husemann the person.

Synopsis

Grafting of 1,2-*O*-isopropylidene- α -D-xylofuranose to commercial cellulose diacetate has been accomplished by using a boron trifluoride catalyst. The reaction proceeds quickly at 25 and 40°C, resulting in degrees of molar substitution (MS) of 0.37 and 0.34, respectively. If monomer and catalyst are added over an extended period of time to maintain low concentrations, MS values as high as 0.89 and 0.85 are obtained at 25 and 40°C, respectively. Major side reactions are depolymerization of the cellulose acetate backbone and grafted D-xylose and the homopolymerization of the monomer. These side reactions may be minimized by conducting the reaction at 40°C for a short time or by adding monomer and catalyst over an extended period of time. Grafting has also been accomplished by using D-xylose derivatives with various reactive groups at the anomeric carbon atom. The grafted material of MS greater than 0.7 is insoluble in acetone and after deacetylation is soluble in water under alkaline, neutral and acidic conditions. Oxalic acid hydrolysis of the deacetylated material indicates that most of the grafted D-xylose units are in the furanose form. Methylation and hydrolysis of the methylated material shows that 75% of the D-xylose residues are terminal units and indicates the presence of many singly grafted D-xylose residues and a few di- and trisaccharide grafts.

INTRODUCTION

Facile opening of the 1,3-dioxolane ring in 1,2-*O*-isopropylidene sugar derivatives with Lewis acids results in the formation of a carbonium ion at carbon C₁ of the sugar which makes these compounds potential derivatizing agents for polysaccharides. This laboratory has already shown¹ that 1,2-*O*-isopropylidene derivatives of D-glucose undergo polymerization in the presence of Lewis acids to produce branched glucans.

The methyl groups attached to the methylenic carbon of the 1,3-dioxolane ring release electrons to the ring oxygens and give the latter sufficient

* Presented in part at the 152nd National Meeting of the American Chemical Society, New York, N. Y., September 1966.

negativity to preferentially complex with the Lewis acid. This ring may then open to produce a partially stabilized carbonium ion at the sugar anomeric position which in turn leads to reaction with available hydroxyl groups to form *D*-glucosidic bonds. Opening of the complexed 1,3-dioxolane through displacement at carbon C₁ by a hydroxyl group can lead to *D*-glucoside formation, but evidence favors the carbonium ion intermediate.¹ Bretschneider and Beran² have prepared aryl glycosides by reacting 1,2,3-, 4,6-penta-*O*-acetyl- β -*D*-glucopyranose with a phenol and boron trifluoride. Further, Bonner and co-workers³ reacted a methyl α -*D*-glucopyranoside-boron trichloride complex with alcohols to produce new *D*-glucosides.

The present work describes the reaction of 1,2-mono-*O*-isopropylidene- α -*D*-xylofuranose with commercial cellulose acetate. This polysaccharide was chosen since maximum grafting of a monomer to a polymer will proceed most efficiently and uniformly in a homogeneous reaction mixture. Both the polysaccharide acetate and the monomer are soluble in similar solvents and particularly in methylene chloride, which is a preferred solvent because it does not react with Lewis acids.

EXPERIMENTAL

Materials

Commercial cellulose acetate with an acetyl degree of substitution (DS) of 2.33 was ground slightly in a mortar and dried at 40°C for 48 hr under reduced pressure. Analysis showed it to contain 15 primary hydroxyl groups per 100 *D*-glucose units. The molecule had a degree of polymerization (DP) of 262.

1,2-*O*-Isopropylidene- α -*D*-xylofuranose was prepared according to standard procedure⁴ and was purified by vacuum distillation, mp 70–71°C. It was converted to 3,5-di-*O*-acetyl-1,2-*O*-isopropylidene- α -*D*-xylofuranose by acetylation in pyridine and acetic anhydride,⁴ bp 121–126°C/0.1 mm. 1,2:5,6-Di-*O*-isopropylidene- α -*D*-glucofuranose⁵ was purified by two recrystallizations from petroleum ether (bp 60–80°C), mp 110°C. 1,2-*O*-Isopropylidene- α -*D*-glucofuranose was prepared as described by Whistler and co-workers⁶ and was purified by two recrystallizations from ethyl acetate, mp 160–161°C. It was acetylated in pyridine and acetic anhydride⁷ to form 3,4,6-tri-*O*-acetyl-1,2-*O*-isopropylidene- α -*D*-glucofuranose, mp 75°C. 2,3,4-Tri-*O*-acetyl-1,6-anhydro-*D*-glucopyranose was prepared according to the procedure of Ward,⁵ mp 109–110°C. 3,4,6-Tri-*O*-acetyl-1,2-anhydro-*D*-glucopyranose was prepared according to standard procedure,⁵ mp 58–59°C.

Methyl α , β -*D*-xylopyranoside was prepared by treatment of dry *D*-xylose with absolute methanol in the presence of dry IR-120 resin (H⁺ form) under reflux for 48 hr. The reaction mixture was filtered and concentrated to a syrup. The α -*D*-form crystallized and was chromatographically pure.

Methylene chloride was dried over calcium chloride. Boron trifluoride etherate was purified by distillation.⁸

Methods

Melting points were determined on a Fisher-Johns apparatus and are corrected. Thin layer chromatography was conducted on 5×13 mm plates coated with silica gel G. Paper chromatography was conducted on Whatman No. 1 paper at 25°C with ethyl acetate, pyridine, and water (25:7:8 v/v) as irrigant. Chromatograms were sprayed with aniline acid phthalate and heated at 110°C for 5 min.

Grafting reactions were conducted in closed containers at 25 and 40°C . Cellulose acetate and monomer were suspended in an appropriate amount of methylene chloride at 25°C and stirred to allow the monomer to dissolve and the polysaccharide to swell. An appropriate amount of boron trifluoride etherate was added by means of a syringe and the reaction allowed to proceed with constant stirring. In another series of reactions, boron trifluoride in methylene chloride and monomer in methylene chloride were added simultaneously and dropwise to cellulose acetate suspended methylene chloride.

The grafted material was isolated by concentrating the reaction mixture to dryness under reduced pressure at 40°C . Homopolymer was removed by washing the solid residue with water. After filtration on a tared, sintered glass funnel, the residue was dried under reduced pressure at 50°C . When the monomer was not water-soluble, the solid residue was also washed with ethyl ether or acetone.

Homopolymer was isolated from the water washings after neutralization with IR-45 resin (OH^- form) and concentration of the filtrate to dryness under reduced pressure. Homopolymer could also be precipitated from a concentrated solution with acetone.

Characterization of Grafted Polymers

The acetyl content of cellulose acetate and grafted material was determined on 100 mg samples dissolved or suspended in 20 ml of absolute acetone at 25°C . A 15 ml portion of 0.5*N* sodium hydroxide solution was added by means of a buret, and the suspension was heated at $60\text{--}70^{\circ}\text{C}$ for 15 min. After standing 1 hr at 25°C the residual sodium hydroxide was titrated with 0.5*N* hydrochloric acid solution. A reagent blank was titrated concurrently.

The degree of molar substitution (MS) of the grafted material was calculated both by weight increases and by acid hydrolysis followed by quantitative paper chromatography. For hydrolysis, 100 mg samples were dissolved in 72% sulfuric acid and allowed to stand overnight. The solution was diluted to 4% acid and hydrolysis continued at 100°C for 4 hr. Hydrolyzates were neutralized with IR-45 resin (OH^- form) and filtered. The resin was washed with small volumes of deionized water and the combined filtrate and washings were concentrated to dryness under reduced pressure; 1 ml of deionized water was added and appropriate aliquots were transferred to Whatman No. 1 paper by means of micropipets. After

development of the chromatograms and spraying with aniline acid phthalate, the quantitative determination was made as described by Wolfrom and co-workers.⁹

The primary hydroxyl content of cellulose acetate and grafted material was measured by the standard procedure with the use of triphenylmethyl chloride.¹⁰

Initial methylation followed standard procedure.¹¹ A 500 mg portion of the partially methylated polymer was treated four times in DMF with 1 ml of methyl iodide and 0.38 g of sodium hydride for 2 hr. Sodium hydride was added to the reaction mixture in small portions at 0°C over a period of 20 min. Excess sodium hydride was destroyed by pouring the reaction mixture into 100 ml of water containing 15 g of sodium chloride. After extraction of the water solution with chloroform and drying over sodium sulfate, the extract was concentrated to dryness under reduced pressure at 70°C. The residue was dissolved in 10 ml of chloroform, and 200 ml of petroleum ether was added. The precipitate was filtered, washed with petroleum ether, and dried. The infrared spectrum showed no hydroxyl absorption at 3500–3600 cm^{-1} .

A 100 mg portion of the completely methylated polymer was refluxed in 20 ml of methanol containing 4% hydrochloric acid for 36 hr, concentrated to dryness under reduced pressure, and hydrolyzed for 8 hr at 100°C in 10 ml of 2*N* sulfuric acid. After neutralization with IR-45 resin (OH⁻ form), the solution was extracted with chloroform and examined by thin-layer chromatography with chloroform and methanol (4:1 v/v). Flow rates were compared with authentic samples of 2,3,4-tri-*O*-methyl and 2,3,5-tri-*O*-methyl-*D*-xylose; and 2,3-di-*O*-methyl and 2,3,6-tri-*O*-methyl-*D*-glucose.

Another sample of completely methylated polymer was hydrolyzed with 3% hydrochloric acid in methanol for 36 hr under reflux. Thin-layer chromatography of the completely methylated sugars was carried out by using ethyl ether and toluene (2:1 v/v).

A 50 mg portion of deacetylated grafted polymer was dissolved in 14 ml. of deionized water and cooled to 0°C.; 6 ml of sodium periodate solution (5.3 g sodium periodate in 100 ml of water) was added and the oxidation allowed to proceed at 0°C. At appropriate intervals, 3 ml aliquots were removed and mixed with 0.5 ml of freshly distilled ethylene glycol. After 1 hr at 25°C the samples were titrated with 0.01*N* sodium hydroxide solution and a 3 ml excess was added. After 0.5 hr, 3 ml of 0.01*N* sulfuric acid solution was added, and the samples were retitrated with base. A cellobiose blank and reagent blank were measured concurrently.

DISCUSSION

Preliminary grafting reactions were conducted with monoacetone *D*-xylose and commercial cellulose acetate. Results show that when monomer, polymer, and boron trifluoride catalyst are mixed at 25°C an initially rapid but relatively small amount of grafting occurs which is not greatly

increased when the reaction is allowed to proceed over a long period of time (Table I). Much homopolymer is rapidly produced under these conditions. The optimal concentrations of catalyst is near a monomer to catalyst ratio of 2:1. Increases or decreases in the catalyst concentration decreases the amount of grafting. Increasing the monomer to polymer ratio does not increase grafting.

It is evident from the data shown in Table I that simultaneous mixing of all reaction components leads to high yields of homopolymer and relatively low degrees of substitution on cellulose. However, when monomer and catalyst are added gradually over the reaction period, grafting proceeds to a greater degree. Under these conditions the same amount of grafting is obtained in 6 hr as is obtained in 24 hr when all reactants are simultaneously

TABLE I
Grafting of 1,2-*O*-Isopropylidene- α -D-xylose to Cellulose Acetate at 25°C

| Molar ratio monomer/catalyst | Molar ratio monomer/cellulose | Reaction time, hr | Yield of homopolymer, % | MS |
|------------------------------|-------------------------------|-------------------|-------------------------|------|
| 2 | 1 | 0.5 ^a | 54.8 | 0.23 |
| 2 | 1 | 8 ^a | 69.5 | 0.32 |
| 2 | 1 | 24 ^a | 65.1 | 0.37 |
| 1 | 1 | 24 ^a | 63.4 | 0.26 |
| 10 | 1 | 24 ^a | 78.0 | 0.23 |
| 100 | 1 | 24 ^a | 45.6 | 0.01 |
| 2 | 2 | 16 ^a | 82.7 | 0.32 |
| 2 | 1 | 6 ^b | — | 0.37 |
| 2 | 2 | 24 ^b | 67.7 | 0.68 |
| 20 | 2 | 24 ^b | 82.1 | 0.10 |
| 2 | 3 | 24 ^b | 71.4 | 0.89 |
| 6 | 3 | 24 ^b | 82.5 | 0.55 |

^a Monomer and catalyst added at 0 reaction time.

^b Monomer and catalyst added dropwise in three portions with initial addition of each beginning at 0, 1/3, and 2/3 total reaction time.

mixed. Furthermore, under gradual addition of monomer and catalyst higher degrees of grafting are obtained with higher monomer to cellulose ratios. Here also, higher monomer to catalyst ratios lead to lower degrees of grafting.

At 40°C grafting proceeds much faster than at 25°C. Thus, when all reactants are simultaneously mixed, the same amount of grafting is obtained in 30 min at 40°C as in 24 hr at 25°C (Table II). Similarly, at 40°C more rapid and often more grafting occurs on gradual addition of monomer and catalyst.

The monomeric 1,2-*O*-isopropylidene- α -D-xylofuranose has two free hydroxyl groups which not only make homopolymerization easy but also permit elongation of side chains produced by grafting of monomer units to free hydroxyl groups of the cellulose acetate. A lower degree of molar substitution might be expected if a fully blocked monomer were used. In

TABLE II
Grafting of 1,2-*O*-Isopropylidene- α -D-Xylose to Cellulose Acetate at 40°C

| Molar ratio monomer/catalyst | Molar ratio monomer/cellulose | Reaction time, hr | MS |
|---------------------------------|----------------------------------|----------------------|------|
| 2 | 1 | 0.5 ^a | 0.34 |
| 2 | 1 | 8 ^a | 0.25 |
| 2 | 1 | 24 ^a | 0.16 |
| 2 | 1 | 0.5 ^b | 0.38 |
| 2 | 1 | 1 ^b | 0.45 |
| 2 | 1 | 2 ^b | 0.49 |
| 2 | 2 | 2.5 ^b | 0.85 |
| 4 | 2 | 3 ^b | 0.72 |

^a Monomer and catalyst added at 0 reaction time.

^b Monomer and catalyst added dropwise in three portions with initial addition of each beginning at 0, 1/3 and 2/3 total reaction time.

increased when the reaction is allowed to proceed over a long period of time fact, it is found that under conditions where monoacetone D-xylose gives a MS of 0.37, 3,5-di-*O*-acetyl-1,2-*O*-isopropylidene- α -D-xylofuranose yields a MS of 0.21 and 3,5,6-tri-*O*-acetyl-1,2-*O*-isopropylidene- α -D-glucofuranose yields a MS of 0.09. Of course, all of these fully blocked monomers would develop a free hydroxyl group at C₂ during the grafting reaction, but the secondary hydroxyl thus produced might be expected to be partially hindered and not easily accessible for further grafting.

All grafted cellulose acetates showed appropriate weight gains corresponding to the calculated amounts of D-xylose added on. They were no longer soluble in acetone. After deacetylation the polymer with MS of 0.34 was insoluble in 1*N* sodium hydroxide solution, while those of MS greater than 0.7 were soluble. The intrinsic viscosity of the grafted cellulose acetate was higher than that of a physical mixture of the same composition containing cellulose acetate previously treated with catalyst and homopolymer.

It is apparent that at 40°C grafting proceeds rapidly in the early phase of the reaction and then diminishes with time (Table II). These observations indicate that boron trifluoride is breaking bonds in the newly formed grafted polymer side chains and in the cellulose acetate polymer as well. Transglycosylation of glycosides and depolymerization of polysaccharides with boron trihalides has been demonstrated.¹² Further direct evidence for depolymerization of the cellulose acetate and possibly accompanying transglycosylation reactions leading to a restructuring of cellulose molecules through branching is illustrated by the data in Table III. It is evident that boron trifluoride rapidly lowers the viscosity of the polymer. Evidence for the branching reaction is the finding of 2,3-di-*O*-methyl-D-glucose when the depolymerized cellulose is fully methylated and hydrolyzed by standard methods.¹⁰

To minimize depolymerization and restructuring of the cellulose acetate during the grafting reaction the concentration of catalyst is maintained at a

TABLE III
Effect of Boron Trifluoride on Cellulose Acetate of Intrinsic Viscosity 1.68

| Temperature, °C | Time of treatment, hr | Molar ratio cellulose/ catalyst | Water-insoluble residue, % | $[\eta]$, dl/g |
|--------------------|-----------------------------|--|-------------------------------|--------------------|
| 25 | 8 | 2 | 94.6 | 0.84 |
| 25 | 24 | 2 | 91.7 | 0.16 |
| 40 | 2 | 2 | 93.8 | 0.60 |
| 40 | 24 | 2 | 65.0 | 0.06 |

low level by gradual addition during the course of the reaction. As grafting proceeds the catalyst complexes with released acetone and this complex is not effective in promoting the main or side reactions.

Acetyl groups are not removed during the grafting reactions, as seen in Table IV.

Homopolymerization is an important side reaction of grafting as indicated in Table I. When monomer and catalyst are mixed and held at different temperatures at concentrations used in grafting, homopolymer forms rapidly as indicated in Table V. As stated earlier, boron trifluoride induces depolymerization as a side reaction of grafting and homopolymerization. The concurrent depolymerization reaction during homopolymerization is suggested by analysis of the residue left from the 24 hr reaction at 40°C. After removal of the 90% of the material converted to homopoly-

TABLE IV
Acetyl Content of Cellulose Acetate Treated with
Boron Trifluoride (2:1 Molar Ratio) at 40°C

| Time of treatment, hr | Acetyl content, % |
|--------------------------|----------------------|
| 0 | 38.6 |
| 2 | 38.6 |
| 8 | 38.6 |
| 24 | 38.6 |

TABLE V
Formation of Homopolymer From 1,2-*O*-Isopropylidene- α -xylofuranose (Monomer:Catalyst Ratio 2:1)

| Temperature, °C | Reaction time, hr | Homopolymer yield, % |
|--------------------|----------------------|-------------------------|
| 25 | 0.5 | 88.7 |
| 25 | 8 | 92.0 |
| 25 | 24 | 100.0 |
| 40 | 0.5 | 92.0 |
| 40 | 24 | 90.0 |

mer the residue is largely D-xylose. This sugar is not found in shorter reaction periods or in reactions conducted at lower temperatures.

Other monomers may also be used in grafting reactions. When all reactants are simultaneously mixed and reacted at 25°C, 1,2-anhydro-D-glucopyranose triacetate grafted to produce a MS of 0.7 and methyl α -D-xylopyranoside to a MS of 0.16, compared to 0.37 for monoacetone D-xylose. Levoglucosan triacetate did not graft under these conditions.

Structure of the Grafted Polymer

The primary hydroxyl content of polymers with a wide range of MS values is shown in Table VI. The commercial cellulose acetate had a total free hydroxyl content of 67 per 100 D-glucose units. Of these, 15 are primary and 52 are secondary. However, as grafting proceeds the number of

TABLE VI
Primary Hydroxyl Content of Grafted Polymers

| | Primary hydroxyl groups |
|-----------------------------|-------------------------|
| | 100 D-glucose units |
| Untreated cellulose acetate | 15 |
| Graft, MS 0.35 | 20 |
| Graft, MS 0.72 | 42 |
| Graft, MS 0.85 | 59 |

primary hydroxyl groups increases. This increase results from the primary hydroxyl groups introduced by D-xylose units and indicates that mainly D-xylofuranose units are being attached to the cellulose chain. From the data in Table VI it appears that the first D-xylofuranosyl units become attached to the primary position of the cellulose since little immediate increase in primary alcohol groups occurs in the polymer at a MS of 0.35. As continued grafting occurs, secondary alcohol functions of the cellulose are derivatized by D-xylofuranosyl units, and the total number of primary hydroxyl groups in the polymer increases. Furthermore, since each newly attached D-xylose unit has three free hydroxyl groups the chances increase for another D-xylose unit to become attached to one of its secondary hydroxyl groups. This would lead to branched side chains and increase in the total number of primary hydroxyl groups.

Complete methylation of the grafted polymer of MS 0.85 followed by hydrolysis gave the methylated derivatives of D-xylose shown in Table VII. The percentages of the various methylated products show that 65% of the grafted sugar is present as terminal D-xylofuranose units and only 10% as terminal D-xylopyranosyl. Ring expansion under grafting conditions has already been demonstrated in work with D-glucose derivatives¹ which seem to show even a greater tendency for expansion than does D-xylose. The

yields of various methyl derivatives of D-xylose show that the average length of graft is only 1.33 D-xylose units. The finding that 65% of the D-xylose is grafted as furanosyl units is substantiated by determination of primary alcohol groups. As indicated in Table VI, the grafted polymer of MS 0.85 has 59 primary hydroxyl groups per 100 D-glucose units. This corresponds to 65% of 85, or 55 D-xylofuranosyl units from the methylation data.

TABLE VII
Per Cent of Total Grafted D-Xylose Obtained as Methyl Ether
From Polymer of MS 0.85

| Methyl ether | Yield, % |
|--------------------------------------|----------|
| 2,3,5-Tri- <i>O</i> -methyl-D-xylose | 65 |
| 2,3,4-Tri- <i>O</i> -methyl-D-xylose | 10 |
| 2,3-Di- <i>O</i> -methyl-D-xylose | 20 |
| 2- and 3- <i>O</i> -methyl-D-xylose | 5 |

The yield of 2,3,4-tri-*O*-methyl-D-xylose indicates 9 D-xylopyranosyl units per 100 D-glucose units. Supporting evidence is provided by periodate analysis of the deacetylated grafted polysaccharide. One mole of formic acid is released by each D-xylopyranosyl terminal unit and three moles from each cellulose molecule. Periodate analysis indicates that 19 moles of formic acid are released per 100 D-glucose units. Subtracting three for formic acid derived from cellulose, the result suggests that the maximum number of D-xylopyranose units per 100 D-glucose units does not exceed this.

Hydrolysis of the grafted and deacetylated polymer of MS 0.85 with 0.05*N* oxalic acid solution removes 60% of the D-xylose. This cleavage of acid labile D-xylofuranosyl bonds is another indication of the extent to which D-xylofuranosyl units are grafted to the polymer. When homopolymers of D-xylose are prepared under grafting conditions and hydrolyzed in the same way, 65% of the D-xylose units are released.

The data suggest that the grafted cellulose acetate molecule is composed of a long cellulose backbone with numerous side chains composed of one or two D-xylose units.

References

1. R. L. Whistler and P. A. Seib, *J. Polymer Sci. A-1*, **4**, 1261 (1966).
2. H. Bretschneider and K. Beran, *Monatsh.*, **80**, 262 (1949).
3. T. G. Bonner, E. J. Bourne, and S. McNally, *J. Chem. Soc.*, **1962**, 761.
4. P. A. Levene and A. L. Raymond, *J. Biol. Chem.*, **102**, 317 (1933).
5. R. L. Whistler and M. L. Wolfrom, *Methods in Carbohydrate Chemistry*, Academic Press, New York, 1963, Vol. II.
6. R. E. Gramera, A. Park, and R. L. Whistler, *J. Org. Chem.*, **28**, 3230 (1963).
7. H. Ohle and K. Spencker, *Ber.*, **59B**, 1836 (1926); *Chem. Abstr.*, **21**, 63 (1927).

8. R. L. Whistler and P. A. Seib, *J. Polymer Sci. A*, **2**, 2595 (1964).
9. M. L. Wolfrom, R. M. deLederkremer, and G. Schwab, *J. Chromatog.*, **22**, 474 (1966).
10. R. L. Whistler, *Methods in Carbohydrate Chemistry*, Academic Press, New York, 1963, Vol. III.
11. R. L. Whistler, *Methods in Carbohydrate Chemistry*, Academic Press, New York, 1965, Vol. V.
12. T. G. Bonner, E. J. Bourne, and S. McNally, *J. Chem. Soc.*, **1960**, 2929.

Received December 28, 1967

Cationic Polymerization of α,β -Disubstituted Olefins.

IV. Stereospecific Polymerization of Propenyl Alkyl Ethers Catalyzed by $\text{BF}_3 \cdot \text{O}(\text{C}_2\text{H}_5)_2$ and $\text{Al}_2(\text{SO}_4)_3\text{-H}_2\text{SO}_4$ Complex*

T. HIGASHIMURA, S. KUSUDO,
Y. OHSUMI, A. MIZOTE, and S. OKAMURA,
Department of Polymer Chemistry, Kyoto University, Kyoto, Japan

Synopsis

The *cis*- and *trans*-propenyl alkyl ethers were polymerized by a homogeneous catalyst [$\text{BF}_3 \cdot \text{O}(\text{C}_2\text{H}_5)_2$] and a heterogeneous catalyst [$\text{Al}_2(\text{SO}_4)_3\text{-H}_2\text{SO}_4$ complex]. Methyl, ethyl, isopropyl, *n*-butyl and *tert*-butyl propenyl ethers were used as monomers. The steric structure of the polymers formed depended on the geometric structures of monomer and the polymerization conditions. In polymerizations with $\text{BF}_3 \cdot \text{O}(\text{C}_2\text{H}_5)_2$ at -78°C ., *trans* isomers produced crystalline polymers, but *cis* isomers formed amorphous ones except for *tert*-butyl propenyl ether. On the other hand, highly crystalline polymers were formed from *cis* isomers, but not from the *trans* isomers in the polymerization by $\text{Al}_2(\text{SO}_4)_3\text{-H}_2\text{SO}_4$ complex at 0°C . The x-ray diffraction patterns of the crystalline polymers obtained from the *trans* isomers were different from those produced from the *cis* isomers, except for poly(methyl propenyl ether). The reaction mechanism was discussed briefly on the basis of these results.

INTRODUCTION

The stereospecific polymerizations of propenyl alkyl ethers were reported by Heck et al.² as the first article on the stereospecific polymerizations of α,β -disubstituted olefins. A more detailed discussion of this problem was given by Natta in which the ditactic structure of poly(propenyl alkyl ether) was confirmed.³ The studies on the polymerization conditions for producing diisotactic polymer will give much knowledge on the mechanism of the propagating step in the ionic polymerization of vinyl monomers. However, in the cationic polymerization, few works have been reported to clarify the relationship between the steric structure of polymer and the polymerization conditions or the geometric structure of monomer, although there were several reports dealing with the structural analysis of diisotactic polymer.

Therefore, *trans*- and *cis*-propenyl alkyl ethers are polymerized and the relationship between polymerization conditions and the steric structure of

* For Part III paper, see Y. Ohsumi et al.¹

polymer are investigated. In this paper, $\text{BF}_3 \cdot \text{O}(\text{C}_2\text{H}_5)_2$ and $\text{Al}_2(\text{SO}_4)_3 \cdot \text{H}_2\text{SO}_4$ complex (SA catalyst) are used as homogeneous and heterogeneous catalysts, respectively, because it has been found that the growing chain controls the steric structure of an incoming monomer in the polymerization of methyl vinyl ether with $\text{BF}_3 \cdot \text{O}(\text{C}_2\text{H}_5)_2$ ⁴ and the catalyst site determines the structure of incoming monomer in the SA catalyst.⁵

EXPERIMENTAL

Materials

Propenyl alkyl ethers, except for *tert*-butyl propenyl ether, were synthesized by the de-alcohol reaction from dialkyl acetal as described in the previous papers.^{1,6} The crude products were obtained as the mixture of *trans* and *cis* isomers, from which the components were fractionated by distillation (45 plates). The isomers of methyl propenyl ether could not be separated satisfactorily in this condition, because their boiling points were very much similar. The purity of these monomers was measured by gas chromatography, and the geometric structure of the purified monomers was determined by infrared and NMR spectra. The purified monomer contained only the geometric isomer as an impurity. The steric purity and physical properties of the monomers used in this paper are summarized in Table I. Also, the spin-spin coupling constant and the chemical shift of α - and β -protons in these monomers are shown in Table II, and these values will be discussed elsewhere.

tert-Butyl propenyl ether was obtained by the isomerization of allyl *tert*-butyl ether catalyzed by potassium *tert*-butoxide.⁷ This procedure produced only the *cis* isomer, by which *trans-tert*-butyl propenyl ether could not be obtained.

SA catalyst was synthesized from $\text{Al}_2(\text{SO}_4)_3 \cdot 18\text{H}_2\text{O}$ and sulfuric acid.⁸ $\text{BF}_3 \cdot \text{O}(\text{C}_2\text{H}_5)_2$, $\text{Al}(\text{C}_2\text{H}_5)\text{Cl}_2$, and the solvents were purified by usual methods as reported in the previous papers.^{4,5} Monomers and solvents were distilled over sodium metal or calcium hydride before use.

Procedure

The polymerization was carried out without stirring in a 100 ml flask having a rubber cap. In the reaction in the presence of $\text{BF}_3 \cdot \text{O}(\text{C}_2\text{H}_5)_2$, the polymerization was initiated by the addition of catalyst solution into monomer solution. In the polymerization with SA catalyst, the monomer was added to a suspension of catalyst particles. The polymerization was stopped and the polymer formed was purified by the same method as in the case of vinyl ethers.^{4,5}

The x-ray diffraction pattern and the melting point of polymers were determined for the unfractionated polymer. The crystalline and amorphous polymers were qualitatively discriminated by comparison with the x-ray diffraction pattern of polymer film prepared from benzene solution of poly-

TABLE I
Steric Purity and Properties of Propenyl Alkyl Ethers ($\text{CH}_3\text{CH}=\text{CHOR}$) Used

| Monomer (R) | <i>cis</i> Isomer | | | <i>trans</i> Isomer | | |
|--------------------|---------------------|--------|-------------|---------------------|--------|-------------|
| | Steric purity, % | bp, °C | n_D (°C) | Steric purity, % | bp, °C | n_D (°C) |
| Methyl | 80 | 45 | — | 89 | 48 | — |
| Ethyl | 99 | 69 | 1.3974 (19) | 98 | 75 | 1.3997 (19) |
| Isopropyl | 99 | 83 | 1.3997 (19) | 98 | 91 | 1.4017 (19) |
| <i>n</i> -Butyl | 99 | 119 | 1.4122 (22) | 98 | 126 | 1.4132 (21) |
| <i>tert</i> -Butyl | ≈ 100 | 101 | 1.4078 (20) | — | — | — |

TABLE II
Chemical Shift and Spin-Spin Coupling Constant of
 α and β Protons in Propenyl Alkyl Ethers ($\text{CH}_3\text{CH}_\beta=\text{CH}_\alpha\text{OR}$)

| Monomer (R) | <i>cis</i> Isomer | | | <i>trans</i> Isomer | | |
|--------------------|--------------------------|-------------------------|---|--------------------------|-------------------------|---|
| | Chemical shift, ppm | | Coupling constant $J_{\text{H}_\alpha\text{H}_\beta}$, cps | Chemical shift, ppm | | Coupling constant $J_{\text{H}_\alpha\text{H}_\beta}$, cps |
| | τ_{H_α} | τ_{H_β} | | τ_{H_α} | τ_{H_β} | |
| Methyl | 4.26 | 5.78 | 7.0 | 3.83 | 5.41 | 12.8 |
| Ethyl | 4.20 | 5.78 | 6.8 | 3.89 | 5.42 | 13.2 |
| Isopropyl | 4.16 | 5.77 | 6.7 | 4.06 | 5.29 | 13.2 |
| <i>n</i> -Butyl | 4.22 | 5.78 | 6.7 | 3.92 | 5.37 | 12.3 |
| <i>tert</i> -Butyl | 3.95 | 5.71 | 6.7 | — | — | — |

mer at room temperature. Highly crystalline polymer was insoluble in benzene, and it was shown clearly by the x-ray diffraction pattern of polymer powder. Polymers were not treated by heating for crystallization. As the differences between crystalline and amorphous polymers was remarkable, the type of stereoregularity by x-ray diffraction pattern was very easily determined for all polymers. The melting point of polymer was determined by a microscopic birefringence method.

RESULTS

Relationship between Crystallinity of Polymers and Conditions of Polymerization

The *cis*- and *trans*-propenyl alkyl ethers were polymerized homogeneously by $\text{BF}_3 \cdot \text{O}(\text{C}_2\text{H}_5)_2$ at -78°C .; the results are summarized in Table III. In toluene solution, the crystalline polymer could be obtained only from the *trans* isomer, but not from the *cis* isomer except for *tert*-butyl propenyl ether. This result agreed with that of Natta.³ Crystalline polymer was produced from the *trans* isomer even in a polar solvent (methylene chloride) as well as in a nonpolar solvent (toluene), and the crystallinities observed by x-ray diffraction pattern were approximately equal in these polymers. This behavior contrasted strongly with the case of the polymerization of vinyl ethers, in which the crystalline polymer was produced only in a nonpolar solvent. However, the behavior of *tert*-butyl propenyl ether was different from that of other propenyl ethers. Although *cis-tert*-butyl propenyl ether formed a highly crystalline polymer in toluene, the amorphous polymer was obtained in methylene chloride.

Heterogeneous polymerization with SA catalyst was carried out without stirring in toluene solution at 0°C . The polar solvent could not be used for SA catalyst, for propenyl alkyl ether was decomposed in methylene chloride by SA catalyst at 0°C . The polymer propagated from the surface of catalyst particles in this system. As shown in Table IV, crystalline polymer was obtained from the *cis* isomer. Moreover, the crystallinity of these polymers was very much high, as qualitatively observed from the x-ray diffraction pattern and the relatively high melting point of the crystalline polymer. The intrinsic viscosity of polymers could not be measured due to poor solubility in benzene or toluene. On the other hand, the *trans* isomers formed only oily polymer products.

With SA catalyst, however, *cis-tert*-butyl propenyl ether did not polymerize, and *cis*-isopropyl propenyl ether converted to polymer only at high monomer concentration. Thus, the monomer having a branched alkoxy group showed low cationic polymerizability with heterogeneous catalyst.

Comparison of Polymer Structures Formed with $\text{BF}_3 \cdot \text{O}(\text{C}_2\text{H}_5)_2$ and SA Catalyst

To compare the steric structures of polymers obtained under various conditions, Table V shows the x-ray diffraction data of crystalline polymers

TABLE III
 Polymerization of Propenyl Alkyl Ethers ($\text{CH}_3\text{CH}=\text{CHOR}$) Catalyzed by Homogeneous Catalyst^a

| Monomer | | Polymerization conditions | | | Properties of polymer | |
|--------------------|--------------|---------------------------|---------------------------|----------------------------|-----------------------|---------|
| R | Structure | Solvent | Catalyst | Crystallinity ^b | $[\eta]^c$ | mp, °C |
| Methyl | <i>trans</i> | Toluene | BF_3OEt_2 | + | 0.30 | 150 |
| | <i>trans</i> | " | AlEtCl_2 | + | — | — |
| Ethyl | <i>cis</i> | " | BF_3OEt_2 | — | 0.27 | — |
| | <i>trans</i> | " | " | + | — ^d | 207 |
| | <i>trans</i> | CH_2Cl_2 | " | + | — ^d | 207 |
| | <i>cis</i> | Toluene | " | — | 0.17 | — |
| Isopropyl | <i>cis</i> | CH_2Cl_2 | " | — | 0.19 | — |
| | <i>trans</i> | Toluene | " | + | — ^d | 211 |
| | <i>trans</i> | CH_2Cl_2 | " | + | 0.23 ^d | 211 |
| | <i>cis</i> | Toluene | " | — | 0.42 | — |
| | <i>cis</i> | CH_2Cl_2 | " | — | 0.15 | — |
| | <i>trans</i> | Toluene | " | + | 0.79 | ca. 100 |
| <i>n</i> -Butyl | <i>trans</i> | " | AlEtCl_2 | + | 0.51 | " |
| | <i>trans</i> | CH_2Cl_2 | BF_3OEt_2 | + | 0.32 | " |
| | <i>cis</i> | Toluene | " | + | 0.46 | — |
| | <i>cis</i> | " | AlEtCl_2 | — | 0.49 | — |
| <i>tert</i> -Butyl | <i>cis</i> | CH_2Cl_2 | BF_3OEt_2 | — | 0.16 | — |
| | <i>cis</i> | Toluene | " | + | — | >250 |
| | <i>cis</i> | CH_2Cl_2 | " | — | 0.06 | — |

^a $[\text{M}]_0 = 5 \text{ vol-\%}$, $[\text{C}] = 2\text{--}4 \text{ mmole/l}$, -78°C .

^b (+) = crystalline; (—) = amorphous.

^c In benzene solution, 30°C .

^d Partially soluble.

TABLE IV
 Polymerization of Propenyl Alkyl Ethers ($\text{CH}_3\text{CH}=\text{CHOR}$)
 Catalyzed by $\text{Al}_2(\text{SO}_4)_3\text{-H}_2\text{SO}_4$ Complex^a

| Monomer | | Properties of polymer | |
|------------------------|--------------|----------------------------|---------|
| R | Structure | Crystallinity ^b | mp, °C |
| Methyl | <i>trans</i> | No polymer | — |
| | <i>cis</i> | + | 230 |
| Ethyl | <i>trans</i> | Oily product | — |
| | <i>cis</i> | + | 191 |
| Isopropyl ^c | <i>trans</i> | No polymer | — |
| | <i>cis</i> | + | 204 |
| <i>n</i> -Butyl | <i>trans</i> | Oily product | — |
| | <i>cis</i> | + | ca. 100 |
| <i>tert</i> -Butyl | <i>cis</i> | No polymer | — |

^a $[\text{M}]_0 = 20$ vol-%; $[\text{C}] = 0.4$ g/100 ml; solvent = toluene; 0°C.

^b (+) = crystalline; (–) = amorphous.

^c $[\text{M}]_0 = 40$ vol-%.

obtained from the *trans* isomers with $\text{BF}_3 \cdot \text{O}(\text{C}_2\text{H}_5)_2$ and from the *cis* isomers with SA catalyst. These x-ray diffraction patterns were measured for the unfractionated polymers. The spacings and relative intensities of the x-ray diffraction pattern of the former polymers were clearly different from those of the latter polymer, except for methyl propenyl ether. Therefore, it is concluded that the crystalline polymers formed from the *trans* isomers have a different steric structure from those derived from the *cis* isomers.

Natta et al. found that the *trans* isomer of β -substituted vinyl ethers produced threo-di-isotactic polymer with a homogeneous catalyst.⁹ Therefore, in our experiments it may be reasonable to estimate that the crystalline polymer obtained from the *trans* isomers seems to have the threo-di-isotactic structure.

It is well known that isotactic polymer has been produced from vinyl ethers with SA catalyst. Accordingly, the crystalline polymer obtained from *cis*-propenyl alkyl ethers with SA catalyst may not have a di-syndiotactic structure, but an erythro-di-isotactic structure. As reported by Natta,⁹ this means that the opening of monomeric double bond of the *trans* isomer is in the *cis* type, and this does not contradict the idea that the surface of heterogeneous catalyst tends to open a monomeric double bond to a *cis*-type. As the *trans* isomer of *tert*-butyl propenyl ether was not synthesized, the steric structure of poly(*tert*-butyl propenyl ether) could not be estimated.

On the other hand, the x-ray diffraction pattern of poly(methyl propenyl ether) obtained from the *cis* isomer with SA catalyst is almost the same as that for the polymer obtained from the *trans* isomer by $\text{BF}_3 \cdot \text{O}(\text{C}_2\text{H}_5)_2$. As already reported,¹ the structure of the latter polymer was recognized to be threo-di-isotactic. To confirm the steric structure of poly(methyl propenyl ether) in more detail, the NMR spectra of polymers were measured

TABLE V
 X-Ray Diffraction of Crystalline Poly(propenyl Alkyl Ethers)

| Polymer | From <i>trans</i> isomer [BF ₃ O(C ₂ H ₅) ₂ catalyst] | | From <i>cis</i> isomer [Al ₂ (SO ₄) ₃ -H ₂ SO ₄ complex] | |
|--|---|-----------|---|-----------|
| | Spacing Å | Intensity | Spacing Å | Intensity |
| Poly(methyl propenyl ether) | 7.8 ₁ | vs | 7.7 ₄ | vs |
| | 6.0 ₁ | w | 6.0 ₁ | w |
| | 5.7 ₂ | s | 5.7 ₂ | s |
| | 4.6 ₆ | w | 4.6 ₂ | w |
| | 3.8 ₆ | s | 3.7 ₉ | s |
| | 3.2 ₇ | w | 3.2 ₈ | w |
| Poly(ethyl propenyl ether) | 10. ₁ | w | 8.6 ₂ | s |
| | 8.3 ₇ | s | 7.7 ₁ | m |
| | 6.3 ₈ | m | 6.4 ₁ | s |
| | 5.2 ₄ | w | 5.2 ₃ | w |
| | 4.4 ₈ | s | 4.4 ₅ | m |
| | 3.8 ₅ | m | 3.9 ₇ | s |
| | 3.0 ₉ | w | 3.6 ₄ | m |
| | | | 3.0 ₉ | w |
| Poly(isopropyl propenyl ether) | 9.9 ₃ | w | | |
| | 8.7 ₈ | vs | 8.0 ₂ | vs |
| | 6.3 ₃ | s | 6.0 ₆ | m |
| | 5.0 ₆ | m | 5.3 ₈ | w |
| | 4.2 ₉ | s | 4.6 ₈ | w |
| | 3.6 ₉ | w | 4.1 ₇ | s |
| | 2.8 ₃ | w | 2.8 ₉ | w |
| | 2.2 ₀ | w | 2.2 ₃ | w |
| Poly(<i>n</i> -butyl propenyl ether) | | | 14.9 | w |
| | 10.1 | s | 10.4 | s |
| | 7.4 | w | 7.5 | s |
| | 5.8 | w | 5.9 | w |
| | 5.1 | s | 5.2 | w |
| | 4.6 | w | 4.6 | s |
| | | | 4.2 | w |
| | | 3.8 | w | |
| Poly(<i>tert</i> -butyl propenyl ether) | | | 9.1 | s |
| | | | 6.1 | s |
| | | | 4.4 | s |
| | | | 3.2 | m |
| | | | 2.8 | w |
| | | 2.2 | w | |

in *o*-dichlorobenzene solution (10% w/v) at 160°C (Varian HR-60). The spin decoupling was performed by the side-band method with a phase-sensitive detector operating at 2 Kcps. As shown in Figure 1, there was no difference between the decoupled NMR spectra of the two polymers,

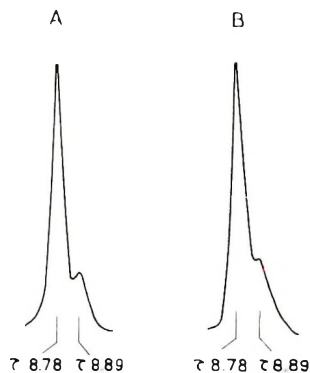
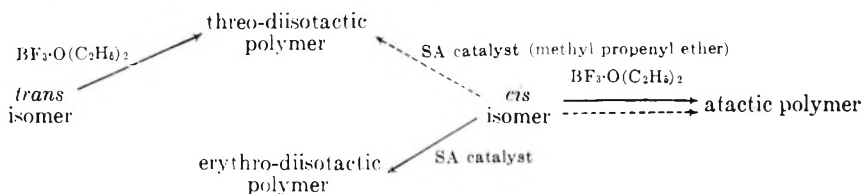


Fig. 1. NMR spectra of β -methyl protons decoupled from β -methine proton in poly-(methyl propenyl ethers): (A) obtained by $\text{BF}_3 \cdot \text{O}(\text{C}_2\text{H}_5)_2$ in toluene at -78°C ; (B) obtained by $\text{Al}_2(\text{SO}_4)_3\text{-H}_2\text{SO}_4$ complex in toluene at 0°C .

and it was thus confirmed that these polymer molecules had the same steric structure. Thus, a *threo*-di-isotactic polymer was confirmed to be produced from *cis*-methyl propenyl ether.

DISCUSSION

Results show that the steric structures of a polymer depends on the geometric structure of monomer and polymerization conditions. According to the relationship between the monomer and polymer structures proposed by Natta,⁹ the results are summarized schematically as shown in eq. (1),



where solid lines and broken lines denote the *cis* and *trans* opening, respectively, of the monomer double bond. Of course, this relationship seems to be valid only in the case when the C—C bond of the newly formed chain end can not be rotated. Therefore, the formation of an atactic polymer from *cis* isomer may be caused by the random opening of a monomer double bond or by the random rotation of a C—C bond of the newly formed chain end.

Homogeneous Polymerization by $\text{BF}_3 \cdot \text{O}(\text{C}_2\text{H}_5)_2$

With $\text{BF}_3 \cdot \text{O}(\text{C}_2\text{H}_5)_2$ as homogeneous catalyst, the *trans* isomers produced crystalline polymer probably having a *threo*-di-isotactic structure. Also, the *trans* isomers were less reactive than the *cis* isomers in the polymerization with $\text{BF}_3 \cdot \text{O}(\text{C}_2\text{H}_5)_2$.^{6,10,11} Some reasons can be considered for the dif-

ferences in reactivity between the geometric isomers,^{10,12} for example, the stability of a monomer.

Here, we assumed that the difference in reactivity of the isomers was caused by the steric effect of substituents in the monomer during the propagation step. The approach of *trans* isomers to a growing chain end is very difficult, because the *trans* isomers have substituents in the opposite side of the monomeric double bond, and a growing chain end has bulky side groups. Otherwise, the steric hindrance for the approach of the *cis* isomers to a growing chain end may be smaller than for the *trans* isomers, because the *cis* isomers have substituents in the same side of the monomer and are able to attack a growing chain end from various directions. Although the *trans* isomers are less reactive, it is expected that the *trans* isomers can add to a chain end from that definite direction from which the steric hindrance is the smallest. This supposition is supported by Stuart-type molecular model.

Also, the effect of solvent can be explained by the same idea. In the polymerization of vinyl ethers, the stereoregularity (isotacticity) of a polymer decreases with increasing polarity of solvent, because the counterion controls the direction of the incoming monomer. However, in polymerization of propenyl alkyl ethers, the polarity of the solvent does not affect the structure of polymer, as shown in Table III. This result suggests that the main factor controlling the steric configuration of an incoming monomer is steric hindrance between the substituents of the incoming monomer and the growing chain end. This explanation is similar to that for the stereospecific polymerization of α -methylstyrene¹³ and the stereospecific copolymerization of ethylene with cycloolefins having an odd number of ring atoms.¹⁴ However, in this model, it is not clear why the *cis* opening of a monomer double bond occurs preferentially in the *trans* isomers with the use of a homogeneous catalyst. Further experiments should be carried out to solve this problem.

As described above, it seems that the usual *cis* isomers produce atactic polymer due to the smaller steric hindrance for the addition of monomer. Nevertheless, *cis-tert*-butyl propenyl ether yielded a stereoregular polymer. The large steric hindrance of the bulky *tert*-butoxy group may cause regular addition of an incoming monomer and decrease the reactivity of *tert*-butyl propenyl ether. In fact, the reactivity of *cis-tert*-butyl propenyl ether was much smaller than that of *tert*-butyl vinyl ether.¹⁵ However, the formation of an amorphous polymer from the *cis* isomer in methylene chloride suggests that steric regulation by the *tert*-butoxy group is not enough in a polar solvent.

Heterogeneous Polymerization by SA Catalyst

With SA catalyst as heterogeneous catalyst, a crystalline polymer was produced from the *cis* isomers from which a crystalline polymer was not obtained with homogeneous catalyst. In the polymerization of methyl

vinyl ether by SA catalyst, it was found that the steric structure of an incoming monomer was controlled by the catalyst site, and the absorption of a monomer on catalyst surface was an important step on the propagation reaction.⁵ If it can be assumed that the absorption on the surface of catalyst is difficult in the *trans* isomers or in the *cis* isomers having a branched alkoxy group, the results shown in Table IV will be able to be easily explained. This assumption is not unreasonable, if the steric hindrance of substituents in a monomer is considered. Otherwise, the *cis* isomers, which are absorbed on the catalyst surface, may be easily polymerized to a crystalline polymer.

One exception was methyl propenyl ether, for which the steric structure of the crystalline polymer was independent of the geometric structures of the monomer. Also, Heck et al.² reported that the crystalline polymer obtained from the *cis* and *trans* isomers had the same steric structures in the polymerization of ethyl and *n*-propyl propenyl ether by the modified Ziegler catalyst.

In the coordination polymerization in which a monomer is absorbed on catalyst surface, *cis* opening of the monomer double bond appears to be a general rule. If so, the behavior of the systems reported here is not easily understandable. If it is valid that the *cis* isomer produces threo-di-isotactic polymer in the polymerization of methyl propenyl ether, SA catalyst causes predominantly *trans* opening of the monomer double bond or the regular rotation of the newly formed chain end. Another possibility is polymerization after isomerization of the *cis* isomer to the *trans* isomer in the presence of SA catalyst. However, as the *trans* isomer was not polymerized by SA catalyst as shown in Table IV, this possibility has to be rejected.

References

1. Y. Ohsumi, T. Higashimura, R. Chujo, T. Kuroda, and S. Okamura, *J. Polym. Sci. A-1*, **5**, 3009 (1967).
2. R. F. Heck and D. S. Breslow, *J. Polym. Sci.*, **41**, 520 (1959).
3. G. Natta, *J. Polym. Sci.*, **48**, 219 (1960).
4. Y. Ohsumi, T. Higashimura, and S. Okamura, *J. Polym. Sci. A-1*, **5**, 849 (1967).
5. Y. Ohsumi, T. Higashimura, K. Kuroda, and S. Okamura, *J. Polym. Sci. A-1*, **5**, 863 (1967).
6. A. Mizote, S. Kusudo, T. Higashimura, and S. Okamura, *J. Polym. Sci. A-1*, **5**, 1727 (1967).
7. C. C. Price and W. H. Snyder, *J. Amer. Chem. Soc.*, **83**, 1773 (1963).
8. S. Okamura, T. Higashimura, and T. Watanabe, *Makromol. Chem.*, **50**, 137 (1961).
9. G. Natta, M. Peraldo, M. Farina, and G. Bressan, *Makromol. Chem.*, **55**, 139 (1962).
10. T. Fueno, T. Okuyama, O. Kajimoto, and J. Furukawa, paper presented at International Symposium on Macromolecular Chemistry, Tokyo-Kyoto, 1966.
11. T. Higashimura, S. Kusudo, Y. Ohsumi, and S. Okamura, *J. Polym. Sci. A-1*, **6**, 2523 (1968).

12. C. G. Overberger, D. H. Tanner, and E. M. Pearce, *J. Amer. Chem. Soc.*, **80**, 4566 (1958).
13. Y. Ohsumi, T. Higashimura, and S. Okamura, *J. Polym. Sci. A-1*, **4**, 923 (1966).
14. F. Danusso, in *Macromolecular Chemistry (J. Polym. Sci. C, 4)*, M. Magat, Ed., Interscience, New York, 1963, p. 1497.
15. T. Higashimura, Y. Kitagawa, and S. Okamura, *Kobunshi Kagaku*, **24**, 655 (1967).

Received August 21, 1967

Revised January 15, 1968

Cationic Polymerization of α,β -Disubstituted Olefins. V. Reactivity of Propenyl Alkyl Ethers in Cationic Polymerization

T. HIGASHIMURA, S. KUSUDO, Y. OHSUMI, and S. OKAMURA,
Department of Polymer Chemistry, Kyoto University, Kyoto, Japan

Synopsis

To elucidate the effect of the introduction of a methyl group in the β -position of a vinyl monomer, propenyl alkyl ethers were copolymerized with vinyl ethers having the same alkoxy group. Propenyl alkyl ethers with an unbranched alkoxy group (ethyl or *n*-butyl propenyl ether) were more reactive than the corresponding vinyl ethers. This behavior is quite different from that of β -methylstyrene derivatives. However, propenyl alkyl ethers with branched alkoxy groups at the α carbon atom (isopropyl or *tert*-butyl propenyl ether) were less reactive than the corresponding vinyl ethers. Also, *cis* isomers were more reactive than the *trans* isomers, regardless of the kind of alkoxy group and the polarity of the solvent.

INTRODUCTION

In radical polymerization, high polymers cannot be produced from α,β -disubstituted olefins due to steric hindrance by the β -substituent, except in the case of cyclic compounds such as vinylene carbonate or an olefinic compound such as 1,2-difluoroethylene in which the size of the substituent is sufficiently small. On the other hand, α,β -disubstituted olefins can be polymerized by the ionic mechanism, and the cationic polymerizations of β -methylstyrenes, stilbene, and β -substituted vinyl ethers have been reported.

Moreover, the effect of the β -methyl group introduced in the vinyl monomer on the polymerizability depends on the kind of monomer in cationic polymerization. A β -methyl group decreased the reactivity of styrene derivatives as expected from the radical polymerization.^{1,2} Otherwise, the introduction of a β -methyl group increased the reactivity of *n*-butyl vinyl ether.³ The same conclusion was also obtained in the case of isobutyl vinyl ether.⁴

Therefore, the first purpose of the present study is to elucidate whether the introduction of a β -methyl group in a vinyl ether generally raises the reactivity of vinyl ether in cationic polymerization or not.

The reactivity of monomers also depends on the geometric structure of the monomers. In the cationic copolymerization of β -methylstyrene with

p-chlorostyrene, the *trans* isomer was more reactive than the *cis* isomer.¹ On the other hand, just the reverse relation was found in the cases of *n*-butyl and isobutyl propenyl ethers.^{3,4} Thus, the second object of this paper is to determine the effect of the geometric structures of monomers on the reactivity of propenyl alkyl ethers in cationic polymerization.

EXPERIMENTAL

Materials

Propenyl alkyl ethers were synthesized and purified by the same method as mentioned in the previous papers.^{3,5} Commercial vinyl ethers were washed with dilute KOH aqueous solution, dried with KOH and repeatedly distilled over metal sodium. The other materials were also purified as reported in the previous papers.^{3,5}

Procedures

A reaction vessel was equipped with a stirrer, thermometer, and stopcock in the bottom, and was sealed with a rubber cap. The polymerization was initiated at constant temperature by adding a catalyst solution to the monomer solution through the rubber cap from a syringe. In this procedure, the reaction system contained a small amount of water (1–2 mmole/l). After a specified time, the contents were removed from the vessel through the stopcock under dry nitrogen and poured into ammoniac methanol.

To determine the amount of monomer consumed, the amount of residual monomer was measured by gas chromatography, as the amount of monomer consumed cannot be determined only by analysis of the polymer. The conditions of gas chromatographic measurement are summarized in Table I.

TABLE I
Conditions of Gas-Chromatographic
Measurement of Propenyl Alkyl Ethers^a

| Monomer | Conditions of measurement | | | |
|-----------------|---------------------------|------------------|---------------------------|---------------------------------------|
| | Column Type ^b | Column Length, m | Temperature of column, °C | Carrier gas (H ₂), ml/min |
| Methyl | DNP | 2 | 45 | 50 |
| | PEG | 1 | | |
| Ethyl | DNP | 1 | 55 | 70 |
| | PEG | 3 | | |
| Isopropyl | DNP | 1 | 60 | 70 |
| | PEG | 3 | | |
| <i>t</i> -Butyl | PEG | 4 ^c | 70 | 50 |

^a Vinyl ether was measured by the same condition as the corresponding propenyl ether.

^b DNP = dinonyl phthalate on Celite 545; PEG = poly(ethylene glycol) 1500 on Celite 545.

^c PEG 400 (2 m) + PEG 1500 (1 m) + PEG 4000 (1 m).

Methylene chloride was used as an internal standard for gas chromatographic measurement for the polymerization in toluene, and toluene was used for the polymerization in methylene chloride. In both systems the amount of internal standard used was 5 vol-%. The amount of monomer consumed coincided well with the amount of methanol-insoluble polymer, except for *tert*-butyl propenyl ether. Reactions other than polymerization were not observed.

The intrinsic viscosity of copolymers was measured in benzene solution at 30°C, and these values were found to be larger than 0.2, except for homopolymer and copolymer of *tert*-butyl propenyl ether.

Polymerization was carried out at -74 to -78°C, and toluene was used as nonpolar solvent and methylene chloride as polar solvent.

RESULTS

Effect of β -Methyl Group on the Reactivity of Vinyl Ethers

To compare the reactivity of the propenyl alkyl ether with that of the corresponding vinyl ether, propenyl alkyl ethers were copolymerized with vinyl ethers having the same alkoxy group. Then, the propagating chain ends formed from both monomers will have a similar structure as described in the case of the copolymerization of β -methylstyrene.²

Figure 1 shows time-conversion curves for the copolymerization of *cis*-ethyl propenyl ether with ethyl vinyl ether. A short induction period was observed. Some systems did not show a good straight line in the first-order plot of the residual monomer concentration for each comonomer

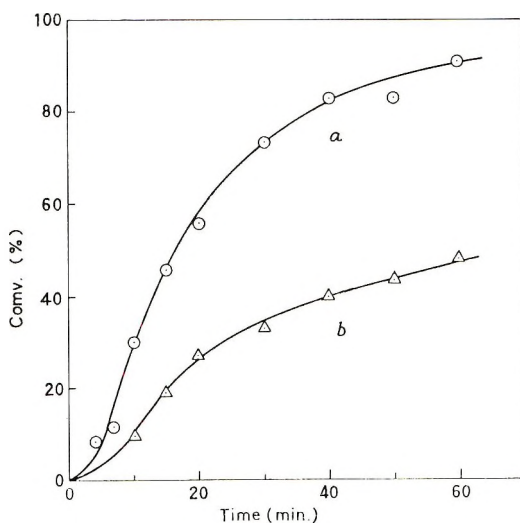


Fig. 1. Time-conversion curve in the copolymerization of ethyl vinyl ether (M_1) with *cis*-ethyl propenyl ether (M_2) catalyzed by $\text{BF}_3 \cdot \text{O}(\text{C}_2\text{H}_5)_2$: (O) *cis*-ethyl propenyl ether; (Δ) ethyl vinyl ether. $[\text{M}]_0 = 10 \text{ vol-\%}$, $[\text{M}_1]/[\text{M}_2] = 1.24$ (mole ratio), $[\text{C}] = 2 \text{ mmole/l}$, solvent; toluene; -74 to -78°C.

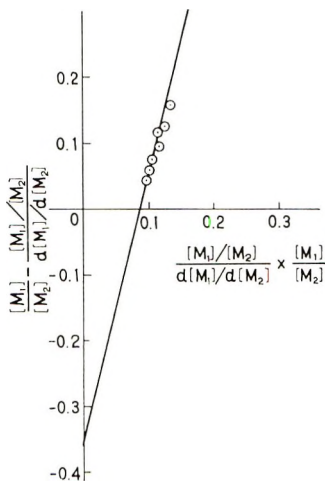


Fig. 2. Fineman-Ross-Sakurada plot for the copolymerization of ethyl vinyl ether (M_1) with *cis*-ethyl propenyl ether (M_2). (Calculated from Fig. 1.)

over the whole range of reaction. The monomer reactivity ratio was calculated from the rate of polymerization of each monomer by the Fineman-Ross-Sakurada equation, eq. (1). This treatment was previously applied to the *n*-butyl propenyl ether-*n*-butyl vinyl ether system.³

$$\frac{[M_1]}{[M_2]} - \frac{[M_1]/[M_2]}{d[M_1]/d[M_2]} = r_1 \frac{[M_1]/[M_2]}{d[M_1]/d[M_2]} \frac{[M_1]}{[M_2]} - r_2 \quad (1)$$

Figure 2 shows the plot of the Fineman-Ross-Sakurada equation calculated from Figure 1, where M_1 is vinyl ether and M_2 is propenyl alkyl ether.

The monomer reactivity ratios calculated by the same method are summarized in Table II, along with the results reported in other papers.^{3,4}

Effect of Geometric Structures of Monomer Reactivity

Table II suggests that *cis*-propenyl alkyl ether is more reactive than the *trans* isomer, from the copolymerization with vinyl ether. To compare directly the reactivity of the two isomers, the *cis* isomers were copolymerized with the *trans* isomers, except for *tert*-butyl propenyl ether, the *trans* isomer of which could not be synthesized.

Time-conversion curves for the copolymerization between *cis*- and *trans*-isopropyl propenyl ether are shown in Figure 3. Figure 4 shows the first-order plot of the residual monomer concentration calculated from Figure 3. The plots were straight lines. Even in a few cases in which the plots were not in a straight line over the whole range of polymerization, the linearity of the plot was established except for the initial stage of the polymerization. This means that the structure of growing chain end produced from the *cis* isomer is the same as that from the *trans* isomer. Therefore, the ratio of the slope of two straight lines in Figure 4 may be regarded

TABLE II
 Monomer Reactivity Ratio in the Copolymerization of Propenyl Alkyl Ether ($\text{CH}_2=\text{CH}=\text{CHOR}$) (M_2) with the
 Corresponding Vinyl Ether ($\text{CH}_2=\text{CHOR}$) (M_1) by $\text{BF}_3 \cdot \text{O}(\text{C}_2\text{H}_5)_2^a$

| Monomer | | Toluene as solvent ^b | | Methylene chloride as solvent ^c | |
|------------------------------|---------------------|---------------------------------|-----------------|--|-----------------|
| R | Geometric structure | r_1 | r_2 | r_1 | r_2 |
| Ethyl | <i>cis</i> | 0.35 ± 0.1 | 4.0 ± 0.5 | — | — |
| | <i>trans</i> | 0.94 ± 0.1 | 0.94 ± 0.1 | — | — |
| <i>n</i> -Butyl ^d | <i>cis</i> | — | — | 0.50 ± 0.2 | 4.0 ± 1.0 |
| | <i>trans</i> | — | — | 0.80 ± 0.3 | 2.3 ± 0.3 |
| Isopropyl | <i>cis</i> | 1.1 ± 0.2 | 0.80 ± 0.4 | — | — |
| | <i>trans</i> | 4.9 ± 0.4 | 0.19 ± 0.05 | — | — |
| <i>tert</i> -Butyl | <i>cis</i> | 2.2 ± 0.4 | 0.28 ± 0.08 | — | — |
| | <i>trans</i> | — | — | 0.29 ± 0.05 | 2.20 ± 0.14 |
| Isobutyl ^e | <i>cis</i> | — | — | 1.04 ± 0.04 | 0.90 ± 0.03 |
| | <i>trans</i> | — | — | — | — |

^a $[\text{M}]_0 = 10 \text{ vol-}\%$, $[\text{C}] = 2 \text{ mmole/l}$, -74 to 78°C .

^b Toluene contains 5 vol-% methylene chloride as an internal standard for the gas-chromatographic measurement.

^c Methylene chloride contains 5 vol-% of toluene for the same reason.

^d Data of Mizote et al.²

^e Data of Fueno et al.³

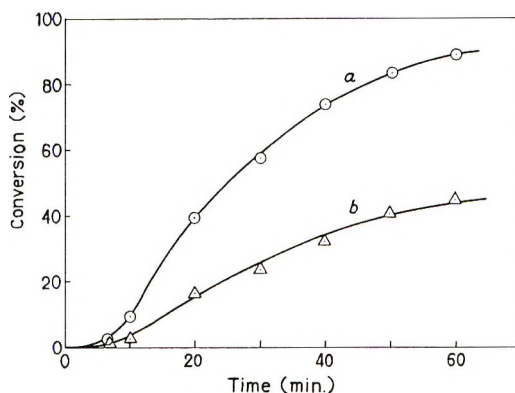


Fig. 3. Time-conversion curve in the copolymerization of *cis*-isopropyl propenyl ether (M_1) with *trans*-isopropyl propenyl ether (M_2) catalyzed by $\text{BF}_3 \cdot \text{O}(\text{C}_2\text{H}_5)_2$: (O) *cis*-isopropyl propenyl ether; (Δ) *trans*-isopropyl propenyl ether. $[\text{M}]_0 = 10 \text{ vol-}\%$, $[\text{M}_1]/[\text{M}_2] = 0.933$ (mole ratio), $[\text{C}] = 2 \text{ mmole/l}$, solvent; toluene; -74 to -78°C .

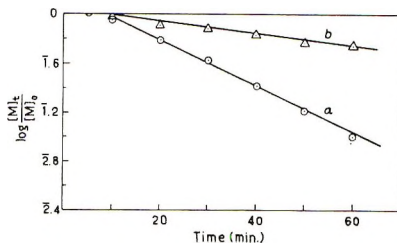


Fig. 4. First-order plot for the monomer concentration in the copolymerization of *cis*- and *trans*-isopropyl propenyl ether. (O) *cis*-isopropyl propenyl ether; (Δ) *trans*-isopropyl propenyl ether. (Calculated from Fig. 3.)

as the reactivity ratio of *cis*- and *trans*-isopropyl propenyl ethers for the growing chain end, that is, $(k_p)_{cis}/(k_p)_{trans}$.

If the conformation of growing chain end affects the reaction rate of an incoming monomer as observed in the stereo-selective polymerization of the *N*-carboxy anhydride of an amino acid,⁶ it is expected that the monomer reactivity of each isomer will be changed by the composition of the initial monomer feed. However, as shown in Table III, the relative reactivity of *cis*- and *trans*-ethyl propenyl ether was independent of the ini-

TABLE III
Relative Reactivity of *cis*- and *trans*-Ethyl Propenyl Ether at
Various Monomer Compositions in Toluene^a

| Mole ratio $([\text{M}]_0)_{cis}/([\text{M}]_0)_{trans}$ | $(k_p)_{cis}/(k_p)_{trans}$ |
|---|-----------------------------|
| 66.6/33.4 | 2.44 |
| 47.4/52.6 | 2.23 |
| 43.0/57.0 | 2.39 |

^a $[\text{M}]_0 = 10 \text{ vol-}\%$, $[\text{BF}_3 \cdot \text{O}(\text{C}_2\text{H}_5)_2] = 2 \text{ mmole/l}$, -74 to -78°C .

tial monomer composition. Therefore, it is not necessary to consider the possibility of the stereoselectivity by a preformed polymer.

Under the conditions of our experiments, *cis* isomer was not observed to be formed during the polymerization of pure *trans* isomer and vice versa, and the linearity of the first-order plot for a monomer concentration was established as shown in Figure 4. It is, therefore, concluded that *cis-trans* isomerization during the polymerization does not take place.

The reactivities of the *cis* isomers relative to the *trans* isomers are summarized in Table IV. The *cis* isomers were more reactive than the *trans*

TABLE IV
Relative Reactivity of *cis*- and *trans*-Propenyl Alkyl Ether by $\text{BF}_3 \cdot \text{O}(\text{C}_2\text{H}_5)_2$ ^a

| Monomer | Solvent ^b | $(k_p)_{cis}/(k_p)_{trans}$ |
|-----------------------|----------------------|-----------------------------|
| Methyl | Toluene | 3.7 |
| | Methylene chloride | — |
| Ethyl | Toluene | 2.4 |
| | Methylene chloride | 1.4 |
| Isopropyl | Toluene | 3.7 |
| | Methylene chloride | 2.2 |
| <i>n</i> -Butyl | Toluene | 1.9 |
| | Methylene chloride | 1.5 |
| Isobutyl ⁴ | Ethyl benzene | 6.4 |
| | Methylene chloride | 2.2 |

^a $[\text{M}]_0 = 10 \text{ vol-}\%$, $[\text{C}] = 2\text{--}4 \text{ mmole/l}$, $-74 \text{ to } 78^\circ\text{C}$.

^b Toluene contains 5 vol-% of methylene chloride as an internal standard for the gas-chromatographic measurement; methylene chloride contains 5 vol-% of toluene for the same reason.

isomers in all systems, as expected from Table II. The difference in reactivity between the *cis* and *trans* isomers decreased with increasing polarity of the solvent. This tendency coincides with the general behavior in ionic reactions in which the difference in reactivity between a reactive reagent and a less reactive reagent decreases in a polar solvent.

The *cis* and *trans* isomers were also copolymerized by $\text{Al}_2(\text{SO}_4)_3\text{--H}_2\text{SO}_4$ complex. Polymer was produced mainly from the *cis* isomer and very little consumption of *trans* isomer was observed. This agrees with the previous observation⁵ that high polymer could not be obtained from the homopolymerization of the *trans* isomer with $\text{Al}_2(\text{SO}_4)_3\text{--H}_2\text{SO}_4$ complex.

DISCUSSION

Effect of β -Methyl Groups on the Reactivity of Vinyl Ethers

The introduction of a methyl group in the β position of an olefinic double bond affected the reactivity of vinyl ethers as shown in Table II. In monomer, with a nonbranched alkoxy group at the α carbon such as ethyl or *n*-butyl propenyl ether, the values of $1/r_1$ and r_2 were both larger than unity, where M_1 was vinyl ether and M_2 was corresponding propenyl alkyl

ether. This relation was not clear in the *trans* isomers, but *cis*-propenyl alkyl ether was several times more reactive than the corresponding vinyl ether. This means that a β -methyl group increases the reactivity of the monomeric double bond in propenyl alkyl ethers.

In *cis*-ethyl and *n*-butyl propenyl ethers, r_2 was larger than $1/r_1$. This result shows that an incoming monomer can approach a growing chain end without steric repulsion of the β -methyl group in a growing chain end against the β -methyl group in an incoming monomer.

Thus, the effect of the β -methyl group on the reactivity of vinyl ethers was just the reverse of that in styrene derivatives whose reactivity was decreased by the steric hindrance between substituents. It is not clear, however, why the introduction of a β -methyl group does not decrease the reactivity of vinyl ether.

On the other hand, when the alkoxy group was branched at the first carbon after the ether oxygen, both r_1 and $1/r_2$ were larger than unity, that is, propenyl alkyl ethers (M_2) were less reactive than the corresponding vinyl ethers (M_1). It is difficult to consider that the electronic effect of β -methyl group on the reactivity of monomeric double bond is reversed by the branching of alkoxy group. Therefore, the bulky alkoxy group in an incoming monomer or a growing chain end may act to repulse sterically the β -methyl group in the growing chain end or incoming monomer, respectively, although steric interactions between an α -substituent and a β -substituent in an addition step have not previously been considered.

Especially, in the case of *cis-tert*-butyl propenyl ether, r_2 was smaller than $1/r_1$, and the rate of homopolymerization was much smaller than that of *tert*-butyl vinyl ether.⁷ These results suggest that the β -methyl group in a growing chain end retards the addition of monomer by steric hindrance. However, it was reported that isobutyl propenyl ether was more reactive than isobutyl vinyl ether.⁴ The branching at the second carbon after the ether oxygen does not sterically repulse a β -methyl group in the addition reaction.

Thus, steric hindrance in the polymerization of propenyl alkyl ether cannot be discussed only with respect to the interaction between a β -methyl group in the growing chain end and a β -methyl group in the incoming monomer, as described in the radical polymerization.⁸

Effect of the Geometric Structures of Monomer on the Reactivity

The reactivities of the *cis* and *trans* isomers were directly compared by the copolymerization between the geometric isomers. As shown in Table IV, the *cis* isomers were more reactive than the *trans* isomers, irrespective of the kind of alkoxy group and solvent.

In the copolymerization between the geometric isomers, it was assumed from Figure 4, that the growing chain end produced from the two isomers was kinetically the same. On the other hand, the relative reactivities of the *cis* and *trans* isomers of propenyl alkyl ethers (M_2) for the chain end produced from vinyl ethers (M_1) are shown in eq. (2).

$$\frac{(k_{12})_{cis}}{(k_{12})_{trans}} = \frac{(k_{12})_{cis}}{k_{11}} \cdot \frac{k_{11}}{(k_{12})_{trans}} = \frac{(r_1)_{trans}}{(r_1)_{cis}} \quad (2)$$

These values were calculated from the data of Table II summarized in the last column of Table V. The corresponding values calculated from the copolymerization between the *cis* and *trans* isomers are shown in the third column of Table V.

TABLE V
Comparison of *cis*- and *trans*-Propenyl Alkyl Ether by Two
Different Methods (Calculated from Tables II and IV)

| Monomer | Solvent | $(k_p)_{cis}/(k_p)_{trans}$ | $(r_1)_{trans}/(r_1)_{cis}$ ^a |
|-----------------|--------------------|-----------------------------|--|
| Ethyl | Toluene | 2.4 | 2.7 |
| <i>n</i> -Butyl | Methylene chloride | 1.5 | 1.6 |
| Isopropyl | Toluene | 3.7 | 4.5 |
| Isobutyl | Methylene chloride | 2.2 | 3.6 |

^a Calculated from Table II.

In ethyl and *n*-butyl propenyl ethers, $(k_p)_{cis}/(k_p)_{trans}$ calculated from Table IV coincided well with $(k_{12})_{cis}/(k_{12})_{trans}$ within experimental error. This supports the assumption that the relative reactivities of the geometric isomers are independent of the existence of β -methyl group in the growing chain end. However, in the branched propenyl alkyl ether, $(k_p)_{cis}/(k_p)_{trans}$ was different from $(r_1)_{trans}/(r_1)_{cis}$.

As already reported in a previous paper,⁵ in considerations of the difference of reactivity between the geometric isomers, we have proposed tentatively an explanation based on greater ease of approach of the *cis* isomer to a growing chain end than the *trans* isomer. Further studies are necessary for detailed discussion of the reactivity of geometric isomers.

References

1. C. G. Overberger, D. H. Tanner, and E. M. Pearce, *J. Am. Chem. Soc.*, **80**, 4566 (1958).
2. A. Mizote, T. Higashimura, and S. Okamura, *J. Polymer Sci. A*, **3**, 2567 (1965).
3. A. Mizote, S. Kusudo, T. Higashimura, and S. Okamura, *J. Polymer Sci. A-1*, **5**, 1727 (1967).
4. T. Fueno, T. Okuyama, O. Kajimoto, and J. Furukawa, paper presented at International Symposium on Macromolecular Chemistry, Tokyo-Kyoto, 1966.
5. T. Higashimura, S. Kusudo, Y. Ohsumi, A. Mizote, and S. Okamura, *J. Polymer Sci. A-1*, **6**, 2511 (1968).
6. R. D. Lundberg and P. Doty, *J. Am. Chem. Soc.*, **79**, 3961 (1957).
7. T. Higashimura, Y. Kitagawa, and S. Okamura, *Kobunshi Kagaku*, **24**, 655 (1967).
8. T. Alfrey, Jr., J. J. Bohrer, and H. Mark, *Copolymerization*, Interscience, New York, 1952, p. 49.

Received August 21, 1967

Revised January 15, 1968

Formaldehyde Equilibria: Their Effect on the Kinetics of the Reaction with Phenol*

ANDREAS A. ZAVITSAS,† *Research Department, Plastic Products and Resins Division, Monsanto Company, Springfield, Massachusetts 01101*

Synopsis

The kinetics of the base catalyzed hydroxymethylation of phenol by aqueous formaldehyde are influenced strongly by the equilibria among the hydrated forms of formaldehyde, and among the hydrates and the alcoholic function of the products. Apparent peculiarities in the kinetics of the system and seemingly anomalous solvent effects are shown to be due to erroneous formulation of the previously accepted rate expression. The correct expression is: $\text{Rate} = k[P_i^-][F]m$, where P_i^- is phenoxide ion, F is unreacted formaldehyde, and m is the fraction of formaldehyde in the form of monomeric hydrate. Formaldehyde tied up in equilibria as α,ω -poly(oxymethylene) diols, and hemiformals of the hydroxymethylphenols, constitutes a potential source of formaldehyde and is detected by the usual analytical procedures, but does not contribute to the rate of the hydroxymethylation reaction.

The base-catalyzed hydroxymethylation of phenol by aqueous formaldehyde is generally accepted to be a second-order ion-molecule reaction whose kinetics follow the general rate expression given by eq. (1):¹⁻⁴

$$\text{Rate} = k[P_i^-][F] \quad (1)$$

where P_i^- depicts phenoxide ion and F unreacted formaldehyde, the latter as determined by titrimetric procedures such as the hydroxylamine hydrochloride method.^{5a} Our investigation of the kinetics of formaldehyde-phenol systems showed eq. (1) to be inadequate in systems containing more than a few tenths molar formaldehyde.

RESULTS AND DISCUSSION

The kinetic experiments were performed with various aqueous mixtures of formaldehyde and phenol, as well as in the presence of added benzyl alcohol. The rate constant for sodium hydroxide catalyzed formation of

* Presented in part at the 151st National Meeting of the American Chemical Society, Pittsburgh, Pennsylvania, March 1966, and at the 153rd National Meeting, Miami Beach, Florida, April 1967.

† Present address: Royal Hellenic Research Foundation, 48 Vassileos Constantinou Avenue, Athens 516, Greece.

TABLE I
Rate Constants for the Formation of the Monohydroxy-
methylphenols According to Eq. (1)

| Run | Temp., °C | $[\text{C}_6\text{H}_5\text{O}^-]_0$, <i>M</i> | $[\text{F}]_0$, <i>M</i> | $[\text{C}_6\text{H}_5\text{OH}]_0$, <i>M</i> | $[\text{H}_2\text{O}]_{\text{tot}}$, <i>M</i> | $k \times 10^4$, l/mole-sec |
|----------------|--------------|--|------------------------------|---|---|---------------------------------|
| A | 57 | 0.0953 | 9.46 | 4.65 | 20.8 | 5.30 |
| B | 57 | 0.0462 | 8.31 | 4.80 | 21.3 | 6.67 |
| C | 57 | 0.0489 | 7.01 | 4.95 | 22.2 | 7.33 |
| D ^a | 57 | 0.0449 | 9.49 | 2.85 | 18.3 | 3.69 |
| E ^b | 57 | 0.0449 | 9.45 | 1.90 | 18.5 | 3.00 |
| F | 57 | 0.0124 | 2.02 | 0.99 | 47.1 | 7.31 |
| G | 30 | 0.0314 | 2.12 | 1.00 | 46.9 | 0.55 |
| H | 30 | 0.0937 | 9.19 | 4.71 | 20.9 | 0.34 |

^a In the presence of 1.88*M* benzyl alcohol.

^b In the presence of 2.85*M* benzyl alcohol.

the monohydroxymethylphenols was determined from the initial rate of disappearance of formaldehyde and the concentration of the reactants at time = 0, according to eq. (1). The concentration of the reactive phenolic species (phenoxide ion) was always kept below 0.1*M*; under these conditions, the large amount of phenol present acts only as a cosolvent, and the total concentration of phenol is not involved in the rate expression. The results are summarized in Table I. Water constituted about 94 mole-% of the system in runs F and G; all other runs were performed in systems that were mostly nonaqueous on a weight basis.

Figure 1 shows some of the kinetic plots. It should be noted at this point that such plots are normally curved in straightforward second-order reactions.

Several irregularities are evident in Table I. The rate constants of

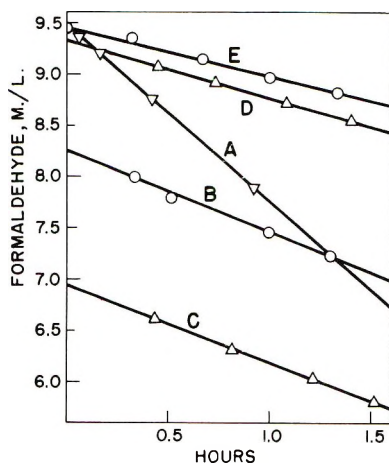


Fig. 1. Total unreacted formaldehyde concentration vs. reaction time, at 57°C. The lines are labeled according to the entries of Tables I and II. The reasons for the unexpected linearity become evident in ref. 15.

ion-molecule reactions are usually not affected drastically by changes of the dielectric constant of the medium in mixed solvents, but they usually increase as the dielectric constant decreases.⁶ Runs G and H demonstrate an opposite behavior in the phenol-formaldehyde reaction; the rate constant decreased by 38% in going from the high-dielectric system G (94 mole-% H₂O) to system H, in which phenol, with a dielectric constant of only 9, is a cosolvent to the extent of about 40 wt-%.* The same unusual solvent effect is evident from a comparison of runs F and A. Much less drastic variations in the dielectric constant of the medium in runs A, B, and C, led to unreasonably large changes in the rate constant. Evidently, the general rate expression, as given by eq. (1), is unsatisfactory.

Formaldehyde Equilibria

Equation (1) makes the implicit assumption that the rate is proportional to total unreacted formaldehyde. This is questionable in view of the well known equilibria of formaldehyde in aqueous solutions.^{5b,7-11}



The hydration equilibrium [eq. (2)] lies far to the right; the polymer equilibria are quite extensive, with detected values of n [eq. (4)] exceeding 10 in concentrated solutions. The usual titrimetric procedures detect the total available formaldehyde that has not reacted irreversibly. We proceeded on the assumption that the rate is proportional to the concentration of the monomeric hydrate only, HOCH₂OH. There are several methods for calculating the fraction of formaldehyde (hereafter denoted by m) present in this form, if the total concentration is known.^{7,11,12} These methods, however, are quite complex in view of the large number of equilibrium reactions that must be taken into account, and are, therefore, of limited value in providing a convenient estimate of the concentration of HOCH₂OH, especially in systems where formaldehyde is a reactant and m must be calculated repeatedly as a function of the changing overall concentration.

We were able to calculate quite accurate values for m by a simple averaging treatment. The average degree of polymerization (excluding monomer) of the α, ω -poly(oxyethylene) diols [eq. (4)] is nearly 3 for concentrated solutions.^{7,11} Consequently, we treated the overall equilibria of hydrated formaldehyde as shown in eq. (5),



and we investigated the possibility that, with the appropriate choice of Q_1 , contributions from dimers would nearly cancel out contributions from

* The dielectric constant of hydrated formaldehyde, HOCH₂OH, is estimated near 45, since for ethylene glycol it is 37.

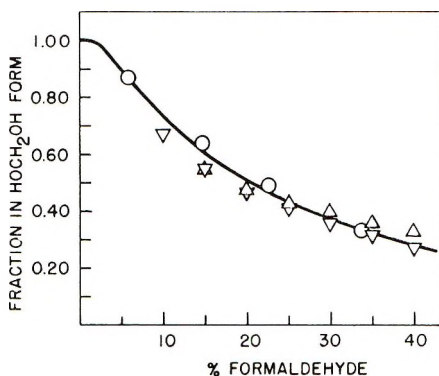


Fig. 2. Fraction of monomeric hydrate vs. wt-% formaldehyde in water: (—) curve calculated according to eq. (6); (O) experimental at 20°C;¹³ (∇) experimental at 35°C;⁷ (Δ) experimental at 100°C.⁷

tetramers, pentamers, etc. A similar equation has been found to fit partial pressure data by the appropriate choice of Q_1 .¹³ Equation (5) implies that, starting from monomer, the initial rate of polymerization would be third order in HOCH_2OH . It is interesting to note that, in a study of similar equilibria in butyraldehyde–polybutyraldehyde systems, the early rates of pressure induced polymerization fit an empirical rate equation with third-order dependence on aldehyde.¹⁴

Some experimentally determined values for m at 20, 30, and 100°C are shown in Figure 2; they all follow a rather smooth pattern. The available data are fitted quite well by eq. (6).

$$Q_1 = 45 = \frac{[\text{HO}(\text{CH}_2\text{O})_3\text{H}][\text{H}_2\text{O}]^2}{[\text{HOCH}_2\text{OH}]^3} \quad (6)$$

The concentration of water in eq. (6) is obtained from the total stoichiometric amount of water placed in the system after subtraction of the amount consumed in hydrating formaldehyde [eq. (7)].

$$[\text{H}_2\text{O}] = [\text{H}_2\text{O}]_{\text{tot}} - [\text{HOCH}_2\text{OH}] - [\text{HO}(\text{CH}_2\text{O})_3\text{H}] \quad (7)$$

The curve in Figure 2 shows the values for m calculated from the equivalent of eq. (6) (see Appendix) after conversion from concentrations to weight per cent. It is fortunate that m is insensitive not only to temperature,^{5b,11} but also to pH;^{5b} only the rate at which the equilibrium value is attained is temperature- and pH-dependent.

Our assumption that the reaction rate is proportional to the monomeric form of hydrated formaldehyde only, is incorporated in the rate expression in eq. (8).

$$\text{Rate} = k[\text{P}_i^-][\text{F}]m = k[\text{C}_6\text{H}_5\text{O}^-][\text{HOCH}_2\text{OH}] \quad (8)$$

Recalculation of rate constants from the data of experiments A–H according to eq. (8) gave the values listed in Table II. The fraction of formaldehyde present in the form of monomeric hydrate (m) was calculated as shown in the Appendix.

TABLE II
Rate Constants for the Formation of the Monohydroxymethylphenols
According to Eq. (8)

| Run | Temp, °C | [HOCH ₂ OH] ₀ , <i>M</i> | [C ₆ H ₅ O ⁻] ₀ , <i>M</i> | [H ₂ O] _{tot} , <i>M</i> | <i>m</i> ₀ | <i>k</i> × 10 ⁴ , l/mole-sec |
|----------------|-------------|---|--|---|-----------------------|--|
| A | 57 | 2.40 | 0.0953 | 20.8 | 0.25 | 21.2 |
| B | 57 | 2.41 | 0.0462 | 21.3 | 0.29 | 23.3 |
| C | 57 | 2.38 | 0.0489 | 22.2 | 0.34 | 21.9 |
| D ^a | 57 | 2.18 | 0.0449 | 18.3 | 0.23 ^c | 16.2 |
| E ^b | 57 | 2.17 | 0.0449 | 18.5 | 0.23 ^c | 13.0 |
| F | 57 | 1.70 | 0.0124 | 47.1 | 0.84 | 8.70 |
| G | 30 | 1.76 | 0.0314 | 46.9 | 0.83 | 0.66 |
| H | 30 | 2.39 | 0.0937 | 20.9 | 0.26 | 1.31 |

^a In the presence of 1.88*M* benzyl alcohol.

^b In the presence of 2.85*M* benzyl alcohol.

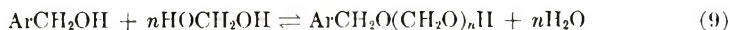
^c Disregarding hemiformal equilibria.

The average value of the rate constant in runs A, B, and C is 22.1×10^{-4} l/mole-sec, the average deviation being only 3.5%. This constancy, over a 36% variation in *m*₀, indicates that the method of calculating *m* is sufficiently accurate and that the rate constants are fairly insensitive to small variations in the dielectric constant of the medium, in accord with the established behavior of ion-molecule reactions. Comparisons of the rate constants for mostly aqueous and mostly nonaqueous conditions both at 30°C (runs G and H) and at 57°C (runs F and A) now show a change of reasonable magnitude and in the expected direction for ion-molecule reactions.

Complete kinetic investigations including analyses for all products up to 70% reaction of phenol¹⁵ gave a value of $k = 22.4 \times 10^{-4}$ l/mole-sec under conditions similar to those of runs A, B, and C of Table II, and 8.5×10^{-4} for the conditions of run F, in good agreement with Table II. Under very dilute conditions (*m*₀ = 0.999) at 30°C, a value of 0.69×10^{-4} has been reported;³ this is in good agreement with run G (*m*₀ = 0.83) and attests to the sufficient accuracy of our method of calculating *m*. The value of *m* in runs A-E and H shows that the equilibria exert a major effect on the rate, in systems composed primarily of phenol and concentrated aqueous formaldehyde; e.g., in run A, 75% of the available formaldehyde does not contribute to the rate at the start of the reaction. The equilibria, therefore, cannot be neglected, except in extremely dilute solutions in which *m* is essentially 1.0.

Hemiformal Equilibria

Runs D and E, in which the dielectric constant of the medium is similar to that of runs A-C, demonstrate the effect on the rate of the well known hemiformal equilibria between formaldehyde and alcohols, eq. (9)^{5b}



It is now reasonable to expect that any formaldehyde tied up as hemiformal is not directly involved in the rate of the hydroxymethylation reaction with phenol. The hemiformal equilibria are quite extensive, and the *m*-correction based on eq. (6) alone is incapable of bringing the rate constants for runs D and E into line with those of runs A-C. Benzyl alcohol was used as a model for the hydroxymethylphenols that are the products of our reaction; its retarding effect is substantial and it indicates that kinetic investigations of the phenol-formaldehyde system that are extended beyond a few per cent conversion,^{16,17} or are carried out with the individual hydroxymethylphenols,^{1,4,16} cannot give meaningful results without accounting for both types of equilibria. This has been accomplished in the accompanying paper.¹⁵ Failure to account for the equilibria has led to a large number of apparently conflicting results among different kinetic investigations.¹⁶

At the temperatures of our experiments and in the pH range employed, 8.0-8.5, we found no indication that the rate at which the formaldehyde and hemiformal equilibria are attained ever became the limiting rate for the base-catalyzed hydroxymethylation reaction with phenol.

The rate retarding effect of alcohols has been noted in a high-temperature uncatalyzed reaction of formaldehyde with resorcinol;¹⁸ evidence for the importance of the formaldehyde equilibria has been reported in a reaction with urea.¹⁹

EXPERIMENTAL

Materials

Phenol was reagent grade, vacuum-redistilled before use. Formaldehyde was 50 wt-% aqueous solution, methanol-free commercial material (less than 0.9 wt-% methanol) and contained traces of formic acid; it was kept warm from the time of its manufacture. Benzyl alcohol was redistilled reagent grade material and was used without further purification.

Kinetic Runs

All experiments were performed as follows: phenol, formaldehyde, and any water or benzyl alcohol, were weighed into a three-necked flask immersed in a constant temperature bath controlled to $\pm 0.3^\circ\text{C}$ at the desired temperature. After temperature equilibration, the required amount of a standard solution of sodium hydroxide was added with stirring; this amount was too small to change the temperature of the mixture appreciably. The time of completion of the addition of base was taken as time zero. An aliquot was removed immediately for determination of initial conditions; phenol was determined by GLC¹⁵ in duplicate, and formaldehyde by titration by the hydroxylamine hydrochloride method.^{5a} Aliquots were removed at proper intervals for formaldehyde analyses and the experiments were terminated when about 10% had reacted. The density

of the kinetic mixture was determined independently on an identical mixture of materials at the temperature of the kinetic run. The total available water was calculated by difference, from the total weight minus the analytically determined weights of phenol and formaldehyde. The concentration of benzyl alcohol was calculated from the weight charged. The concentration of sodium hydroxide was calculated from the amount charged minus the amount required to neutralize traces of formic acid present in each batch of formaldehyde (determined independently); it was converted to concentrations by the appropriate density corrections. For the limited extent of reaction studied the density was found to remain essentially invariant.

APPENDIX

Equation (10) is equivalent to eq. (6):

$$45 = (1/3)[F](1 - m) [H_2O]^2/[F]^3m^3 \quad (10)$$

Equation (11) is equivalent to eq. (7):

$$[H_2O] = [H_2O]_{tot} - m[F] - (1/3)(1 - m) [F] \quad (11)$$

[F] in eqs. (10) and (11) denotes the total titrimetric^{5a} amount of formaldehyde that has not reacted irreversibly. The above two equations can be combined by elimination of one of the unknowns, [H₂O], and solved explicitly for *m*. We solved eq. (10) by an iterative procedure²⁰ by making an initial estimate of *m* and updating eq. (11) after each iteration; initially we set [H₂O] = [H₂O]_{tot}. The procedure succeeds because [H₂O] converges fast.

The skillful technical assistance of Mr. K. Kozlowski is gratefully acknowledged; we thank Mrs. L. R. Zavitsas for her assistance in the writing of the *m*-function programs, and Mr. R. D. Beaulieu for many helpful discussions.

References

1. J. H. Freeman and C. W. Lewis, *J. Amer. Chem. Soc.*, **76**, 2080 (1954).
2. H. G. Peer, *Rec. Trav. Chim.*, **78**, 851 (1959).
3. R. Dijkstra, J. de Jonge, and M. F. Lammers, *Rec. Trav. Chim.*, **81**, 285 (1962).
4. L. M. Yeddanapalli and V. V. Gopalakrishna, *Makromol. Chem.*, **32**, 112 (1959).
5. J. F. Walker, *Formaldehyde*, 3rd ed., Reinhold, New York, 1964, (a) p. 493; (b) Chap. 3.
6. C. K. Ingold, *Structure and Mechanism in Organic Chemistry*, Cornell Univ. Press, Ithaca, N. Y., 1953, p. 345.
7. A. Iliceto, S. Bezzi, N. Dallaporta, and G. Giacommetti, *Gazz. Chim. Ital.*, **81**, 915 (1951).
8. P. Skell and H. Suhr, *Ber.*, **94**, 3317 (1961).
9. Y. Ihashi, K. Sawa, and S. Morita, *J. Chem. Soc. Japan*, **68**, 1427 (1964).
10. A. A. Babushkin, L. M. Krylova, and A. I. Gorshin, *Zh. Fiz. Khim.*, **38**, 2365 (1964).
11. K. Moedritzer and J. R. Van Wazer, *J. Phys. Chem.*, **70**, 2025 (1966).

12. L. C. D. Groenweghe, J. R. Van Wazer, and A. W. Dickinson, *Anal. Chem.*, **36**, 303 (1964).
13. J. F. Walker, *J. Phys. Chem.*, **35**, 1104 (1931).
14. Y. Ohtsuka and C. Walling, *J. Amer. Chem. Soc.*, **88**, 4167 (1966).
15. A. A. Zavitsas, R. D. Beaulieu, and J. R. LeBlanc, *J. Polym. Sci. A-1*, **6**, 2541 (1968).
16. R. W. Martin, *The Chemistry of Phenolic Resins*, Wiley, New York, 1956, chap. 10.
17. M. M. Sprung, *J. Amer. Chem. Soc.*, **63**, 334 (1941).
18. R. A. V. Raff and B. H. Silverman, *Can. J. Chem.*, **29**, 857 (1951).
19. G. A. Crow and C. C. Lynch, *J. Amer. Chem. Soc.*, **71**, 3731 (1949).
20. L. Lapidus, *Digital Computations for Chemical Engineers*, McGraw-Hill, New York, 1963.

Received August 18, 1967

Revised January 15, 1968

Base-Catalyzed Hydroxymethylation of Phenol by Aqueous Formaldehyde. Kinetics and Mechanism*

ANDREAS A. ZAVITSAS,† RAYMOND D. BEAULIEU,
and JOHN R. LEBLANC,

*Research Department, Plastic Products and Resins Division,
Monsanto Company, Springfield, Massachusetts 01101*

Synopsis

The effects of formaldehyde and hemiformal equilibria on the rates of the base-catalyzed and hydroxymethylations of phenol by aqueous formaldehyde have been treated quantitatively. A kinetic model treating all seven simultaneous, parallel, consecutive, and competing reactions, as well as the equilibria, has been shown to apply to a wide variety of conditions and to data from other works. Concentration-induced solvent effects on the rates and on the *ortho/para*-substitution patterns have been studied. The temperature dependence of the rate constants, both for dilute systems and systems composed primarily of phenol and aqueous formaldehyde, has been determined.

Previous extensive work on the base-catalyzed hydroxymethylation of phenol by aqueous formaldehyde has failed to establish the kinetic order of the reaction under any but extremely dilute conditions. The reaction has been described as kinetically first-order, second-order, or of fractional orders;^{1,2} in addition, there have been reports of dependence of the rate constants on the ratio of formaldehyde to phenol,^{3,4} on the concentration of phenol,⁵ and on empirical functions of the concentration of catalyst.^{3,4} No plausible explanation has been advanced for these apparent peculiarities. At high dilutions and pH not exceeding 10, the established rate expression is given by eq. (1).^{6,7}

$$\text{Rate} = k[\text{P}_i^-][\text{F}] \quad (1)$$

where P_i^- denotes phenoxide anion, and F unreacted formaldehyde as determined by the usual titrimetric procedures, commonly the hydroxylamine hydrochloride method.^{8a}

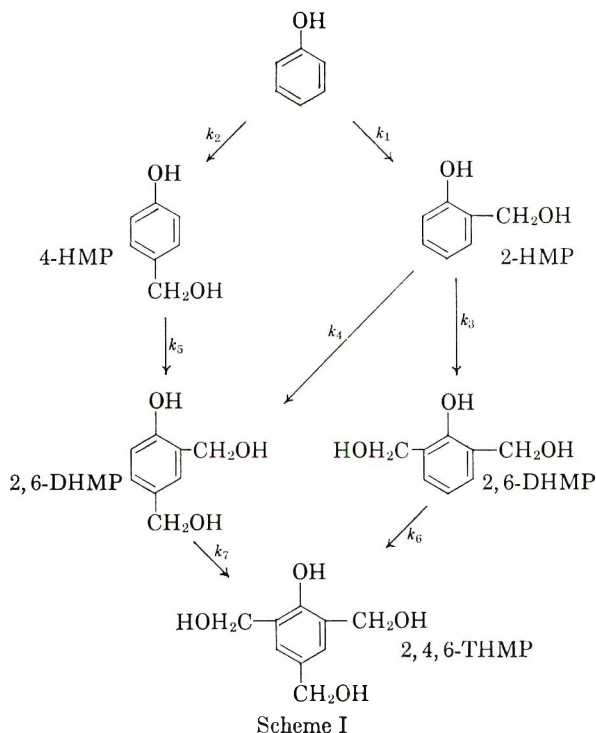
All but one of the previous kinetic investigations have been handicapped by one or more of the following limitations: only the disappearance of formaldehyde was followed; the reaction was followed for only a few per

* Presented in part at the 153rd Meeting, American Chemical Society, Miami Beach, Florida, April 9-14, 1967.

† To whom inquiries should be addressed. Present address: Royal Hellenic Research Foundation, 48 Vassileos Constantinou Avenue, Athens 516, Greece.

cent conversion, and artificial restrictions were imposed on the ratio of the reactants.^{1,2}

The only investigation that followed the rates of appearance and disappearance of all phenolic components (scheme I)⁹ has been that of Free-



man and Lewis;¹⁰ it has remained as the cornerstone of our understanding of the reaction. Under concentrated conditions (phenoxide anion about 1.8*M*, formaldehyde about 6*M*), the general rate expression of eq. (1) was used, at high pH. The present availability of high-speed digital computers has allowed us to check the accuracy of the rate constants thus obtained; we found that they would not fit the data from which they were derived.

In addition, the *ortho* to *para* ratio of initial substitution with sodium hydroxide catalysis at 30°C has been reported as 1.1,⁶ 1.5⁷ and 1.7,¹⁰ in apparent contradiction.

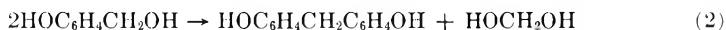
We can show now that much of the existing confusion can be attributed to the unsuspected effect of formaldehyde equilibria on the rate of the reaction.¹¹

RESULTS

Our kinetic investigation concentrated primarily on the two regions of composition that are of major interest and in which most of the previous data have been collected; our systems either contained well in excess of 90

mole-% water, or were essentially mixtures of phenol and concentrated aqueous formaldehyde (50 wt-%). The concentration of reactive phenolic species (phenoxide anions) was, in all cases, of the order of 0.1*M*, usually less; any additional un-ionized phenols present simply act as cosolvents and are not directly involved in the kinetic expressions.

We analyzed for all components in scheme I and for formaldehyde; the kinetic runs were terminated when diphenylmethane-type dimers from self-condensation of the hydroxymethylphenols, eq. (2), amounted to 2–4 mole-% of the phenolic components. This limitation did not prove too



restrictive, for reaction (2) is slow¹⁰ at the temperature of our experiments. In all cases, at the termination of the run, the rate of disappearance of phenol had decreased to less than one-tenth of its initial value (65–70% reaction of phenol).

Kinetic Model

When the rate constants are known, the system of scheme I can be simulated on a computer by a numerical solution of the seven rate equations that describe the rate of change of the concentration of each component, eqs. (3)–(9). The rate equations involve the concentration of each

$$-d[\text{C}_6\text{H}_5\text{OH}]/dt = [\text{HOCH}_2\text{OH}](k_1 + k_2)[\text{C}_6\text{H}_5\text{O}^-] \quad (3)$$

$$d[2\text{-HMP}]/dt = [\text{HOCH}_2\text{OH}]\{k_1[\text{C}_6\text{H}_5\text{O}^-] - (k_3 + k_4)[2\text{-HMP}^-]\} \quad (4)$$

$$d[4\text{-HMP}]/dt = [\text{HOCH}_2\text{OH}]\{k_2[\text{C}_6\text{H}_5\text{O}^-] - k_5[4\text{-HMP}^-]\} \quad (5)$$

$$d[2,6\text{-DHMP}]/dt = [\text{HOCH}_2\text{OH}]\{k_3[2\text{-HMP}^-] - k_6[2,6\text{-DHMP}^-]\} \quad (6)$$

$$d[2,4\text{-DHMP}]/dt = [\text{HOCH}_2\text{OH}]\{k_4[2\text{-HMP}^-] + k_5[4\text{-HMP}^-] - k_7[2,4\text{-DHMP}^-]\} \quad (7)$$

$$d[2,4,6\text{-THMP}]/dt = [\text{HOCH}_2\text{OH}]\{k_6[2,6\text{-DHMP}^-] + k_7[2,4\text{-DHMP}^-]\} \quad (8)$$

$$-d[F]/dt = [\text{HOCH}_2\text{OH}]\{(k_1 + k_2)[\text{C}_6\text{H}_5\text{O}^-] + (k_3 + k_4)[2\text{-HMP}^-] + k_5[4\text{-HMP}^-] + k_6[2,6\text{-DHMP}^-] + k_7[2,4\text{-DHMP}^-]\} \quad (9)$$

phenolic species in the anion form; these are related to total (analytical) concentrations by a system of six simultaneous algebraic equations, e.g., eqs. (10), (11), (12), etc., which involve the acid ionization constant (*K*_{*i*})

$$\Sigma[\text{P}_i^-] = [\text{base}]$$

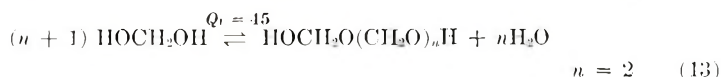
$$\frac{[\text{P}_2^-]}{[\text{P}_1^-]} = \frac{K_2}{K_1} \frac{[\text{P}_2]_{\text{tot}} - [\text{P}_2^-]}{[\text{P}_1]_{\text{tot}} - [\text{P}_1^-]} \quad (11)$$

$$\frac{[\text{P}_3^-]}{[\text{P}_2^-]} = \frac{K_3}{K_2} \frac{[\text{P}_3]_{\text{tot}} - [\text{P}_3^-]}{[\text{P}_2]_{\text{tot}} - [\text{P}_2^-]} \quad (12)$$

of each phenolic component and the total amount of base. The acid constants¹² and their temperature dependence have been determined.^{13*} The total amount of base would be known in each case.

In addition, to obtain the concentration of HOCH₂OH, the fraction of formaldehyde in the form of monomeric hydrate, m ,¹¹ must be calculated from the total (analytical) concentration at each step of the numerical solution of the rate equations.

The equilibria of formaldehyde with itself have been described by eq. (13), and the method for calculating their effect on m has been given.¹¹



In the presence of the hydroxymethylphenols (scheme I), m will also become dependent on hemiformal equilibria of the type shown in eq. (14).



The following section describes the derivation of a method for calculating the effects of both equilibria on m .

Thus, given a set of rate constants, k_1 – k_7 , and the acid ionization constants, K_1 – K_6 , for each compound in scheme I, a numerical solution of the rate equations [with simultaneous evaluation of m and the algebraic equations (10), (11), (12), etc., at each step] will give the composition of a reacting system as a function of time for any combination of initial concentrations of phenol, formaldehyde, base, and total available water in the system.

Hemiformal Equilibria

Hemiformal equilibria between alcohols and formaldehyde are known to be quite extensive.^{8b,14} The hemiformals of the hydroxymethylphenols have been shown to be stable enough to yield acetate derivatives which have been analyzed by chromatography and nuclear magnetic resonance spectrometry.^{15,16} We have demonstrated the retarding effect of alcohols on the rate of the hydroxymethylation reaction.¹¹

Available information regarding the relative importance of the reactions shown in eqs. (13) and (14) indicates that they are roughly comparable, the hemiformal equilibria being somewhat more extensive. In experiments in which formaldehyde was allowed to partition itself among equal volumes of water and immiscible alcohols, usually more than half was found in the alcohol layer.¹⁷ The heats of solution of gaseous formaldehyde in water and methanol are -14.8 and -15.0 kcal/mole, respectively.¹⁸

Qualitatively, the effects of the formaldehyde and the hemiformal equilibria on m will be in opposite directions in this kinetic system; the decrease in the concentration of formaldehyde with extent of reaction will

* No temperature dependence data are available for the 2,6-isomer and the values used were obtained from data at 25°C.,¹² assuming a temperature coefficient similar to that of the other isomers.

tend to increase m , but the concurrent increase in the concentration of hydroxymethyl groups will tend to decrease its value [eq. (14)]. Each effect dampens the other and the overall reactivity of phenol-formaldehyde systems is kept from changing very drastically during reaction. This fortuitous partial cancellation of two major effects has allowed the use of apparent rate constants (without m -corrections) in describing the reaction without gross discrepancies.^{5,10}

A quantitative description of the hemiformal equilibria can be based on the obvious similarity between eqs. (13) and (14). The terminal alcoholic hydroxy groups are virtually the same, $-\text{CH}_2\text{OCH}_2\text{OH}$. Equation (14) makes no distinction among *ortho* and *para* hydroxymethyl groups or mono-, di-, and trihydroxymethylated phenols in terms of their tendency toward hemiformal formation. The work of Higginbottom et al.¹⁶ on the analysis of the hemiformals in mixtures of phenol, the five possible *ortho*- and *para*-substituted hydroxymethylphenols, and small amounts of formaldehyde, has shown, in a qualitative fashion, that the amount of each isomer in the hemiformal form depends on its number of hydroxymethyl groups and on the concentration of formaldehyde. No hemiformals of the phenolic hydroxy were found. We confirmed these findings by quickly freezing a similar mixture, acetylating and analyzing by GLPC. We found that the fraction of each hydroxymethylphenol present as hemiformal was very nearly proportional to its total number of hydroxymethyl groups; the type of group, *ortho* or *para*, was immaterial. The assignment of equal reactivity to all hydroxymethyl groups [eq. (14)] is therefore justified.

Because of the virtually identical endgroups in both equilibria, the average degree of polymerization would be expected to be the same and we assigned $n = 2$ in eq. (14), by analogy with eq. (13). The equilibria would be expected to behave very similarly, even though the polyoxymethylene diols can grow from either end of the molecule, whereas the hemiformals cannot; this statistical factor is completely cancelled out by the opposing statistical factor for depolymerization. The chemical behavior in terms of temperature and pH effects would also be expected to be very similar, and these factors have been shown not to be very significant in the equilibria of formaldehyde with itself.^{3b,11}

The hemiformal equilibria can now be summarized by a pseudoequilibrium expression [eq. (15)], where ArCH_2OH denotes the concentration

$$Q_2 = \frac{[\text{ArCH}_2\text{O}(\text{CH}_2\text{O})_2\text{H}][\text{H}_2\text{O}]^2}{[\text{ArCH}_2\text{OH}][\text{HOCH}_2\text{OH}]^2} \quad (15)$$

of hydroxymethyl groups. Our extensive kinetic data allowed us to determine a value for Q_2 .

Early attempts to fit the data with a set of rate constants, without any account being taken of the equilibria, had shown an apparent decrease in the reactivity of the system with extent of reaction, i.e., numerical solutions of the rate equations could be made to fit the data only if the rate constants used were arbitrarily but uniformly decreased as the reaction proceeded.

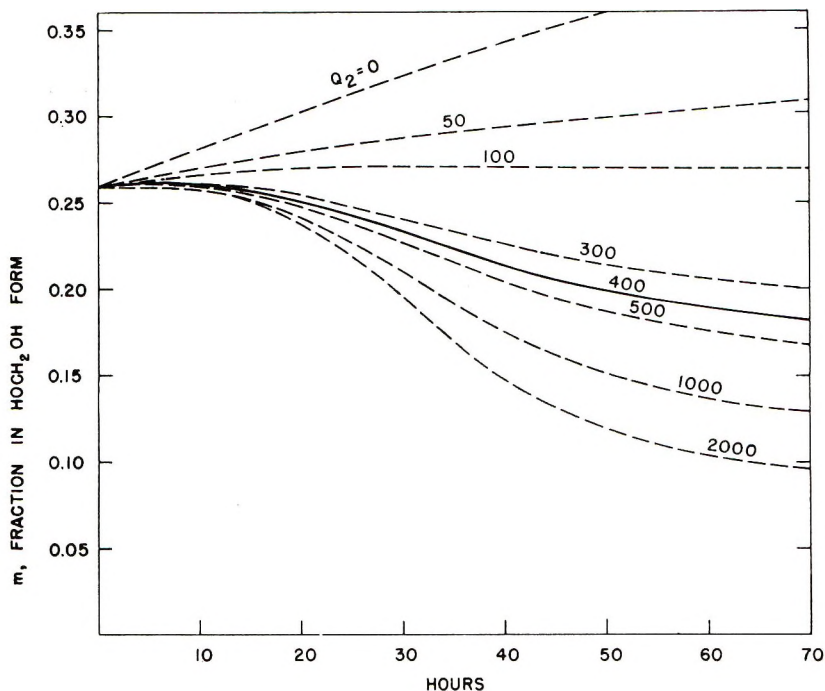


Fig. 1. Fraction of monomeric hydrated formaldehyde vs. time, for run K, as a function of Q_2 .

Quantitative estimates of this decrease were made, and inverted S-shaped curves similar to those in Figure 1 were obtained. Apparently, the value of m was decreasing during the run. The pseudo-equilibrium equations describing the formaldehyde and the hemiformal equilibria were combined, and m was calculated at various stages of our reactions as a function of arbitrarily chosen values of Q_2 (see Appendix). Plots for kinetic run K (Table I) are shown in Figure 1. A value of $Q_2 = 400$ accounted best for the observed apparent decrease in the reactivity of the system. The procedure was repeated for runs L and M, and a value of $Q_2 = 400 \pm 30$ was obtained. Other values of n in eq. (14) were also investigated, including fractional values; the point of inflection was found to be a function of n . A value of $n = 2$ best fits the observed inflection in the apparent reactivity. Figure 1 shows that the value of m is not affected much by small uncertainties in Q_2 ; it is also seen that the opposing nature of the two equilibria keeps the value of m from changing more drastically. This partial cancellation of two major effects has effectively concealed the importance of the equilibria in extensive kinetic studies over the last several decades.^{1,2}

Determination of the Rate Constants

The type of experimental data obtained are exemplified by the points in Figures 2-5, corresponding to runs L and M. An initial estimate was obtained for the rate constants by solving the seven simultaneous rate

TABLE I
 Experimental Conditions and Calculated Rate Constants^a

| | Run I | Run J | Run K | Run L | Run M |
|--|----------|----------|----------|----------|----------|
| Temp., °C. | 30.0 | 57.0 | 30.0 | 57.0 | 57.0 |
| [F] ₀ | 2.119 | 2.030 | 9.189 | 9.456 | 9.963 |
| [C ₆ H ₅ O ⁻] ₀ | 0.03138 | 0.01250 | 0.09369 | 0.09615 | 0.2320 |
| [C ₆ H ₅ OH] ₀ | 1.003 | 0.9583 | 4.710 | 4.680 | 4.815 |
| [H ₂ O] _{tot} | 46.9 | 47.2 | 20.9 | 20.8 | 21.0 |
| pH, approx. | 8.5 | 8.1 | 8.3 | 8.3 | 8.7 |
| <i>m</i> ₀ | 0.83 | 0.84 | 0.26 | 0.25 | 0.24 |
| <i>k</i> ₁ | 0.387 | 5.10 | 0.835 | 14.63 | 12.86 |
| <i>k</i> ₂ | 0.275 | 3.39 | 0.479 | 7.81 | 2.37 |
| <i>k</i> ₃ | 0.482 | 4.95 | 0.848 | 13.50 | 19.35 |
| <i>k</i> ₄ | 0.349 | 3.60 | 0.776 | 10.21 | 4.82 |
| <i>k</i> ₅ | 0.415 | 5.58 | 0.768 | 13.45 | 12.38 |
| <i>k</i> ₆ | 1.028 | 10.77 | 1.552 | 21.34 | 9.91 |
| <i>k</i> ₇ | 0.246 | 2.65 | 0.619 | 8.43 | 7.08 |
| <i>k</i> ₁ / <i>k</i> ₂ | 1.41 | 1.51 | 1.74 | 1.88 | 5.43 |

^a Rate constants in l/mole-sec × 10⁴. The base was NaOH for runs I-L, and MgO for run M.

equations in the derivative form; the slopes at each point were estimated in conjunction with the two adjacent points. The equations are redundant, and they were solved as a set of simultaneous linear regression equations.¹⁹ These rate constants were used as initial values in a nonlinear least squares iterative procedure which operates as follows:^{20,21} the approximate set of rate constants is used to simulate the reaction on a digital computer and the differences between experimental and calculated values are obtained. Then each rate constant is perturbed individually by a small amount (2-5%) and the effect of each perturbation on the differences is obtained

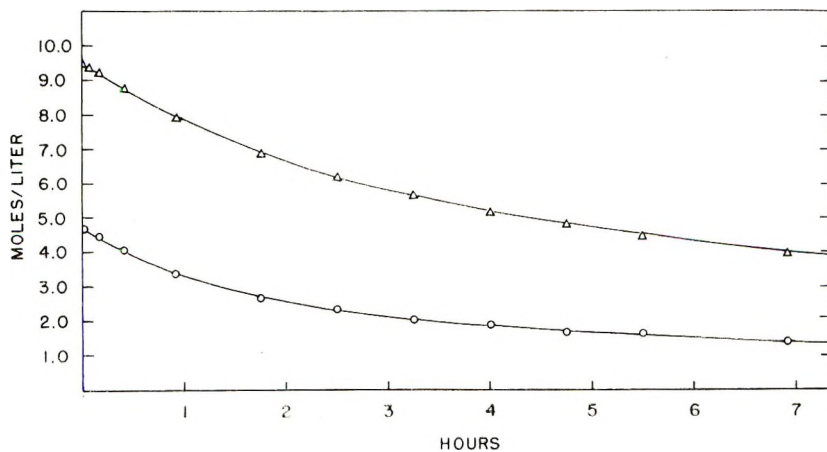


Fig. 2. Reactants vs. reaction time, for run L, at 57°C: (O) phenol; (Δ) formaldehyde. The curves were calculated with the corresponding rate constants from Table I.

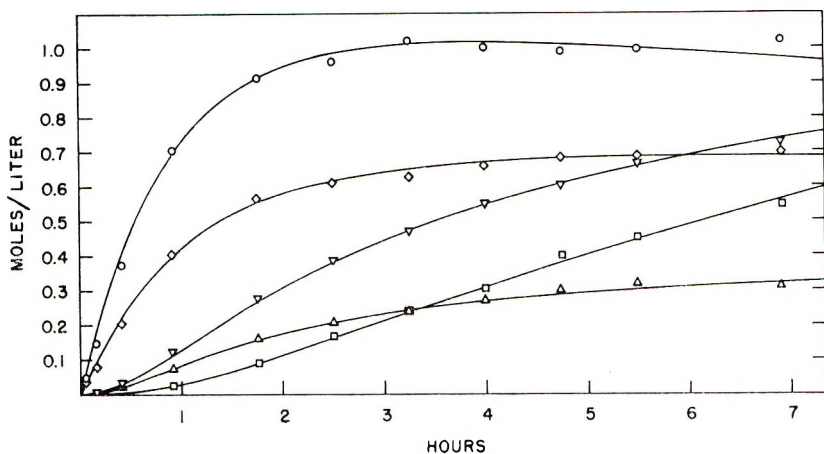


Fig. 3. Products vs. reaction time, for run L, at 57°C: (O) 2-HMP; (◇) 4-HMP; (△) 2,6-DHMP; (▽) 2,4-DHMP; (□) 2,4,6-THMP. Curves calculated as for Fig. 2.

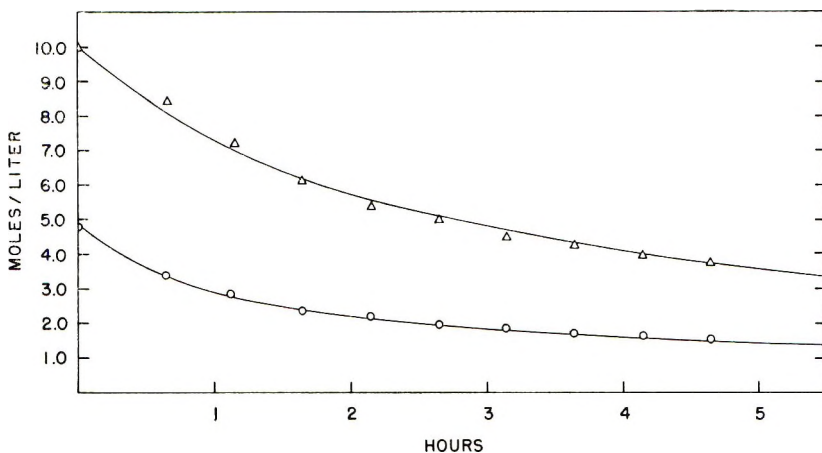


Fig. 4. Reactants vs. reaction time, for run M, at 57°C: (O) phenol; (△) formaldehyde. Curves calculated with the corresponding rate constants from Table I.

and used to derive a new set of improved rate constants. The whole procedure is repeated until the rate constants are no longer substantially affected by further iterations; thus all rate constants are derived simultaneously from all the data. The criterion used was maximization of the multiple correlation coefficients,¹⁹ a procedure that is nearly equivalent to minimizing the sum of the squares of the per cent error for all points.

The results of our five complete kinetic experiments are summarized in Table I. Runs K, L, and M, were essentially mixtures of phenol and concentrated aqueous formaldehyde; I and J were predominantly aqueous systems. The curves in Figures 2–5 were calculated by numerical solution of the rate equations (incorporating the m function of the Appendix) with the rate constants listed in columns L and M respectively, of Table I.

We investigated the general applicability of the rate constants listed in

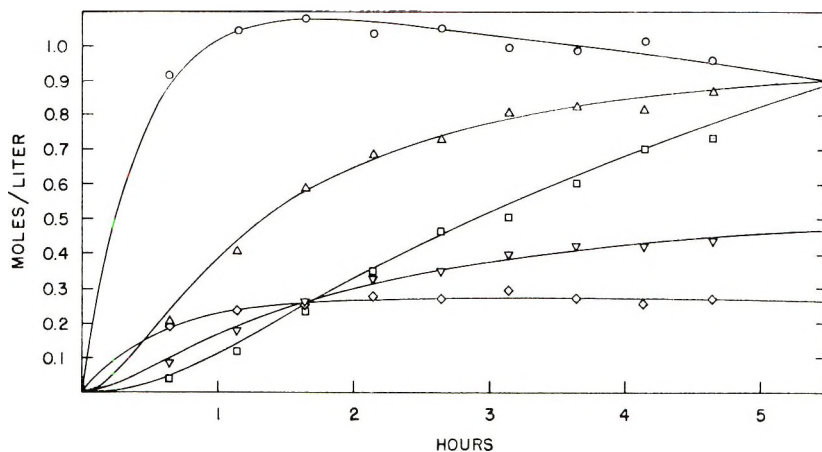


Fig. 5. Products vs. reaction time, for run M, at 57°C: (○) 2-HMP; (◇) 4-HMP; (△) 2,6-DHMP; (▽) 2,4-DHMP; (□) 2,4,6-THMP. Curves calculated as for Fig. 4.

Table I to a variety of reaction conditions and to several sets of data available from other works, and we found them successful. The following paragraphs summarize this phase of our investigation.

The limited sensitivity of the rate constants of ion-molecule reactions to small changes of the dielectric constant of the medium¹¹ would indicate that the rate constants listed in columns I and J of Table I will be applicable to all systems containing more than 90 mole-% water, and those of columns K and L to systems catalyzed by sodium hydroxide that are essentially mixtures of phenol and concentrated aqueous formaldehyde.

Data on the rate of disappearance of formaldehyde in very dilute systems at 30°C are available from the work of Dijkstra and de Jonge.^{7,22} We carried out a numerical solution of the rate equations including the m function, with the reported initial conditions and the rate constants of run I, Table I. The results are summarized in Table II. The agreement between calculated and reported values is excellent. The reported ratio of $k_1/(k_1 + k_2)$ was 0.59; column I, Table I, gives 0.585. It should be noted that our rate constants were determined with less than 2% of the phenolic components neutralized, whereas some of the data of Table II were obtained with up to 50% neutralization, in considerably more dilute systems, and with an eightfold smaller ratio of phenol to formaldehyde.

Variations in reactant ratio and amount of base were investigated in kinetic runs N and O. The rate constants derived from run L were used to predict the formaldehyde curve with the following system (run N; NaOH catalysis): temp = 57°C, $[C_6H_5O^-]_0 = 0.04388M$, $[F]_0 = 7.270M$, $[C_6H_5OH]_0 = 4.694M$, $[H_2O]_{tot} = 23.2M$, $m_0 = 0.33$. The calculated curve and the experimental points are essentially superimposable (Fig. 6).

The rate constants of run K were used to predict the reaction path in the following system (run O; NaOH catalysis): temp = 30°C, $[C_6H_5O^-]_0 = 0.2861M$, $[F]_0 = 8.470M$, $[C_6H_5OH]_0 = 4.770M$, $[H_2O]_{tot} = 21.5M$,

TABLE II
Experimental Values of Dijkstra et al.^{7,22} and Values Calculated
with the Rate Constants of Column I, Table I.

| Series A ^a | | | Series B ^b | | |
|-----------------------|------------------------|--------------------|-----------------------|------------------------|--------------------|
| Time, hr | Formaldehyde, <i>M</i> | | Time, hr | Formaldehyde, <i>M</i> | |
| | Exptl | Calcd ^c | | Exptl | Calcd ^c |
| 0.167 | 0.09527 | 0.0952 | 0.0458 | 0.04999 | 0.0499 |
| 0.333 | 0.09476 | 0.0945 | 0.5153 | 0.04965 | 0.0497 |
| 0.667 | 0.09316 | 0.0930 | 2.1528 | 0.04866 | 0.0487 |
| 1.000 | 0.09156 | 0.0915 | 4.6778 | 0.04713 | 0.0473 |
| 1.500 | 0.08955 | 0.0893 | 6.7500 | 0.04607 | 0.0461 |
| 2.000 | 0.08693 | 0.0872 | | | |
| 2.584 | 0.08472 | 0.0849 | | | |
| 3.100 | 0.08313 | 0.0828 | | | |
| 3.500 | 0.08141 | 0.0812 | | | |

^a Series A: $[C_6H_5OH]_0 = 0.4000M$; $[F]_0 = 0.09602M$; $[NaOH] = 0.2000M$; $m_0 = 0.999$.

^b Series B: $[C_6H_5OH]_0 = 0.2000M$; $[F]_0 = 0.05002M$; $[KOH] = 0.05000M$; $m_0 = 0.999$.

^c Our computer output format was written to truncate after the fourth decimal.

$m_0 = 0.28$. Analyses for each component after 28.0 hr of reaction gave values in good agreement with those calculated, as follows (experimental values in parentheses): $[F] = 3.914M$ (3.96 ± 0.08), $[C_6H_5OH] = 1.844M$ (1.86 ± 0.03), $[2\text{-HMP}] = 0.965M$ (0.95 ± 0.02), $[4\text{-HMP}] = 0.717M$ (0.71 ± 0.02), $[2,6\text{-DHMP}] = 0.236M$ (0.25 ± 0.01), $[2,4\text{-DHMP}] = 0.609M$ (0.61 ± 0.02), $[2,4,6\text{-THMP}] = 0.395M$ (0.39 ± 0.01).

The reliability of interpolations and extrapolations of the values of the rate constants listed in Table I to other temperatures was also tested with a run at 45°C and with data from other investigations, as shown below.

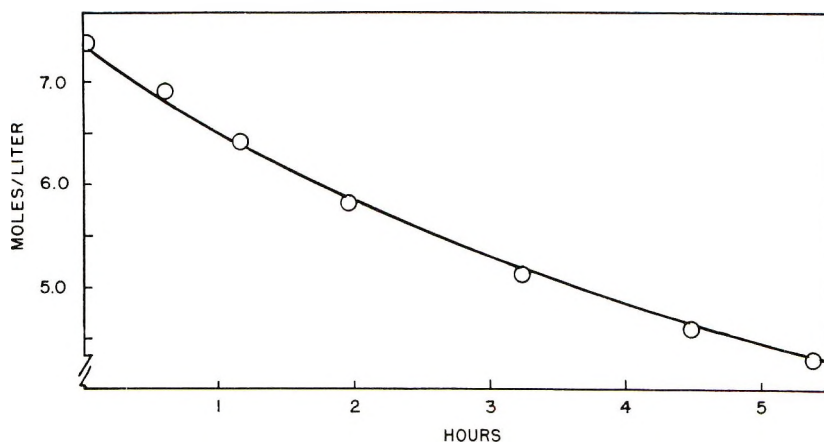


Fig. 6. Unreacted formaldehyde vs. reaction time, for run N, at 57°C. Curve calculated with the rate constants of run L from Table I.

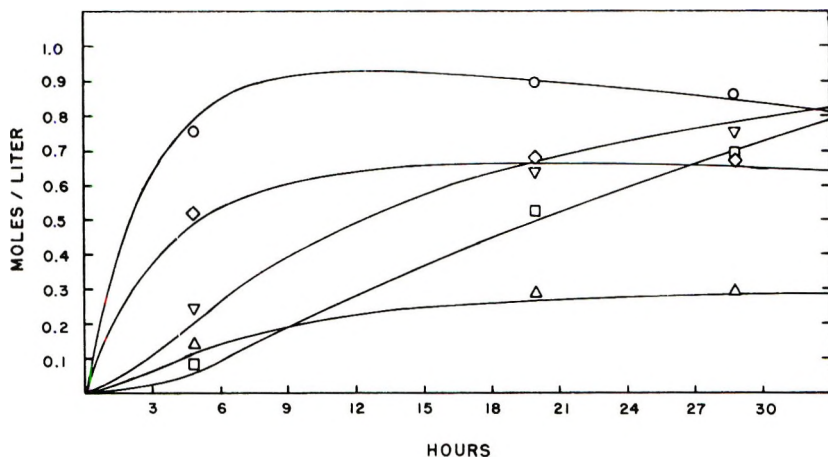


Fig. 7. Products vs. reaction time, for run P, at 45°C: (O) 2-HMP; (\diamond) 4-HMP; (Δ) 2,6-DHMP; (∇) 2,4-DHMP; (\square) 2,4,6-THMP. Curves calculated with temperature-interpolated rate constants from runs K and L.

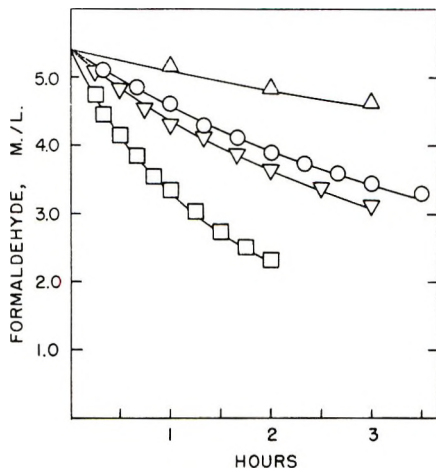


Fig. 8. Unreacted formaldehyde vs. reaction time (data of Debing et al.⁴): (Δ) $[\text{Na}^+]/[\text{P}]_0 = 0.02$, 40°C; (O) $[\text{Na}^+]/[\text{P}]_0 = 0.02$, 50°C; (∇) $[\text{Na}^+]/[\text{P}]_0 = 0.01$, 60°C; (\square) $[\text{Na}^+]/[\text{P}]_0 = 0.02$, 70°C. Curves calculated with temperature interpolated and extrapolated rate constants from runs K and L.

An experiment was performed with NaOH catalysis under the following conditions (run P): temp = 45°C $[\text{C}_6\text{H}_5\text{O}^-]_0 = 0.09370M$, $[\text{F}]_0 = 9.300M$, $[\text{C}_6\text{H}_5\text{OH}]_0 = 4.420M$, $[\text{H}_2\text{O}]_{\text{tot}} = 20.9M$, $m_0 = 0.26$. The experimentally determined concentrations of the products are shown in Figure 7; the curves were calculated with the rate constants obtained from a plot of $\log k$, from runs K and L versus $1/T^\circ\text{K}$. The agreement is within experimental error; the reactants were also predicted well with the interpolated rate constants.

Debing et al. have studied the kinetics of systems composed essentially

of phenol and aqueous 37 wt-% formaldehyde with a few per cent of the phenol neutralized by sodium hydroxide at different temperatures.⁴ The available data pertain to the rate of disappearance of formaldehyde at a formaldehyde to phenol ratio of 1.00; we made use of their experimental data up to the point where dimerization, eq. (2), would be expected to become significant.²³ Our calculated curves with the reported initial conditions and with rate constants obtained from plots of $\log k_i$ versus $1/T^\circ\text{K}$. from runs K and L are superimposable on their data (Fig. 8).

DISCUSSION

The effect of hydroxymethyl substitution on the reactivity of the remaining position of phenol can be derived from the rate constants of Table I. Contrary to previous reports,^{5,10,12} we find that *para* hydroxymethyl substitution has little effect (compare k_1 to k_5), as would be expected from the small value of the Hammett substituent constant for this group ($\sigma_p = 0.06$).¹³ Substitution in the *ortho* position, however, enhances the reactivity of both remaining positions (compare $k_1/2$ to k_3 , and k_2 to k_5); evidently *ortho* hydrogen bonding with the phenolic oxygen in the anion enhances the partial negative charge density on the remaining *ortho* and the *para* position.¹⁰

The substitution-induced reactivity increase more than compensates for the overall loss of available reactive phenolic positions at the early stages of the reaction; it contributes, along with the early slight increase in m (Fig. 1), to making the rate of disappearance of formaldehyde appear time-independent at the early stages of the reaction (Figs. 2 and 4).¹¹

We have shown that, in predominantly aqueous systems, the rate constants obtained with sodium hydroxide catalysis are also applicable with great accuracy to systems catalyzed by potassium hydroxide (Table II). Lithium hydroxide, under such conditions, is reported to lead to the same rates and *ortho* to *para* ratios.⁶ Magnesium hydroxide, under similar conditions, has been reported to lead to the same *ortho* to *para* ratio of substitution, within experimental error.²² These results with cations of different chelating tendencies and e/r indicate little, if any, involvement of the metal in the transition state for hydroxymethylation in predominantly aqueous systems.

In systems of lower dielectric constant, such as those containing large amounts of phenol, an increase in the *ortho* to *para* ratio of substitution is evident from the values of k_1/k_2 in Table I (compare runs I and K, and J and L). The different solvent effects exhibited by k_1 and k_2 are a clear indication of different mechanisms for *ortho* and *para* substitution in systems of lower dielectric constant. The effect is probably best explained in terms of increased likelihood of the existence of ion-pairs between phenoxide and metal ions in media of low dielectric, leading to *ortho* chelate type structures for the transition state of *ortho* substitution. Such structures have been proposed previously;^{1,2} they are not necessary for the reaction

to occur, but in media of low dielectric they promote *ortho* substitution. Bivalent metal ions would be expected to exhibit a greater tendency toward ion-pair formation and it is generally known that, in industrial systems, catalysis by barium, calcium, and magnesium hydroxides leads to higher extents of *ortho* substitution. The drastically different distribution of products between sodium and magnesium hydroxide catalysis in such systems can be seen from a comparison of Figures 3 and 5.

When a 15-fold excess of phenol was used as solvent for the reaction, sodium hydroxide catalysis at 30°C gave $k_1/k_2 = 4$. In toluene solvent with magnesium hydroxide catalysis and paraform (solid formaldehyde polymers, about 8 wt-% water content) at steam bath temperature, k_1/k_2 increased to 50, or 98% *ortho* substitution at the early stages of the reaction. Qualitative data on higher *ortho* substitution patterns with acid catalysts in organic solvents have been reported.^{24, 25}

In view of the involvement of the metal ion in systems containing large amounts of phenol, the rate constants for runs K and L (Table I) cannot be used to calculate rigorous activation parameters, because they essentially include the temperature dependence of the equilibrium constants for ion-pair formation; temperature extrapolations of the rate constants are successful for this reason. The activation energies that can be calculated from the high dielectric runs I and J are all quite similar, as would be expected for these seven closely related reactions, and they range from 17 to 19 kcal/mole; $\log A$ varies from 8 to 9.4 for the several reactions. Because of the relatively small differences and the uncertainties involved in calculating activation parameters, it would not be fruitful to attempt to derive mechanistic inferences from them.

The often encountered linear correlations between $\log k$ and functions of the dielectric constant of the medium²⁶ suggest a possible correlation between $\log k_i$ and the ratio of *ortho* to *para* substitution at the early stages of reaction, o/p . Such a correlation, if valid, would allow estimates of the rate constants to be made for aqueous systems intermediate between those studied here in detail, by the relatively easier evaluation of o/p at the outset of the reaction.²² The only complete kinetic data available from another investigation to date have been obtained by Freeman and Lewis under such intermediate conditions (water constituted approximately 82 mole-%);¹⁰ with sodium hydroxide catalysis at 30°C, the data¹ indicate $k_1/k_2 = 1.57$.

A plot of $\log k_i$ versus the initial *ortho* to *para* ratio for the rate constants of runs I (high dielectric) and K (low dielectric), allows interpolation of the rate constants at $o/p = 1.57$. A numerical solution of the rate equations, with the initial conditions reported¹⁰ and our interpolated rate constants, gave a good fit to the data, considering the high concentration of phenoxide ion used (approximately 1.8M) and the scatter of the experimental points. The agreement for the two most critical components (phenol and the ultimate product) is shown in Figure 9, along with the curves calculated by using the kinetic model and the rate constants of

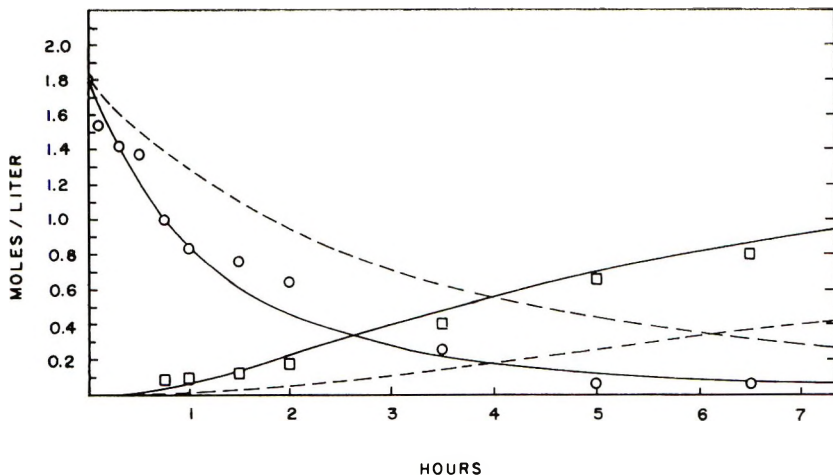


Fig. 9. Data of Freeman and Lewis¹⁰ at 30°C: (O) phenol, (□) 2,4,6-THMP; (---) calculated with the rate constants reported;¹⁰ (—) calculated with values interpolated from plots of $\log k_i$ vs. o/p (see text).

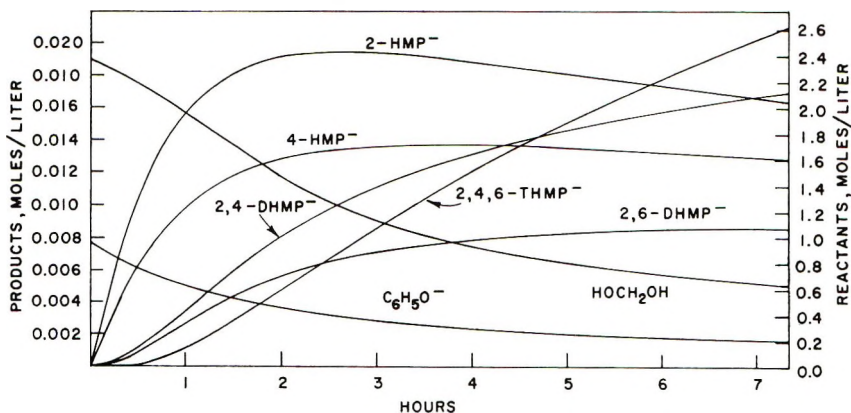


Fig. 10. Reactive species (anions and HOCH_2OH) vs. reaction time, for run L, at 57°C. Curves calculated with the corresponding rate constants from Table I. The phenoxide ion concentration is shown ten times greater than actual.

Freeman and Lewis.* The intermediate products were also predicted fairly well, but probably further work would be needed to firmly establish the linear relationship between $\log k_i$ and the dielectric constant of the medium as indicated by o/p .

The behavior of the curves describing the disappearance of phenol in seemingly approaching an asymptote at high levels such as shown in

* In experiments with the individual hydroxymethylphenols,¹⁰ the individual rate constants were determined under conditions leading to widely different values of m_0 . Combination of these rate constants with the complete experiment starting from phenol, with yet a different value of m_0 , could not give a self-consistent result. Also, the kinetic linearization procedure used to derive the rate constants from the data eliminated all dependence on formaldehyde and completely obscured the importance of the equilibria.

Figures 2 and 4 has led to speculation that the hydroxymethylation reaction may be a reversible process.¹ Work with model compounds has shown that the rate of the reverse reaction is nil.¹⁰ The approach of a quasi-equilibrium in phenol can be shown now to be due to three factors: (a) phenol, being the weakest acid,¹³ cannot compete favorably for the limited amount of base available once the concentration of the hydroxymethylphenols builds up; (b) the unreactive ultimate product, the strongest acid, in effect removes catalyst from the system; and (c) the overall reactivity of the system is suppressed at the later stages by the adverse effect of the hemiformal equilibria on m (Fig. 1).

An insight into the general behavior of the system and into the effects of the different acid strengths and the variation in m can be gained from a comparison of Figures 2 and 3 with Figure 10; the latter gives the concentration of the reactive species as a function of time for run L.

EXPERIMENTAL

Materials Used

Phenol was reagent grade, vacuum redistilled before use. Formaldehyde was 50 wt-% aqueous solution, methanol-free commercial material (less than 0.9% methanol) and it contained traces of formic acid (less than 0.05%). It was kept warm from the time of its manufacture to avoid precipitation of polymers. Standard solutions of sodium hydroxide were used for the kinetic runs. The magnesium oxide was reagent grade powder, higher than 99% assay. The paraform used assayed at 92% formaldehyde.

Kinetic Runs

All kinetic experiments were performed essentially as described below for run I, Table I: 37.6 g phenol, 48.0 g 50 wt-% aqueous formaldehyde, and 282.0 g distilled water, were mixed and placed in a 500-ml flask equipped with stirrer and thermometer and immersed in a constant temperature bath thermostatted at 30°C and cycling over a 0.3°C range. After temperature equilibration, a 25.00 ml portion of 0.5000*N* sodium hydroxide was added with stirring. The completion of the addition of the base was taken as time zero. An aliquot was withdrawn for determination of the starting concentrations and sampling was continued periodically. Each aliquot was placed in a vial, was tightly capped, and was immediately frozen in a mixture of Dry Ice and acetone; the vials were subsequently kept in a Dry Ice chest until they were analyzed. It was not found necessary to vigorously exclude air from the system; there was no significant color development, indicative of the highly colored quinoid oxidation products, during the kinetic runs. Dinuclear species amounted to less than 4% at the termination of the kinetic runs.

Analytical Procedures

The concentration of sodium hydroxide was calculated from the amount of standard solution added minus the amount needed to neutralize the

traces of formic acid usually present in our aqueous formaldehyde (determined independently of the kinetic run).

The density of the reacting mixture did not change appreciably during runs I and J; in runs K, L, and M the density increased about 4% during the times studied. For our calculations of concentrations, we assumed that the increase was linear with time. Density corrections were applied to all calculations. Formaldehyde was determined by the hydroxylamine hydrochloride method^{8a} as weight per cent, and the values were converted to molar concentrations. Duplicate determinations were run for each point.

Phenol was determined as weight per cent by GLPC of very dilute solutions of the reaction mixture (not greater than 1%) in acetone containing a known amount of *p*-cresol and one drop of dilute HCl. The analyses were performed on a 6 ft \times $\frac{1}{8}$ in. copper column packed with 2% Versamid-900 on 60-80 mesh Diatoport-S, maintained at 140°C (injector at 212°C). The instrument was equipped with a hydrogen flame ionization detector. At the temperatures employed, phenol can react with the hydroxymethylphenols and the formaldehyde present subsequent to injection; evidence of this is found at high sample concentrations. Values obtained for phenol by this method increase with increasing dilution and reach a plateau in the vicinity of 3-5 wt-% sample content. Our use of less than 1% assures correct values.²⁷ *p*-Cresol was advisedly used as the internal standard since its reactivity is similar to that of phenol. We ran an additional check on the accuracy of the phenol analyses by determining the phenol content of a sample and then adding known amounts of phenol to it and analyzing for the increment; the analytical values agreed with those calculated. The accuracy was found to be $\pm 2\%$. Triplicate determinations were run for each point.

The hydroxymethylphenols were determined by GLPC of their acetates. The hemiformals present in the aliquots were destroyed with SO₂-pyridine and the mixture was subsequently acetylated with acetic anhydride-pyridine. Exact details can be found in the literature¹⁶ along with proof that the composition of the mixture under analysis is not altered by this type of handling. The accuracy of the acetate determinations was checked occasionally with the pure model compounds, synthesized essentially by the procedures of Freeman,⁹ as modified by Higginbottam et al.¹⁶ Accuracy was 2-4%, depending on the compound. Duplicate determinations were run for each point; in cases of differences greater than 5% on any one component in the duplicates, two more determinations were performed and the average of all four was used. The presence of dinuclear materials is detected by this method.

Handling of the Data

The concentrations of phenol and formaldehyde were used as calculated from the experimental weight per cent with the appropriate density corrections. The experimental values for each acetate of the hydroxymethyl-

phenols were converted to mole fractions of product. The amount of reacted phenol (determined by difference from initial and current phenol values) times each mole fraction at each sampling point, gave the concentration of each hydroxymethylphenol. The data for all phenolic components are thus normalized; their sum is equal to the initial concentration of phenol.

Rate constants were determined as outlined in the section on Results. Rigorous statistical analyses could not be performed on the nonlinear method. A rigorous error analysis on the regression calculation of the initial rough estimates of the rate constants does, however, give the maximum possible bounds of error. The standard deviations calculated for each initial rate constant estimate in run L are typical: k_1 , 3.7%; k_2 , 5.5%; k_3 , 4.6%; k_4 , 17.6%; k_5 , 24.5%; k_6 , 9.2%; and k_7 , 13.0%. From the effect of small perturbations of the rate constants on the fitting of the data, we estimate that the rate constants derived by our nonlinear method probably carry uncertainties about one third as large as the values listed above. The kinetic data were extensive enough to allow evaluation of eight parameters, i.e., Q_2 and the seven rate constants. Our method evaluates each constant from independent analytical data for several different components; as a result, reliable rate constant estimates can be obtained despite the complexity of the kinetic system.

The reliability of the rate constants is borne out not only by good internal consistency in our sixteen kinetic experiments but also by the excellent agreement with data from other investigations. Even though data were available only on formaldehyde, our calculation of formaldehyde curves is dependent on all rate constants. Despite their generality and overall superiority, nonlinear methods²⁰ have not yet been applied widely in chemical kinetics.

The reliability of our method of calculating m (see Appendix) is evident from the remarkably successful application of the rate constants from run I ($m_0 = 0.83$) to the data of Dijkstra et al. (Table II, $m_0 = 0.999$); also those of run L ($m_0 = 0.25$) to run N ($m_0 = 0.33$), those of run K ($m_0 = 0.26$) to run O ($m_0 = 0.28$), and those interpolated from runs K and L to the data of Debing et al. ($m_0 = 0.39$, Fig. 8). In an additional check, standard linearization methods of calculating the rate constants, which eliminate time and formaldehyde dependence,²⁸ were used to calculate rate constant ratios. These values are independent of our treatment of the equilibria and they were in excellent agreement with the corresponding ratios that can be obtained from Table I. For runs K and L the average discrepancy in $k_i/(k_1 + k_2)$ was 1.9% and the maximum 6.9%.

CONCLUSION

The same set of rate constants from run I, Table I, has been shown to apply to systems varying in base from 2 to 50 mole-% of the phenol initially present, over a 40-fold variation in the concentration of formaldehyde, and

an eightfold variation in the ratio of the reactants. In systems composed primarily of phenol and concentrated aqueous formaldehyde, variations in base concentration, reactant ratio, and temperature, also have been described successfully by our kinetic model. Our rate constants have been shown to apply equally well to data from other investigations. The reported peculiarities of the system, as mentioned in the Introduction, can now be seen to have been the result of failure to recognize the effect of substantial changes in concentrations on m , on the rate constants, and on the ratio of *ortho* to *para* substitution.

APPENDIX

The average behavior of the hemiformal equilibria is described by eq. (16) which is equivalent to eq. (15):

$$Q_2 = 400 = \frac{([F]_0 - [F])(1 - n)[H_2O]^2}{([F]_0 - [F])n([F]m)^2} \quad (16)$$

where n is the fraction of the total hydroxymethyl groups that are free (not tied up as hemiformals) and the other symbols are as described in the text.

The equilibria of hydrated formaldehyde with itself in the presence of the hydroxymethylphenol products is described by eq. (17).¹¹

$$Q_1 = 45 = \frac{(^{1/3})\{[F] - [F]m - 2([F]_0 - [F])(1 - n)\}[H_2O]^2}{([F]m)^3} \quad (17)$$

Combination of eqs. (16) and (17) by elimination of n gives eq. (18).

$$f(m) \equiv 3Q_1Q_2[F]^5m^5 + (3Q_1 + Q_2)[F]^3[H_2O]^2m^3 + Q_2(2[F]_0 - 3[F])[F]^2[H_2O]^2m^2 + [F][H_2O]^4(m - 1) = 0 \quad (18)$$

Equation (18) was solved by the Newton-Raphson method,²⁹ starting from some reasonable initial estimate of m . The concentration of water in eqs. (16)–(18) does not include water consumed in hydrating formaldehyde, eq. (19).

$$[H_2O] = [H_2O]_{tot} - m[F] - (^{1/3})(1 - m)[F] \quad (19)$$

The concentration of water is updated after every iteration around eq. (18). The procedure succeeds because $[H_2O]$ converges fast.

Our thanks are extended to Dr. H. P. Higginbottom for many helpful discussions, to Mr. A. N. MacDonald for calculating the rate constant ratios by linearization, to Mr. K. Kozłowski for skillful technical assistance, and to Mr. F. E. Gore for some analog computer simulations.

References

1. R. W. Martin, *The Chemistry of Phenolic Resins*, New York, 1956, Chap. 10.
2. N. J. L. Megson, *Phenolic Resin Chemistry*, Academic Press, New York, 1958, p. 229.

3. M. M. Sprung, *J. Am. Chem. Soc.*, **63**, 334 (1941).
4. L. M. Debing, G. E. Murray, and R. J. Schatz, *Ind. Eng. Chem.*, **44**, 356 (1952).
5. L. M. Yeddapanalli and V. V. Gopalarkrishna, *Makromol. Chem.*, **32**, 112 (1959).
6. H. G. Peer, *Rec. Trav. Chim.*, **78**, 851 (1959).
7. R. Dijkstra, J. de Jonge, and M. F. Lammers, *Rec. Trav. Chim.*, **81**, 295 (1962).
8. J. F. Walker, *Formaldehyde*, 3rd ed., Reinhold New York, 1964, (a) p. 493; (b) chap. 3.
9. J. H. Freeman, *J. Am. Chem. Soc.*, **74**, 6257 (1952).
10. J. H. Freeman and C. W. Lewis, *J. Am. Chem. Soc.*, **76**, 2080 (1954).
11. A. A. Zavitsas, *J. Polymer Sci. A-1*, **6**, 2533 (1968).
12. G. R. Sprengling and C. W. Lewis, *J. Am. Chem. Soc.*, **75**, 5709 (1953).
13. A. A. Zavitsas, *J. Chem. Eng. Data*, **12**, 94 (1967).
14. Y. Ihashi, K. Sawa, and S. Morita, *J. Chem. Soc. Japan*, **68**, 1427 (1964).
15. J. C. Woodbrey, H. P. Higginbottom, and H. M. Culbertson, *J. Polymer Sci. A*, **3**, 1079 (1965).
16. H. P. Higginbottom, H. M. Culbertson, and J. C. Woodbrey, *Anal. Chem.*, **37**, 1021 (1965).
17. H. G. Johnson and E. L. Piret, *Ind. Eng. Chem.*, **40**, 743 (1948).
18. J. F. Walker, *J. Am. Chem. Soc.*, **55**, 2825 (1933).
19. A. W. Dickinson, *Chem. Eng. Progr., Symp. Ser.*, **59**, 84 (1963).
20. D. W. Marquardt, *J. Soc. Ind. Appl. Math.*, **2**, 431 (1963).
21. G. E. P. Box, *Biometrika*, **52**, 355 (1965).
22. R. Dijkstra and J. de Jonge, *Rec. Trav. Chim.*, **76**, 92 (1957).
23. R. J. Schatz, Monsanto Co.; the raw data were made available to us by private communication.
24. H. G. Peer, Thesis, The University of Leyden, Leyden, The Netherlands, 1956; and references therein.
25. S. Murayama, *Bull. Chem. Soc. Japan*, **39**, 1025 (1966).
26. K. B. Wiberg, *Physical Organic Chemistry*, Wiley, New York, 1974, p. 388.
27. H. P. Higginbottom, Monsanto Co., unpublished data.
28. S. W. Benson, *The Foundations of Chemical Kinetics*, McGraw Hill, New York, 1960, p. 43.
29. L. Lapidus, *Digital Computations for Chemical Engineers*, McGraw-Hill, New York, 1963.

Received August, 1967

Revised January 15, 1968

Autoxidation of Polypropylene Catalyzed by Cobalt Salt in the Liquid Phase

YOSHIO KAMIYA, *Faculty of Engineering, University of Tokyo,
Hongo, Tokyo, Japan*

Synopsis

The autoxidation of isotactic polypropylene suspended in the organic solvent was found to proceed very rapidly in the presence of cobalt salts. The rate of oxidation increases and the induction period decreases as the concentration of cobalt is increased. The rate of oxidation depends on solvent and is quite fast in fatty acids. Polypropylene has shown a rapid decrease in molecular weight at the initial stage of oxidation, and the volatile products were mainly composed of carbon dioxide and small amount of carbon monoxide. Other oxidation products were acetic acid-soluble resinous materials, having molecular weights of 250-730, with a molar ratio of carbon to oxygen of 3.0-5.4. Atactic polypropylene, relatively stable against oxidation, was oxidized easily in the presence of cobalt and bromide ion. The difference in the rate of oxidation depending on the tacticity of polypropylene is attributed primarily to steric hindrance to the intramolecular hydrogen abstraction step.

INTRODUCTION

Although the autoxidation of polymers in the liquid phase^{1,2} is an advantageous method for the study of oxidation mechanism, there is a problem involved, in that organic solvents are also oxidized at high temperatures, in some cases even faster than the polymers. Moreover, when such a relatively stable solvent as chlorobenzene is used, side reactions, e.g., dehalogenating decomposition of the solvent, complicates the reaction scheme.

The autoxidation studies on polymers to elucidate the oxidation mechanism should be carried out at temperatures below 100°C.

According to our experiments, the autoxidation of polymers catalyzed by metal salts is a very useful method, since it proceeds very rapidly at temperatures as low as 80°C.

We intended to clarify the various effects, especially the effect of tacticity, on the autoxidation of polypropylene. The effect of tacticity on the rate of oxidation of polymer has not yet been clarified, although Dulog et al.¹ suggested that dimeric decomposition of hydroperoxide takes place in the oxidation of isotactic polypropylene while monomeric decomposition occurs in the oxidation of the atactic polymer in trichlorobenzene at 120°C.

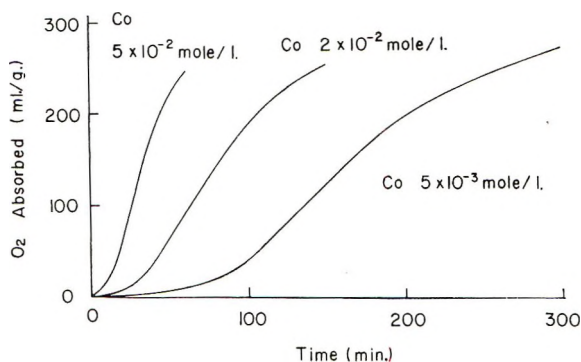


Fig. 1. Oxygen absorption curves of isotactic polypropylene (1.0 g) suspended in acetic acid (10 ml) in the presence of cobalt acetate.

RESULTS

Autoxidation of Isotactic Polypropylene

Typical oxygen absorption curves are shown in Figure 1. The induction period decreases and the rate of oxidation increases as the concentration of cobalt salt is increased. The oxidation appears to reach a steady state after absorption of about 35 ml of oxygen per 1.0 g of isotactic polypropylene (IP) and to start decreasing after absorption of about 140 ml of oxygen. According to the following results, the decrease in the rate of oxidation can be attributed to the formation of inhibitors in the solution and not to the deactivation of metal catalyst.

Although the rate of oxidation of IP with 2×10^{-2} mole/l cobalt, as shown in Figure 1, is decreased by a factor of two after 120 min and absorption of 200 ml oxygen per 1.0 g of IP as compared with the steady rate of oxidation, the addition of the same amount of fresh cobalt acetate as initially added after 120 min has no effect on the rate of oxidation. Furthermore, it was found that the acetic acid solution of 2×10^{-2} mole/l cobalt, after 120 min of oxidation of IP, is hardly able to oxidize a fresh sample of IP.

The amount of solvent used affects the rate of oxidation until the ratio of volume solvent (in milliliters) to weight polypropylene (in grams) reaches about 10:1 as shown in Figure 2, but the rate maintains a constant value at a ratio above 10:1, showing that the rate is a function of cobalt concentration and not of the amount of solvent when a sufficient amount of solvent is present. The cobalt concentration in the solution at the ratio of 10:1 was exactly constant before and after the oxidation, showing that the amount of cobalt adsorbed on IP or dissolved in IP is little. The solvent effect is quite marked, as given in Table I and Figure 3. In acetic or propionic acids, the oxidation proceeds much faster than in neutral solvents.

In acetic acid the rate of cobalt-catalyzed autoxidation appears to reach a constant value at cobalt concentrations above 0.1 mole/l and it is nearly of one-half order with respect to cobalt at concentrations below 5×10^{-2} mole/l.

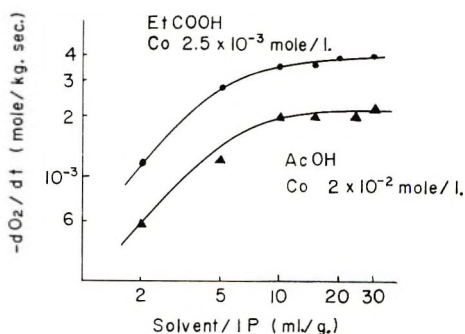


Fig. 2. Effect of the ratio of volume of solvent to weight of isotactic polypropylene on the rate of oxidation catalyzed by cobalt in acetic acid or in propionic acid.

The activation energy of the overall reaction in acetic acid, according to the Arrhenius plot at temperatures from 70 to 90°C, was determined to be 15 kcal/mole.

The high dependence of the rate of the metal concentration over a wide range of concentration seems to suggest that direct initiation by cobalt and hydrocarbon occurs. However, in the autoxidation of IP catalyzed by 5×10^{-2} mole/l cobalt acetate in the presence of 5×10^{-3} mole/l 2,6-di-*tert*-butyl-4-methylphenol, no appreciable oxygen absorption is observed within 360 min at 80°C, showing the direct initiation should be very slow.

In the case of neutral solvents (Table I), the rate of oxidation apparently tends to increase as the dielectric constant of the solvent is increased. The rate of oxidation in neutral solvents has starts to decrease after a shorter period at a steady state than in the acidic solvents.

The hydroperoxide concentration in the course of oxidation indicates a steady value at a steady state of oxidation as shown in Figure 4.

Nickel, copper, and manganese salts are very weak catalysts as compared with cobalt salt in acidic solvent, as reported previously.³ However, copper salts are very effective catalysts in a neutral solvent, as shown in Figure 5, even though it can be seen that copper becomes an inhibitor at high concentrations.

TABLE I

Effect of Solvent on the Rate of Oxidation of Isotactic Polypropylene^a

| Solvent | $-d[O_2]/dt \times 10^4$, (mole/kg-sec) |
|---------------------------|---|
| Propionic acid | 40 |
| Acetic acid | 30.5 |
| Dimethyl phthalate | 4.4 |
| Acetophenone | 3.0 |
| <i>o</i> -Dichlorobenzene | 1.85 |
| Monochlorobenzene | 1.5 |

^a Ratio of solvent to polymer, 10 ml/g; cobalt concentration, 5×10^{-2} mole/l.

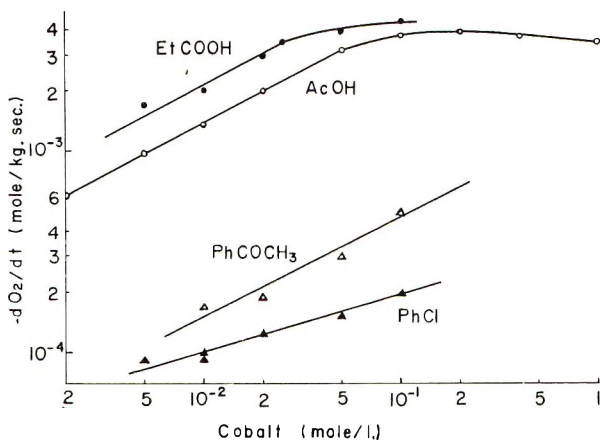


Fig. 3. Rate of oxidation of isotactic polypropylene as a function of cobalt concentration in various solvents at the ratio of solvent to polymer of 10 ml/g.

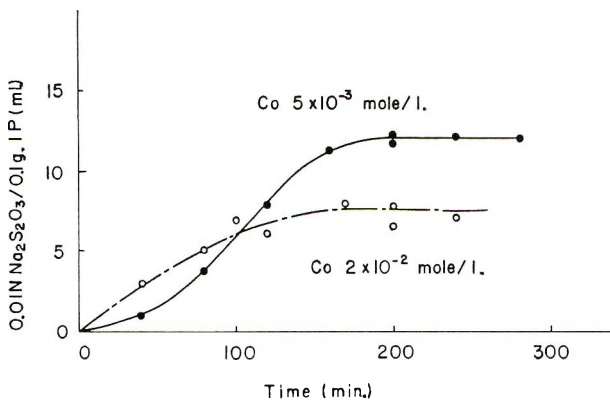


Fig. 4. Hydroperoxide concentration in the course of oxidation of isotactic polypropylene (10.0 g) in acetic acid (200 ml) catalyzed by cobalt.

The solvent effect in Figure 3 and Table I as well as the catalyst effect in Figure 5 are quite unique as compared with the ordinary autoxidation of liquid hydrocarbons,^{4,5} since the oxidation of IP proceeds much faster in acidic solution than in neutral solvents and copper salt has shown a stronger activity than cobalt.

When acetic acid solvent is partly replaced by chlorobenzene, the rate of oxidation shows only small deviations from a constant value until more than 90% is replaced (Fig. 6). The rate of oxidation starts to decrease after a shorter steady-state period as the concentration of acetic acid is decreased. These results indicate that the active form of cobalt can be retained in acetic acid but is deactivated easily in a neutral solvent.

Oxidation Products of Isotactic Polypropylene

The molecular weight of oxidized isotactic polypropylene, which is insoluble in acetic acid, during the oxidation with 5×10^{-3} mole/l cobalt

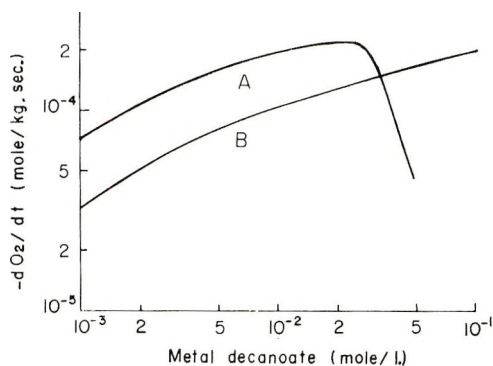


Fig. 5. Rate of oxidation of isotactic polypropylene (1.0 g) in chlorobenzene (10 ml) as a function of catalyst concentration with (A) copper decanoate or (B) cobalt decanoate.

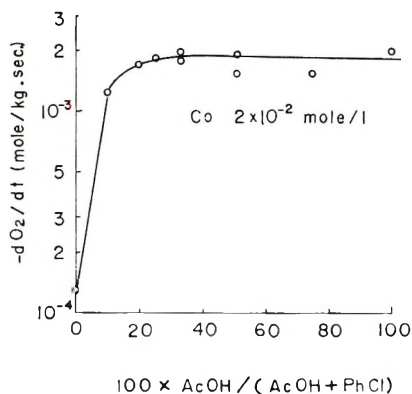


Fig. 6. Effect of concentration of acetic acid on the rate of oxidation of isotactic polypropylene (0.2 g) catalyzed by cobalt in a mixture (2 ml) of chlorobenzene and acetic acid.

at 80°C is shown in Table II. According to infrared spectra the oxidized polypropylene contains a small amount of carbonyl groups.

Carbon dioxide and smaller amounts of carbon monoxide are evolved after the oxygen absorption reaches a steady state, and they reach maximum values a little later than the oxygen absorption. The ratio of the rate

TABLE II
Depolymerization of Isotactic Polypropylene in Oxidation Catalyzed by 5×10^{-3} mole/l Cobalt Acetate in Acetic Acid

| Time, min | Molecular weight |
|-----------|--------------------|
| 0 | 23.5×10^4 |
| 30 | 13.6×10^4 |
| 60 | 7.8×10^4 |
| 90 | 2.7×10^4 |
| 120 | 1.05×10^4 |

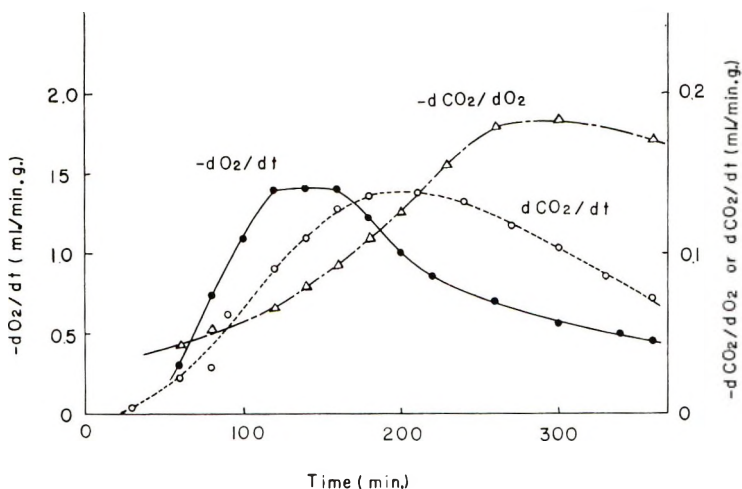


Fig. 7. Comparison of the rate of oxygen absorption with the rate of formation of carbon dioxide in the course of oxidation of isotactic polypropylene (10.0 g) in acetic acid (200 ml) catalyzed by 5×10^{-3} mole/l cobalt.

of carbon dioxide formation to the rate of oxygen absorption increases gradually as the oxidation proceeds, and the ratio seems to approach a value of 1:5 at the later stage of oxidation (Fig. 7).

The surface area of IP after oxidation according to the BET method* shows just the same value of $2.5 \text{ m}^2/\text{g}$ as the feed after 120 min with 2×10^{-2} mole/l cobalt in acetic acid.

Various oxidation products other than gaseous products were examined by gas-liquid chromatography, but only small amounts of acetaldehyde and acetone were found in the condensates recovered from the cold trap. No appreciable amount of acetic acid could be detected in the oxidation products of IP in propionic acid.

Other important oxidation products are acetic acid-soluble resinous materials consisting of neutral and acidic products, as shown in Table III. The yields for each product were only several per cent (based on polypropylene) after 2 hr but increased markedly after 4 hr. These products showed very strong absorption spectra due to carbonyl and hydroxyl groups.

Autoxidation of Atactic Polypropylene Catalyzed by Cobalt Salt

Although the atactic polypropylene is completely soluble in chlorobenzene or in a 1:1 mixture by volume of chlorobenzene and acetic acid, the maximum rate of oxidation is lower than that of isotactic propylene by a factor of 3-7 as shown in Table IV. The rate of oxidation of atactic polypropylene (AP) is not so accurate as that of IP, because the oxygen absorp-

* The surface area according to the BET method may be somewhat different from the true value, because nitrogen gas might dissolve in IP.

TABLE III
Yields and Properties of Acetic Acid-Soluble Products from Oxidation of Isotactic Polypropylene in Acetic Acid

| Oxidation conditions | | Products yield, wt-% | |
|-----------------------|-----------|----------------------|---------------------|
| Cobalt concn., mole/l | Time, min | Neutral ^a | Acidic ^b |
| 2×10^{-2} | 120 | 5.3 | 3.5 |
| 2×10^{-2} | 240 | 14.5 | 5.8 |
| 5×10^{-3} | 120 | 2.2 | 0.7 |
| 5×10^{-3} | 360 | 16.7 | 5.4 |

^a Neutral products: molecular weight 630-730; empirical formula $C_{33}H_{61}O_7$.

^b Acidic products: molecular weight 250-400; empirical formula $C_{15}H_{22}O_5$.

TABLE IV
Effect of Tacticity on the Maximum Rate of Oxidation of Polypropylene Catalyzed by Cobalt

| Oxidation conditions | | $-d[O_2]/dt \times 10^3$, mole/kg-sec | |
|--|--|--|---------|
| Solvent | Cobalt concn., mole/l | Isotactic | Atactic |
| Chlorobenzene | 1×10^{-2} | 10 | 3.2 |
| Chlorobenzene | 5×10^{-2} | 17 | 4.2 |
| Acetic acid-chlorobenzene ^a | 2×10^{-2} | 205 | 27 |
| Acetic acid-chlorobenzene ^a | 5×10^{-2} | 300 | 40 |
| Acetic acid-chlorobenzene ^a | 2×10^{-2} , NaBr, 4×10^{-2} | 245 | 300 |

^a 20 ml of a 1:1 mixture by volume of chlorobenzene and acetic acid was used per 1.0 g of polymer.

tion curve of AP decreases markedly after a small amount of oxygen has been absorbed.

However, the autoxidation of atactic polypropylene catalyzed by cobalt acetate and sodium bromide in a 1:1 mixture by volume of chlorobenzene and acetic acid proceeds very rapidly after a short induction period, and the catalyst retains its activity for a long time. The rate of oxidation is exactly first-order with respect to polypropylene concentration (Fig. 8) and is increased with the increase of cobalt concentration, as shown in Figure 9, in which the molar ratio of bromide ion to cobalt is kept 2:1 because the rate is confirmed to be constant at the ratio of Br^- to cobalt above 1:1.

DISCUSSION

Mechanism of Autoxidation of Isotactic Polypropylene

The oxidation of isotactic polypropylene proceeds surprisingly fast in the presence of cobalt salts at 80°C, but this result is quite reasonable because

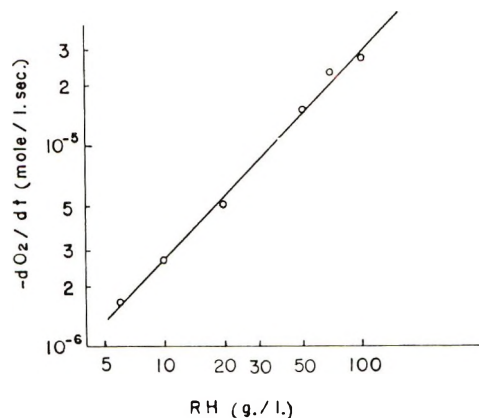


Fig. 8. Effect of concentration of atactic polypropylene on the rate of oxidation catalyzed by 2×10^{-2} mole/l cobalt acetate and 4×10^{-2} mole/l NaBr in a 1:1 mixture by volume of chlorobenzene and acetic acid.

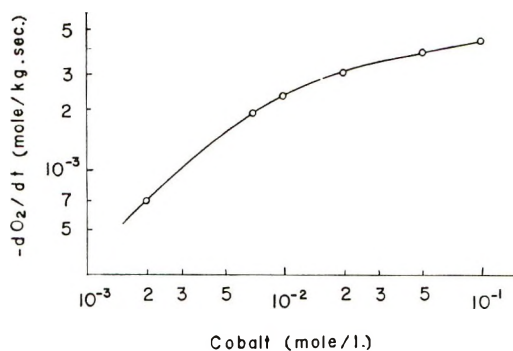


Fig. 9. Rate of oxidation of atactic polypropylene as a function of cobalt acetate concentration at a ratio of solution to polymer of 20 ml/g.

IP has a tertiary hydrogen, which is located in the preferred position for intramolecular chain propagation.

Cobalt salt initiates the autoxidation chain by decomposing hydroperoxide as in the case of ordinary metal catalysis, since cobalt is not responsible for the direct initiation reaction. The results of Figure 4 indicate that the hydroperoxide formed is relatively stable, since the hydroperoxide concentration is still appreciable at high concentration of cobalt. Also it supports the above conclusion that cobalt initiates the chain by decomposing hydroperoxide, because the rate of oxidation increases and the steady concentration of hydroperoxide decreases as the cobalt is increased.

The result that the rate of oxidation increases with the increase in the dielectric constant of solvent indicates that the propagation step includes the dipolar transition stage.^{7,8}

The higher rate of oxidation in acidic solvents than in neutral solvents may be due to a highly active form of cobalt in acidic solvents. The

higher rate of oxidation in propionic acid than in acetic acid can be explained by the fact that the rate of decomposition of hydroperoxide⁹ increases as the molecular weight of acidic solvent is increased.

It is of interest that the acid-soluble products retard the oxidation reaction but the partially oxidized polypropylene, which is insoluble in acid, can be oxidized faster than the fresh sample of polypropylene.

Since the induction period of oxygen absorption is 75 min at 5×10^{-3} cobalt, as seen in Figure 1, scission of the carbon-carbon bond at a large molecular unit appears to occur rather preferentially at the initial stage of oxidation, according to the results of Table II. In the photooxidation of polystyrene in chloroform, Lawrence and Weir¹⁰ observed that after a rapid initial decrease in molecular weight, the rate of chain scission gradually decreases.

In this experiment considerable amount of carbon dioxide was found in the volatile products, but many workers¹¹⁻¹³ found just carbon monoxide but no carbon dioxide. Therefore, the formation of carbon dioxide is presumably due to the oxidation of intermediate products, such as formaldehyde, catalyzed by cobalt salt. It seems also a feature of metal-catalyzed autoxidation at low temperatures that very small amounts of acetone and acetic acid are produced. Bevilacqua et al.¹³ regarded the two- or three-carbon products to result from intramolecular attack by radicals leading to β -oxidation at high temperatures.

As for acid-soluble products, most of the tertiary hydrogen of polypropylene seems to have been oxidized, since the ratio of carbon to oxygen is between 3.0 and 5.4. As can be seen in Table III and Figure 1, the low molecular weight products increase at the later stage of oxidation, in spite of the decrease in the rate of oxidation.

The fast oxidation of isotactic polypropylene catalyzed by cobalt in acetic acid corresponds to the lower activation energy of 15 kcal/mole as compared with the values for the gas phase (22 kcal/mole,¹⁴ 27 kcal/mole¹⁵).

Steric Effect on the Rate of Oxidation of Polypropylene

The steric effect on the oxidation of polypropylene (Table IV) seems to be so large that it overcomes the effect of solubility.

However, the higher rate of oxidation of IP may be partly caused by other reasons, that is, in a heterogeneous system hydrocarbon concentration is very high locally, and inhibitors formed by the oxidation will be removed easily.

Since the chain length of the autoxidation of atactic polypropylene initiated by azobisisobutyronitrile in chlorobenzene at 80°C was about three, the difference in rates due to the tacticity can be attributed to steric hindrance to the propagation step. A similar short chain length of atactic polymers was reported by Tobolsky et al.¹⁶ Metz and Mesrobian¹⁷ suggest the relative inertness of polystyrene compared with isopropylated polystyrene toward hydroperoxide formation is due to either steric hindrance or to a steric inhibition of resonance of the propagation step. In contrast, it

is well known that the chain length of tertiary peroxy radicals, such as cumyl peroxy radical,¹⁸ is long.

The steric effect can be elucidated by the oxidation catalyzed by cobalt bromide. As we have suggested previously,¹⁹ cobalt monobromide in acetic acid operates as a chain carrier of autoxidation. With cobalt bromide catalysis, the steric hindrance to the intramolecular hydrogen abstraction is expected to be eliminated completely.

With addition of bromide ion, the rate of oxidation of hydrocarbons catalyzed by cobalt in acidic solvent increases markedly in the cases of methylbenzenes and *n*-paraffins, affecting the rate of hydrogen abstraction reaction. However, this effect may be as small in the case of polypropylene as cumene, because the rate of oxidation of cumene catalyzed by 2×10^{-2} mole/l cobalt increases only by a factor of two in the presence of 4×10^{-2} mole/l NaBr.

The rate of oxidation of atactic polypropylene with 2×10^{-2} mole/l cobalt in a 1:1 mixture by volume of chlorobenzene and acetic acid increases in the presence of 4×10^{-2} mole/l NaBr from 2.7×10^{-4} to 3.0×10^{-3} mole/kg-sec (Table IV), while the rate of oxidation of isotactic polypropylene under the same conditions increases only from 2.05×10^{-3} to 2.45×10^{-3} mole/kg-sec in the presence of NaBr.

The marked increase in the rate of oxidation of atactic polymer due to bromide ion may be due mainly to the elimination of steric hindrance to the intramolecular hydrogen abstraction step, since the hydrogen abstraction reaction should be independent of steric configuration. In other words, it may be said that the chain propagation step of polypropylene proceeds mostly intramolecularly rather than intermolecularly.

Other evidence for the steric hindrance to the oxidation can be observed in the co-oxidation of polypropylene with liquid hydrocarbons. When small amounts of isotactic or atactic polymers are added to the solution of ethylbenzene or cumene, the steady rate of oxidation increases in the case of isotactic polypropylene, but it shows a minimum value in the case of atactic polypropylene, as shown in Figure 10.

These results demonstrate that the inhibition effect due to atactic structure is ascribed to the short chain length.

EXPERIMENTAL

Powdered isotactic polypropylene with molecular weight of 2.35×10^5 and surface area of $2.5 \text{ m}^2/\text{g}$ was suspended in organic solvents and treated by oxygen under vigorous agitation in the presence of metal catalyst. The catalysts used were cobalt acetate in acetic acid and cobalt decanoate in other solvents.

The oxidation procedure was carried out in an oxygen absorption apparatus⁴ or by a three-mouthed flask with stirrer; in the latter, 10.0 g of polypropylene suspended in 200 ml of acetic acid was treated with oxygen at a flow rate of 100 ml/min, and the oxidation products in the gas phase as

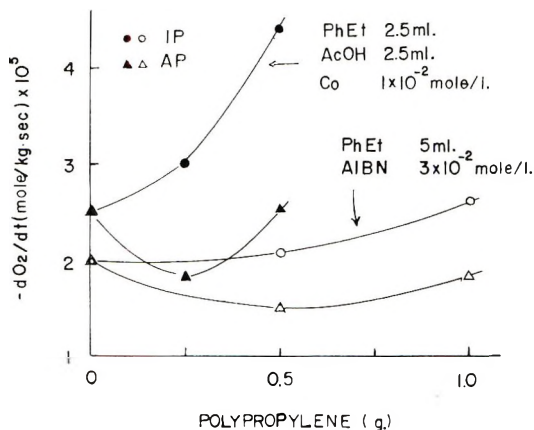


Fig. 10. Rate of oxidation of ethylbenzene in the presence of small amounts of atactic polypropylenes catalyzed by cobalt or initiated by azobisisobutyronitrile.

well as in the liquid phase were analyzed by gas-liquid chromatography. The oxidation was carried out at 80°C except as noted.

In order to separate the oxidation products, the polypropylene was filtered off from the solution after cooling, and the filtrate was distilled to dryness under vacuum. The remaining viscous materials were dissolved in benzene and washed with an aqueous solution of sodium hydroxide; the alkaline solution was acidified with hydrochloric acid and extracted with diethyl ether. Thus, the neutral products were recovered from benzene solution and the acidic products from ether solution.

Atactic polypropylene with a molecular weight of 10^4 was dissolved in chlorobenzene or in a 1:1 mixture by volume of chlorobenzene and acetic acid, and treated with oxygen in the presence of cobalt salt as for the case of isotactic polymer.

The molecular weight was determined with a Mechrolab osmometer or calculated from the viscosity.⁶

References

1. L. Dulog, E. Radlmann, and W. Kern, *Makromol. Chem.*, **60**, 1 (1963).
2. F. Grafmüller and E. Husemann, *Makromol. Chem.*, **40**, 172 (1960).
3. Y. Kamiya, *J. Polym. Sci. B*, **4**, 999 (1966).
4. Y. Kamiya and K. U. Ingold, *Can. J. Chem.*, **42**, 1027 (1964).
5. Y. Kamiya, *Kogyo Kagaku Zasshi*, **69**, 897 (1966).
6. P. Parrini, *Makromol. Chem.*, **24**, 265 (1957).
7. J. A. Howard and K. U. Ingold, *Can. J. Chem.*, **42**, 1044 (1964).
8. D. G. Hendry and G. A. Russell, *J. Amer. Chem. Soc.*, **86**, 2371 (1964).
9. Y. Kamiya, *Bull. Chem. Soc. Japan*, **38**, 2156 (1965).
10. J. B. Lawrence and N. A. Weir, *Chem. Commun.*, 257 (1966).
11. F. Geleji and Z. Holly, *Osterr. Chemiker-Z.*, **67**, 189 (1966).
12. V. S. Pulov, B. A. Gromov, M. B. Neiman, and E. G. Sklyarova, *Neftekhimiya*, **5**, 100 (1963).

13. E. M. Bevilacqua, E. S. English, and J. S. Gall, *J. Appl. Polym. Sci.*, **8**, 1691 (1964).
14. S. S. Stivala, L. Reich, and P. G. Kelleher, *Makromol. Chem.*, **59**, 28 (1963).
15. R. H. Hansen, C. A. Russell, T. DeBenedictis, W. M. Martin, and J. V. Pascale, *J. Polym. Sci. A*, **2**, 587 (1964).
16. A. V. Tobolsky, P. M. Norling, N. H. Frick, and H. Yu, *J. Amer. Chem. Soc.*, **86**, 3925 (1964).
17. D. J. Metz and R. B. Mesrobian, *J. Polym. Sci.*, **16**, 345 (1955).
18. H. S. Blanchard, *J. Amer. Chem. Soc.*, **82**, 2014 (1960).
19. Y. Kamiya, *Tetrahedron*, **22**, 2029 (1966).

Received February 2, 1968

Polymerization of 2,2,2-Trifluoroethyl Vinyl Ether

C. K. CHIKLIS and H. C. HAAS, *Chemical Research Laboratories,
Polaroid Corporation, Cambridge, Massachusetts 02139*

Synopsis

The polymerization of 2,2,2-trifluoroethyl vinyl ether by six different catalyst systems was examined. Low-temperature studies (-78°C) with boron trifluoride etherate catalyst in hydrocarbon and chlorinated solvents slowly yielded low molecular weight polymers which were amorphous and noncrystallizable upon cold drawing. Under similar conditions, polymerizations with boron trifluoride gas were spontaneous, quantitative, and gave relatively high molecular weight, form-stable, amorphous polymer. Heterogeneous polymerizations with chromium trioxide crystals in toluene at 68°C and bulk reactions with ethylmagnesium bromide-carbon tetrachloride catalyst at 40°C failed to produce polymer. Room temperature runs with triisobutylaluminum-titanium tetrachloride catalyst gave amorphous, tacky material. Aluminum hexahydrosulfate heptahydrate (AHS) initiated polymerizations conducted at 25 and 60°C gave low yields of mixtures of amorphous and crystalline polymers, the ratio depending upon the polymerization solvent employed. The infrared spectra and x-ray diffraction intensity curves of crystalline and amorphous poly(trifluoroethyl vinyl ether) are reported and compared herein for the first time.

INTRODUCTION

The low-temperature polymerization of alkyl vinyl ethers with boron trifluoride etherate in hydrocarbon and chlorinated solvents, which gives stereoregular and crystallizable polymers, was first reported by Schildknecht and co-workers.¹⁻³ Since that time, a multitude of catalyst systems capable of yielding high molecular weight, tactic and atactic polymers over a broad range of polymerization temperatures have been reported. From a practical standpoint, the complex organic metal sulfate and Ziegler-type catalysts disclosed by Vandenberg⁴⁻⁸ and the metal sulfate hydrates of Mosley⁹ and Lal¹⁰ are of particular interest, since they give stereoregular polymers at or near room temperature.

Schildknecht¹¹ polymerized 2,2,2-trifluoroethyl vinyl ether with boron trifluoride etherate at -80°C in chloroform and described the product as a relatively high molecular weight, nontacky, rubberlike polymer. Using an aluminum isopropoxide-sulfuric acid complex catalyst, Vandenberg and co-workers^{5,6} prepared crystalline, presumably isotactic, poly(2,2,2-trifluoroethyl vinyl ether). During the course of our work with this monomer, we observed that some of the reported catalyst systems for alkyl vinyl were partially or totally ineffective. Based on our investigation, the virtues and limitations of six different catalyst systems are reported herein.

EXPERIMENTAL

Reagents

2,2,2-Trifluoroethyl vinyl ether, obtained from Ohio Chemical, was washed three times with aqueous sodium carbonate, water-washed, and dried over sodium sulfate followed by calcium sulfate. It was distilled over calcium hydride under nitrogen and the fraction coming over at 43.2°C collected.

Chloroform and carbon tetrachloride (Mallinckrodt AR grade) were washed thoroughly with water, dried over sodium sulfate and then calcium sulfate, and distilled under nitrogen. Pentane and heptane (Eastman practical grade) were treated with concentrated sulfuric acid, washed thoroughly with water and aqueous sodium carbonate, and dried over sodium sulfate and calcium sulfate successively. Thereafter, they were distilled over phosphorus pentoxide under nitrogen. Benzene (Fisher reagent, thiophene-free); toluene, acetone, carbon disulfide (Mallinckrodt AR grade); and hexafluoro-*p*-xylene (Columbia Organic) were dried over calcium sulfate and distilled over calcium hydride under nitrogen. The above distillations were run on a spinning band column (28 theoretical plates) at a reflux ratio of 9/1.

Boron trifluoride-diethyl ether (Eastman white label) was distilled under nitrogen through a 10-in. Vigreux column. The main fraction (bp 126°C) of water-white liquid was collected and the receiving flask capped with a serum stopper.

Boron trifluoride gas, obtained from the Matheson Company, was used directly from the lecture bottle.

Chromium trioxide crystals (Mallinckrodt AR grade) were used as received and after two recrystallizations from water. The melting point of the commercial and recrystallized material was the same, 199–200°C.

A freshly prepared 3*M* solution of ethylmagnesium bromide in diethyl ether, obtained from Arapahoe Chemicals, was used as received.

Aluminum hexahydrosulfate heptahydrate (AHS) was prepared by heating aluminum sulfate octadecahydrate with concentrated sulfuric acid as described by Mosley.⁹

Triisobutylaluminum was purchased from Texas Alkyls, Inc. and titanium tetrachloride from Matheson.

Polymerizations

Polymerization conditions and references are given in Table I.

Polymer Characterization

The x-ray diffraction intensity curves of unstretched films, stretched films, and finely ground powders were measured by using nickel-filtered copper radiation.

Crystalline melting points were determined by differential thermal

analysis (DTA). The DTA cell was equipped with a window which allowed visual observation of the sample during the melting transition. A typical run consisted of heating a sample in the instrument to 15°C above the expected (or observed) melting point, cooling and holding it for approximately 30 min at a temperature about 5°C below the melting point to permit recrystallization, cooling to room temperature, and then reheating and recording its thermogram.

Films for infrared studies were cast from acetone on silver chloride disks and dried for 30 min in a circulating air oven at 50°C. Crosslinked, insoluble fractions were run as potassium bromide pellets.

Inherent viscosities were obtained at 0.5% concentration in acetone at 25°C.

RESULTS AND DISCUSSION

The polymerization conditions and results for trifluoroethyl vinyl ether are given in Table I.

Polymerization in liquid propane at -78°C with boron trifluoride etherate was slow and gave a 50% yield of a low molecular weight, tacky polymer. Its infrared spectrum is shown in Figure 1 (designated as amorphous polymer). Since the rate of polymerization of alkyl vinyl ethers catalyzed by boron trifluoride-etherate is greatest when the alkyl group is strongly electron-donating,³ it was expected that trifluoroethyl vinyl ether would polymerize even more slowly than methyl vinyl ether, and this might account for the low yield observed.

Low-temperature polymerizations in "activating" solvents with boron trifluoride etherate catalyst¹¹ gave quantitative yields of somewhat higher molecular weight, nontacky polymers. The inherent viscosities are relatively low but are typical of polymers derived from the lower alkyl vinyl ethers with boron trifluoride etherate catalyst.¹² Their infrared spectra were identical to that of the polymer prepared in liquid propane. Okamura and co-workers¹² have shown that these "activating" halogenated solvents

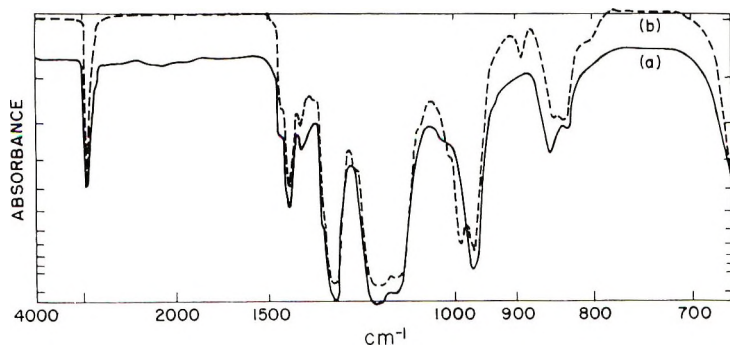


Fig. 1. Infrared spectra of: (a) amorphous and (b) crystalline poly(trifluoroethyl vinyl ether).

TABLE I
 Polymerization Conditions and Results for 2,2,2-Trifluoroethyl Vinyl Ether

| Run | Solvent | Vol. ratio solvent monomer | Catalyst | Molar ratio monomer/catalyst | Polymerization temperature, °C, and time | Yield, % | Inherent viscosity in acetone, (25°C, (concn. = 0.5 g/dl)) | Reference |
|-----|------------------------------------|----------------------------|-------------------------------------|------------------------------|--|----------|--|-----------|
| 1 | Liquid propane | 5:0 | BF ₃ ·Et ₂ O | 9.62 × 10 ¹ | -78, 2 hr | 50 | 0.25 | 1,3 |
| 2 | Chloroform | 3:5 | BF ₃ ·Et ₂ O | 1.1 × 10 ¹ | -78, 1.5 hr | 100 | 0.43 | 11 |
| 3 | Chloroform | 1:8 | BF ₃ ·Et ₂ O | 2.2 × 10 ¹ | -78, 1.5 hr | >95 | 0.50 | 11 |
| 4 | Bulk polymerization | | BF ₃ ·Et ₂ O | 2.0 × 10 ¹ | -78, 2 hr | 100 | 0.32 | — |
| 5 | Chloroform-pentane (70/30 vol/vol) | 4:3 | BF ₃ gas (20 cc at 25°C) | 1.07 × 10 ² | -78, 30 min | 100 | 0.99 | 1,3,11 |
| 6 | Chloroform-pentane (70/30 vol/vol) | 4:3 | BF ₃ gas (10 cc) | 2.14 × 10 ² | -78, 30 min | 100 | 1.17 | 1,3,11 |
| 7 | Chloroform-pentane (70/30 vol/vol) | 4:3 | BF ₃ gas (8 cc) | 2.67 × 10 ² | -78, 30 min | 100 | 0.82 | 1,3,11 |
| 8 | Chloroform-pentane (70/30 vol/vol) | 4:3 | BF ₃ ·Et ₂ O | 1.1 × 10 ² | -78, 21 hr | ~90 | 0.29 | 1,3,11 |

| | | | | | | | | |
|----|----------------------------------|------|---|--|----------------------------|----------------|-------------------|----|
| 9 | Toluene | 2.0 | CrO ₃ | 8.97 × 10 ¹ | 67.5, 3 hr (then 24 hr) | 0 | — | 15 |
| 10 | Bulk polymer- ization | | EtMgBr-CCl ₄ | 3.59 × 10 ² (based on EtMgBr) | 25, 24 hr 40, 24 hr | 0 0 | — — | 16 |
| 11 | Heptane | 6.0 | 75% AHS | 3.0 × 10 ³ | 25, 20 days | 25 | — | 18 |
| 12 | Chloroform | 6.0 | 75% AHS | 3.0 × 10 ³ | 25, 20 days | 25 | 0.40 ^a | 18 |
| 13 | Acetone | 6.0 | 75% AHS | 3.0 × 10 ³ | 25, 20 days | 4 | 0.30 ^a | 18 |
| 14 | Hexafluoro- <i>p</i> - xylene | 6.0 | 75% AHS | 3.0 × 10 ³ | 25, 20 days | <1 | 0.30 ^a | 18 |
| 15 | Benzene | 6.0 | 75% AHS | 3.0 × 10 ³ | 25, 20 days | <1 | 0.19 ^a | 18 |
| 16 | Carbon disulfide | 6.0 | 75% AHS | 3.0 × 10 ³ | 25, 20 days | <1 | 0.18 ^a | 18 |
| 17 | Heptane | 2.26 | 75% AHS | 8.96 × 10 ² | 60, 40 hr | 31 | — | 18 |
| 18 | Chloroform | 2.26 | 75% AHS | 8.96 × 10 ² | 60, 40 hr | — ^b | — | 18 |
| 19 | Carbon disulfide | 2.26 | 75% AHS | 8.96 × 10 ² | Reflux, 40 hr | 39 | — | 18 |
| 20 | Acetone | 2.26 | 75% AHS | 8.96 × 10 ² | Reflux, 40 hr | 52 | — | 18 |
| 21 | Hexafluoro- <i>p</i> - xylene | 2.26 | 75% AHS | 8.96 × 10 ² | 60, 40 hr | 50 | — | 18 |
| 22 | Petroleum ether | 3.0 | (<i>i</i> -Bu) ₃ Al- TiCl ₄ | 1.12 × 10 ² | 25, 24 hr | ca. 50 | 0.33 | 19 |

^a Viscosity of acetone soluble fraction.

^b Spillage; unable to determine yield but estimated to be ca. 50%.

are simply much better solvents than liquid propane, *n*-hexane, and *n*-heptane for the less reactive monomers, e.g., methyl vinyl ether, and their corresponding polymers and that similar results can be obtained in toluene.

The polymerizations conducted with boron trifluoride gas at -78°C in chloroform-pentane solvent were instantaneous upon catalyst injection and quantitative. This technique is analogous to the flash-type polymerization reported by Schildknecht¹ and yielded higher molecular weight polymers as compared to the boron trifluoride etherate runs. These polymers were soluble in acetone, methanol, tetrahydrofuran, and hexafluoro-*p*-xylene. They were insoluble in monomer, aliphatic hydrocarbons, chlorinated hydrocarbons, dioxane, benzene, toluene, dimethylformamide, dimethyl sulfoxide, carbon disulfide, and nitrobenzene. A few remarks regarding these runs seem appropriate. Upon cooling the monomer-solvent system under nitrogen with stirring prior to catalyst injection, the solution became slushy as the temperature approached -78°C . If the gaseous catalyst was injected at this point, the yield and inherent viscosity of the resultant polymer were decreased. The preferred technique involved lowering the cooling bath, momentarily thereby allowing the slush to liquify and then immediately injecting the catalyst through a hypodermic needle. It was also observed that if the chloroform solvent was distilled over calcium hydride, after drying over calcium sulfate as reported in the experimental section, the flash polymerization did not occur. No polymer formation was discernible after 2 hr at -78°C , however, upon addition of a few water droplets from a syringe, a slow growth of polymer was observed at the surface of the frozen water droplets. The level of water, or some other protonic material, in the chloroform which was dried over calcium sulfate was beyond the detectability limits of Karl Fisher titrations or vapor phase chromatography but was sufficient to act as co-catalyst with boron trifluoride gas.

The infrared spectra of films of poly(trifluoroethyl vinyl ether) prepared with boron trifluoride gas and boron trifluoride etherate were found to be identical. This was surprising since we expected the latter to be stereoregular. Our own work (unpublished) and that of Vandenberg⁵ with solvent-cast films of atactic and isotactic poly(methyl vinyl ether) has shown that the spectra are quite similar but some of the bands of the fine structure are discernibly sharper and slightly shifted for the crystalline polymer. A similar observation was reported by Schildknecht¹³ for crystalline and amorphous poly(isobutyl vinyl ether).

The x-ray diffraction intensity curves were measured of unstretched and stretched films of polymer prepared with boron trifluoride etherate and boron trifluoride gas (runs 1-8, Table I). None of the films showed signs of crystallinity. It was quite difficult to obtain highly stretched films of the polymers prepared with boron trifluoride etherate, since they lacked cohesive strength and often ruptured during measurement. Schildknecht recollected that the poly(trifluoroethyl vinyl ether) prepared by him in chloroform at -78°C with boron trifluoride etherate¹¹ did not

exhibit a crystalline x-ray diffraction pattern upon cold drawing.¹⁴ Based on the infrared and x-ray data it appears that the polymer discussed thus far are all amorphous.

Iwasaki¹⁵ reported that isotactic poly(vinyl isobutyl ether) could be prepared at 80°C by using chromium trioxide crystals as catalyst and toluene as solvent. The polymerization is heterogeneous and a magnetic stirrer, to mill the catalyst during reaction, was found necessary to obtain polymer with a high crystalline fraction. This technique was attempted by us with trifluoroethyl vinyl ether except that our reaction temperature (reflux) was 67.5°C as dictated by the composition of our monomer-solvent system. No polymer formation was observed. Numerous additional runs were made which encompassed the use of commercially available and recrystallized chromium trioxide and stabilizer (2,6-di-*tert*-butyl-*p*-cresol) crystals, fresh monomer, and toluene which were distilled over sodium directly into the polymerization flask, longer reaction times (24 hr), longer initial heating times in dry air at 100°C to activate the catalyst, and finally, the use of different sizes of glass- and Teflon-coated stirring magnets. No evidence of polymer formation was ever observed. Our attempts to reproduce Iwasaki's work with vinyl isobutyl ether resulted in very low yields of polymer (ca. 3%); therefore, the source of our difficulty remains unanswered but probably involves insufficient milling of the heterogeneous catalyst.

The bulk polymerization of vinyl isobutyl ether with ethylmagnesium bromide-carbon tetrachloride catalyst at 80°C was reported by Iwasaki and co-workers¹⁶ to give a 69% conversion of high molecular weight polymer. We studied this catalyst system with trifluoroethyl vinyl ether using lower reaction temperatures (bp of monomer is 43°C) and longer times. Runs conducted at 25 and 40°C for 24 hr failed to produce polymer. Interestingly, when a control polymerization was conducted with carefully purified vinyl isobutyl ether,¹⁷ which was distilled over sodium under nitrogen immediately before use, the monomer polymerized violently within seconds at room temperature.

Trifluoroethyl vinyl ether was polymerized with Mosley's catalyst,⁹ aluminum hexahydrosulfate heptahydrate (AHS), in six solvents for 20 days at room temperature with the use of monomer-solvent-catalyst ratios as reported by Lal and co-worker.¹⁸ The yields were very low (Table I) but the polymer characteristics are interesting (Table II). The polymers prepared in chloroform, acetone, hexafluoro-*p*-xylene, and benzene were crystalline and gave x-ray diffraction intensity curves as shown in Figure 2. Average diffracting distances calculated from 2θ values are given in Table III. The melting points were determined by using differential thermal analysis. The fine structure region of their infrared spectra was distinctly different from that of the previously prepared amorphous polymers (see Fig. 1, crystalline polymer). The principal differences are the appearance of a doublet at 968 and 990 cm^{-1} , the presence of a new band at 890 cm^{-1} , and a change (or possibly a shift) in the relative intensities of the bands at

TABLE II
 Characteristics of Poly(trifluoroethyl Vinyl Ether)
 Polymerized with 75% AHS at 25°C in Various Solvents

| Polymer- ization solvent | Physical form | Solubility data | Crystallinity of unfrac- tionated polymer ^a | Melting point, °C |
|----------------------------------|---------------------------|--|--|-------------------------|
| Heptane | Syrupy, viscous liquid | Sol. in methanol, acetone, etc. | — | — |
| Carbon disulfide | Crosslinked powder | Small fraction of methanol- and acetone-soluble material | Amorphous | — |
| Chloroform | Powder | Methanol-soluble and -insoluble frac- tions; latter com- pletely soluble in acetone. | Crystalline | 130 |
| Acetone | Powder | Methanol-soluble and -insoluble frac- tions; latter in- completely soluble in acetone; small fraction of cross- linked polymer | Crystalline | 136 |
| Hexafluoro- <i>p</i> - xylene | Crosslinked powder | 5-10% of acetone- soluble polymer | Crystalline | 130 |
| Benzene | Crosslinked powder | 5-10% of acetone- soluble polymer | Crystalline | 130 |

^a As determined by DTA, IR and X-ray analyses.

853 and 830 cm^{-1} . These spectral differences are similar to those observed by Iwasaki¹⁵ for amorphous and crystalline poly(isobutyl vinyl ether). The inherent viscosities of the acetone soluble fractions of these powders ranged between 0.20 and 0.40 dl/g.

The acetone insoluble fractions also showed signs of crystallinity by infrared, x-ray, and differential thermal analyses, but we verified that their insolubility was due to crosslinking by heating them in hexafluoro-*p*-xylene at temperatures above the crystalline melting point ($> 136^\circ\text{C}$), whereupon they swelled but did not dissolve. The low yields obtained in the hexafluoro-*p*-xylene, benzene, and carbon disulfide runs might be explained by the observation that the polymers formed were coated on the surface of the heterogeneous catalyst. This suggests that the competitive crosslinking reaction insolubilized the polymer thereby rendering the surface of the catalyst inactive. No mention of this crosslinking reaction has been made by Mosley⁹ or Lal¹⁸ in their studies of AHS-catalyzed polymerizations of alkyl vinyl ethers. Therefore, we feel that this crosslinking reaction is peculiar to trifluoroethyl vinyl ether and might involve abstraction of a

TABLE III
 2θ Values and Calculated Diffracting Distances for Crystalline
 Poly(trifluoroethyl Vinyl Ether)

| 2θ | $d, \text{\AA}$ |
|-----------|-----------------|
| 13.6 | 6.55 |
| 17.4 | 5.09 |
| 18.6 | 4.75 |
| 18.9 | 4.68 |
| 19.4 | 4.57 |
| 24.6 | 3.62 |

methylenic proton (alpha to the trifluoromethyl group) by an anionic coordination site on the heterogeneous catalyst¹⁸ to yield a carbanion capable of creating intermolecular crosslinks.

A second series of AHS-catalyzed polymerizations were conducted in five solvents at 60°C at higher monomer and catalyst concentrations (Table I). The results were similar to those obtained at room temperature. The yields were higher and so was the extent of the crosslinking reaction, but more material was available for characterization (Table IV). Although the polymers obtained from the heptane and carbon disulfide runs appeared to be amorphous, infrared and differential thermal analyses hinted that their methanol-insoluble fractions might have contained a very small amount (ca. 1%) of crystalline polymer.

Lal¹⁸ reported that AHS yields stereoregular (isotactic) and crystallizable poly(alkyl vinyl ethers) and measured the apparent first order rate constants for a series of alkyl vinyl ethers which decreased in the order: ethyl > *n*-butyl > *n*-hexyl = *n*-octyl. From our qualitative observation of the polymerization rate of trifluoroethyl vinyl ether in heptane and the overall rate constants given by Lal, we roughly estimate that trifluoroethyl vinyl ether is as unreactive as *n*-hexyl or *n*-octyl vinyl ether toward AHS, which

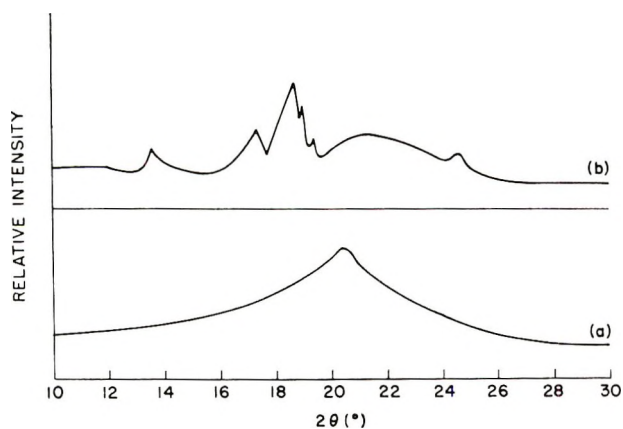


Fig. 2. X-ray scattering from (a) amorphous and (b) crystalline poly(trifluoroethyl vinyl ether).

TABLE IV
 Characteristics of Poly(trifluoroethyl Vinyl Ether)
 Polymerized in Various Solvents with 75% AHS at 60°C

| Polymerization solvent | Polymer characteristics and solubility data |
|------------------------------|---|
| Heptane | Rubbery polymer: methanol-soluble (12.8%) and -insoluble fractions; latter incompletely soluble in acetone (small fraction of crosslinked polymer); no evidence of crystallinity in either fraction ^a |
| Carbon disulfide | Mixture of viscous liquid (61%) and powder; powder has methanol-soluble (11.5%) and -insoluble fractions; latter incompletely soluble in acetone (small fraction of crosslinked polymer); no evidence of crystallinity in either fraction |
| Chloroform | Rubbery powder (mp 130°C), methanol-soluble (<5%) and -insoluble fraction; latter partially soluble and largely swollen by acetone (cross-linked); both fractions show signs of crystallinity |
| Acetone | Mixture of viscous liquid (80%) and powder (mp 130°C); powder has methanol-soluble (27%) and -insoluble fractions; latter incompletely soluble in acetone; both fractions show signs of crystallinity |
| Hexafluoro- <i>p</i> -xylene | Mixture of viscous liquid (50%) and powder (mp 130°C); powder has methanol-soluble (89%) and -insoluble fractions; latter incompletely soluble in acetone; both fractions show signs of crystallinity |

* As determined by DTA, IR, and x-ray analyses.

further demonstrates the deactivating effect of the trifluoromethyl group.

Vandenberg and co-workers^{5,6} reported the preparation of crystalline (presumably isotactic) poly(trifluoroethyl vinyl ether) by using a group III metal alkoxide-sulfuric acid complex catalyst. The polymer had a melting point of 128°C and a higher molecular weight than the crystalline polymers prepared by us. A reduced specific viscosity of 0.6 was cited for a 0.1% acetone solution at 25°C.

Our triisobutylaluminum-titanium tetrachloride-catalyzed polymerization of trifluoroethyl vinyl ether yielded a rubbery and slightly tacky polymer. Infrared, DTA, and x-ray analyses indicated that it was amorphous and noncrystallizable. These observations are in general agreement with those of Lal,¹⁸ who showed that if vinyl isobutyl ether was polymerized with triisobutylaluminum-titanium tetrachloride at temperatures above -20°C, the polymer produced was amorphous. Natta and co-workers²⁰ reported that if the polymerization of vinyl isobutyl ether with triamylaluminum-biscyclopentadienyltitanium dichloride was carried out at -30°C or higher, amorphous polymers were obtained.

In conclusion it can be said that trifluoroethyl vinyl ether is comparatively unreactive and polymerizes slowly with boron trifluoride etherate catalyst

due to the negative inductive effect of the fluoroalkyl group. In hydrocarbon solvents at -78°C , low molecular weight, tacky polymers are formed presumably due to poor solvency effects. Nontacky, rubbery polymers are formed in chlorinated hydrocarbon solvents, but as films they lack cohesive strength and rupture easily upon cold drawing. Despite this apparent unreactivity, polymerizations with boron trifluoride gas in chloroform or chloroform-pentane solvents proceed spontaneously and quantitatively to give high molecular weight, form-stable polymers.

The reason for the complete ineffectiveness of the Grignard-carbon tetrachloride catalyst system can only be speculated upon at this time. Perhaps the monomer was simply too unreactive toward this catalyst at 40°C and higher temperatures are required (pressure polymerizations). We intend to study this at a later date. The mechanism of this polymerization and the nature of the active catalyst is not known but we assume it to be cationic. Kray²¹ has suggested that when a Grignard reagent dissolved in diethyl ether (an etherate) is added to an alkyl vinyl ether, an early step in the formation of the active catalyst might involve the replacement of the diethyl ether by each of two vinyl ether oxygens (or double bonds). It is conceivable that the electron-withdrawing effect of the trifluoromethyl group (and not steric effects since isobutyl vinyl ether polymerizes readily) could sufficiently reduce the electron density about the vinyl ether oxygen atom or double bond so as to inhibit formation of the active catalyst.

As future work we plan to study the factors responsible for the termination of the chain growth reaction, particularly for the boron trifluoride etherate-catalyzed system (no complicating crosslinking reaction). Copolymerization studies would also be desirable to determine Alfrey-Price Q and e values in order to assess more quantitatively the deactivating effect of the 2,2,2-trifluoroethyl group.

The authors are indebted to Dr. M. Manning for the DTA studies and to Mrs. Mary McCann for the x-ray analyses.

References

1. C. E. Schildknecht, S. T. Gross, H. R. Davidson, J. M. Lambert, and A. O. Zoss, *Ind. Eng. Chem.*, **40**, 2104 (1948).
2. C. E. Schildknecht, S. T. Gross, and A. O. Zoss, *Ind. Eng. Chem.*, **41**, 1998 (1949).
3. C. E. Schildknecht, A. O. Zoss, and F. Grosser, *Ind. Eng. Chem.*, **41**, 2891 (1949).
4. E. J. Vandenberg, *Ital. Pat.* 571,741 (1958).
5. E. J. Vandenberg, R. F. Heck, and D. S. Breslow, *J. Polymer Sci.*, **41**, 519 (1959).
6. E. J. Vandenberg and D. L. Christman, U.S. Pat. 3,025,282 (1962).
7. E. J. Vandenberg and R. F. Heck, U.S. Pat. 3,025,283 (1962).
8. E. J. Vandenberg, in *First Biannual American Chemical Society Polymer Symposium (J. Polym. Sci. C, 1)*, H. W. Starkweather, Ed., Interscience, New York, 1963, p. 207.
9. S. A. Mosley, U.S. Pat. 2,549,921 (1951).
10. J. Lal, U.S. Pat. 2,984,656 (1961).
11. C. E. Schildknecht, U.S. Pat. 2,820,025 (1958).
12. S. Okamura, T. Higashimura, and H. Yamamoto, *J. Polym. Sci.*, **33**, 510 (1958).
13. C. E. Schildknecht, *Ind. Eng. Chem.*, **50**, 107 (1958).

14. C. E. Schildkuecht, private communication.
15. K. Iwasaki, *J. Polym. Sci.*, **56**, 27 (1962).
16. K. Iwasaki, H. Fukutani, Y. Tsuchida, and S. Nakano, *J. Polym. Sci. A* **1**, 2371, (1963).
17. J. G. Shukys, U.S. Pat. 2,830,007 (1958).
18. J. Lal and J. E. McGrath, *J. Polym. Sci.* **2**, 3369 (1964).
19. W. R. Sorenson and T. W. Campbell, *Preparative Methods of Polymer Chemistry*, Interscience, New York, 1961, p. 223.
20. G. Natta, G. Dall'asta, G. Mazzanti, U. Giannini, and S. Cesca, *Angew. Chem.*, **71**, 205 (1959).
21. R. J. Kray, *J. Polym. Sci.*, **44**, 264 (1960).

Received February 7, 1968

Relative Reactivities of Cyclic Ethers in Cationic Copolymerizations: Effects of Ring Strain and Basicity

SHUZO AOKI, YOSHIYUKI HARITA, YOSHIAKI TANAKA,
HIROSHI MANDAI, and TAKAYUKI OTSU, *Faculty of Engineering,
Osaka City University, Sugimotocho, Sumiyoshi-ku, Osaka, Japan*

Synopsis

The relative reactivities of α -monosubstituted cyclic ethers having rings of three to six members toward a cation were estimated from their copolymerizations with 3,3-bis(chloromethyl)oxetane (M_1) catalyzed by boron trifluoride etherate in methylene chloride at 0°C. It was found that the reactivity of these cyclic ethers was dominated by both the ring strain and the basicity. The following empirical equation was derived to represent the relative reactivity of cyclic ethers: $\log(1/r_1) = -0.086\Delta RS - 0.31\Delta B + 0.57$, where ΔRS and ΔB are constants, characteristic of ring strain and basicity of the cyclic ethers and determined from the differences in free energy of polymerization of the corresponding cycloalkanes and in basicity between M_1 and M_2 monomers, respectively. A good linear correlation was observed between the reactivities calculated from this equation and those obtained from the experiments.

Introduction

Although many studies have been made on the homo- and copolymerizations of cyclic ethers, quantitative and systematic studies of the relation between the structure and the reactivity of cyclic ethers to a cation have been few. In 1964 Iwatsuki et al.¹ reported that the relative reactivities of cyclic compounds to a growing polymer cation are correlated with their basicities. This treatment was extended to various copolymerization systems and discussed in detail.² Sakai et al.³ also investigated the competitive ring-opening reactions of cyclic ethers with stannic chloride and described the correlation between the relative reactivities and the basicities of cyclic ethers.

In a previous paper⁴ we reported that the relative reactivities of α -substituted ethylene oxides, which were estimated from copolymerizations with 3,3-bis(chloromethyl)oxetane (BCMIO), were higher than expected from their basicities, and we assumed that the ring strain of cyclic ethers might be the cause.

The present work was done to clarify the effects of both ring strain and basicity of α -monosubstituted cyclic ethers on their reactivities. The relative reactivities to a given cation were estimated from copolymeriza-

tions with BCMO catalyzed by boron trifluoride etherate as well as from those mentioned in the previous paper.⁴

Experimental

The experimental procedures have been described in previous papers.^{4,5} All copolymerizations were carried out under similar reaction conditions. The concentration of monomer mixtures was kept constant at 3 mole/l., and a suitable concentration of boron trifluoride etherate was used in methylene chloride at 0°C. The copolymers obtained were isolated at a lower conversion. The composition of the resulting copolymers was determined from their chlorine analysis, and the monomer reactivity ratios were calculated by the Fineman-Ross method.⁶

Results and Discussion

The monomer reactivity ratios in the copolymerization of various α -substituted cyclic ethers (M_2) and BCMO (M_1) are summarized in Table I.

TABLE I
Monomer Reactivity Ratios in Copolymerization of Various α -Substituted Cyclic ethers (M_2) and 3,3-Bis(chloromethyl)oxetane (M_1) catalyzed by $\text{BF}_3 \cdot \text{O}(\text{C}_2\text{H}_5)_2$ in CH_2Cl_2 at 0°C.

| α -Substituent | r_1 | r_2 | $1/r_1$ | Ref. |
|------------------------------------|-------|-------|------------|--------------|
| Three-membered ring: | | | | |
| C_2H_5 | 0.3 | 2.0 | 3.33 | present work |
| CH_3 | 0.3 | 0.65 | 3.33 | 4 |
| $\text{C}_6\text{H}_5\text{CH}_2$ | 0.45 | 1.1 | 2.22 | present work |
| H | 0.5 | 0.2 | 2.00 | 4 |
| CH_3OCH_2 | 0.7 | 0.1 | 1.45 | present work |
| C_6H_5 | 0.8 | 0.8 | 1.25 | 4 |
| $\text{C}_6\text{H}_5\text{OCH}_2$ | 1.1 | 0.25 | 0.91 | present work |
| Four-membered ring: | | | | |
| CH_3 | 0.04 | 3.4 | 25 | present work |
| H | 0.01 | 10.8 | 100 | present work |
| C_6H_5 | 0.05 | 2.7 | 20 | present work |
| Five-membered ring: | | | | |
| CH_3^a | — | — | 0.77 | 7 |
| H^b | 0.82 | 1.00 | 1.22 | 8 |
| C_6H_5 | 2.6 | 0 | 0.38 | present work |
| $\text{C}_6\text{H}_5\text{OCH}_2$ | 3.8 | 0 | 0.26 | present work |
| Six-membered ring: | | | | |
| CH_3 | 7.2 | 0 | 0.14 | present work |
| H^a | — | — | 0.66 | 7 |
| C_6H_5 | — | — | very small | present work |

^a Copolymerization was carried out in bulk.

^b Copolymerization was carried out in toluene.

When the relative reactivities of cyclic ethers to the poly(BCMO) cation given in Table I were plotted against their basicities (pK_b), which were determined by Iwatsuki et al.¹ and Sakai et al.,⁹ no linear relationship was observed. As has been known, this might suggest that the reactivity of the cyclic ethers was influenced not only by the basicity but also by the ring strain.

Then an attempt was made to derive an empirical equation between the reactivity and the structure of the cyclic ethers by using these two parameters. The free energies of polymerization (ΔG) of unsubstituted and methyl-substituted cycloalkanes, which were estimated by Dainton et al.,¹⁰ might be assumed to be used as a measure of the extent of their ring strains, RS ; see Table II. Furthermore, it was hypothesized that the free energies of polymerization of cyclic ethers are comparable to those of the corresponding cycloalkanes¹¹ and that the substituents other than the methyl group have only as much effect as the methyl group. Thus, when the contribution of ring strain was eliminated from the relative reactivities ($1/r_1$) with the term of $0.086\Delta G$, a fairly good linear correlation was observed, as is shown in Figure 1. Therefore, the relative reactivities of cyclic ethers to the poly-(BCMO) cation are empirically expressed by

$$\log (1/r_1) = -0.086\Delta G - 0.31(pK_b) + C \quad (1)$$

where C is a constant mainly determined by the M_1 used. A similar equation was also made by using the ring strain parameter ΔRS , rather than ΔG (see footnote of Table II).

To clarify further the basicity term in eq. (1), the polar effect of the α substituents on the reactivity was examined. Figure 2 shows the relationship between the relative reactivities of three- and five-membered cyclic ethers and their polar substituent constants σ^* ,¹² the relative reactivities appeared on different straight lines with the same slope ($\rho^* = -0.62$), except for the values of unsubstituted cyclic ethers. As is shown in Figure 3, a similar relationship appeared between the pK_b values and the σ^* constants; again the slopes of the resulting straight lines were the same ($\tan \theta = 1.9$). In the case of four- and six-membered cyclic ethers similar correlations might be predicted, but the available data were limited.

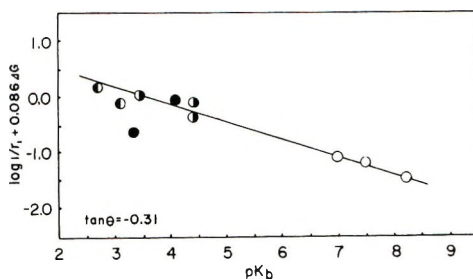


Fig. 1. Relationship between $\log 1/r_1 + 0.086\Delta G$ and pK_b of M_2 : (O) three-membered ring; (◐) four-membered ring; (◑) five-membered ring; (●) six-membered ring.

TABLE II
 Values of ΔG , $\Delta B/S$, and ΔB_1 for Cyclic Ethers

| Ring size | Substituent | ΔG of cyclo-alkane, ^a kcal/mole | $\Delta B/S$ ^b | pK_b of α -methyl-subst. cyclic ether | ΔB_1 ^c |
|-----------|---------------------------|---|---------------------------|--|---------------------------|
| 3 | H | -22.1 | -8.1 | | |
| 3 | α -Methyl | -18.1 | -4.1 | 6.94 ¹ | 1.3 |
| 3 | α,α -Dimethyl | -13.7 | 0.3 | | |
| 4 | H | -21.5 | -7.5 | | |
| 4 | α -Methyl | -17.7 | -3.7 | 2.7 | -3.0 |
| 4 | α,α -Dimethyl | -14.0 | 0.0 | | |
| 5 | H | -2.2 | 11.8 | | |
| 5 | α -Methyl | 1.5 | 15.5 | 3.47 ⁹ | -2.2 |
| 5 | α,α -Dimethyl | 4.8 | 18.8 | | |
| 6 | H | 1.4 | 15.4 | | |
| 6 | α -Methyl | 5.5 | 19.5 | 3.3 | -2.4 |
| 6 | α,α -Dimethyl | 7.8 | 21.8 | | |

^a Data for the polymerization of cycloalkanes.¹⁰

^b Indicated difference in ΔG between cycloalkanes and standard 1,1-dimethylcyclobutane taken as a model of BCMO.

^c Indicated difference in pK_b between cyclic ethers and standard BCMO ($pK_b = 5.65$).¹

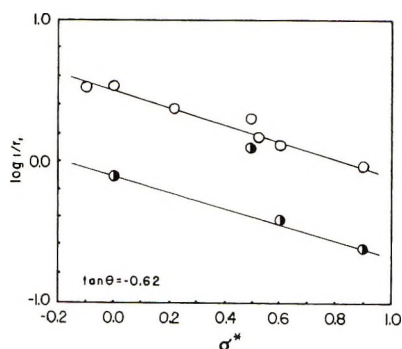


Fig. 2. Relationship between $\log 1/r_1$ and σ^* values: (O) three-membered ring; (●) five-membered ring.

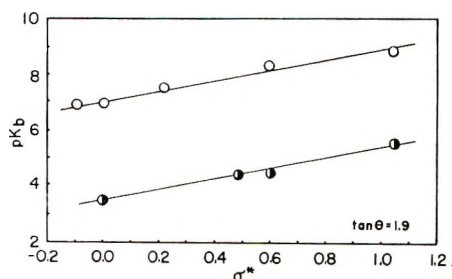


Fig. 3. Relationship between pK_b and σ^* values: (O) three-membered ring; (●) five-membered ring.

From the results of Figure 3 it is considered that the basicity of the cyclic ethers may be separated into two terms, in which the first term, B_1 , is dependent on the ring size and second one, B_2 , on the inductive effect of the substituent: $\text{p}K_b \equiv B = B_1 + B_2$. Hence, eq. (1) can be transformed into the following general equation:

$$\log (1/r_1) = \alpha \Delta RS + \beta \Delta B + C \quad (2)$$

where ΔB is given by $\Delta B = \Delta B_1 + B_2$, where $B_2 = \rho^* \sigma^* / \beta = 2.0 \sigma^*$

In eq. (2) the constants $\Delta RS \equiv \Delta \Delta G$ and ΔB are characteristic of the ring strain and basicity of the cyclic ethers used and are calculated from the differences in free energy of polymerization and in basicity between M_1 and M_2 , respectively (see footnote of Table II). The parameters α and β are the empirical constants depending on the contributions from ring strain and basicity, respectively, and C is a correction constant. In this equation the ΔB 's of the substituted cyclic ethers are easily obtained from the equation $\Delta B = \Delta B_1 + 2.0 \sigma^*$. Here eq. (2) may be rewritten in the empirical form

$$\log (1/r_1) = -0.086 \Delta RS - 0.31 \Delta B + 0.57 \quad (3)$$

This equation is substantially the same as eq. (1), but it is more useful; the relative reactivities of the cyclic ethers whose $\text{p}K_b$ values are not available may be predicted from this equation whenever the σ^* value of the substituent is obtainable from the literatures.

The comparison between the values calculated from eq. (3) and those observed (Table I) is shown in Figure 4. The good agreement between them emphasizes that the equation may be used under the conditions described for expressing the reactivity of cyclic ethers to the poly(BCMO) cation.

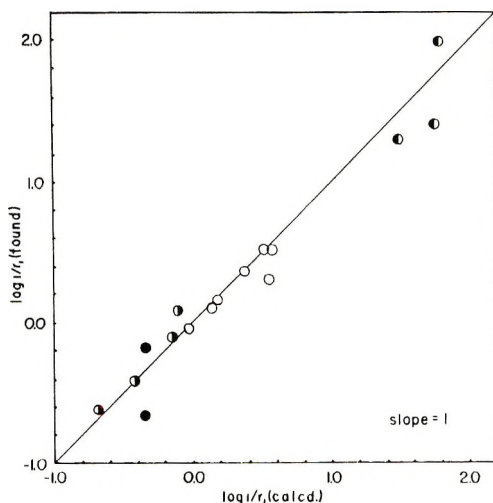


Fig. 4. Relationship between relative reactivities found and those calculated from eq. (3): (○) three-membered ring; (◐) four-membered ring; (●) five-membered ring; (●) six-membered ring.

The results mentioned above suggest that cationic polymerizations of cyclic ethers of different ring sizes proceed by similar reaction mechanisms; the growing polymer end is an oxonium ion, even in the case of ethylene oxides, as it is in oxetanes and tetrahydrofurans.^{4,13}

In the previous paper⁴ the reactivity of isobutene oxide to the poly-(BCMO) cation was found to be lower than that of propylene oxide in spite of the increased polar substituent effect. The relative reactivity of isobutene oxide calculated from eq. (3) was 2.74, and this value was smaller than that of propylene oxide, 3.33. Therefore it was concluded that the lower reactivity of isobutene oxide was understandable by its decreased ring strain.

References

1. S. Iwatsuki, N. Takikawa, M. Okada, Y. Yamashita, and Y. Ishii, *J. Polymer Sci. B*, **2**, 549 (1964); *idem.*, *Kogyo Kagaku Zasshi*, **67**, 1236 (1964).
2. Y. Yamashita, T. Tsuda, M. Okada, and S. Iwatsuki, *J. Polymer Sci. A-1*, **4**, 2121 (1966).
3. S. Sakai, T. Sugiyama, H. Tanaka, and Y. Ishii, paper presented at the 14th Annual Symposium on Polymer Chemistry, Japan, Kyoto, 1965, *Preprints*, p. 141.
4. S. Aoki, K. Fujisawa, T. Otsu, and M. Imoto, *Kogyo Kagaku Zasshi*, **69**, 131 (1966).
5. S. Aoki, Y. Harita, T. Otsu, and M. Imoto, *Bull. Chem. Soc. Japan*, **38**, 1922 (1965).
6. M. Fineman and S. D. Ross, *J. Polymer Sci.*, **5**, 269 (1950).
7. T. Tsuda, T. Nomura and Y. Yamashita, *Makromol. Chem.*, **86**, 301 (1965).
8. T. Saegusa, H. Inai, and J. Furukawa, *Makromol. Chem.*, **56**, 55 (1962).
9. S. Sakai, H. Tanaka, and Y. Ishii, *Kogyo Kagaku Zasshi*, **69**, 1388 (1966).
10. F. S. Dainton, T. R. E. Devlin, and P. A. Small, *Trans. Faraday Soc.*, **51**, 1710 (1955).
11. P. A. Small, *Trans. Faraday Soc.*, **51**, 1717 (1955).
12. R. W. Taft, Jr., in *Steric Effects in Organic Chemistry*, M. S. Newman, Ed., Wiley, New York, 1956, p. 619.
13. H. Haubenstock and W. Naegle, *Makromol. Chem.*, **97**, 248 (1966).

Received November 24, 1967

Revised February 8, 1968

1,5-Polymerization of 1-Thioacylaziridines

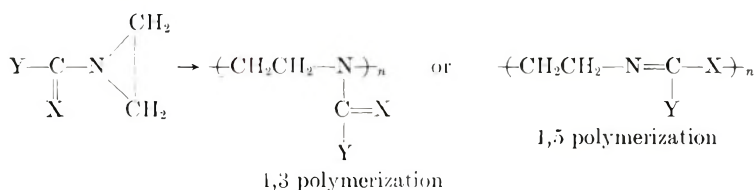
YOSHIO IWAKURA, AIKO NABEYA, and TAKESHI NISHIGUCHI,
*Department of Synthetic Chemistry, Faculty of Engineering,
 University of Tokyo, Bunkyo-ku, Tokyo, Japan*

Synopsis

Four thioacylaziridines, 1-thioaroyl-, 1-(*N*-phenylthiocarbonyl)-, 1-(aryloxythiocarbonyl)-, and 1-(aryldithiooxycarbonyl)aziridines, were found to undergo 1,5-polymerization to giving polymers of polyiminothioether, polyisothioureia, polyiminothiocarbonate, and polyiminodithiocarbonate structure, respectively. The 1,5 polymerization may be explained by the kinetic factors rather than the thermodynamic ones.

INTRODUCTION

Aziridines possessing an α -unsaturated substituent at the 1 position are able to form polymers by either of two processes:



where X is =O, =S, =N—, etc., and Y is —O—Ar, —S—Ar, —NH—Ar, —Alkyl, etc.

In a previous paper,¹ we reported the syntheses and reactions of new thioacylaziridines, 1-thioaroyl-, 1-(aryloxythiocarbonyl)-, and 1-(aryldithiooxycarbonyl)aziridines. They were unstable and polymerized either gradually or rapidly on standing at room temperature.

The 1,3 polymerization of specific 1-acylaziridines, such as the 1-(perfluoroacyl)aziridines² and 1-(alkoxycarbonyl)aziridines,³ has been reported. However, in the case of 1-thioacylaziridines, including 1-(*N*-phenylthiocarbonyl)aziridine, the 1,5 polymerization was observed exclusively. In view of this difference it seemed to be of interest to elucidate the factors governing the polymerization processes.

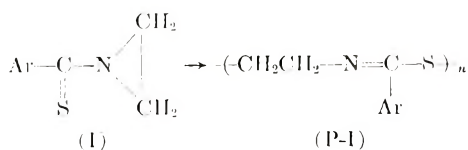
RESULTS AND DISCUSSION

Polymerization of 1-Thioaroylaziridines (I)

1-Thiobenzoyl- and 1-(*p*-chlorothiobenzoyl)aziridine, (Ia) and (Ib), polymerized explosively when kept at room temperature for several min-

utes, while 1-(*p*-methylthiobenzoyl)- and 1-(*p*-methoxythiobenzoyl)-aziridine, (Ic) and (Id), did so more gently.

In solution (I) polymerized rapidly with nucleophilic initiators such as *n*-butyllithium, triethylamine, and sodium cyanide, and did so very slowly without initiators. It was found that the polymers (P-I) from (I) had polyiminothioether structure, resulting from 1,5 polymerization.



where Ar is (a) phenyl, (b) *p*-chlorophenyl, (c) *p*-tolyl, or (d) *p*-methoxyphenyl.

The structure of (P-I) was established from the following facts.

(a) The infrared spectra resemble those of 2-arylthiazolines, which have iminothioether linkage, and showed a strong peak ascribable to C=N linkage near 1610 cm.^{-1} .

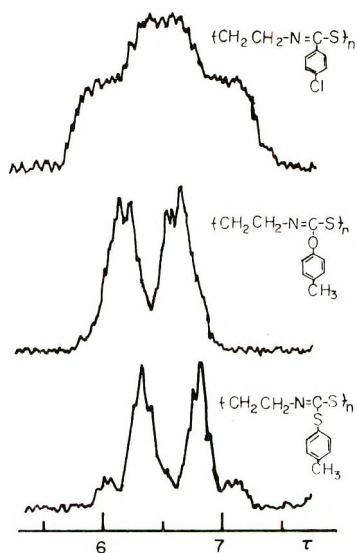
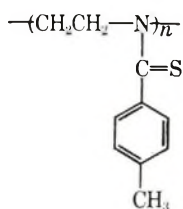


Fig. 1. NMR spectra of methylene regions of polymers at 60° in *o*-dichlorobenzene at 60 mc./sec.: (top) polymer (P-Ib); (middle) polymer (P-IIIa); (bottom) polymer (P-IVa). Tetramethylsilane was internal standard.

(b) In the nuclear magnetic resonance (NMR) spectra broad peaks of methylene protons assignable to the A_2B_2 type⁴ of structure were observed. A part of the spectrum of (P-Ib) is shown in Figure 1 as an example.

(c) Poly(*N*-*p*-methylthiobenzoyl)ethylenimine (P-I'c), which would result from 1,3 polymerization of (Ic), was prepared in the condensation reaction of polyethylenimine and sodium *p*-methylthiobenzoylthioglycolate.

The infrared spectrum and chemical behavior of (P-I'c) were quite different from those of (P-Ic).



(P-I'c)

The results of the polymerization of (Ia-d) are summarized in Table I.

The results indicate that the smaller the amount of *n*-butyllithium, the higher the viscosities of the resultant polymers. Figure 2 shows reduced viscosity versus time for the polymerization of (Ib): when 3 mole-% of *n*-butyllithium was added to a 0.3*M* solution of (Ib) in tetrahydrofuran, the polymerization was almost complete within 3 hr.

The infrared analysis demonstrated that appreciable polymerization of (Ib) took place within 1 hr. when 5 wt.-% of (P-I) or *N*-methylbenzthioamide was added to a solution of (Ib), whereas no polymerization of (Ib) was observed within 1 day when 2-aryltiazolines or *N,N*-dimethylbenz-

TABLE I
Polymerization^a of 1-Thioaroylaziridines (I)

| (I) | Solv. | Init. | Concn., mole-% | Yield, % | η_{sp}/c^b | P-I m.p., °C. | \bar{M}_n^c ($\times 10^3$) |
|------|------------------|------------------|-------------------|-------------|-------------------|------------------|------------------------------------|
| (Ia) | d | d | d | d | 0.09 | 55-58 | 2.8 |
| | d | d | d | d | 0.55 ^e | 84-98 | |
| (Ib) | THF ^f | <i>n</i> -BuLi | 5 | 82 | 0.11 | 90-100 | 4 |
| | " | " | 1 | 90 | 0.14 | | 8 |
| | " | " | 0.5 | 94 | 0.15 | | |
| | " | " | 0.2 | 93 | 0.16 | | |
| | " | " | 0.05 | 92 | 0.28 | | |
| | " | DMF ^g | Et ₃ N | 1 | 86 | 0.14 | |
| (Ic) | THF | <i>n</i> -BuLi | 1 | 81 | 0.14 | 142-153 | |
| | | | 1 | 90 | 0.14 | | |

^a Unless otherwise noted 2.5 mmoles of (I) in 1.5 ml. of the designated solvent was allowed to stand for 1 day at room temperature.

^b Reduced viscosity in *N*-methylpyrrolidone (1% concn. at 30°).

^c Number-average molecular weight measured by a vapor-pressure osmometer in benzene.

^d See under "Experimental."

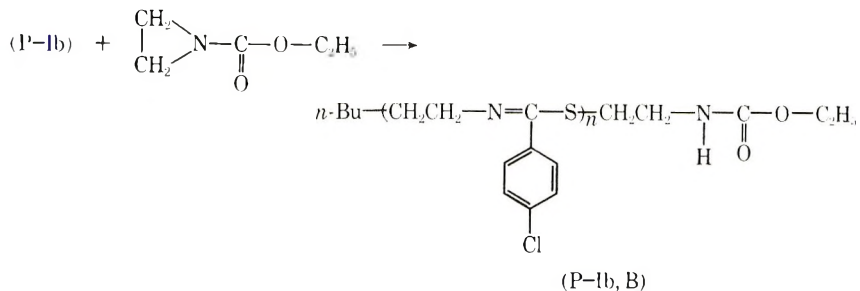
^e The intrinsic viscosity was 0.45 in *N*-methylpyrrolidone at 30°.

^f Tetrahydrofuran.

^g Dimethylformamide.

^h Substance (Ib) in DMF was allowed to stand for 5 days at room temperature.

To see whether the acid-catalyzed depolymerization would proceed only from that polymer chain end which has an active hydrogen or from any place in the chain a comparison was made between the acid-catalyzed depolymerization of an alkylated and a nonalkylated (P-Ib). Alkylation of (P-Ib) was performed by the ring-opening addition reaction of 1-ethoxycarbonylaziridine with the polymer endgroup, ($-\text{SH}$).



In the reaction of the alkylated (P-Ib), or (P-Ib,B), and picric acid in tetrahydrofuran an induction period of 30 min. was observed, whereas in the control run of non-alkylated (P-Ib), or (P-Ib,A), no induction period was observed; see Figure 3. This fact indicates that the acid-catalyzed depolymerization of (P-I) can be initiated not only from the polymer end having an active hydrogen but also from the inner part of the polymer chain, though with slightly more difficulty. Moreover, NMR analysis and vapor-pressure osmometer measurement revealed that (P-I) depolymerized slowly even in inert solvents at room temperature.

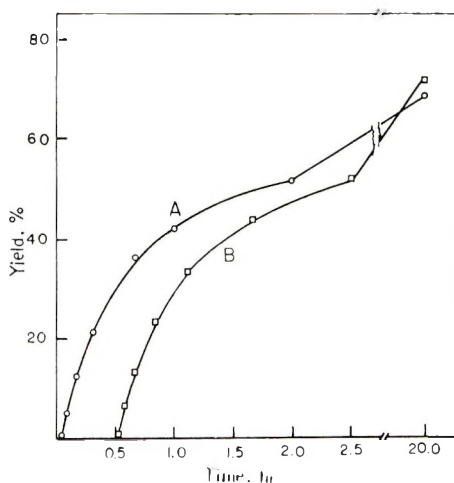
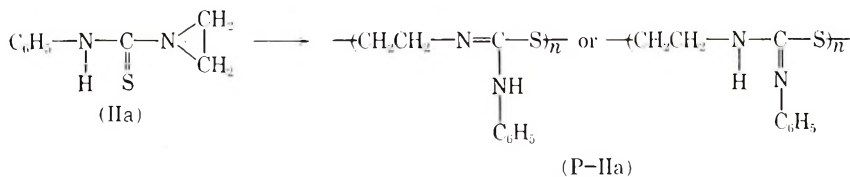


Fig. 3. Time versus conversion to picrate of 2-(*p*-chlorophenyl)thiazoline for depolymerization of (A) nonalkylated (P-Ib) and (B) alkylated (P-Ib) with picric acid.

Polymerization of 1-(*N*-Phenylthiocarbamyl)aziridine (IIa)

1-(*N*-Alkyl- or arylthiocarbamyl)aziridines⁵⁻⁹ and their polymers are known in the literatures, but no structural study of them has been reported. Substance (IIa) polymerized gradually on standing at room temperature, and its polymerization was initiated with basic substances such as triethylamine, *tert*-BuONa, and piperidine. The results of this polymerization are detailed under "Experimental." All the solvents examined dissolved the polymer (P-IIa) only incompletely. The infrared spectra of the polymers from (IIa) were essentially the same, regardless of the polymerization conditions or the solubility.

The tetrahydrofuran-insoluble part of (P-IIa) which was soluble in *N*-methylpyrrolidine had a reduced viscosity of 0.2-0.3 in *N*-methylpyrrolidone (1% concn. at 30°). The structure of (P-IIa),



was found to be of the polyisothiourea type resulting from 1,5 polymerization, according to the following itemized observations.

(a) The infrared spectrum of (P-IIa) exhibited a strong absorption assignable to the C=N stretching band at 1580 cm.⁻¹ (with a shoulder at 1605 cm.⁻¹).

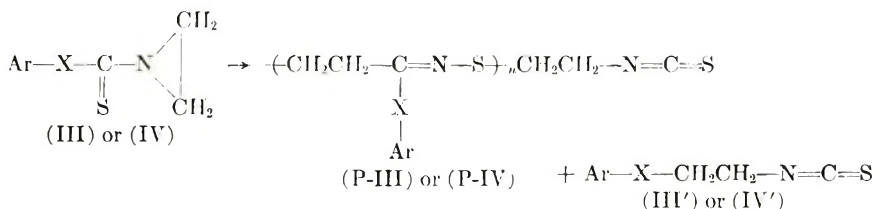
(b) Poly-*N*-(*N'*-phenylthiocarbamyl)ethylenimine (P-II'a), which would result from 1,3 polymerization of (IIa), was synthesized from polyethylenimine and phenylisothiocyanate. The infrared spectrum and chemical behavior of (P-II'a) are quite different from those of (P-IIa).

(c) In the presence of acids (P-IIa) depolymerized, giving 2-anilinothiazoline. For example, (P-IIa) and picric acid gave the picrate of 2-anilinothiazoline in 84% yield after a refluxing in benzene for 2 hr. However, (P-II'a) did not depolymerize under the same conditions.

Polymerization of 1-(Aryloxythiocarbonyl)- and 1-(Aryldithiooxycarbonyl)-aziridines, (III) and (IV)

As mentioned in the previous paper,¹ (III) and (IV) were fairly unstable at room temperature and rapidly underwent 1,5 polymerization, giving polyiminothiocarbonates (P-III) and polyiminodithiocarbonates (P-IV), which have an isothiocyanate group at the polymer chain end.

In some cases aniline adducts of 2-aryloxyethyl- or 2-aryldithioethylisothiocyanates, (III') and (IV') respectively, were isolated by treating the polymerization mixtures with aniline.



where

- (IIIa), (P-IIIa), (III'a): X = O, Ar = *p*-tolyl
 (IIIb), (P-IIIb), (III'b): X = O, Ar = *p*-nitrophenyl
 (IVa), (P-IVa), (IV'a): X = S, Ar = *p*-tolyl
 (IVb), (P-IVb), (IV'b): X = S, Ar = *p*-chlorophenyl
 (IVc), (P-IVc), (IV'c): X = S, Ar = *p*-methoxyphenyl

In the polymerization of 1-(*p*-nitrophenyloxythiocarbonyl)aziridine (IIIb) the substance 2-(*p*-nitrophenyloxy)ethylisothiocyanate (III'b) was isolated. Table III reports the results of the polymerization of (III) and (IV).

The structures of (P-III) and (P-IV) were confirmed by the following facts.

TABLE III
 Polymerization^a of 1-(Aryloxythiocarbonyl)aziridines (III) and
 1-(Aryldithiooxycarbonyl)aziridines (IV)

| Monomer | Solv. | Initiator | Yield, % | η_{sp}/c^b | \bar{M}_n^c | Yield ^d of (III') and (IV'), % |
|---------|-------|-------------------|-------------|-----------------|---------------|---|
| (IIIa) | none | none | 13 | 0.08 | 2800 | 4 |
| | THF | <i>n</i> -BuLi | 54 | 0.09 | | 0 |
| | " | Et ₃ N | 58 | 0.09 | | 0 |
| | " | "(e) | 57 | 0.09 | | 0 |
| (IIIb) | " | <i>n</i> -BuLi | 9 | 0.08 | | 16 ^f |
| | " | Et ₃ N | trace | | | 49 ^f |
| (IVa) | " | " | 33 | 0.04 | 1500 | 14 |
| | DMF | NaCN | 34 | 0.05 | | 12 |
| | " | none | 53 | 0.04 | | 5 |
| (IVb) | THF | Et ₃ N | 23 | 0.09 | 3100 | 8 |
| (IVc) | none | none | 6 | | | 29 |
| | THF | Et ₃ N | 24 | 0.08 | | 14 |
| | " | <i>n</i> -BuLi | 27 | 0.07 | | 24 |

^a Unless otherwise noted, 0.1 mmole (1 mole-%) of initiator was added to 10 mmoles of monomer in solvents.

^b Reduced viscosity measured at a concentration of 1% in *N*-methyl pyrrolidone at 30°.

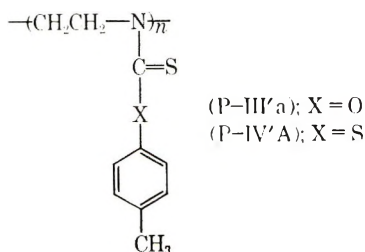
^c Number-average molecular weight measured by vapor-pressure osmometer in benzene.

^d Yield of (III') and (IV') was evaluated as adducts of aniline, ArXCIL₂CH₂NH-CSNHC₃H₅.

^e A 5 mole-% amount of initiator was added.

^f A part of (III'b) was isolated.

(a) The infrared spectra and chemical behavior of (P-IIIa) and (P-IVa) were quite different from those of *N*-substituted polyethylenimines, (P-III'a) and (P-IV'a), which were synthesized by the condensation reactions of polyethylenimine with chlorothionformic acid *p*-tolylester and chlorodithioformic acid *p*-tolylester.



(b) The methylene protons of (P-IIIa) appeared as two multiplets centered at 6.6 and 6.2 τ with equal areas in the NMR spectrum, in *o*-dichlorobenzene at 60°. Those of (P-IVa) were shown as two strong multiplets at 6.8 and 6.4 τ and two weak ones at 7.1 and 6.0 τ . These absorption patterns are assignable to the A₂B₂ type.⁴ The NMR spectra are shown in Figure 1.

The fact that the triethylamine-initiated polymers showed a very weak triplet at 8.9 τ and that triethylbenzylammonium chloride exhibited a triplet in the vicinity of 9 τ in aromatic solvents suggests that the initiator is attached at the end of the polymer.

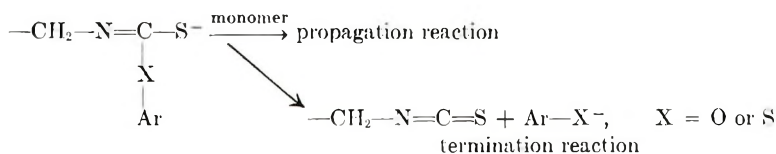
(c) The infrared spectra of (P-III) and of (P-IV) showed strong peaks attributable to C=N near 1640 and 1580 cm.⁻¹, respectively, and weak ones characteristic of the isothiocyanate group in the regions of 2150 and 2240

TABLE IV
Polyiminothiocarbonates (P-III) and Polyiminodithiocarbonates (P-IV)

| Polymer and formula | Analysis, % | | | $\nu_{\text{C=N}}$, cm. ⁻¹ | $\nu_{\text{N=C=S}}$, cm. ⁻¹ | (shoulder) |
|--|-------------|------|-------|---|---|------------|
| | C | H | N | | | |
| (P-IIIa) (C ₁₀ H ₁₁ NOS) _n | | | | | | |
| Calcd. | 62.15 | 5.74 | 7.25 | 1640 | 2150 | (2240) |
| Found | 62.26 | 5.81 | 7.43 | | | |
| (P-IIIb) (C ₁₀ H ₈ N ₂ O ₂ S) _n | | | | | | |
| Calcd. | 48.21 | 3.60 | 12.49 | 1670 | 2140 | (2230) |
| Found | 48.43 | 3.82 | 12.60 | | | |
| (P-IVa) (C ₁₀ H ₁₁ NS ₂) _n | | | | | | |
| Calcd. | 57.41 | 5.30 | 6.70 | 1580 | 2140 | (2230) |
| Found | 57.79 | 5.25 | 6.89 | | | |
| (P-IIIb) (C ₁₀ H ₈ ClNS ₂) _n | | | | | | |
| Calcd. | 47.05 | 3.51 | 6.10 | 1580 | 2140 | (2240) |
| Found | 46.63 | 3.69 | 5.86 | | | |
| (P-IVc) (C ₁₀ H ₁₁ NOS ₂) _n | | | | | | |
| Calcd. | 53.33 | 4.92 | 6.22 | 1590 | 2150 | (2240) |
| Found | 53.47 | 5.11 | 6.70 | | | |

cm.⁻¹ (shoulder). The analytical and infrared spectral data are summarized in Table IV.

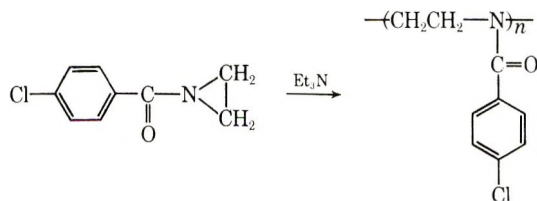
The higher the molecular weight of the polymers, the weaker the absorption intensity of the isothiocyanate group. On treating of the polymers with aniline the absorption of the isothiocyanate group disappeared. A mixture of (P-IIIa) and picric acid exhibited no change except for the disappearance of the peaks of the isothiocyanate group in its infrared spectrum, by refluxing in benzene. The existence of an isothiocyanate group at the polymer end suggests that the termination reaction of the polymerization was caused by the elimination of phenols or thiophenols (perhaps phenolates or thiophenolates).



General Discussion

The 3 → 5 ring-expansion reactions of 1-acyl- and 1-thioacylaziridines correspond to 1,5 polymerization in the sense that the keto form is converted to the enol form, and the ring-opening addition reactions are analogous to the 1,3 polymerization, because the carbonyl or the thiocarbonyl groups are still maintained.

Since previous studies^{6,7} revealed that the 1-acylaziridines isomerize less readily than the 1-thioacyl derivatives, they were expected to undergo 1,3, in preference to 1,5, polymerization. With triethylamine as initiator 1-(*p*-chlorobenzoyl)aziridine was polymerized and gave polymer of a reduced viscosity of 0.22 in 33% yield along with a trace of 2-(*p*-chlorophenyl)oxazoline. The polymer was found to have the expected structure, poly(*N*-*p*-chlorobenzoyl)ethylenimine, from the fact that its infrared spectrum was essentially the same as that of the sample obtained by the acylation of polyethylenimine with *p*-chlorobenzoyl chloride.



Similar examples of the 1,3 polymerization of 1-acylaziridines have previously been reported.^{2,3}

It seems to be evident that in amides the keto form (amide form) is more stable than the enol form (imino form) thermodynamically, for the rearrangement of *N*-substituted iminoethers to *N,N*-disubstituted amides is

well known (Chapman rearrangement¹⁰). Similarly, in benzthioamides the keto form (thione form) appears to be more stable than the enol form (imino form) from the following facts.

(a) *N*-methylbenzthioamide was found to have the keto form at various temperatures in a comparison of its infrared and NMR spectra with those of *N,N*-dimethylbenzthioamide and methyl *N*-methylbenzthioimidate. Most workers have concluded that thioamides,¹¹⁻¹⁴ thiourcas,^{15,16} and dithiourethanes¹⁷ also exist essentially in the keto form, although some reports¹⁸⁻²⁰ have described the presence of greater or lesser amounts of the enol form.

(b) It has been reported²¹ that phenyl *N*-phenylbenzthioimidate rearranges thermally to *N,N*-diphenylbenzthioamide at 280-290° and that the latter compound is recovered unchanged under the same conditions. Consequently, 1,5 polymerization of 1-thioacylaziridines might be the result of kinetic, rather than thermodynamic, control of the reaction.

It is known that alkylation of thioamides by saturated alkylating reagents generally occurs at the sulfur atom (S alkylation),²² although N alkylation of benzthioamide by tritylchloride in pyridine has been reported.²³

Generally, S alkylation of thioamides may be explained by the kinetic factor rather than the thermodynamical one.

EXPERIMENTAL

The melting points and boiling points given in this section are uncorrected. The NMR spectra were measured in a specified solution with tetramethylsilane as the internal standard at 60 Mc./sec.

Preparation of 1-Thiobenzoyl aziridine (Ia) and Its Polymerization

Thiobenzoylthioglycolic acid (21.2 g., 0.1 mole) was neutralized with sodium bicarbonate (9.2 g.) in 50 ml. of water. To the aqueous solution a cold solution of 6.5 g. (0.15 mole) of aziridine in 50 ml. of water was added at 0-5°, and the mixture was stirred for 5 min.

The mixture was extracted with *n*-hexane, and the organic layer was washed with ice water several times, filtered from solid impurities, and cooled in a Dry Ice-acetone bath. Yellow needles (Ia) of low melting point (ca. 5°) were collected on a filter in a cold chamber and dissolved in dimethylformamide. The solution was allowed to stand for 3 days at room temperature. Polymer (P-Ia) was precipitated by addition of the solution to methanol and weighed about 8 g. (50% based on thiobenzoylthioglycolic acid); m.p. 55-58°. The reduced viscosity was 0.09 measured at a concentration of 1% in *N*-methylpyrrolidone at 30°. Molecular weight was measured by vapor-pressure osmometer in benzene and was found to be 2.8×10^3 . After the polymer was washed with methanol in a Soxhlet extractor for 3 hr., the residue weighed 3.2 g. (20%), m.p. 84-98°, and had an intrinsic viscosity (in *N*-methylpyrrolidone, at 30°) of 0.45.

Polymerization of 1-Thioaroylaziridines (I)

Substance I was prepared by the procedure previously reported.¹ To a solution of 1-(*p*-chlorothiobenzoyl)aziridines (Ib) (0.49 g., 2.5 mmoles) in 1.5 ml. of dry tetrahydrofuran was added 0.025 mmole (1 mole-%) of *n*-butyllithium in *n*-heptane with a syringe under cooling in an ice-salt bath. The operation was carried out quickly to avoid exposure to moisture. The solution was allowed to stand for 2 days at room temperature and poured into methanol to precipitate the polymer (P-Ib). The polymer was dissolved in tetrahydrofuran, reprecipitated again in methanol, and dried *in vacuo*, giving 0.45 g. (90%) of yellowish powder melting at 90°–110°. The reduced viscosity of the polymer was 0.14 at 30° (1% solution in *N*-methylpyrrolidone), and the molecular weight measured by a vapor-pressure osmometer in benzene was about 8×10^3 . The polymerization of (I), shown in Table I, was carried out in the same manner as in the case of (Ib) described above. The analytical data of (P-I) are summarized in Table V.

TABLE V
Polyiminothioethers (P-I)

| Polymer and formula | Analysis, % | | | | | | $\nu_{C=N}$, cm. ⁻¹ |
|--|-------------|------|------|-------|------|------|------------------------------------|
| | Calcd. | | | Found | | | |
| | C | H | N | C | H | N | |
| (P-Ia), (C ₉ H ₉ NS) _n | 66.22 | 5.56 | 8.65 | 66.25 | 5.75 | 8.55 | 1612 |
| (P-Ib), (C ₉ H ₈ ClNS) _n | 54.68 | 4.08 | 7.09 | 54.39 | 4.16 | 7.05 | 1612 |
| (P-Ic), (C ₁₀ H ₁₁ NS) _n | 67.76 | 6.26 | 7.90 | 67.90 | 6.26 | 7.93 | 1608 |
| (P-Id), (C ₁₀ H ₁₁ NOS) _n | 62.15 | 5.74 | 7.25 | 62.26 | 5.72 | 7.15 | 1605 |

Polymerization of (Ib) in a Viscometer

An Ubbelohde viscometer containing 1.20 g. (ca. 6 mmoles) of (Ib) and 20 ml. of anhydrous tetrahydrofuran was flushed with nitrogen and closed to air with rubber tubes. To the viscometer kept at 30° was added 0.18 mmole (3 mole-%) of *n*-butyllithium in *n*-heptane with a syringe, and the reduced viscosity was measured at appropriate time intervals. The results are shown in Figure 2.

Synthesis of Poly(*N-p*-methylthiobenzoyl)ethylenimine (P-I'c)

A commercially available aqueous solution of polyethylenimine (molecular weight ca. 2×10^3) was dehydrated by repeated azeotropic distillations with benzene. 1-*p*-Methylthiobenzoylthioglycolic acid (2.26 g., 10 mmoles) was neutralized with sodium hydroxide (0.4 g.) in methanol, and the solvent was evaporated. To the residue was added 0.3 g. of polyethylenimine dissolved in 10 ml. of dimethylformamide, and the mixture was stirred for 8 hr. Polymer (P-I'c) was precipitated by addition to water,

reprecipitating from tetrahydrofuran to methanol, and it weighed 0.27 g. (22%); m.p. 94–98°.

ANAL. Calcd. for $C_{10}H_{11}NS$ (%): C 67.76, H 6.26, N 7.90. Found (%): C 65.88, H 7.34, N 7.99.

Acid-Catalyzed Depolymerization of (P-I)

(a) Substance (P-Ia) (1.63 g.) and picric acid (2.29 g., 10 mmoles) were heated under reflux for 1 hr. in 10 ml. of benzene. After cooling, the yellow crystals were collected on a filter and washed with benzene. The dried picrate weighed 3.64 g. (93%); m.p. 170–173° (lit.²⁴ 172.0–173.5°).

ANAL. Calcd. for C_9H_5NS (%): N 14.28. Found (%): N 14.46.

Other reactions between (P-I) and picric acid were carried out in the same manner as that described above.

Substance (P-I'c) and picric acid were heated in a manner similar to that described above, and benzene was removed. The infrared spectrum of the residue was lacking in absorption bands characteristic of the picrate of 2-tolylthiazoline and showed those of the unchanged (P-I'c) and picric acid.

(b) Substance (P-Ia) (1.63 g.) and *p*-toluenesulfonic acid (1.72 g., 10 mmoles) were refluxed in benzene (10 ml.) for 1 hr. From the reaction mixture, benzene was removed, and the residue was washed with acetone to give 2.41 g. (72%) of white crystals melting at 131–133°. Recrystallization from tetrahydrofuran raised the melting point to 132–135°.

ANAL. Calcd. for $C_{16}H_{17}NO_3S_2$ (%): C 57.31, H 5.11, N 4.18. Found (%): C 57.46, H 5.32, N 4.07.

(c) A mixture of 1.63 g. of (P-Ia) and 1.42 g. (10 mmoles) of boron trifluoride etherate in 10 ml. of benzene was refluxed for 1 hr. The oily product solidified after being left overnight, and the product was filtered and washed with a small quantity of tetrahydrofuran to give 2.05 g. (89%) of white powder melting at 103–106°. Recrystallization from tetrahydrofuran gave 1.42 g. (62%) of white needles melting at 109–110°.

ANAL. Calcd. for $C_9H_9BF_3NS$ (%): C 46.79, H 3.93, N 6.06. Found (%): C 46.81, H 4.48, N 5.83.

Alkylation of Polymer Chain End of (P-Ib) with 1-Ethoxycarbonylaziridine

Method A. Substance (Ib) (3.95 g., 20 mmoles) dissolved in anhydrous tetrahydrofuran (10 ml.) was cooled in a Dry Ice–acetone bath, and 1 mmole of *n*-butyllithium in *n*-heptane was added with a syringe. The solution was left at room temperature for 1 day and divided into two equal portions. One portion was precipitated into methanol and gave non-alkylated (P-Ib,A). To the other portion 2 g. of 1-ethoxycarbonylaziridine²⁵ was added, and tetrahydrofuran was removed at reduced pressure from the solution. After 3 days the reaction mixture was poured into methanol to precipitate the alkylated (P-Ib,B). Both of the polymers (A and B) were washed with pentane–ether in a Soxhlet extractor for 10 hr.

They had the same reduced viscosity, 0.08, at 30° (1% solution in *N*-methylpyrrolidone). The infrared spectra of (P-Ib,B) had a very weak C=O stretching band at 1700 cm.⁻¹.

Method B. To 1.5 g. of the isolated (P-Ib) was added 2 g. of 1-ethoxy-carbonylaziridine. The mixture was allowed to stand for 3 days at room temperature and then was poured into methanol. The precipitate was filtered, washed with methanol, and dried *in vacuo*, giving 1.3 g. of alkylated (P-Ib,B).

Depolymerization of Non-alkylated (P-Ib,A) and Alkylated (P-Ib,B) with Picric Acid

In 5 ml. of tetrahydrofuran 1.06 g. of (P-Ib,A) or (P-Ib,B) and 1.22 g. of picric acid were dissolved. The two tetrahydrofuran solutions were combined, and the precipitated picrate was separated by filtration from the reaction mixture at appropriate time intervals and weighed. The results are shown in Figure 3.

Polymerization of 1-(*N*-Phenylthiocarbamyl)aziridine (IIa)

To a solution of 0.59 g. (3.3 mmoles) of (IIa)⁵ in 5 ml. of tetrahydrofuran a specified initiator was added, and the solution was allowed to stand at 60° for 3 days. The white polymer (P-IIa) that precipitated was filtered, dried *in vacuo*, and weighed. Then the polymer was washed with acetone, to remove polymer of low molecular weight. The organic solvents examined, such as *m*-cresol, chloroform, dimethylformamide, dimethylacetamide, methylcellosolve, dimethylsulfoxide, benzene, toluene, and pyridine, did not dissolve the polymer completely. The *N*-methylpyrrolidone-soluble part, which was insoluble in tetrahydrofuran, had a reduced viscosity of 0.2–0.3 in *N*-methylpyrrolidone (1% concn. at 30°). See Table VI.

TABLE VI

| Initiator | Amount | Tetrahydrofuran-insoluble part | | Acetone-insoluble part | |
|--------------------|---------|--------------------------------|-----------|------------------------|-----------|
| | | Yield, % | M.p., °C. | Yield, % | M.p., °C. |
| <i>tert</i> -BuONa | 2.3 mg. | 93 | 145–153 | 64 | 184–188 |
| Et ₃ N | 2 drops | 95 | 145–155 | 66 | 167–177 |
| Piperidine | 1 drop | 51 | | 36 | |

Synthesis of Poly(*N*-Phenylthiocarbamyl)ethylenimine (P-II'a)

To the dehydrated polyethylenimine (2.15 g.) dissolved in 50 ml. of anhydrous benzene 11 g. of phenylisothiocyanate was added portionwise with stirring. After additional stirring for 5 hr. the solvent (benzene) was removed at reduced pressure, and the residue was washed with methanol in

a Soxhlet extractor for 8 hr. The purified (P-II'a) weighed 7.9 g. (89%); m.p. 155–172°.

ANAL. Calcd. for $C_9H_{10}N_2S$ (%): N 15.72. Found (%): N 16.10.

Depolymerization of (P-IIa) with Picric Acid

A mixture of 5.34 g. of (P-IIa) and 6.87 g. (30 mmoles) of picric acid in 30 ml. of benzene was refluxed for 2 hr. After cooling, the yellow precipitate was filtered, washed with benzene, and dried. The crude picrate weighed 10.14 g. (84%) and melted at 198 to 203°. Two recrystallizations from ethanol gave an analytical sample; m.p. 204–206°. (lit.⁶ 206–207°).

ANAL. Calcd. for $C_{15}H_{13}N_5O_7S$ (%): N 17.20. Found (%): N 17.52.

Polymer (P-II'a) and picric acid were heated in the manner described above, and benzene was removed. The infrared spectrum of the residue was lacking in absorptions characteristic of the picrate of 2-anilinothiazoline and showed peaks due to unchanged (P-II'a) and picric acid.

Polymerization of 1-(*p*-Tolyloxythiocarbonyl)aziridine (IIIa)

Substance (IIIa) was prepared by the method previously reported.¹

(a) When (IIIa) (3.16 g., 18 mmoles) was dried at room temperature in a desiccator over calcium chloride, it polymerized exothermically and gave glassy material. The polymeric substance was dissolved in tetrahydrofuran and poured into methanol. The resultant precipitate was separated by decantation and dried, giving glassy polymer (P-IIIa), which was purified further by washing with methanol in a Soxhlet extractor for 5 hr. to give 0.48 g. (13%) of (P-IIIa), melting at 45–48°. The supernatant solution was evaporated, and the oily residue was washed with 30 ml. of hot *n*-hexane. After addition of 0.5 g. of aniline to the washings the mixture was refluxed for 3 hr. and cooled.

The precipitated crystals were filtered and gave 0.24 g. (5%) of 1-phenyl-3-[2'-(*p*-tolyloxy)ethyl]thiourea, melting at 126–129°.

Recrystallization from benzene and *n*-hexane gave the analytical sample of m.p. 129–130°.

(b) To a solution of (IIIa) (1.93 g., 10 mmoles) in 3 ml. of anhydrous tetrahydrofuran 14 μ l. (0.1 mmole) of triethylamine was added with a microsyringe under cooling in an ice-salt bath. The solution was left in a refrigerator for 1 day and at room temperature for an additional 3 days and was poured into methanol to precipitate the polymer (P-IIIa).

The purification of (P-IIIa) and an attempt to obtain 1-phenyl-3-[2'-(*p*-tolyloxy)ethyl]thiourea were carried out in a way similar to that described in (a) above.

(c) Polymerization of (IIIa) initiated with 5 mole-% of triethylamine and 1 mole-% of *n*-butyllithium was carried out in a manner similar to that described in (b) above.

Polymerization of 1-(*p*-Nitrophenyloxythiocarbonyl)aziridine (IIIb)

Substance (IIIb) was prepared by the published method.¹ To a solution of (IIIb) (2.24 g., 10 mmoles) in 10 ml. of dry tetrahydrofuran 14 μ l. (0.1 mmole) of triethylamine was added under cooling in an ice-salt bath. The solution was allowed to stand in a refrigerator for 1 day and at room temperature for an additional 3 days and was then poured into hot *n*-hexane.

The oily precipitate, which was separated by decantation, was dissolved in tetrahydrofuran and poured into methanol to precipitate the polymer (P-IIIb). Polymer (P-IIIb) was filtered and dried *in vacuo*; it weighed 0.04 g. (2%) and had a melting point of 77–84°. 2-(*p*-Nitrophenyloxy)ethylisothiocyanate (III'b), which was separated out by cooling the hot *n*-hexane layer, was filtered, and it weighed 0.02 g. (1%), melting at 77–80°. Recrystallization from *n*-hexane raised the melting point to 80–82°.

The infrared spectrum of (III'b) showed peaks assignable to the isothiocyanate group at 2220 and 2280 cm.^{-1} (shoulder).

ANAL. Calcd. for $\text{C}_9\text{H}_8\text{N}_2\text{O}_2\text{S}$ (%): C 48.21, H 3.60, N 12.49. Found (%): C 48.41, H 3.56, N 12.35.

The two filtrates (methanol and *n*-hexane) were combined, and the solvents were removed under reduced pressure. Substance (III'b) was extracted with hot ether from the residue and after removal of ether was heated with 0.8 g. of aniline in 5 ml. of refluxing acetone for 8 hr.

After cooling of the mixture the precipitate was filtered and washed with a small quantity of acetone. It weighed 1.53 g. (48%); m.p. 166–169°.

Polymerization of (IIIb) initiated by *n*-butyllithium was carried out in a manner similar to that described above.

Preparation of 1-(*p*-Tolyldithiooxycarbonyl)aziridine (IVa)

Chlorodithioformic acid *p*-tolyl ester was prepared in 68% yield by the method described^{1,26} the synthesis of *p*-chlorophenyl- or *p*-methoxyphenyl ester; and had b.p. 94–105° at 1 mm.

Substance (IVa) was prepared from chlorodithioformic acid *p*-tolyl ester and aziridine in 66% yield by the methods described for (IVb) and (IVc).¹ It melted at about 43°, and its NMR spectrum (in CCl_4) showed two singlets, at 7.58 (CH_2) and 7.53 (CH_3), with 3:4 area ratio.

ANAL. Calcd. for $\text{C}_{10}\text{H}_{11}\text{NS}_2$ (%): C 57.41, H 5.30, N 6.70. Found (%): C 57.13, H 4.99, N 6.63.

Polymerization of (IVa)

(a) The polymerization of (IVa) (2.09 g., 10 mmoles), which was initiated with 0.1 mmole of triethylamine, was performed in a manner similar to that of (IIIa). The polymerization mixture was poured into methanol. The oily precipitate was separated from the supernatant layer by decantation and purified by reprecipitation from tetrahydrofuran to methanol, yielding 0.63 g. (33%) of sticky polymer (P-IVa). From the

supernatant solution solvents were removed at diminished pressure. To the residue 0.5 g. of aniline was added, and the mixture was allowed to stand for 2 days. To the mixture ether and *n*-hexane were added, and the precipitate was filtered and dried; it weighed 0.63 g.; m.p. 120–122°. Recrystallization from ethanol gave 0.47 g. (14%) of 1-phenyl-3-(2'-tolylthioethyl)thiourea, melting at 124–125°.

(b) To 2.09 g. of (IVa) was added 4 ml. of dimethylformamide containing 4.9 mg. (0.1 mmole) of sodium cyanide under cooling in an ice-salt bath. The solution was kept in a refrigerator for 1 day and at room temperature for 3 days. The purification of (P-IVa) and the isolation of the aniline adduct of (IV'a) were carried out described as in (a).

(c) A solution of (IVa) in 4 ml. of dimethylformamide was allowed to stand at room temperature for 5 days. The purification of (P-IVa) and the isolation of the derivatives of (IV'a) were carried out in the way described above.

Polymerization of 1-(*p*-Chlorophenyldithiooxycarbonyl)aziridine (IVb)

Polymerization of (IVb) (2.23 g., 10 mmoles) initiated with 0.1 mmole of triethylamine was carried out as described for (IVa). The polymerization mixture was poured into methanol. The precipitate (P-IVb) was collected on a filter, and it weighed 0.73 g. (33%); m.p. 116–125°. Polymer (P-IVb) was washed with methanol in a Soxhlet extractor for 3 hr. to give 0.51 g. (23%) of purified (P-IVb) melting at 122–127°. From the filtrate methanol and tetrahydrofuran were removed, and 0.5 g. of aniline was added to the residue. After 2 days 10 ml. of ether was added, and the resultant precipitate was collected on a filter. Recrystallization from ethanol gave 0.23 g. (8%) of 1-[2'-(*p*-chlorophenylthio)ethyl]-3-phenylthiourea melting at 148–149.3°.

Polymerization of 1-(*p*-Methoxyphenyldithiooxycarbonyl)aziridine (IVc)

The polymerization of (IVc) and the treatment of the products were carried out in essentially the same way as for (IVa), except that P-IVc was purified by being washed with methanol in a Soxhlet extractor.

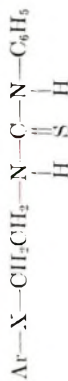
In the other polymerizations of (IVc) the purification of (P-IVc) and the isolation of the aniline adduct of (IV'c) were performed as described above.

The analytical data on (P-III) and (P-IV) are summarized in Table IV; those of the aniline adducts of 2-aryloxyethyl- and 2-arylthioethylisothiocyanates, (III') and (IV'), in Table VII.

Synthesis of (P-III'a)

Into a solution of 1.09 g. (10 mmoles) of chlorothionformic acid *p*-tolylester in 15 ml. of benzene was added a solution of 0.3 g. of dehydrated polyethylenimine and 1.0 g. (10 mmoles) of triethylamine in 15 ml. of benzene with stirring. The mixture was allowed to stand overnight, and triethyl-

TABLE VII
1-(2'-Aryloxyethyl)- and 1-(2'-Arylthioethyl)-3-phenylthioureas



| Ar | N | m.p., °C. | Formula | Analyses | | | | | | |
|-------------------------|---|-----------|--|----------|------|-------|-------|------|-------|-----------|
| | | | | Calcd. | | | Found | | | |
| | | | | C | H | N | C | H | N | |
| <i>p</i> -Tolyl | O | 129-130 | C ₁₆ H ₁₈ N ₂ O ₂ S | 67.11 | 6.34 | 9.78 | 66.67 | 6.33 | 9.76 | 3400,3160 |
| <i>p</i> -Nitrophenyl | O | 169-170.5 | C ₁₆ H ₁₃ N ₃ O ₃ S | 56.77 | 4.76 | 13.24 | 57.10 | 4.89 | 13.01 | 3400,3180 |
| <i>p</i> -Tolyl | S | 124-125 | C ₁₆ H ₁₈ N ₂ S ₂ | 63.56 | 6.00 | 9.27 | 63.76 | 6.49 | 9.10 | 3340,3160 |
| <i>p</i> -Chlorophenyl | S | 148-149.5 | C ₁₅ H ₁₃ ClN ₂ S ₂ | 55.80 | 4.86 | 8.68 | 56.10 | 4.64 | 8.47 | 3350,3160 |
| <i>p</i> -Methoxyphenyl | S | 117-118 | C ₁₆ H ₁₈ N ₂ O ₂ S ₂ | 60.34 | 5.70 | 8.80 | 60.38 | 5.71 | 8.62 | 3450,3170 |

amine hydrochloride was removed by filtration. From the filtrate benzene was removed, and the residue was dissolved in tetrahydrofuran. The solution was poured into methanol to give 0.5 g. (24%) of (P-III'a) melting at 111–115°.

ANAL. Calcd. for $(C_{10}H_{11}NOS)_n$ (%): C 62.15, H 7.54, N 7.25. Found (%): C 61.30, H 5.61, N 7.42.

Synthesis of (P-IV'a)

Polymer (P-IV'a) was prepared from chlorodithioformic acid *p*-tolyl-ester and purified polyethylenimine in the presence of triethylamine in the same manner as for (P-III'a). It melted at 78–85°.

ANAL. Calcd. for $(C_{10}H_{11}NS_2)_n$ (%): C 57.41, H 5.33, N 6.70. Found (%): C 56.59, H 5.23, N 6.90.

Polymerization of 1-(*p*-Chlorobenzoyl) Aziridine

To a solution of 1-(*p*-chlorobenzoyl)aziridine²⁷ (1.82 g., 10 mmoles) in tetrahydrofuran was added triethylamine (0.03 g., 0.3 mmole), and the resultant solution was kept at 30° for 2 days. The solvent was evaporated under reduced pressure, and the residue was washed with methanol in a Soxhlet extractor for 10 hr.; it yielded 0.60 g. (33%) of white polymer melting at 185–220°. The reduced viscosity of the polymer was 0.22 in dimethylformamide (1% concn. at 30°). The infrared spectrum (Nujol) showed a C=O stretching band at 1638 cm^{-1} .

ANAL. Calcd. for (C_9H_8ClNO) (%): C 59.52, H 4.44, N 7.71. Found (%): C 59.18, H 4.59, N 7.70.

Methanol was removed from the washings, and the residue was washed with ether to give 0.59 g. of white powder melting at 110–160°. The infrared spectrum of the powder was essentially identical with that of the methanol-insoluble polymer. Adding of picric acid to the ether-soluble liquid gave 0.09 g. (2%) of the picrate of 2-(*p*-chlorophenyl)oxazoline; m.p. 186–187° (lit.^{28,29} 190–191°, 180–182°).

ANAL. Calcd. for $C_{15}H_{11}ClN_2O_5$ (%): C 43.86, H 2.70, N 13.69. Found (%): C 43.69, H 2.79, N 13.59.

The authentic sample of poly[*N*-(*p*-chlorobenzoyl)]ethylenimine was synthesized in the following way. A solution of dehydrated polyethylenimine (0.8 g.), *p*-chlorobenzoylchloride (5.3 g.), and triethylamine (3 g.) in 50 ml. of dimethylformamide was stirred for 3 hr., and the solution was concentrated under reduced pressure. On pouring of the concentrated solution into water a white polymer precipitated. It was filtered, dried, and washed with ether in a Soxhlet extractor. The infrared spectrum was quite identical with that of the polymer obtained from 1-(*p*-chlorobenzoyl)-aziridine.

The authors wish to thank Nippon Soda Company, Ltd., for the generous supply of thiophosgene.

References

1. Y. Iwakura, A. Nabeya, and T. Nishiguchi, *J. Org. Chem.*, **32**, 2362 (1969).
2. A. G. Pittman and R. E. Lundin, *J. Polymer Sci. A*, **2**, 3803 (1964).
3. R. E. Lane, Jr. and G. E. Ham, Belg. Pat. 668,007 (1966).
4. K. B. Wiberg and B. J. Nist, *The Interpretation of NMR Spectra*, Benjamin, New York, 1962, pp. 309-562.
5. S. Gabriel and R. Stelzner, *Ber.*, **28**, 2929 (1895).
6. Y. Iwakura and A. Nabeya, *Bull. Tokyo Inst. Technol.*, **42**, 69 (1961).
7. Y. Iwakura and A. Nabeya, *J. Chem. Soc. Japan Pure Chem. Sect.*, **77**, 773 (1956).
8. A. S. Deutsch and P. E. Fanta, *J. Org. Chem.*, **21**, 892 (1956).
9. M. Tisler, *Archiv. Pharm.*, **291**, 457 (1958).
10. For a review see R. Roger and D. Neilson, *Chem. Rev.*, **61**, 179 (1961).
11. N. Bacon, A. J. Boulton, R. T. C. Brownlee, A. R. Katritzky, and R. D. Topson, *J. Chem. Soc.*, **1965**, 5230.
12. M. G. Ettlinger, *J. Am. Chem. Soc.*, **72**, 4699 (1950).
13. W. Walter and H. P. Kubersky, *Ann.*, **694**, 56 (1966).
14. I. D. Rae, *Can. J. Chem.*, **45**, 1 (1967).
15. A. K. Chibisov and Yu. A. Pentin, *Zh. Obshchei Khim.*, **31**, 359 (1961).
16. K. W. F. Kohlrausch and J. Wagner, *Z. Physik Chem.*, **45**, 229 (1940).
17. M. St. C. Fett, *J. Chem. Soc.*, **1953**, 347.
18. A. Hantzsch, *Ber.*, **64**, 661 (1931).
19. G. Hopkins and L. Hunter, *J. Chem. Soc.*, **1942**, 638.
20. A. J. Speziale and L. R. Smith, *J. Org. Chem.*, **28**, 3492 (1963).
21. A. W. Chapman, *J. Chem. Soc.*, **1926**, 2296.
22. For a review see R. N. Hurd and G. D. Matler, *Chem. Rev.*, **61**, 45 (1961).
23. H. Bredereck, R. Gompfer, and D. Bitzer, *Chem. Ber.*, **92**, 1139 (1959).
24. A. Lawson and C. E. Searle, *J. Chem. Soc.*, **1957**, 1556.
25. H. Bestian, *Ann.*, **566**, 210 (1950).
26. Y. Iwakura, A. Nabeya, T. Nishiguchi, and K. Ohkawa, *J. Org. Chem.*, **31**, 3352 (1966).
27. H. W. Heine, M. E. Fetter, and E. M. Nicholson, *J. Am. Chem. Soc.*, **81**, 2202 (1959).
28. J. A. Boyer and J. Hamer, *J. Am. Chem. Soc.*, **77**, 951 (1955).
29. R. N. Boyd and R. C. Rittner, *J. Am. Chem. Soc.*, **82**, 2032 (1960).

Received August 10, 1967

Revised February 8, 1968

Polymerization of Isocyanates. V. Thermal Degradation of Polyisocyanates

YOSHIO IWAKURA, KEIKICHI UNO, and NORIO KOBAYASHI

*The Department of Synthetic Chemistry, Faculty of Engineering,
University of Tokyo, Bunkyo-ku, Tokyo, Japan*

Synopsis

Thermal degradation of polyisocyanates was investigated. The only degradation products were monomer and trimer. The main product was trimer for most aliphatic polymers, and monomer for aromatic polymers. Poly(cyclohexyl isocyanate) gave only its monomer on account of steric requirements. The apparent activation energy was calculated for aromatic polymers by using TGA and DTA curves.

INTRODUCTION

It is known that polyisocyanates are thermally unstable. Shashoua and co-workers have reported that aliphatic polyisocyanates degraded to monomer and trimer when heated to their melting points.¹ In relation to a previous paper dealing with degradation of polyisocyanates in solution,² we have investigated thermal behavior of polyisocyanates. In the present paper, differential thermal analyses (DTA) and thermogravimetric analyses (TGA) of polyisocyanates will be described.

EXPERIMENTAL

The polymers were prepared with sodium cyanide in DMF by the method described by Shashoua.¹ DTA and TGA curves were obtained by the use of the Rigaku Denki differential thermal and thermogravimetric analyzers.

RESULTS AND DISCUSSION

Thermal Degradation of Aliphatic Polyisocyanates

Most of the aliphatic polymers gave DTA and TGA curves of a similar type. Figure 1 shows the DTA and TGA curves for poly(*n*-butyl isocyanate) as a representative aliphatic polymer. For this study, approximately 50 mg of sample was heated in a stream of nitrogen at a programmed heating rate of 2.5°C/min. Table I summarizes the TGA data and DTA data.

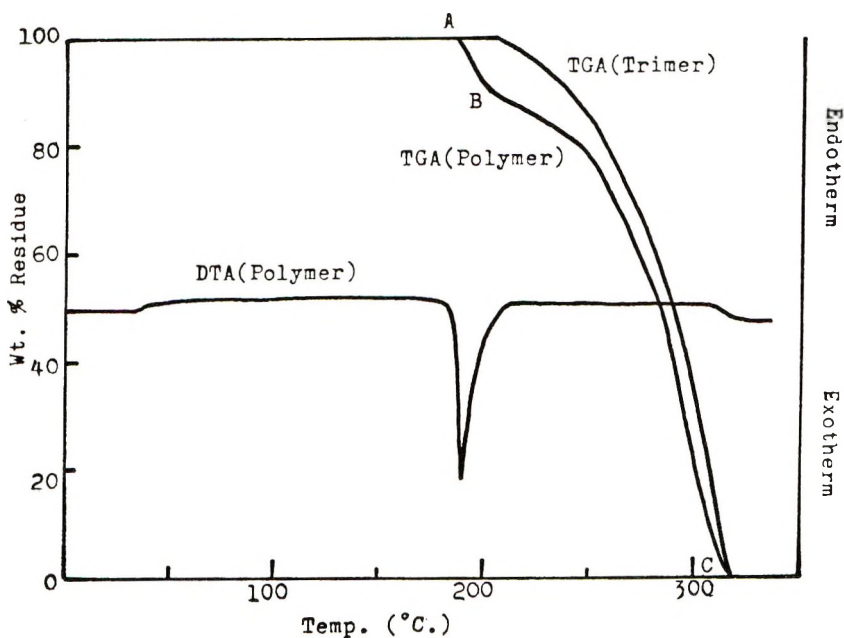


Fig. 1. TGA and DTA curves of poly(*n*-butyl isocyanate) and trimer of *n*-butyl isocyanate under nitrogen; $\phi = 2.5^\circ\text{C}/\text{min}$.

These polymers exhibited a small weight loss (A to B in Fig. 1) ranging from 7 to 17% of the original weight within a relatively narrow temperature range with a sharp endotherm which indicates the decomposition temperature. A second step occurred in the TGA curve successively (B to C), during which almost all of the residue was lost up to $262\text{--}427^\circ\text{C}$.

When poly(*n*-butyl isocyanate) was kept at 190°C in air, the sample was liquefied in a few minutes. *n*-Butyl isocyanate was isolated by distillation of the reaction mixture, and the residue was only the trimer of *n*-butyl isocyanate. This is the same observation as that of Shashoua and co-

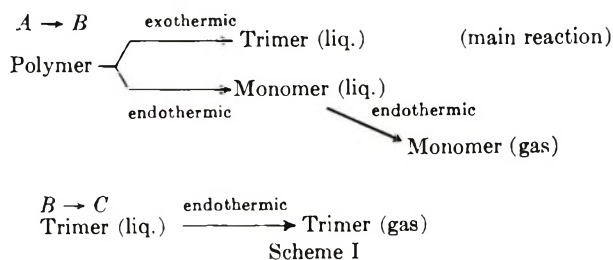
TABLE I
Summary of DTA Data and TGA Data for Aliphatic Polyisocyanates

| R | DTA peak | | Weight loss | |
|---|------------------------|-----------|------------------------|----|
| | Temp, $^\circ\text{C}$ | Type | Temp, $^\circ\text{C}$ | % |
| $\text{C}_2\text{H}_5\text{—}$ | 170 | Exotherm | 151–177 | 14 |
| | | | 177–262 | 86 |
| $\text{C}_4\text{H}_9\text{—}$ | 190 | Exotherm | 184–202 | 10 |
| | | | 202–315 | 90 |
| $\text{C}_8\text{H}_{17}\text{—}$ | 184 | Exotherm | 181–188 | 7 |
| | | | 188–341 | 93 |
| $\text{C}_6\text{H}_5\text{CH}_2\text{—}$ | 181 | Exotherm | 170–216 | 17 |
| | | | 216–427 | 83 |
| $\text{C}_6\text{H}_{11}\text{—}$ | 212 | Endotherm | 177–311 | 89 |

workers.¹ The amount of isocyanate was smaller than that of the trimer. Thus it would be reasonable to suppose that the first weight loss (*A* to *B*) corresponds to a loss of monomer and the second weight loss (*B* to *C*) to a loss of trimer.

Furthermore, when trimer of *n*-butyl isocyanate, 1,3,5-tri-*n*-butyl isocyanurate, was subjected to thermogravimetric analysis, the sample has lost approximately 100% of its original weight from 204°C up to about 320°C. The TGA curve of the trimer is also shown in Figure 1. This temperature range corresponds to that of the second weight loss (*B* to *C*) for poly(*n*-butyl isocyanate). This fact supports the above assumption.

Accordingly, TGA curve and DTA curve of most aliphatic polymers are interpreted as shown in scheme I.



The main product was trimer. Depolymerization to monomer should be an endothermic reaction, since polymerization is exothermic. Then degradative trimerization would be exothermic because the net reaction is exothermic as shown in DTA curve.

Thermal behavior of poly(cyclohexyl isocyanate) is very different from those of common aliphatic polymers. Figure 2 shows TGA and DTA curves of poly(cyclohexyl isocyanate). For this polymer, a rapid loss in weight occurred at 175°C, and the sample has lost approximately 80% of its original weight at 245°C. The weight loss continued at a much slower rate up to 310°C, and the polymer exhibited a broad endotherm which peaks at 212°C. When the polymer was heated at 220°C for 10 min, it degraded completely; the products were monomer and a small amount of resin which could not be identified. Thus the weight loss mentioned above would correspond to a loss of monomer. This anomalous behavior of poly(cyclohexyl isocyanate) could be ascribed to steric factors, since there are steric limitations in trimerization of isocyanates. Brauner has reported that tertiary butyl isocyanate did not trimerize even with triethyl phosphine as a catalyst.³ Although we have succeeded in polymerization of cyclohexyl isocyanate to low conversion by using sodium cyanide as a catalyst,⁴ attempts to prepare 1,3,5-tricyclohexyl isocyanurate, the trimer of cyclohexyl isocyanate, were unsuccessful. Possibly steric factors may exert much more influence upon trimerization than upon homopolymerization. Thus, it could be said that thermal degradation of poly(cyclohexyl isocyanate) to its trimer is impossible.

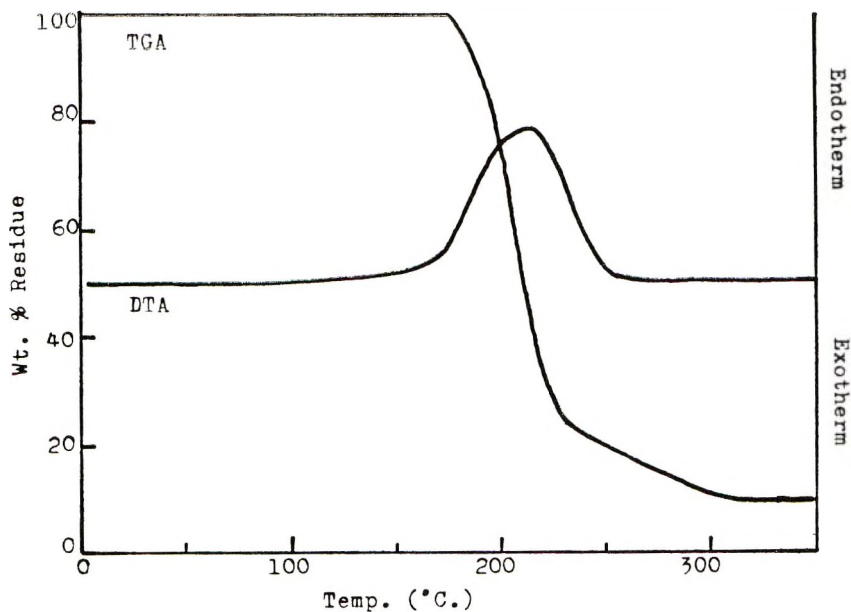


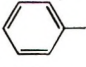
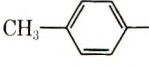
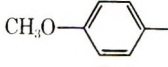
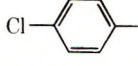
Fig. 2. TGA and DTA curves of poly(cyclohexyl isocyanate) under nitrogen; $\phi = 2.5^\circ\text{C}/\text{min}$.

Thermal Degradation of Aromatic Polyisocyanates

Figure 3 shows TGA and DTA curves of aromatic polyisocyanates. They were obtained under the same conditions as employed for aliphatic polymers. TGA and DTA data are summarized in Table II.

All of these polymers exhibited a large weight loss, ranging from 76 to 87% of the original weight from 170°C up to about 240°C . This weight loss is believed to correspond to a loss of monomer formed by thermal degradation of the polymer. After the loss of monomer no weight loss was

TABLE II
Summary of DTA Data and TGA Data for Aromatic Polyisocyanates

| R | DTA peak | | Weight loss | |
|---|------------------------|-----------|------------------------|----|
| | Temp, $^\circ\text{C}$ | Type | Temp, $^\circ\text{C}$ | % |
|  | 204 | Endotherm | 170-238 | 87 |
| | | | 331-385 | 13 |
|  | 190 | Endotherm | 171-224 | 83 |
| | | | 309-400 | 17 |
|  | 184 | Endotherm | 181-233 | 76 |
| | | | 349-431 | 24 |
|  | 177 | Endotherm | 170-242 | 80 |
| | | | 359-428 | 14 |

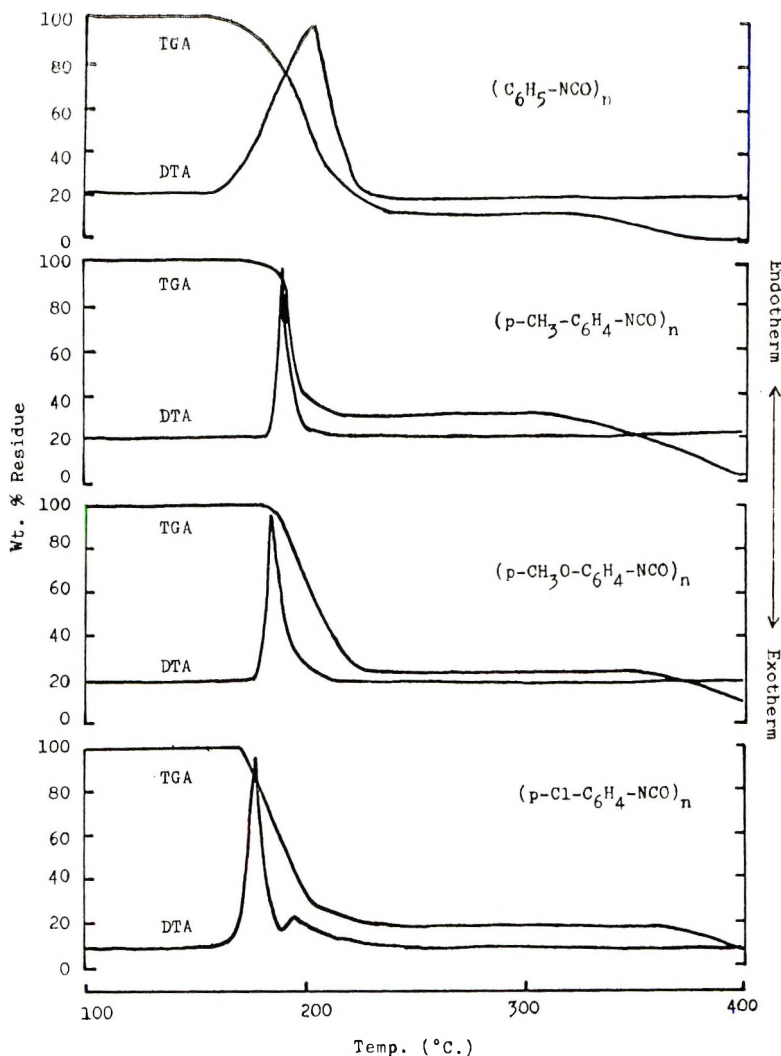


Fig. 3. TGA and DTA curves of aromatic polyisocyanates in nitrogen; $\phi = 2.5^\circ\text{C}/\text{min}$.

seen up to a temperature range of $310\text{--}360^\circ\text{C}$; above these temperatures a small loss in weight occurred and continued up to approximately $390\text{--}430^\circ\text{C}$.

All the polymers exhibited a sharp endotherm, which, according to Akita's theory,⁵ coincides with the maximum rate of the reaction. For poly(phenyl isocyanate), the peak value of the DTA curve coincides with the maximum rate of weight loss. Then the TGA curve can be considered to express the extent of the reaction. For other polymers, however, the DTA peak was already observed at an earlier stage of weight loss. Namely, the peak of DTA curve does not coincide with the maximum rate of weight loss. This is a rather unusual phenomenon. This fact suggests

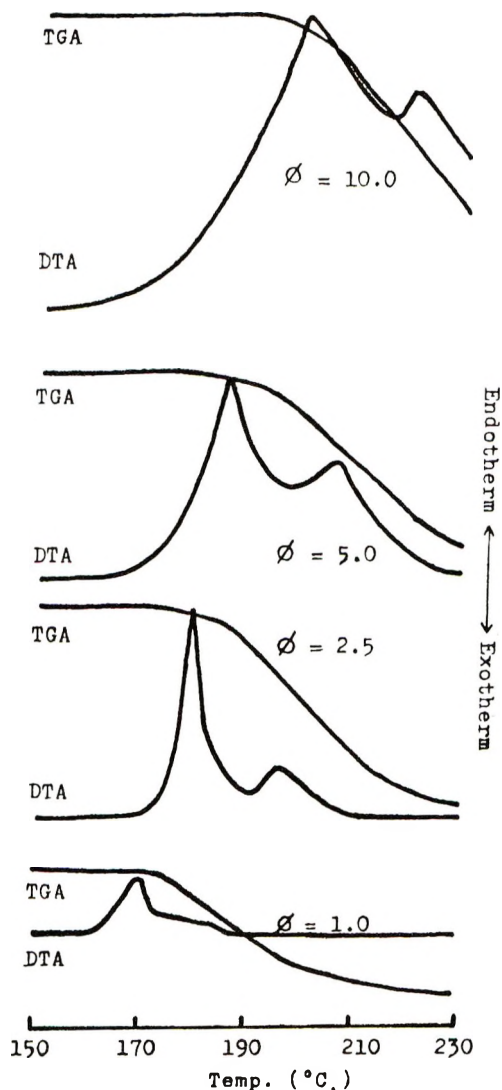
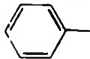
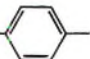
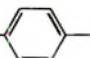


Fig. 4. Effect of heating rate on the DTA curves of poly(*p*-chlorophenyl isocyanate).

that the rate of depolymerization is very fast, and the TGA curve no longer expresses the extent of the reaction. In the case of poly(*p*-chlorophenyl isocyanate) there appeared endotherms, one corresponding to the maximum rate of reaction and the other to maximum rate of weight loss. When the heating rate was raised, the latter peak became more distinct, as shown in Figure 4.

When poly(phenyl isocyanate) was subjected to thermal degradation at 205°C, only monomer and trimer were obtained, and the yield of monomer was more than 80%. This value is very close to that of the first weight loss (see Table II). Then it can be said the first weight loss in the TGA

TABLE III
Summary of DTA Data and TGA Data for Trimers

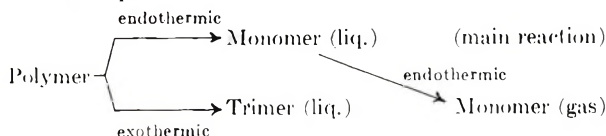
| R | DTA peak | | Weight loss | |
|---|----------|-----------|-------------|-----|
| | Temp, °C | Type | Temp, °C | % |
|  | 280 | Endotherm | 336-459 | 100 |
| CH ₃ -  | 269 | Endotherm | 349-400 | 100 |
| Cl-  | 333 | Endotherm | 359-518 | 90 |
| C ₆ H ₅ - | — | — | 204-324 | 100 |

curve corresponds to the loss of monomer, and the subsequent trimerization of monomer produced is negligible under the present conditions, if any. Stollé has reported that thermal degradation of 1,3,5-triphenyl isocyanurate at 300°C gave carbon dioxide and diphenyl carbodiimide.⁶ However, when 1,3,5-triphenyl isocyanurate was heated up to 400°C in a stream of nitrogen at a heating rate of 2.5°C/min, formation of neither carbon dioxide nor diphenyl carbodiimide was observed, and only sublimation of trimer occurred. Furthermore, trimers of aromatic isocyanates were submitted to thermogravimetric analyses, and differential thermal analyses under the same conditions as those employed for polymers. Table III lists the results. All of these trimers exhibited a simple weight loss in the temperature ranges which correspond to those of the second weight loss of polymers, and they showed an endotherm at a temperature corresponding to their melting points.

From these facts it would be concluded that thermal degradation of aromatic polyisocyanates gives only monomer and trimer. The second weight loss corresponds to loss of trimer.

Accordingly, TGA and DTA curves of aromatic polymers would be interpreted as shown in scheme II.

First Step:



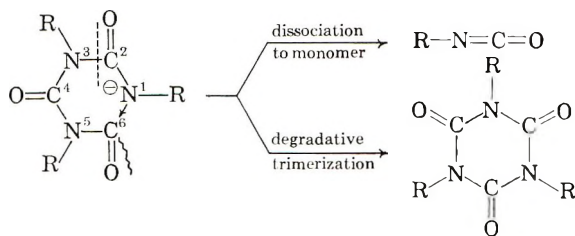
Second Step:



Unlike aliphatic polymers, aromatic polymers give their monomers as a main product, so the net reaction is endothermic. Trimer would be formed as liquid, since there is no endotherm corresponding to fusion of trimer in the DTA curve of polymer.

Factors Influencing the Mode of Depolymerization

As described above, thermal degradation of polyisocyanates gives generally both monomer and trimer. Depolymerization would be initiated by abstraction of hydrogen attached to nitrogen atom at the chain end or by cleavage of the main chain.* Since the activation energy is low as described later, the reaction would not be homolytic. Then dissociation to monomer and degradative trimerization would occur competitively as shown in scheme III.

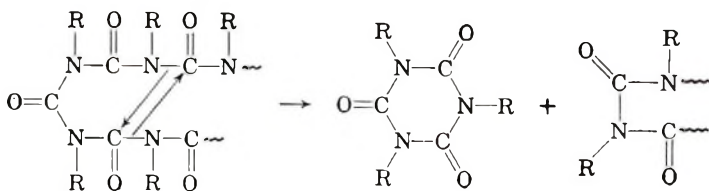


Scheme III

The results shown in Tables I and II indicate that there are some factors which influence the mode of depolymerization. They can be classified as either the electronic character of the *N*-substituent or steric factors. The latter plays an important role in depolymerization of poly(cyclohexyl isocyanate), which does not give trimer when subjected to thermal degradation.

In Figure 5, yields of monomer in thermal depolymerization of aromatic polymers are plotted against Hammett's σ values, along with the data in depolymerization by di-*n*-butylamine in DMF at 30°C.² There seems to be an optimum σ region for the highest yield of monomer in both series of reactions. Although close discussion is impossible at present since only a few data are available, it could be said that monomer yields are influenced to some extent by the electronic character of *N*-substituents. There seem to be two types of electronic factors which act in the opposite direction. As shown in scheme III, nucleophilicity of the nitrogen anion (N^1), the electron density on carbonyl carbon at the 6 position (C^6), and carbon-nitrogen bond (C^2-N^3) strength may influence the mode of depolymerization. These factors would be affected by electronic character of *N*-substituents in various ways.

* The referee suggested that it is possible to imagine a bond reorganization mechanism not involving an endgroup.



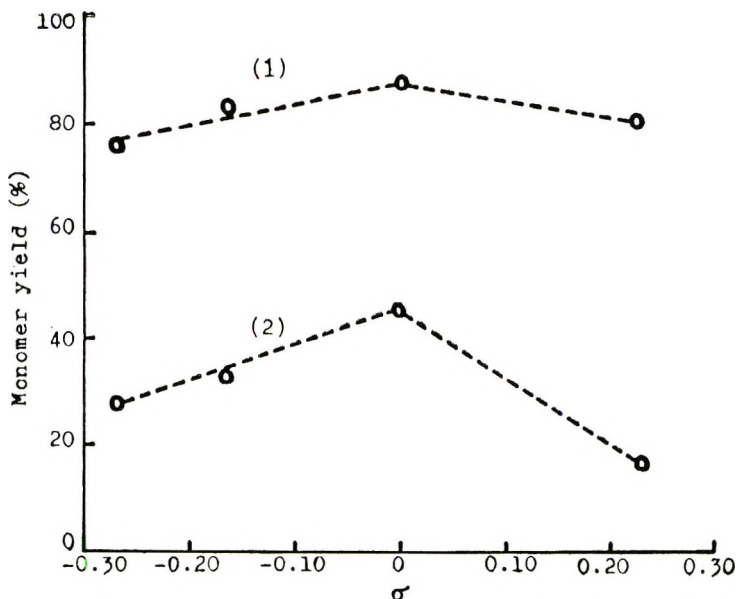


Fig. 5. Correlation between monomer yield and σ value: (1) thermal degradation of polyisocyanates; (2) degradation of polyisocyanates by di-*n*-butyl amine in DMF at 30° C.

A similar relationship is also observed between monomer yields in the thermal degradation of aliphatic polymers and Taft's σ^* values.

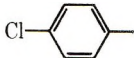
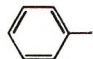
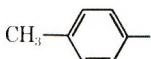
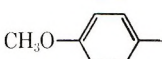
Determination of Kinetic Parameters by TGA and DTA

In the pyrolysis of poly(phenyl isocyanate) the peak value of the DTA curve coincides with the maximum rate of weight loss as mentioned above. Then, reaction order n , activation energy E , and pre-exponential factor k_0 were determined for pyrolysis of poly(phenyl isocyanate) by means of TGA and DTA following the method given by Akita and Kase.⁵ Results were obtained from four different TGA and DTA curves having different heating rates ϕ . They are summarized in Table IV. The average of n is nearly equal to unity, so the pyrolysis reaction is considered to be first order with respect to the weight of the residual polymer. The activation energy E

TABLE IV
Kinetic Parameters for Pyrolysis of Poly(phenyl isocyanate)

| No. | Heating rate ϕ , °C/min | n | E , kcal/mole | $\log k_0$, min ⁻¹ |
|---------|------------------------------|------|-----------------|--------------------------------|
| 1 | 1.0 | 1.06 | 24.9 | 10.6 |
| 2 | 2.5 | 1.08 | 25.9 | 10.6 |
| 3 | 5.0 | 1.13 | 24.4 | 10.7 |
| 4 | 10.0 | 1.08 | 24.5 | 10.5 |
| Average | | 1.09 | 24.9 | 10.6 |

TABLE V
Activation Energies for Pyrolysis of Aromatic Polyisocyanates

| R | E_a , kcal/mole |
|---|----------------------|
|  | 23.3 |
|  | 24.6 |
|  | 28.6 |
|  | 30.0 |

and the pre-exponential factor of Arrhenius equation k_0 are independent of heating rate and the averages are 24.9 kcal/mole and $10^{10.6} \text{ min}^{-1}$, respectively. The activation energy for poly(phenyl isocyanate) was also obtained by the differential method,⁷ and the value obtained is 24.4 kcal/mole, which is in good agreement with the above result.

For other aromatic polymers, Akita's method can not be employed since the peak value of DTA does not coincide with the maximum rate of weight loss. Thus Kissinger's method⁸ was used to calculate the activation energy for these polymers. They are shown in Table V. It may be said that there is some relationship between activation energy and electronic character of *N*-substituent. However, it must be noted that the activation energy obtained here is an apparent value, and it is very difficult to know the real value on account of following two reasons. First, in the thermal degradation of polyisocyanates there are two competitive reactions, one is dissociation to monomer and the other degradative trimerization. Secondly, TGA curves do not express the rate of degradation for most aromatic polymers. The latter prevents the isolation of competing reactions.

References

1. V. E. Shashoua, W. Sweeny, and R. F. Tietz, *J. Amer. Chem. Soc.*, **82**, 866 (1960).
2. Y. Iwakura, K. Uno, and N. Kobayashi, *J. Polymer Sci.*, in press.
3. B. Brauner, *Ber.*, **12**, 1874 (1879).
4. Y. Iwakura, K. Uno, and N. Kobayashi, *J. Polymer Sci. A-2*, **4**, 1013 (1966).
5. K. Akita and M. Kase, *J. Polymer Sci. A-1*, **5**, 838 (1967).
6. R. Stollé, *Ber.*, **41**, 1125 (1908).
7. J. H. Flynn and L. A. Wall, *J. Res. Natl. Bur. Std.*, **70A**, 487 (1966).
8. H. E. Kissinger, *Anal. Chem.*, **29**, 1702 (1957).

Received January 4, 1968

Revised February 15, 1968

Cupric Sulfate-Hydrazine System as an Initiator of Vinyl Polymerization. II. Polymerization of Methyl Methacrylate in Aqueous Solution in the Absence of Oxygen

JOAN BOND and P. I. LEE, *The University of Salford, Salford, Lancashire, England*

Synopsis

The cupric sulfate-hydrazine system has been used to initiate the aqueous solution polymerization of methyl methacrylate at pH 9.25 in the absence of oxygen. There is no decomposition of hydrazine on the surface of the reduced cupric hydroxide until a flocculant precipitate is formed (cupric sulfate concentration of about 10^{-3} mole/l). Below this concentration, the initiating reaction occurs solely in solution, the rate of polymerization decreasing when the reaction mixture becomes depleted in cupric ions. When a suitable surface area of the precipitated polymer is attained, adsorption and decomposition of hydrazine occurs on its surface, causing further initiation of polymerization.

The polymerization of methyl methacrylate in aqueous solution, initiated by the cupric sulfate-hydrazine system in the presence of oxygen, was described in Part I of this series.¹ The work discussed in this paper deals with the polymerization which occurs in the absence of oxygen and of which there is very little mention in the available literature, Menon and Kapur² simply quoting the fact that the rate of polymerization of methyl methacrylate increases with increasing initial concentration of cupric ions.

Experimental

The experimental techniques were identical to those described in Paper I of this series,¹ except that all solutions were prepared in water which had previously been boiled and then cooled while nitrogen was bubbling through it. The reaction mixtures were further deoxygenated by bubbling nitrogen through them for 2 hr. after which polymerization was initiated by the addition of hydrazine. The British Oxygen Company's oxygen-free nitrogen was used, and this was further purified by passing it first through a solution of alkaline pyrogallol and then through distilled water.

Results

The results are expressed graphically (Figs. 1-4).

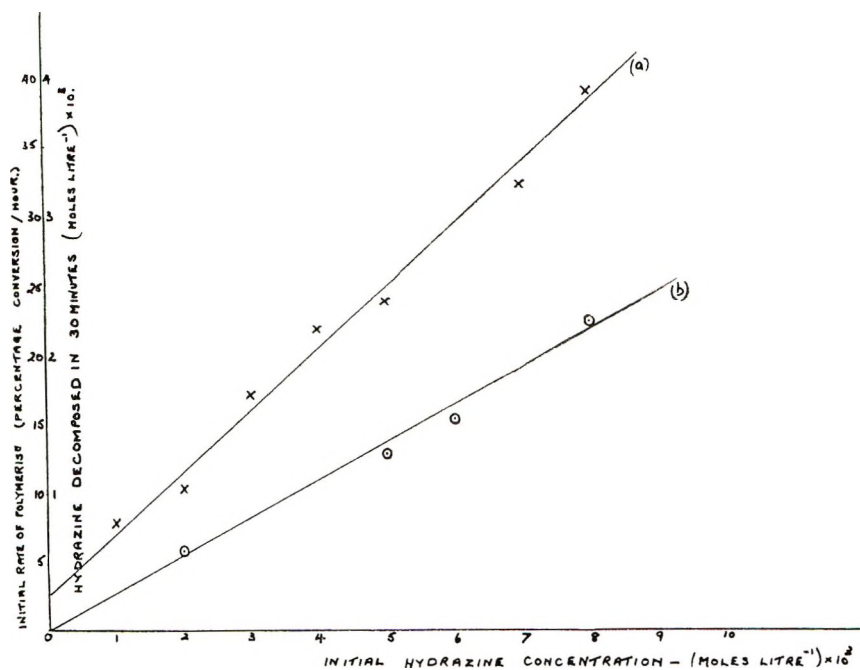


Fig. 1. Dependence of (a) the amount of hydrazine decomposed in 30 min and (b) the initial rate of polymerization on the initial hydrazine concentration. Methyl methacrylate, 0.02 mole/l; cupric sulfate, 5×10^{-5} mole/l.

Discussion

At an initial cupric sulfate concentration of 5×10^{-5} mole/l, the rate of hydrazine decomposition and the corresponding rate of polymerization both increase with increasing alkalinity and reach a maximum at pH 9.5. At this pH value there is no detectable decomposition of hydrazine over a 2 hr period in the absence of cupric sulfate, while in its presence the rate of hydrazine decomposition is directly proportional to the initial concentration of cupric ions (Fig. 2) until a flocculant precipitate of cupric hydroxide forms (10^{-3} mole/l). The rate of decomposition then increases appreciably and some hydrazine is removed instantaneously from the solution as a result of its adsorption onto the surface, the amount adsorbed increasing with increasing amount of precipitate.

Below 10^{-3} mole/l cupric sulfate there is some instantaneous disappearance of hydrazine; this is 0.4×10^{-3} mole/l (at an initial cupric sulfate concentration of 5×10^{-5} mole/l) compared with 2×10^{-3} mole/l in the presence of oxygen.¹ A comparison between Figure 1 of the present report and Figure 4 of the previous paper¹ shows that the reaction between the initial cupric ions and hydrazine takes place in solution in the absence of oxygen. It would thus appear that the small particles of cuprous hydroxide sol which have been formed as a result of the original adsorption and oxida-

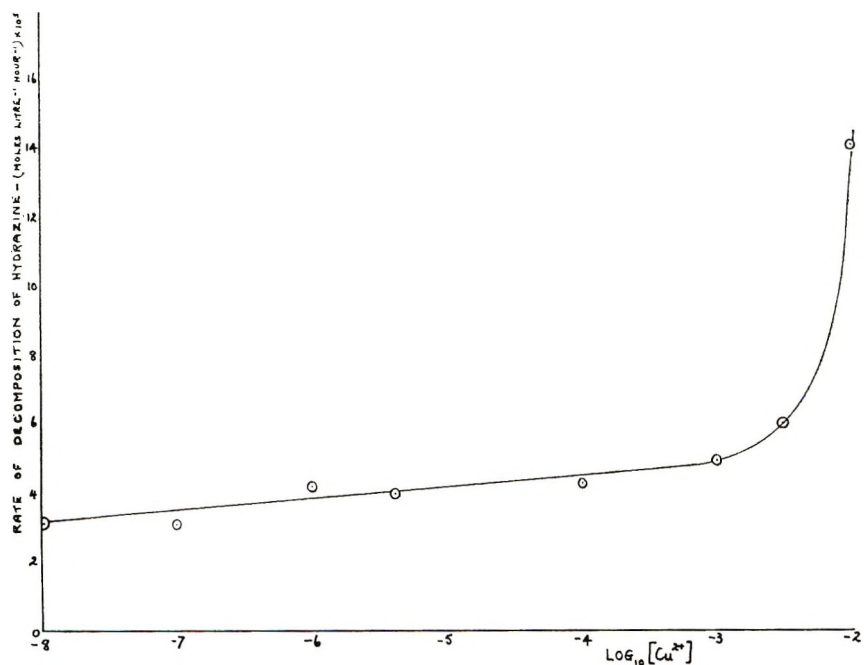


Fig. 2. Dependence of the initial rate of the decomposition of hydrazine on the concentration of cupric sulfate. Hydrazine, 0.08 mole/l; methyl methacrylate, 0.02 mole/l.

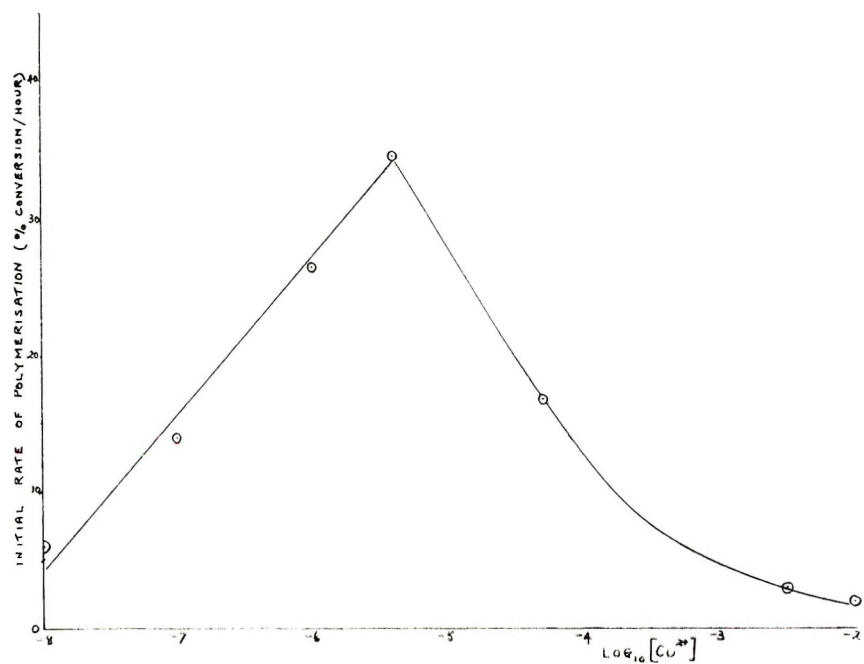


Fig. 3. Dependence of the initial rate of polymerization on the concentration of cupric sulfate. Hydrazine, 0.08 mole/l; methyl methacrylate, 0.02 mole/l.

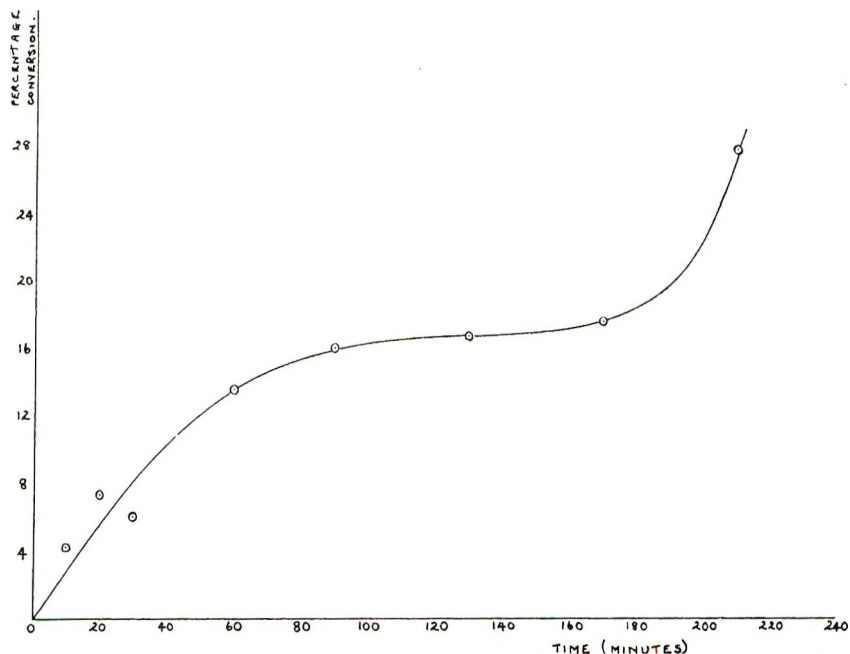


Fig. 4. Rate curve for the polymerization of methyl methacrylate. Hydrazine, 0.08 mole/l; methyl methacrylate, 0.02 mole/l; cupric sulfate, 5×10^{-5} mole/l.

tion of hydrazine, do not present a suitable surface for further hydrazine adsorption. At cupric sulfate concentrations $>10^{-3}$ mole/l the increased rate of hydrazine decomposition indicates that decomposition must take place on both the initial cupric, and resultant cuprous, hydroxide precipitates.

Since there is no oxygen present in the system to convert cuprous ions to cupric ions, a given reaction mixture becomes progressively depleted in cupric ions; the initiating reaction is therefore not maintained, and a decrease in the rate of decomposition of hydrazine is observed with a resultant slowing down of the polymerization when a plateau is produced in the rate curve (Fig. 4). The increased rate of polymerization which occurs after the plateau can be attributed to the adsorption and subsequent decomposition of hydrazine on the surface of the polymer which is of a suitable nature and area. This effect was verified qualitatively by observing the decomposition of hydrazine in solution when a finely divided sample of purified polymer was added to it.

The graph of initial rate of polymerization versus monomer concentration is of the same form as that of percentage conversion versus time and can be interpreted in a similar manner, because a change in the initial monomer concentration represents a change in the total surface area of polymer produced.

At cupric sulfate concentrations below the saturation solubility of cupric

hydroxide, the rate of polymerization is directly proportional to the initial concentration of cupric ions in solution, as was observed by Menon and Kapur.² At cupric sulfate concentrations above the saturation solubility of cupric hydroxide, the rate of polymerization decreases in a similar manner to that observed in the presence of oxygen,¹ and this again is probably the result of adsorption and recombination of initiating radicals at the surface (Fig. 3).

The authors wish to thank Geigy (U.K.) Ltd., Manchester 22, England, for a grant to one of us (P.I.L.) which allowed this work to be carried out.

References

1. J. Bond and P. I. Lee, *J. Polymer Sci.*, in press.
2. C. C. Menon and S. L. Kapur, *J. Polymer Sci.*, **54**, 45 (1961).

Received November 18, 1967

Revised January 29, 1968

Polymerization Studies on Allylic Compounds. III. α -(Substituted Methyl)styrenes

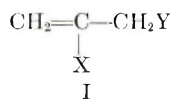
M. G. BALDWIN and SAMUEL F. REED, JR.,
*Rohm and Haas Company, Redstone Research
Laboratories, Huntsville, Alabama 35807*

Synopsis

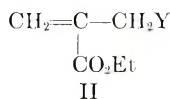
The free-radical polymerization of a series of α -(substituted methyl)styrenes was investigated. These compounds were found to be inactive in homopolymerizations but copolymerized with methyl methacrylate and styrene with a retarding effect. Copolymerization characteristics were followed by rate and viscosity measurements.

INTRODUCTION

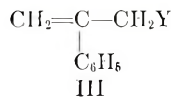
This series of papers describes the free-radical polymerization characteristics of 2,3-disubstituted propenes having the general formula I.



Previous papers in the series were concerned with compounds of type II



where Y was varied over twelve common functional groups. The present paper extends the study to include α -(substituted methyl)styrenes of the general structure III, where Y substituents are H, OH, OCH₃, OCOCH₃,



F, Cl, and CN, and thus affords a comparison of the effects of the carboethoxy and phenyl groups in the 2 position on the polymerizability of 3-substituted propenes.

Homopolymerization of the compounds III was attempted, and copolymerizations with methyl methacrylate and styrene were studied. In the copolymerization studies emphasis was placed on the effects of small concentrations of the monomers III on the polymerization rate and on the intrinsic viscosity of the resulting polymers. Only in the case of the fluoro

compound were the actual copolymer compositions determined. The cyano compound could not be obtained in pure form, so polymerization data concerning it were not obtained.

RESULTS

Homopolymerization

None of the monomers polymerized to a detectable extent with either azo or peroxide initiators (azobisisobutyronitrile and benzoyl peroxide). Samples containing no solvent, when heated in the absence of air at 60–80°C with as much as 2% of the initiators, failed to increase in viscosity, and no solids were precipitated in hexane. Dilatometric studies with α -(acetoxymethyl)styrene with benzoyl peroxide at 2% concentrations at 80° for 16 hr led to shrinkage corresponding to polymerization of less than 1% of the monomer.

Three of the monomers underwent unexpected reactions during attempted homopolymerization. These were the fluoromethyl, methoxymethyl, and chloromethyl derivatives.

α -Fluoromethylstyrene. From analogy with the series of compounds II it was thought that the α -fluoromethylstyrene would have the least retarding effect on polymerization of methyl methacrylate and styrene, and in fact, it was expected to homopolymerize. As shown below, however, it had as great or greater retarding effect in copolymerizations than any of the other compounds except the α -chloromethylstyrene.

This observation led to repeated experiments with the fluoro compound and to extra care in its purification, as described in the Experimental section. Although the samples used in the polymerization studies are considered to have been of high purity, they underwent an unexpected decomposition during homopolymerization attempts which were carried out in glass containers. For example, when the monomer, containing 1% AIBN, was heated in the absence of air at 70°C, no visible change in the sample occurred for 72 hr, but in the ensuing 8 hr period it changed to a dark green, viscous oil, evolved about 3 cc of gas per gram of sample, and severely etched the glass container. Previous experiments had shown that the same behavior occurred in the absence of AIBN.

Apparently, a strongly autocatalytic fluoride ion elimination occurs, perhaps initiated by impurities on the glass surface or by trace impurities in the sample. In the copolymerization experiments to be described there was no evidence of any degradation. We believe that the kinetic results obtained represent the free-radical behavior of the fluoro compound and that the decomposition just described is a separate phenomenon. However, the results obtained in experiments with the fluoro compound must remain in doubt until the cause of the decomposition is better understood.

The fact that significant amounts of fluorine were incorporated in the copolymer with both methyl methacrylate and styrene further supports the conclusion that the fluoro monomer is not an active terminator or

transfer agent, but rather, is an active comonomer. The retarded copolymerization rate in the case of methyl methacrylate is due to the relative stability of the propagating radical derived from the fluoro compound. The reason for the relative sluggishness of the fluoro compound in this series of monomers (III) compared with its high reactivity in the carboethoxy series (II) is not understood.

α -Methoxymethylstyrene. In homopolymerization experiments in which benzoyl peroxide was the initiator, fairly rapid evolution of gas was observed, presumably due to a reaction between the peroxide and the ether portion of the molecule.

α -Chloromethylstyrene. This compound reacted rapidly with the exposed mercury surface within the dilatometer during the rate experiments; therefore, all polymerization rate studies involving it were carried out in sealed NMR tubes by a technique previously described.¹

Copolymerization

The effects of the monomers III on the polymerization of methyl methacrylate and of styrene were investigated. Copolymerizations were carried out at 60°C, and the rates of copolymerization were observed dilatometrically² for all except the chloro compound, which was studied in sealed NMR tubes. Results are given in Tables I and II where R_{p0} refers to the rate of polymerization of methyl methacrylate and styrene in the absence of comonomer, otherwise under the same conditions as those employed in the copolymerizations.

In the case of the chloro compound, polymerization of methyl methacrylate was completely inhibited (no detectable decrease in the MMA vinyl proton area from NMR after 48 hr). Copolymerization of the chloro compound with styrene was not attempted.

In a separate series of experiments the monomers III were copolymerized with methyl methacrylate and with styrene and the intrinsic viscosities of

TABLE I
Effect of α -Methylstyrene Derivatives on the Rate of
Polymerization of MMA at 60°C in Benzene^a

| Y substituent in monomer | Concentration of monomer, mole/l | Initial polymerization rate | |
|-----------------------------|--|-----------------------------------|--------------|
| | | R_p , %/min | R_p/R_{p0} |
| Blank ^b | — | 0.74 (R_{p0}) | 1.00 |
| —OH | 1.49 | 0.064 | 0.086 |
| —OCH ₃ | 1.23 | 0.058 | 0.079 |
| —H | 1.69 | 0.035 | 0.047 |
| —OCOCH ₃ | 1.14 | 0.031 | 0.041 |
| —F | 1.24 | 0.013 | 0.018 |
| —Cl | 1.5 | 0 | 0 |

^a [MMA] = 7.54 mole/l; [AIBN] = 0.049 mole/l.

^b Benzene replaced comonomer.

TABLE II
Effect of α -Methylstyrene Derivatives on the Rate of
Polymerization of Styrene at 60°C in Benzene^a

| Y substituent in monomer | Concentration of monomer, mole/l | Initial polymerization rate R_p , %/min | R_p/R_{p0} |
|-----------------------------|--|--|--------------|
| Blank | — | 0.113 (R_{p0}) | 1.00 |
| —OCH ₃ | 1.23 | 0.089 | 0.79 |
| —OH | 1.49 | 0.079 | 0.71 |
| —OCOCH ₃ | 1.14 | 0.065 | 0.58 |
| —H | 1.69 | 0.061 | 0.54 |
| —F | 1.24 | 0.054 | 0.48 |

^a [Styrene] = 6.96 mole/l; [AIBN] = 0.049 mole/l.

the resulting copolymers determined. Lower concentrations of the comonomers III were used then in the polymerization rate studies to assure formation of copolymer with molecular weight high enough to permit isolation and purification. In the copolymerization experiments, the reaction mixtures were precipitated in hexane after about 10% reaction, and the intrinsic viscosities of the copolymers were measured in acetone solution at 30°C. Results are shown in Tables III and IV. In these tables $[\eta]_0$ refers to the intrinsic viscosity of homopolymers of methyl methacrylate and styrene prepared under the same conditions as the copolymers listed.

Analysis of the copolymers containing the fluoro monomer were performed and the resulting copolymer compositions calculated. The copolymer of α -fluoromethylstyrene and methyl methacrylate (Table III) contained 22 wt-% of the fluoro monomer, which corresponds to a mole ratio of 4.8:1 of MMA to fluoro monomer. The comonomer mole ratio in the copolymerization mixture was 28.9:1; hence, the fluoro monomer is shown to be an active comonomer although it greatly retards the rate of polymerization of methyl methacrylate.

The copolymer of styrene with α -fluoromethylstyrene contained 38.9 wt-% of the fluoro monomer. This gives a styrene to α -fluoromethylstyrene mole ratio of 2.1:1 compared to a value of 28.0:1 for their mole

TABLE III
Effect of α -Methylstyrenes on the Intrinsic Viscosity of MMA Copolymers

| Y substituent in monomer | Concentration of monomer, mole/l | $[\eta]$ | $[\eta]/[\eta]_0$ |
|-----------------------------|--|---------------------|-------------------|
| Blank | — | 0.41 ($[\eta]_0$) | 1.00 |
| —OCH ₃ | 0.37 | 0.17 | 0.41 |
| —OH | 0.31 | 0.20 | 0.48 |
| —OCOCH ₃ | 0.42 | 0.13 | 0.31 |
| —H | 0.29 | 0.15 | 0.36 |
| —F | 0.31 | 0.15 | 0.36 |

TABLE IV
Effect of α -Methylstyrenes on the Intrinsic Viscosity of Styrene Copolymers^a

| Y substituent in monomer | Concentration of monomer, mole/l | $[\eta]$ | $[\eta]/[\eta]_0$ |
|-----------------------------|--|---------------------|-------------------|
| — | — | 0.28 ($[\eta]_0$) | 1.00 |
| —OCH ₃ | 0.37 | 0.26 | 0.93 |
| —OH | 0.31 | 0.25 | 0.89 |
| —OCOCH ₃ | 0.42 | 0.22 | 0.79 |
| —H | 0.29 | 0.25 | 0.89 |
| —F | 0.31 | — ^b | — |

^a [Styrene] = 8.67 moles/l; [AIBN] = 0.049 moles/l.

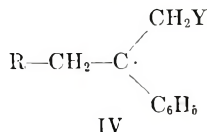
^b Copolymer was insoluble in acetone, so viscosity was not obtained. Copolymer was soluble in benzene.

ratio in the copolymerization mixture, and further emphasizes the reactive nature of the fluoro monomer in these copolymerizations.

From the above tables it is noted that addition of a relatively low concentration of the α -(substituted methyl)styrenes retards the polymerization of both methyl methacrylate and of styrene, but has a much greater effect of MMA than on styrene. Correspondingly, the viscosities of the resulting polymers were lower than those obtained in the absence of added comonomer. The degree of lowering of $[\eta]$ was not great (except in the case of the chloro compound) however, and reflects retarded polymerization rate rather than extensive chain transfer. Except for the halogens, the nature of the Y group is seen to have a rather small effect on the degree of retardation of both MMA and styrene polymerizations.

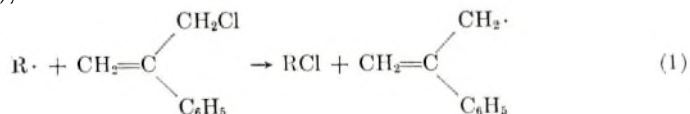
DISCUSSION

The retarding effect of the compounds studied in this work (except the chloro compound) results from the low energy of the radical IV



derived from the comonomer through attack by a growing polymer chain radical R \cdot . Radical IV is stabilized by resonance associated with the phenyl group and by steric effects caused by the two bulky substituents on the central carbon atom. The combined effects of these properties cause the addition of IV to another monomer unit to occur much less readily than is the case for chain radicals derived from MMA or styrene.

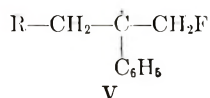
In the case of the chloro compound degradative chain transfer occurs as shown in eq. (1),



in which $R\cdot$, an initiator fragment or a growing chain radical, abstracts a Cl atom from the chloro monomer and forms a stable allylic radical, which does not initiate another chain. The difference in bond energy between $C-Cl$ and $C-H$ is sufficient to make loss of Cl much easier than loss of H. This was discussed³ for compounds II¹.

Since the monomers do not exhibit homopolymerization under free radical initiation it can be concluded that radical IV does not add to a monomer molecule of the same type. In the case of methyl methacrylate, addition of IV to MMA must occur, since the polymerization is not completely stopped by addition of the monomers studied here, but addition to MMA is slow. In the case of styrene, addition of IV to styrene monomer occurs readily, as shown by the minor retardation that was observed.

Although the monomers studied contain labile allylic hydrogen atom, none of the radicals in the system studied were sufficiently reactive to abstract them readily; addition to the stabilized double bond is favored. The nature of the Y group, therefore, had little effect on the system, as was shown to be the case of monomers II, as long as the $C-Y$ bond is not appreciably weaker than the corresponding $C-H$ bond. For weaker bonds, such as $C-Cl$, chain transfer involving the substituted atom occurs. The apparent stability of the radical derived from the fluoro derivative (V), as shown by its retardation of the rate of polymerization of MMA



compared to the other nonhalogen derivatives is not understood.

EXPERIMENTAL

Monomer Preparation

α -Methylstyrene was obtained from a commercial source and distilled just prior to use in the polymerization studies. The method of Hatch and Patton³ was employed for the preparation of α -acetoxymethylstyrene and α -hydroxymethylstyrene. The reaction of α -bromomethylstyrene with sodium methoxide gave α -methoxymethylstyrene. Each of the monomers was doubly distilled through an 18-in. semimicro spinning band column and checked for purity by vapor-phase chromatography. These compounds were considered to be of greater than 99.5% purity.

α -Acetoxymethylstyrene. This was prepared by the selenium dioxide oxidation of α -methylstyrene; bp 94–94.5°C/0.9 mm; n_D^{20} 1.5281.

ANAL. Calcd for $C_{11}H_{12}O_2$: C, 75.00%; H, 6.80%. Found: C, 74.87%; H, 6.95%.

α -Hydroxymethylstyrene. This derivative was prepared by the hydrolysis of α -acetoxymethylstyrene with aqueous sodium hydroxide; bp 94–95/1.0 mm; n_D^{20} 1.5672.

ANAL. Calcd for $C_9H_{10}O$: C, 80.6%; H, 7.5%. Found: C, 80.52%; H, 7.41%.

α -Bromomethylstyrene. This was prepared by the *N*-bromosuccinimide bromination of α -methylstyrene;⁴ bp 90–91°C/5 mm; n_D^{20} 1.5917.

ANAL. Calcd for C_9H_9Br : C, 54.82%; H, 4.57%; Br, 40.61%. Found: C, 54.71%; H, 4.52%; Br, 40.37%.

α -Methoxymethylstyrene. To a mixture of 58.0 g (0.29 mole) α -bromomethylstyrene in 150 ml of ethanol was added in increments 16.2 g (0.3 mole) sodium methoxide over a period of 30 min with rapid stirring. After standing for 1 hr, 150 ml ether was added and the total mixture was filtered to remove solids. The filtrate was thoroughly washed with water, dried over anhydrous magnesium sulfate and the ether removed at reduced pressure. The resulting residue was distilled through an 18-in. spinning band column to give 33.62 g (75.7%) of α -methoxymethylstyrene; bp 62–63°C/2 mm; n_D^{20} 1.5410.

ANAL. Calcd for $C_9H_{12}O$: C, 79.41%; H, 8.82%. Found: C, 79.53%; H, 8.86%.

Preparation of α -Fluoromethylstyrene. A mixture of 18.6 g (0.094 mole) of α -bromomethylstyrene and 25.2 g (0.2 mole) silver fluoride in 200 ml dry acetonitrile was stirred at ambient temperature for a period of 12 hr. After filtration to remove solids, the filtrate was added to 500 ml of water and extracted with three 100 ml portions of ether. The ether extracts were combined, washed thoroughly with water and dried over anhydrous magnesium sulfate. Ether was removed by evaporation and the residue distilled through an 18-in. semimicro spinning band column to give 9.63 g (36.5%) of α -fluoromethylstyrene, bp 50°C/2.7 mm; $n_D^{21.5}$ 1.5283. It was observed that this compound attacks glass, since both the distillation column and glass containers become etched on contact. It could be stored for extended periods in glass containers at 0°C after distillation without etching, however. Final purification was accomplished by preparative gas chromatography employing a 5'-dinonyl phthalate on Chromosorb column in an Aerograph Model A-100-C instrument.

ANAL. Calcd for C_9H_9F : C, 79.42%; H, 6.63%; F, 13.95%. Found: C, 79.14%; H, 6.74%; F, 13.70%.

Attempted Preparation of α -Cyanomethylstyrene. A mixture of 39.2 g (0.2 mole) α -bromomethylstyrene, 19.5 g (0.3 mole) potassium cyanide, and 100 ml of dry acetonitrile was introduced into a 200-ml three-necked flask fitted with magnetic stirrer, condenser, thermometer, and dropping funnel (all outlets covered with Drierite-filled drying tubes). This mixture was stirred at ambient temperature over a period of three days and then examined by gas chromatography, which indicated the presence of only a trace of the unreacted bromide. The reaction was poured into 500 ml of water, extracted three times with 100 ml portions of ether, the combined ether extracts washed thoroughly with water, and dried over anhydrous magnesium sulfate. After evaporation of the ether, the liquid

residue was distilled to give 18.0 g (63%) of cyano compounds; bp 84°C/0.65 mm; n_D^{20} 1.5824. Identification was based on elemental analysis and the proton NMR spectrum. The H^1 NMR spectrum* showed the following signals: α -methyl- β -cyanostyrene was characterized by a doublet at 2.32 ppm (CH_3), $J \sim 1$ cps, a quartet at 5.55 ppm (vinyl proton) and phenyl protons at 7.36 ppm, α -cyanomethylstyrene displayed a quartet at 3.35 ppm ($-CH_2-$), a multiplet centered at 5.48 ppm (vinyl protons), and phenyl protons at 7.30 ppm. The two compounds were present in approximately equal quantities.

ANAL. Calcd for $C_{10}H_9N$: C, 83.90%; H, 6.29%; N, 9.78%. Found: C, 83.85%; H, 6.57%; N, 9.70%.

In the course of several attempts to prepare α -cyanomethylstyrene, mixtures of it with α -methyl- β -cyanostyrene were obtained as shown by NMR spectra of the reaction product. Suitable techniques were not found to separate the two isomers. In still other experiments, the vinyl cyanide was the only product isolated. Our failure to isolate the desired α -cyanomethylstyrene is attributed to its ease of isomerization under either thermal or base catalyzed conditions. Gas chromatography of the crude or distilled product showed only one peak representing the α -methyl- β -cyanostyrene. Apparently the α -cyanomethylstyrene contained in the mixture undergoes complete isomerization on the chromatographic column and during distillation.

Polymerization Studies

The dilatometric and viscometric techniques used in this study were described previously.³

SUMMARY

Comparison of the effects of the carboethoxy and phenyl groups in the X position in I leads to the general observation that those compounds with the phenyl group are much less reactive in homopolymerization than those with the carboethoxy group, but, generally, are active comonomers with MMA and styrene. This is due to the low energy of the chain carrying radical from the phenyl substituted monomers compared with those derived from the carboethoxy monomers. Increased resonance stabilization and steric hindrance associated with the phenyl group give rise to this effect. All of the α -methylstyrene derivatives retarded the polymerization of methyl methacrylate and of styrene, and decreased the molecular weight of the resulting polymers. The molecular weight decrease is not great except in the case of the chloro compound, however, and probably does not reflect significant chain transfer. The fluoro derivative was shown to undergo

* All H^1 NMR spectra were obtained in 10–15% carbon tetrachloride solutions with tetramethylsilane as external standard and with the use of a Varian Associates A-60 instrument with 40 Mcps probe.

autocatalytic decomposition with elimination of fluoride ion when stored in glass, but it copolymerized extensively with methyl methacrylate and styrene to form the copolymers. The cyano derivative could not be prepared because of isomerization to β -cyano- α -methylstyrene.

This work was performed under the sponsorship of the U. S. Army Missile Command, Redstone Arsenal, Alabama, under Contract DA-01-021 ORD-11878 (Z).

References

1. C. P. Haney, F. A. Johnson, and M. G. Baldwin, *J. Polymer Sci. A-1*, **4**, 1791 (1966).
2. M. G. Baldwin and S. F. Reed, *J. Polymer Sci.*, **1**, 1919 (1963).
3. S. F. Reed and M. G. Baldwin, *J. Polymer Sci. A*, **2**, 1355 (1964).
4. L. F. Hatch and T. L. Patton, *J. Amer. Chem. Soc.*, **27**, 2705 (1954).
5. S. F. Reed, *J. Org. Chem.*, **30**, 3258 (1965).

Received December 6, 1967

Revised February 2, 1968

X-Ray Degradation of Penton and Its Potential Use as a Dosimeter for the 4-15 keV Range

BARBARA J. MALLON, *Lawrence Radiation Laboratory, University of California, Livermore, California 94550*

Synopsis

Exposure of poly-3,3-(bischloromethyl)oxetane (Penton) to x-rays produces a linear reduction of the molecular weight, heat of fusion, and melting point with increasing absorbed dose. Optical density measurements fit a smooth curve with absorbed dose. Exposures were made with 25, 50, and 100 cal/cm² integrated incident energy at 50 peak keV with and without zinc and titanium-aluminum filters. Because the molecular weight of Penton is relatively uniform from lot to lot, and because it is difficult to obtain spectral measurement in the 4-15 keV range to which Penton is particularly sensitive, it is believed that the data contained in this report can be used with an iterative computer code to determine the spectrum and intensity of radiation in this region.

INTRODUCTION

The fact that poly-3,3-(bischloromethyl)oxetane (Penton, Hercules, Inc., Wilmington, Delaware) degrades by chain scission with absorption of γ -rays has been shown by Golden and Hazell.¹ Although, according to their report, the decomposition products change somewhat with increasing weight was found to hold. They also report a decrease in softening temperature with increasing dose.

Absorbed dose on exposure to x-rays is very spectrum-dependent, in contrast to that due to exposure to γ -rays. In the x-ray spectral region, the mass absorption coefficients are changing rapidly, whereas in the γ region they are nearly constant. This makes dosimetry of x-rays from commercial machines more difficult because the spectrum must be known to determine the absorbed dose in different compounds. The few spectra available in the literature^{2,3} do not resolve the spectral region below 10 keV. Penton is an ideal candidate for the study of this region, since it is relatively transparent to radiation above 15 keV and it becomes increasingly absorbant below this energy (see Fig. 1). Successive layers of stacks of Penton disks would be expected to be graduated in radiation damage for two reasons: first, each layer absorbs a fraction of the energy incident upon it and thereby decreases the amount incident upon the next; second, the lower-energy x-rays are preferentially absorbed, creating a less damaging spectrum of higher-energy x-rays for the next layer.

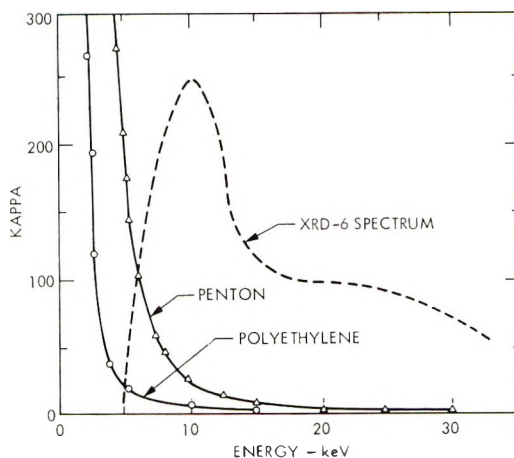


Fig. 1. Mass absorption coefficient (κ) as a function of energy.

A preliminary study⁴ made with x-rays and a measured spectrum⁵ showed linear relationships between calculated absorbed dose and the experimental melting points and heats of fusion. The relationships held even though the exposures and filters were varied. These promising results prompted further investigation of the degradation and dosimetric possibilities.

EXPERIMENTAL

Penton 9215G (Hercules, Inc., Wilmington, Delaware) was used in this study. The material used in the melting points and heat of fusion experiments was prepared by Battelle Memorial Institute from sheet and machined to the specified thickness. Samples were then punched from the sheets to give $\frac{1}{2}$ -in. diameter disks which were assembled into layered stacks for irradiation. The sample temperature during irradiation was 61°C at the front surface, with a gradient of 5°C for each 2 mm depth in the sample. [Temperatures were measured by the melting points of various waxes (Will Corp. and Subsidiaries, Rochester, New York) placed between disks in a calibration run. A wax which melted at 61 – 62°C softened slightly but did not melt at the front surface, and a 56 – 56.5°C wax did the same between disks 2 mm back.]

After irradiation, samples to be used in intrinsic viscosity measurements were dissolved in cyclohexanone (Matheson, Coleman, and Bell, Rutherford, New Jersey) which contained 0.5% antioxidant 2246 (American Cyanamid Company, New York, New York). This was accomplished by heating to 125°C . Viscosity measurements were made at $50 \pm 0.01^{\circ}\text{C}$. (Model H-1 high temperature bath, Cannon Instrument Co., State College, Pa.) with Cannon-Ubbelohde viscometers (Cannon Instrument Company, State College, Pa.) with constants of approximately 0.02 cS/sec.

Measurements of the heats of fusion and melting points of Penton samples were made with the calorimeter module of the duPont 900 Thermal-analyzer (E. I. duPont de Nemours and Co., Wilmington, Delaware). The instrument plots the temperature of the reference against the difference in temperature between the reference and the sample. The reference and sample are heated simultaneously in isolated cups in a dual-chamber oven. The area of the endotherm obtained with melting is proportional to the heat of fusion,

$$H_f = ACT\Delta T/WR$$

where A is the area of the endotherm, C is a calibration coefficient, T is the scale of the abscissa, ΔT is the scale of the ordinate, W is the weight of the sample, and R is heating rate.

After irradiation, each sample was heated under nitrogen to 230°C in the calorimeter, allowed to cool until it crystallized, and then annealed. Annealing was done by reheating and holding the sample for 15 min at $8 \pm 1^\circ\text{C}$ below the peak of the highest temperature endotherm of a sample which had cooled naturally (cooled in the calorimeter from 230 to 25°C by gradual heat loss). After annealing, the sample was shock-cooled with Dry Ice to prevent transition to the β -crystalline form.⁶ (It was found that slow cooling after annealing caused this transition to occur.)

Precision between individual runs is better than $\pm 3\%$. Accuracy should also be in the same range since the instrument is calibrated with pure metals whose heats of fusion are well established. Precision on the more severely damaged samples was poorer because the gradient of damage is sharper in these samples and the endotherms are broader, making the determinations more difficult.

Melting points are either the intersection of the extrapolated highest melting endotherm to the base line or the peak of the highest temperature endotherm. These are referred to as "Mp (extrap)" and "Mp (peak)," respectively.

The need for better surface characteristics and thinner samples for optical measurements resulted in the development of special samples for these experiments. These 10 mil-thick samples were prepared from Penton powder (generously donated by Dr. Frank H. McTigue, Hercules Research Center, Wilmington, Delaware) pressed between two polished metal plates with 10-mil thick shims at 400°F.

Optical density measurements were made with a Carey Model 14 recording spectrometer (Applied Physics Corp., Monrovia, Calif.) at 580 nm and a slit width of 0.14 mm.

Zinc and titanium-aluminum filters were prepared and loaned by Dr. Nancy del Grande of this Laboratory.

An XRD-6 x-ray machine (General Electric Co., Milwaukee, Wisc.) was operated at 50 peak kV and 50 mA. The sample of Penton was

approximately 31.8 mm from the tungsten target and was separated from the beryllium window by a 1.6-mm thick disk of carbon foam. A stream of helium was passed over the sample during irradiation. (Results from a 100 cal/cm² sample exposed in air were found to be indistinguishable.) Exposure times ranged from 79 min for the 25-cal/cm² exposure to 316 min. for the 100-cal/cm² exposure.

The intensity of the impinging radiation of the XRD-6 was determined by Taylor.⁵ The method consisted briefly of absorbing all the x-ray energy in a lead cylinder and measuring the temperature rise. Beam intensity was found to be constant over the 1/2-in. diameter of the Penton disks.

The spectrum used in this study for this machine was proposed by Taylor⁵ and is shown in Figure 1. The spectrum was obtained by counting photons obtained by Compton scatter of the beam per unit time per channel with a 100-channel analyzer. The detector was a NaI (Tl) crystal with a photomultiplier tube. A correlation of channel with energy was established by fluorescence of various materials. Further corrections were made to change number of pulses to intensity, to correct slight energy changes in the Compton scatter, and to correct changes in channel width at different energies.

Calculation of absorbed dose was done by means of a computer code.⁷ This code calculates the absorbed dose with a one-dimensional exponential absorption code, based on the photoelectric cross sections of the elements involved plus a linear correction for Compton absorption for each 0.2 keV increment of the given spectrum. Each input must supply, in addition, the density of the materials, the weight fraction of each element, the thickness of each disk, the spectrum, and the total intensity of the impinging radiation on the first disk. It then calculates the average absorbed dose for each successive disk, ignoring any scattering. A further correction was then applied for the $1/r_2$ (r = radius) loss in intensity with distance from the source.

The validity of the above approach was checked by using a detailed Monte Carlo type code with 10,000 initial particles, mathematically weighted in successive layers to provide enough particles for numerically significant absorbed doses. The geometry used for this calculation consisted of a point source with the stack of Penton disks located at the same distance as in the XRD-6 x-ray machine. The code used a stack of 10 lead disks surrounding the Penton to calculate the effect of scatter from the lead shield of the machine. This code takes into account both photoelectric and Compton absorption, the density of the materials and the weight fraction of the composing elements, and yields the average absorbed dose per disk. Agreement between the simple approach and the Monte Carlo approach was in all cases better than 2% and well within the 3-9% standard deviations of the Monte Carlo output. Since 2% error in dose would be lost in the experimental error of the rest of this study, a Monte Carlo calculation using more particles was not done.

RESULTS AND DISCUSSION

After irradiation, the disks of each exposed sample were spread on a white sheet of paper. The change of color with depth was striking: the slice closest to the source was nearly black, and the colors of the others graduated with depth to the pale beige of the control. In exposures at 100 cal/cm², at 100 cal/cm² with a zinc filter, and at 50 cal/cm², the surface of the first disk was foamed. The amount of foaming decreased in the order listed. In the exposures at 25 cal/cm², at 25 cal/cm² with a zinc filter, and at 100 cal/cm² with a titanium-aluminum filter, the surfaces were not foamed but merely darkened. Foaming is easily explained by the lowering of the melting point of the front of the surface disk below 61°C by radiation deposition.

It is necessary to investigate the effect of the 5°C temperature gradient for each 2 mm depth on the amount of damage as measured by viscosity, melting points, heats of fusion, and optical density. There is some question in the literature⁸⁻¹⁸ as to whether temperature below that at which the compound flows significantly affects the amount of decomposition per given dose in poly(methyl methacrylate), polyethylene, and polyisobutylene. The most logical compound of the three to compare with Penton is polyethylene since it, like Penton, is between its glass transition point and its melting point at 61°C. While Taubman and Ianova¹¹ and Turner¹² claim no effect to polyethylene with temperature until melting, Charlesby and Davison⁸ and Black¹⁰ claim the opposite. Using the data of Black¹⁰ one finds that an increase in temperature from 56 to 61°C increases the absorption coefficient, G (crosslinks), a measure of absorbed dose, by only 0.14%. This would be indeed a negligible effect in this study.

The dependence of absorbed dose with depth changes with a change in spectrum. Figure 2 is a theoretical plot of absorbed dose versus depth for two assumed spectra; in one case a rectangular band from 5 to 7 keV and in the other another such band from 15 to 17 keV. After comparing these curves, one can see that the steeper the damage gradient, the less energetic the spectrum. Presumably, one could determine the spectrum from 4 to 15 keV from the depth results in Penton, using a property such as molecular weight which has a theoretical relationship with dose.¹ Since there was already a proposed spectrum,² the author decided instead to test that spectrum against a theoretical molecular weight relationship and to study the dose depth effect on such properties as heat of fusion, melting point, and optical density.

Molecular Weight

The best test for the proposed spectrum is to plot the calculated absorbed dose against a theoretical relationship. Chapiro¹⁴ derives the relationship

$$\frac{1}{\bar{M}_n} = \frac{1}{\bar{M}_{n_0}} + \frac{D}{E_d N} \quad (1)$$

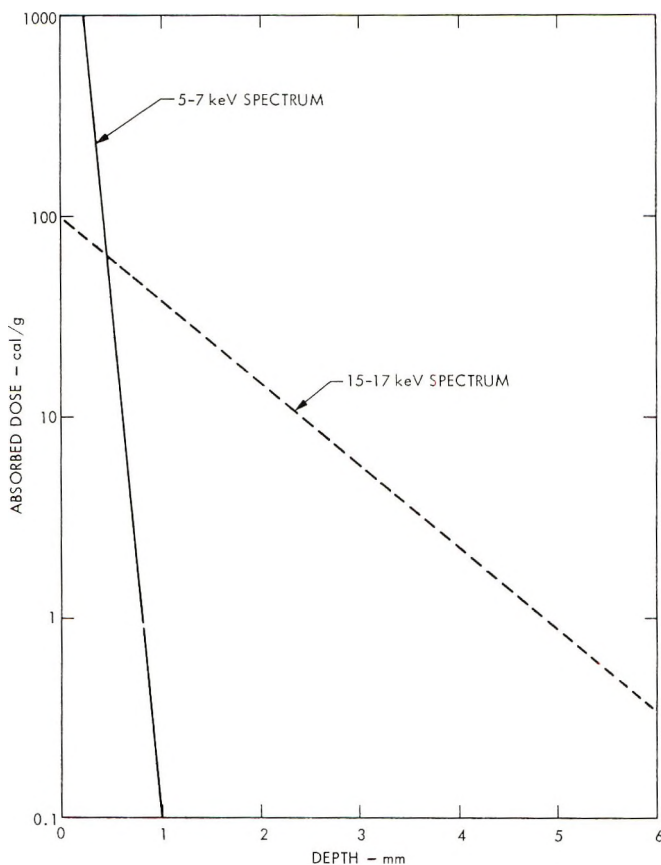


Fig. 2. Log calculated absorbed dose of Penton as a function of depth for two assumed spectra.

where \bar{M}_n is the number-average molecular weight, D is the absorbed dose, E_d is the average energy absorbed per main chain scission, N is Avogadro's number, and \bar{M}_{n_0} is initial number-average molecular weight.

Substituting the relationships given in eqs. (2) and (3)

$$[\eta] = K' \bar{M}_v^\alpha \quad (2)$$

where $[\eta]$ is the intrinsic viscosity and \bar{M}_v is the viscosity-average molecular weight, and

$$\bar{M}_v = [(\alpha + 1)(\Gamma(\alpha + 1))]^{1/\alpha} \bar{M}_n = C \bar{M}_n \quad (3)$$

where Γ is the gamma function and C a constant, eq. (1) becomes

$$\left(\frac{K'}{[\eta]}\right)^{1/\alpha} = \left(\frac{K'}{[\eta_0]}\right)^{1/\alpha} + \frac{D}{CE_d N} \quad (4)$$

Therefore, the absorbed dose should be a linear function of the reciprocal of the intrinsic viscosity to the $1/\alpha$ power. The value of α was obtained from

the unpublished work of Chiang¹⁵ by least squares of $\log [\eta]$ in cyclohexanone at 50°C as a function of $\log \bar{M}_w$ obtained by light scattering. A value of 0.83 for α was obtained. Substituting in eq. (3), yields

$$\bar{M}_v = 1.92\bar{M}_w$$

Although Chiang's values of M were of unfractionated Penton samples, they have a consistent linear relationship between $\log [\eta]$ and $\log \bar{M}_w$. According to Flory¹⁷ the value of α obtained should be valid and any error from least-squares fit should reside in K' instead.¹⁶

Intrinsic viscosity and absorbed dose values for various samples obtained in this study are shown in Table I. A plot of the reciprocal of the intrinsic viscosity to the $1/\alpha$ power as a function of absorbed dose is shown in Figure 3. The linearity of this plot is taken as strong support of the Taylor spectrum.^{5*}

TABLE I
Experimental Intrinsic Viscosity and Calculated
Absorbed Doses of Penton with Taylor Spectrum

| Exposure cal./cm. ² | Sample | Thickness, mm | Absorbed dose, cal/g | Intrinsic viscosity |
|-----------------------------------|--------|------------------|-------------------------|------------------------|
| 100 (air) | 4 | 0.719 | 83.88 | 0.120 |
| | 6 | 0.70 | 34.83 | 0.230 |
| | 9 | 0.70 | 15.37 | 0.356 |
| 100 (helium) | 3 | 0.716 | 62.24 | 0.158 |
| | 4 | 0.716 | 40.47 | 0.220 |
| 50 cal/cm. ² | 4 | 0.437 | 28.71 | 0.249 |
| | 6 | 0.66 | 20.03 | 0.390 |
| | 10 | 0.66 | 10.31 | 0.465 |
| | 25 | | | |
| | 4 | 0.701 | 10.52 | 0.490 |
| | 8 | 0.701 | 3.49 | 0.788 |
| Control | | 0.712 | 0 | 1.188 |

On correcting Chiang's molecular weights by the relationship

$$\bar{M}_v = (1.92/2.0)\bar{M}_w$$

the value of K' is corrected from 3.61×10^{-6} to 3.74×10^{-6} . By substituting this value into eq. (4), a value of 35.4 eV per scission is obtained.

Charlesby et al.⁹ prefer to rearrange eq. (4) to the form

$$(1/\eta)^{1/\alpha} = \text{constant} (D + D_0).$$

* When the Erlich spectrum² is used to calculate absorbed dose, a curve with more scatter is obtained for this plot. These effects are greatest for the surface disks because the effect of the incident spectrum is greatest (see Introduction).

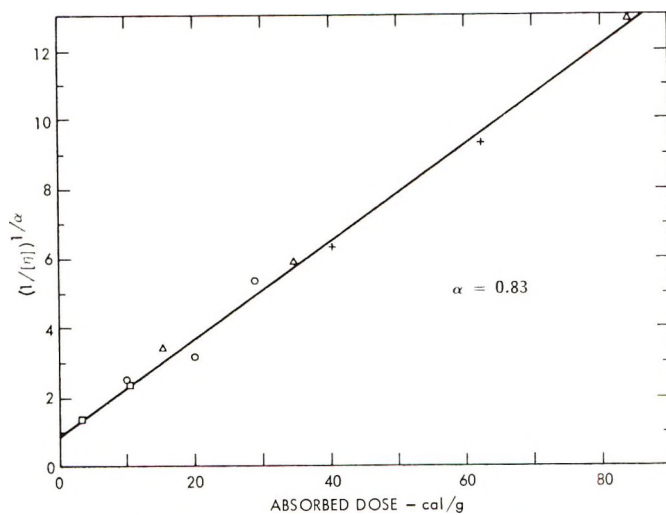


Fig. 3. Reciprocal of the intrinsic viscosity to the $1/\alpha$ power as a function of x-ray absorbed dose (Taylor spectrum⁶): (Δ) 100 cal/cm², in air; (+) 100 cal/cm², in helium; (O) 50 cal/cm²; (\square) 25 cal/cm²; (\times) control.

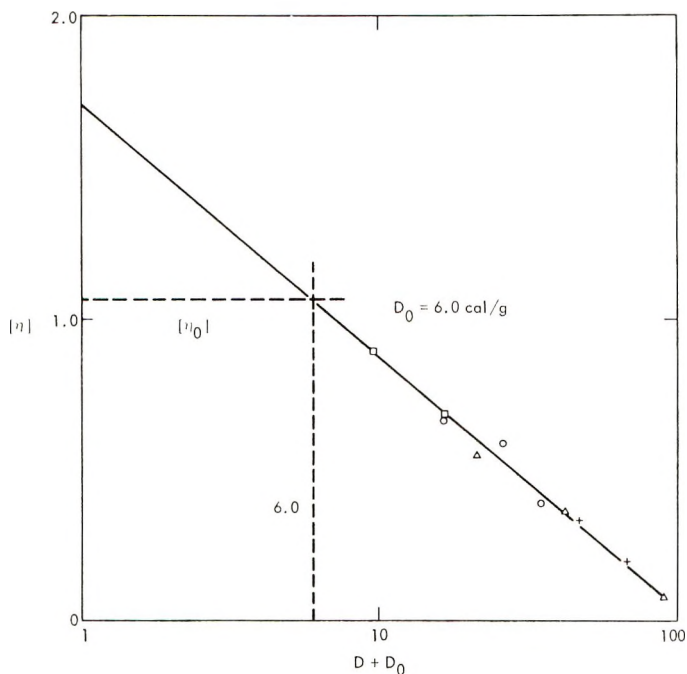


Fig. 4. Log-log plot of intrinsic viscosity as a function of $D + D_0$. (Δ) 100 cal/cm², in air; (+) 100 cal/cm², in helium; (O) 50 cal/cm²; (\square) 25 cal/cm²; (\times) control.

From the slope obtained from a least-squares fit of the reciprocal of the intrinsic viscosity to the $1/\alpha$ power as a function of dose (Fig. 3) and the intrinsic viscosity of a nonirradiated sample, a value of 6.0 cal/g was

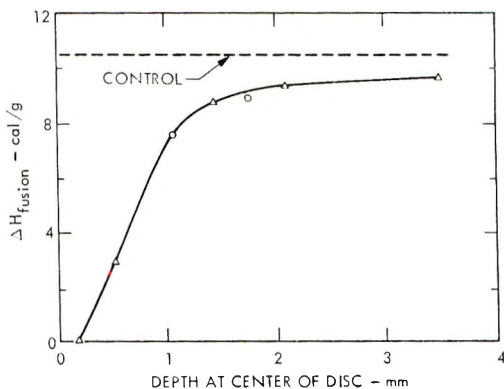


Fig. 5. Heat of fusion for Penton as a function of depth for samples exposed to 100 cal/cm²: (Δ) in air; (○) in helium.

calculated for D_0 . A log-log plot of intrinsic viscosity as a function of $D + D_0$ is shown in Figure 4. Again, a linear relationship with a slope of -0.83 is observed as required.

Heat of Fusion

A specimen exposed at 100 cal/cm² in air showed a marked decrease of the heat of fusion with depth, as shown in Figure 2. Another sample with thicker disks near the surface was exposed to 100 cal/cm² in helium to confirm that results are independent of sample thickness and atmosphere. These results also are shown in Figure 5.

A linear relationship between heats of fusion of annealed samples and calculated absorbed dose was found (see Table II and ref. 4, Fig. 2). The equation obtained by least-squares fit of these values is

$$\Delta H = -0.910 D + 10.68$$

where ΔH and D are in calories per gram. When the samples were not annealed, much more scatter of the data was observed. This is reasonable in view of the fact that the naturally cooled samples have varied proportions of the α and β crystalline forms, whereas the annealed samples are all the higher melting, α -crystalline form.

Melting Points

Melting points were obtained simultaneously with heat of fusion values. The values basically provide the same correlation as the heats of fusion (see Fig. 6).

The best correlation, surprisingly, is obtained from the melting points of the samples which cooled naturally (see Fig. 6). It is surprising in that these samples were mixtures of the α and β forms of Penton which have melting points approximately 20°C apart, and the errors on these determinations were larger than in the other three cases shown in Table II. (The

TABLE II
Experimental Heats of Fusion and Melting Points and Calculated Absorbed Doses of Penton with XRD-6 Spectrum^a

| Exposure, cal/cm ² | Sample | Thickness, mm | Absorbed dose, cal/g | Naturally cooled samples | | | Annealed samples | | |
|--|--------|---------------|----------------------|--------------------------|-------------------|---------------|----------------------|-------------------|---------------|
| | | | | ΔH_f , cal/g | Mp (extrap), °C | Mp (peak), °C | ΔH_f , cal/g | Mp (extrap), °C | Mp (peak), °C |
| 100, unfiltered (air) | Disk 1 | 0.35 | 802 | 0 ^b | None ^b | 121 ± 2 | 0 ^b | None ^b | |
| | Disk 2 | 0.35 | 264 | 3.0 ± 0.3 | 108 ± 6 | 120 ± 2 | 3.0 ± 0.2 | 120 ± 2 | |
| | Disk 4 | 0.70 | 85 | 7.5 ± 0.2 | 151 ± 3 | 161 ± 1 | 8.8 ± 0.2 | 160 ± 1 | |
| | Disk 5 | 0.70 | 51 | 8.6 ± 0.2 | 158 ± 2 | 166 ± 1 | 9.4 ± 0.2 | 162 ± 2 | |
| | Disk 7 | 0.70 | 26 | 8.7 ± 0.2 | 163 ± 2 | 172 ± 1 | 9.7 ± 0.1 | 171 ± 1 | |
| | Disk 2 | 0.70 | 118 | 7.1 ± 0.2 | 139 ± 4 | 159 ± 1 | 7.6 ± 0.2 | 154 ± 1 | |
| | Disk 3 | 0.70 | 63 | 8.5 ± 0.2 | 157 ± 2 | 167 ± 1 | 9.0 ± 0.2 | 162 ± 1 | |
| 100, 0.0533-mm Ti + 0.0254-mm Al filter | Disk 1 | 0.44 | 132 | 6.0 ± 0.2 | 137 ± 3 | 156 ± 1 | 6.5 ± 0.3 | 152 ± 3 | |
| | Disk 2 | 0.44 | 84 | 7.7 ± 0.3 | 150 ± 3 | 160 ± 1 | 8.5 ± 0.2 | 159 ± 2 | |
| 100, 0.0139-mm Zn filter | Disk 1 | 0.44 | 304 | 3.1 ± 0.2 | 106 ± 5 | 129 ± 1 | 3.0 ± 0.3 | 149 ± 2 | |
| | Disk 2 | 0.44 | 106 | 7.4 ± 0.4 | 148 ± 3 | 162 ± 1 | 8.4 ± 0.2 | 156 ± 1 | |
| 50, unfiltered | Disk 6 | | 38 | | 163 ± 1 | 171 ± 1 | | | |
| | Disk 1 | 0.44 | 355 | 1.9 ± 0.2 | 86 ± 5 | 124 ± 2 | 1.6 ± 0.3 | 143 ± 2 | |
| | Disk 2 | 0.44 | 103 | 7.9 ± 0.2 | 150 ± 4 | 163 ± 1 | 8.1 ± 0.2 | 156 ± 1 | |
| | Disk 5 | | 25 | | 165 ± 1 | 173 ± 1 | | | |
| | Disk 1 | 0.254 | 235 | 3.2 ± 0.3 | 116 ± 3 | 135 ± 1 | 3.5 ± 0.3 | 135 ± 1 | |
| Control | | 0.35 | | | | | | | |
| | | 0.254 | 0 | 9.0 ± 0.2 | 165 ± 2 | 175 ± 1 | 10.4 ± 0.2 | 172 ± 1 | |
| | | 0.44 | | | | | | | |

^a Error values include only measuring errors of all types. They do not include the error caused by the sharp "damage gradient" in the surface disks.

^b No endotherm was found in the DTA trace of the calorimeter.

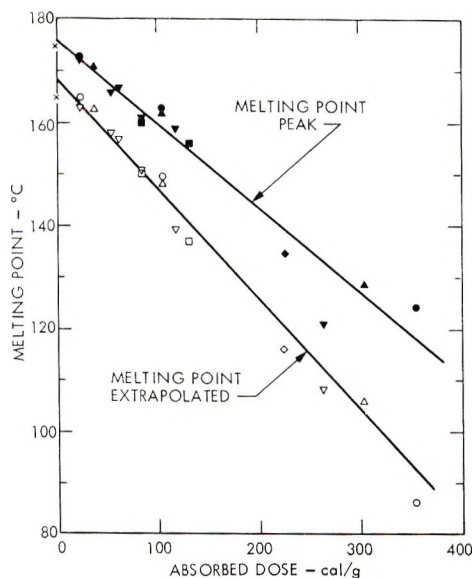


Fig. 6. Melting point values for naturally cooled Penton samples as a function of absorbed x-ray dose (Taylor spectrum⁵): peak values filled, extrapolated values unfilled; (∇) 100 cal/cm², unfiltered; (Δ) 100 cal/cm², Zn filter; (\square) 100 cal/cm², Ti-Al filter, (\circ) 50 cal/cm², unfiltered; (\diamond) 25 cal/cm², unfiltered.

relative amount of Penton in the high-melting form tended to shift its melting point.) Equations for these relationships are

$$M_p(\text{extrap}) = -0.1799D + 169.6$$

and

$$M_p(\text{peak}) = -0.1610D + 175.9$$

The only major discrepancy is in the melting points for the annealed top disks of the specimens exposed at 50 cal/cm² unfiltered and at 100 cal/cm² with a zinc filter (Fig. 7). The fact that these values are so high is easily explained. The damage gradient in the top disk is the greatest. In these samples the top disk is 0.44 mm thick; therefore, although the average dose is about 300 cal/g, the top of the disk received much more radiation and the bottom of the disk received considerably less. The high melting point is, therefore, the melting point of the less damaged bottom of the top disk; this appeared as a peak near the end of the broad melting endotherm in the naturally cooled samples. The samples were, therefore, annealed 8°C below this temperature (see experimental section). Better data for surface disks would have been obtained if they had been thinner.

It is interesting to compare x-ray damage with γ -ray damage for an equivalent absorbed dose. Golden and Hazell¹ report that a dose of 100 Mrad of γ -radiation linearly reduces the softening temperature from 148°C to 125–126°C, and 200 Mrad lowers it to 89–90°C. Converting the 100

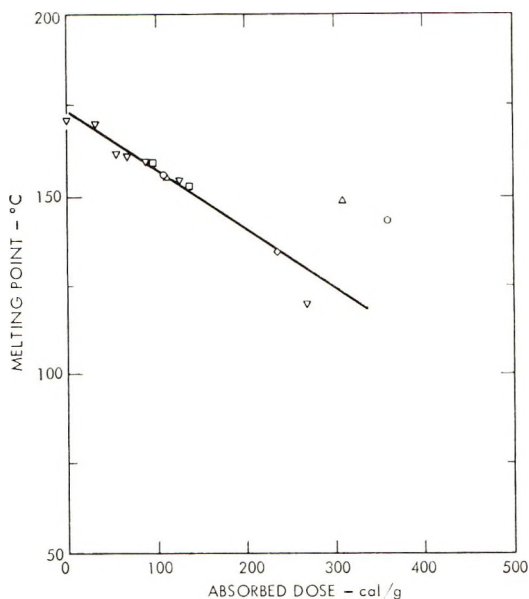


Fig. 7. Melting point extrapolated values for annealed Penton samples as a function of absorbed x-ray dose (Taylor spectrum⁶): (∇) 100 cal/cm², unfiltered; (Δ) 100 cal/cm², Zn filter; (□) 100 cal/cm², Ti Al filter; (○) 50 cal/cm², unfiltered; (◇) 25 cal/cm², unfiltered.

and 200 Mrad to the units cal/g absorbed dose, one obtains 240 and 480 cal/g, respectively. Further comparison of the results of Golden and Hazell¹ and the present results is difficult because rads in the above-cited study are evidently a measure of absorbed dose in tissue which is not quite equivalent to that in Penton, and the softening point of 148°C is difficult to translate into melting point. However, it is noteworthy that both the x-ray and γ -ray absorbed doses do produce roughly the same degree and type of damage. The approximate linearity of the above-cited softening points with dose lends credence to the linearity of the relationship between melting points versus dose obtained in this study. Golden and Hazell¹ also state that Penton degrades up to doses of 500 Mrad by chain scission with no evidence of crosslinking, as determined by solubility and viscosity studies.

Although no other reports of decrease in melting point and heat of fusion with dose in Penton were found, similar results were observed for other compounds. A linear decrease in melting point with dose was observed by Charlesby¹⁷ for *n*-dodecane, C₂₄C₅₀, and C₃₆H₇₄. Although these compounds crosslink as well as degrade by chain scission, the linear reduction in melting point is attributed to production of lower paraffins by main-chain fracture.

A similar observation on the behavior of poly(methyl methacrylate) with both γ - and pile radiation is reported by Ross and Charlesby.¹⁹ The "bubbling" temperature (probably glass transition temperature) is shown

to lower as a linear function of radiation dose. Poly(methyl methacrylate) is known to degrade like Penton by random chain scission.

Optical Density

Since all the irradiated Penton samples were graduated in color with depth, optical measurements seemed an obvious means to establish a correlation with absorbed dose. The change in optical density with depth was examined on the specimen exposed at 100 cal/cm² in air. A smooth curve was obtained. However, further disks were cut from a second sheet of Penton which was thicker (0.44 mm as compared to 0.35 mm) and had a much rougher, less regular surface. Optical measurements on samples from a latter sheet were very irregular because of uneven scattering by the rough surface. Comparison would have been difficult anyway, since Penton, being partially crystalline, is somewhat opaque and therefore does not obey Beer's Law. Therefore, special 10-mil thick samples were prepared from Penton powder, as described in the experimental section.

Optical measurements on these samples after exposure at 25 cal/cm² both with and without the zinc filter (see Fig. 3 of the previous communication⁴) are listed in Table III. Deviations are more likely due to imperfections in the sample than in resolution of the instrument or in error in the spectrum. This premise is supported by the fluctuations of the data for

TABLE III
Optical Density and Absorbed Dose Calculated with the XRD-6 Spectrum

| Exposure cal/cm ² | Sample | Thickness, mm | Absorbed dose, cal/g | Optical density at 580 mμ |
|---------------------------------|--------|------------------|----------------------------|------------------------------|
| 25, unfiltered | Disk 1 | 0.254 | 235 | 1.520 |
| | Disk 2 | 0.254 | 89 | 1.050 |
| | Disk 3 | 0.254 | 52 | 0.727 |
| | Disk 4 | 0.254 | 36 | 0.702 |
| | Disk 5 | 0.254 | 27 | 0.645 |
| | Disk 6 | 0.254 | 20 | 0.595 |
| | Disk 7 | 0.254 | 17 | 0.592 |
| | Disk 8 | 0.254 | 14 | 0.540 |
| | Disk 9 | 0.254 | 13 | 0.533 |
| 25, 0.0139-mm. Zn filter | Disk 1 | 0.254 | 98 | 1.049 |
| | Disk 2 | 0.254 | 41 | 0.665 |
| | Disk 3 | 0.254 | 26 | 0.565 |
| | Disk 4 | 0.254 | 20 | 0.560 |
| | Disk 5 | 0.254 | 16 | 0.552 |
| | Disk 6 | 0.254 | 14 | 0.532 |
| | Disk 7 | 0.254 | 12 | 0.520 |
| | Disk 8 | 0.254 | 10 | 0.552 |
| | Disk 9 | 0.254 | 9 | 0.546 |
| Control | | 0.254 | 0 | 0.525 |

disks 7, 8, and 9 of the specimens exposed at 25 cal/cm² with a zinc filter. These disks were purposely chosen as the ones with the worst surfaces when the samples were prepared.

The marked dependence of optical density upon absorbed dose, together with the ease of measurement, make this approach of much interest for dosimetry. However, fading or deepening of color of irradiated plastics upon subsequent storage is well-known. This suggests the need for additional studies of aging (time/temperature/oxygen) before optical density can be depended upon as an indication of exposure.

For comparison, Mallon⁴ shows the Taylor spectrum⁵ for the 50 keV spectrum and that proposed in 1955 by Erlich² for commercial x-ray machines. This is a much more energetic spectrum. The Erlich spectrum peaks at about 26 keV in contrast to 10 keV for the spectrum proposed by Taylor.⁵ In Figure 8, absorbed dose calculated with the Erlich spectrum is plotted against the experimental melting points for naturally cooled specimens. The inconsistency of the points is readily apparent. The same is true for plots of absorbed energy with melting point or optical density.

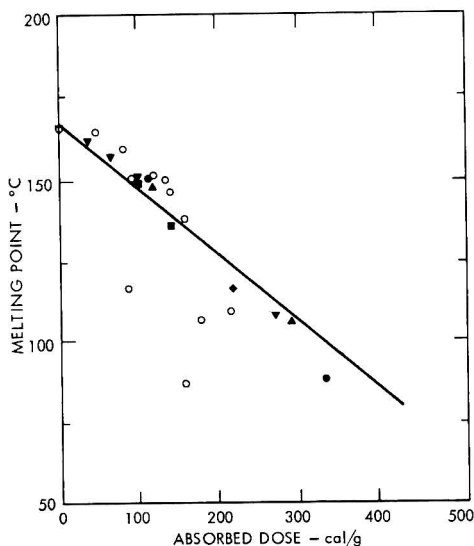


Fig. 8. Effect of changing from Taylor spectrum;⁵ extrapolated melting point vs. absorbed dose: (O) Erlich spectrum; (●) modified 10% Taylor spectrum; (—) Taylor spectrum.⁵

It is desirable to have some measure of how much a given degree of deviation from the proposed spectrum would affect the correlations. To provide a reference for this question, the coordinates of the Taylor spectrum were reduced by 10% below 10 keV and raised 10% above 10 keV. The resulting correlation of this modified spectrum with the melting points of the naturally cooled samples is shown in Figure 8. Although the points all fit reasonably on a curve, the plot is no longer a straight line.

The fact that Penton powder is of relatively uniform molecular weight from lot to lot¹⁸ definitely increases its value as a dosimeter. To test the above statement, the intrinsic viscosity of the powder (donated by Dr. F. H. McTigue of Hercules Research) was measured. This was found to be 1.124 in contrast to the intrinsic viscosity of 1.188 of the machined Penton sheets supplied by Battelle. The values of $(1/\eta)^{1/\alpha}$ of these samples are 0.8684 and 0.8333, respectively. This corresponds to a difference in absorbed dose of 0.25 cal/g. This dosage would be lost in the experimental error of the heat of fusion and melting point measurements.

CONCLUSIONS

The potential use of a stack of Penton disks as a dosimeter for 4–15 keV x-rays appears promising. Theoretical molecular weight dependence upon absorbed dose was observed. Equations for absorbed dose, based on melting points and heats of fusion, have been experimentally derived. The relationship between absorbed dose and optical density also appears promising. It is believed that the above relationships will provide calibrations which could be used for determining the spectra of other x-ray sources.

The author would especially like to acknowledge the assistance and encouragement given by Grover Taylor who not only ran the XRD-6, but also provided the flux and the spectrum.⁵ In addition, the loan of the zinc and titanium–aluminum filters by Dr. Nancy L. del Grande, plus several beneficial conversations, is deeply appreciated. The author also wishes to thank Harry Conrad for preparing the samples for the optical measurements, Dr. Roman Bystroff for the use of his Carey spectrometer, and Dr. Lyman E. Lorensen for many helpful discussions. Appreciation is also expressed for generous donation of information and material by Dr. Frank McTigue of Hercules Research.

This work was performed under the auspices of the U.S. Atomic Energy Commission.

References

1. J. H. Golden and E. A. Hazell, *J. Polym. Sci. A*, **2**, 4017 (1964).
2. M. Erlich, *J. Res. Nat. Bur. Std.*, **54**, 107 (1955).
3. H. Kulenkampff and L. Schmidt, *Ann. Physik*, **43**, 494 (1943).
4. B. J. Mallon, *J. Polym. Sci. B*, **5**, 977 (1967).
5. G. Taylor, Lawrence Radiation Laboratory, Livermore, Calif., private communication.
6. K. Iimura and S. Kondo, *J. Appl. Polymer Sci.*, **6**, S52 (1962).
7. D. Ruchonnet and P. Robinson, Lawrence Radiation Laboratory, Livermore, Calif., private communication.
8. A. Charlesby and W. H. T. Davison, *Chem. Ind. (London)*, **1957**, 232 (1957).
9. A. Charlesby, M. Ross, and P. Alexander, *Proc. Roy. Soc. (London)*, **A223**, 392 (1954).
10. R. M. Black, *Nature*, **178**, 305 (1956).
11. A. B. Taubman and L. P. Ianova, *Proc. Acad. Sci. USSR, Chem. Sect. (Engl. Transl.)*, **114**, 103 (1958).
12. D. T. Turner, *J. Polym. Sci. B*, **1**, 101 (1963).
13. P. Alexander, R. M. Black, and A. Charlesby, *Proc. Roy. Soc. (London)*, **A232**, 31 (1955).

14. A. Chapiro, *Radiation Chemistry of Polymeric Systems*, Interscience Publishers, New York, 1962, p. 379.
15. R. Chiang, Internal Report, Hercules Research Center, Wilmington, Delaware, 1953.
16. P. J. Flory, *Principles of Polymer Chemistry*, Cornell Univ. Press, New York, 1953, p. 313.
17. A. Charlesby, *Proc. Roy. Soc. (London)*, **A222**, 60 (1954).
18. F. H. McTigue, Hercules Research Center, Wilmington, Delaware, private communication.
19. M. Boss and A. Charlesby, *Atomics*, **4**, 189 (1953).

Received November 29, 1967

Revised January 23, 1968

Syndiotactic and Isotactic Poly(*tert*-butylethylene Oxide)

CHARLES C. PRICE and H. FUKUTANI, *Department of Chemistry,
University of Pennsylvania, Philadelphia, Pennsylvania 19104*

Synopsis

The rate of polymerization of *t*-BuEO by *t*-BuOK in DMSO is about one-tenth that of propylene oxide. The slow rate of propagation was accompanied by considerable chain transfer. In the absence of solvent, the polymer obtained was crystalline, different from the isotactic form and therefore must be syndiotactic. The NMR spectra indicate the isotactic polymer exists in solution preferentially in the skew₁ form, while syndiotactic is about 60% skew₁, 40% skew₂. Amorphous polymer accompanying isotactic exists about 50% in the *trans* conformer, by NMR data.

There have been very few reports of the polymerization of *tert*-butylethylene oxide (*t*-BuEO).¹⁻⁴ Because of the extra bulk of its alkyl group, and the absence of reactive α -hydrogens leading to chain transfer,³ because of the earlier observations of very low molecular weight and also solid apparently crystalline polymer by base catalysis,³ and the report of isotactic polymer by coordination catalysts,⁴ we felt a more careful study of the polymerization of *tert*-butylethylene oxide was of interest.

RESULTS AND DISCUSSION

Relative Rates of Polymerization

Earlier reports have indicated that *t*-BuEO polymerizes more slowly than EO or propylene oxide (PO).¹⁻³ We have found that the kinetics of base-catalyzed polymerization in DMSO (dimethyl sulfoxide) were easily followed by NMR. Both monomer and polymer have sharp singlets at 9.1 τ , but the monomer multiplet centered at 7.45 τ (7.25-7.8 τ) shifts to a complex set of broad peaks between 5.5 and 7.25 τ for the polymer. Conversion was thus readily estimated from the integrated areas in these two regions of the NMR spectra. The data are summarized in Table I.

The rate constant at 26°C indicates a rate of about one-tenth that reported for PO in DMSO.* The activation energy, estimated from an Arrhenius plot of the values for k_2 in Table I, was 24 kcal/mole. This

* In other solvents, the rate constant for KOH-catalyzed polymerization of PO is reported⁶ to be 1.2×10^{-4} and for ethylene oxide $\sim 5 \times 10^{-3}$. Snyder⁶ reports $k_2 = 1.8 \times 10^{-6}$ and $\Delta H^\ddagger = 17.6$ for neopentylethylene oxide polymerization by *t*-BuOK.

TABLE I
Rate of Polymerization of *t*-BuEO (0.1 g) in DMSO (0.3 g)
Catalyzed by $4.7 \times 10^{-2}M$ *t*-BuOK^a

| Temperature, °C | Time, min. | Conversion, % | k_1' , sec ⁻¹ ^b | k_2 , l/mole-sec |
|-----------------|------------|---------------|---|-----------------------|
| 100 | 5 | 50 | 2.0×10^{-3} | 4.3×10^{-2} |
| | 12 | 74 | | |
| 75 | 10 | 26 | 3.2×10^{-4} | 6.8×10^{-3} |
| | 37 | 50 | | |
| | 60 | 63 | | |
| 60 | 60 | 21 | 5.8×10^{-5} | 1.23×10^{-3} |
| | 120 | 34 | | |
| 26 | 6 days | 31 | 5.8×10^{-7} | 1.23×10^{-5} |
| | 14 days | 46 | | |

^a Potassium *tert*-butoxide.

^b $k_1' [t\text{-BuEO}] = k_2 [t\text{-BuOK}] [t\text{-BuEO}]$; rate constants were estimated graphically.

value, which is considerably larger than those for EO (17.4) and PO (17.8),^{7,8} undoubtedly is due to increased steric hindrance from the bulky *tert*-butyl group.

Molecular Weight and Chain Transfer

Since the molecular weight of poly(propylene oxide) (PPO) is limited by a chain-transfer reaction involving the methyl hydrogens α to the oxirane ring,³ it was not expected that chain transfer would be a major factor in polymerization of *t*-BuEO, since it has no such hydrogens. However, the polymer formed in base-catalyzed polymerization has had low molecular weight.³ The results of experiments changing monomer-catalyst and monomer-DMSO ratios are summarized in Tables II and III, respectively.

At a catalyst-monomer ratio of 200 to 1, the expected molecular weight without chain transfer would be 20 000, compared with only 1040 observed. That chain transfer could involve DMSO in this case is shown by the data in Table III.

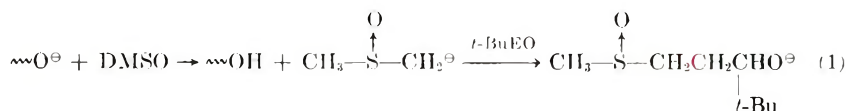


TABLE II
Effect of Changing Monomer-Catalyst Ratio on Molecular Weight of Poly(*t*-BuEO)^a

| <i>t</i> -BuEO, mmole | <i>t</i> -BuOK, mmole | \bar{M}_n ^b |
|-----------------------|-----------------------|--------------------------|
| 20 | 2.0 | 630 |
| 20 | 0.4 | 1030 |
| 20 | 0.2 | 1020 |
| 20 | 0.1 | 1040 |

^a Temperature 60°C, 1 week, 6.0 ml of DMSO; all conversions were essentially quantitative.

^b Number-average molecular weight measured by vapor osmometer.

TABLE III
Effect of Changing Monomer-DMSO Ratio on Molecular Weight of Poly(*t*-BuEO)^a

| <i>t</i> -BuOK, mmole | DMSO, ml | DMSO / <i>t</i> -BuEO | \bar{M}_n^b | S, % |
|-----------------------|----------|--------------------------|---------------|-------------------|
| 0.2 | 3 | 2.1 | 1270 | 0.70 |
| 0.2 | 6 | 4.3 | 1020 | 0.84 ^c |
| 0.2 | 12 | 8.5 | 910 | 1.03 |
| 2.0 | 0.5 | 0.35 | 1310 | — |
| 2.0 | 6 | 4.3 | 630 | 0.85 |

^a Temperature 60°C, 1 week, 20 mmole of *t*-BuEO; all conversions were over 90%.

^b Number-average molecular weight measured by vapor osmometer.

^c The small peak at 7.55 τ indicated about 1% sulfur as sulfoxide in the polymer.

The presence of a sulfoxide endgroup was confirmed both by sulfur analyses and by a small NMR peak at 7.55 τ for poly(*t*-BuEO) prepared in DMSO.

Extrapolation of the data in Table III to zero DMSO concentration indicated a molecular weight of only about 2000, in excellent agreement with observed values without solvent (Table IV) but still much lower than expected.

TABLE IV
Polymerization of *t*-BuEO in Bulk and in Diglyme^a

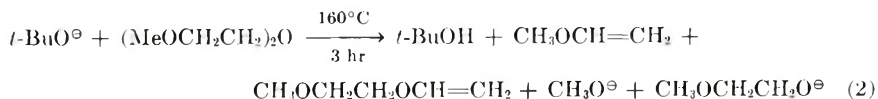
| <i>t</i> -BuEO/ <i>t</i> -BuOK | (MeOCH ₂ CH ₂) ₂ O, ml | Temper- ature, °C | Time, days | Yield, % | \bar{M}_n |
|-----------------------------------|---|----------------------|------------|----------|---------------------|
| 50 | 6 | 75 | 14 | 98 | 690 |
| 50 | 6 | 100 | 14 | ~100 | 750 |
| 50 | 0 | 75 | 10 | 81 | 1900 ^b |
| 110 | 0 | 90 | 21 | ~100 | 2200 ^{b,c} |

^a (CH₃OCH₂CH₂)₂O.

^b These polymers were solids, mp ~50°C; polymers of lower molecular weight were oils.

^c Calculated from $[\eta] = 0.038$, others by vapor osmometer.

The low molecular weights observed in diglyme, (CH₃OCH₂CH₂)₂O, suggest there is some kind of transfer possible with this solvent also. Perhaps it may be related to the base cleavage of diglyme reported by Snyder.⁹



Even in bulk, the molecular weight of 1900 observed is appreciably below the value of 5000 expected, if no chain transfer were possible. Perhaps the molecular weight limiting reaction is one involving a similar attack on the polymer chains, but we have no evidence to offer at this time on this possibility.

TABLE V
Physical Properties of Poly(*t*-BuEO) Prepared by *t*-BuOK Catalysis

| \bar{M}_n^a | $[\eta]$ | mp, °C |
|---------------|----------|--------------------------|
| 630 | 0.0185 | < room temp |
| 690 | — | < room temp |
| 750 | — | < room temp |
| 1040 | 0.0245 | ~30 |
| 1120 | — | < room temp ^b |
| 1270 | 0.0255 | ~30 |
| 1270 | — | 42 |
| — | 0.03 | 44 ^b |
| 1900 | 0.035 | 51 |
| (~2000) | 0.038 | 53 |

^a By vapor osmometer, except last value was calculated from $[\eta] = 3.2 \times 10^{-6} \bar{M}_n^{0.97}$, the best line defined by \bar{M}_n data in Tables V and VI. This equation compares with $[\eta] = 6.4 \times 10^{-5} \bar{M}_v^{0.82}$ for PEO in water at 35°C¹⁰ and $[\eta] = 1.25 \times 10^{-4} \bar{M}_v^{0.77}$ for PPO in benzene at 25°C.¹¹

^b Data of Carmelite.³

The fact that the higher molecular weight samples of poly(*t*-BuEO) prepared in bulk were solid and crystalline (see Table V), suggested some stereoregular polymerization was occurring. For comparison, we prepared samples of isotactic poly(*t*-BuEO) by two different coordination catalysts (Table VI). The benzene-insoluble material was also crystalline but of much higher molecular weight and melting point than that from base. The x-ray patterns were also distinctly different (see Fig. 1).

The comparison of these two crystalline polymers is summarized in Table VII. Certainly some differences might be expected from the large difference in molecular weight. Even the melting point difference, however, was too great to be explained by molecular weight differences and the x-ray and NMR data are conclusive evidence that I and II are indeed of different crystalline form. Since there is no reason to doubt that the coordination catalysts would give isotactic polymer (I),² this suggests that II must be the syndiotactic form.

TABLE VI
Polymerization of *t*-BuEO by Coordination Catalysts^a

| Catalyst | Coordination catalyst | Yield, % | | $[\eta]$ | |
|-----------------------------|--------------------------|-------------------|-----------------|--------------------------------|------------------------------|
| | | Benzene-insoluble | Benzene-soluble | Benzene-insoluble ^b | Benzene-soluble ^c |
| Et ₂ Zn | H ₂ O, 0.11 g | 8.0 | 30.9 | 3.82 | 0.083 ^d |
| Et ₂ Zn | Amyl alcohol, 1.35 ml | 3.8 | — | 0.42 | — |
| Et ₂ Zn | <i>d</i> -Borneol, 2 g | 4.2 | — | — | — |
| <i>i</i> Bu ₃ Al | H ₂ O, 0.11 g | 13.4 | 55.0 | 2.53 | 0.099 |

^a *t*-BuEO, 4 g; C₆H₆, 5 ml; catalyst, 6.5 mmole; 60°C for 1 day.

^b 90°C in tetralin.

^c 30°C in benzene.

^d \bar{M}_n (osmometric) = 2780.

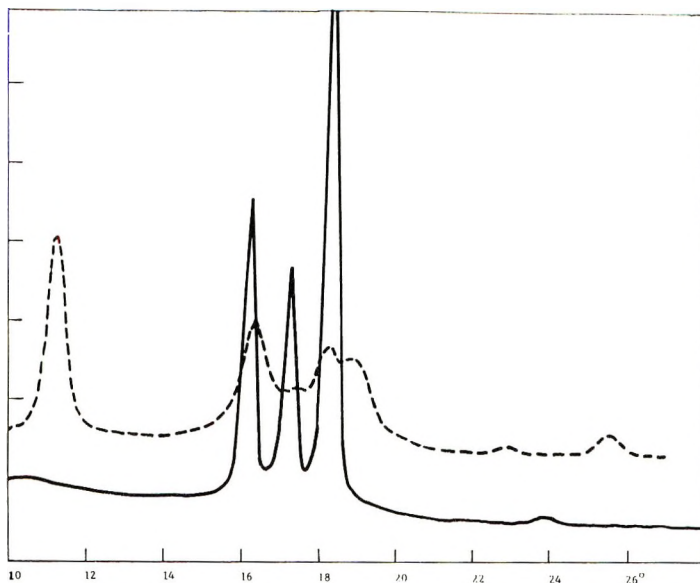


Fig. 1. X-ray powder scattering for (---) isotactic and (—) syndiotactic poly(*t*-BuEO).

The formation of a crystalline syndiotactic polyepoxide by base catalysis is unique, although there are several reports of crystalline isotactic poly(phenyl glycidyl ether) (PPGE) by base catalysis.¹²⁻¹⁵ In this case, it seems reasonable to assume that the *tert*-butyl group will provide considerable steric hindrance to polymerization. This view is supported by the high activation energy reported above as well as the NMR data (Fig. 2) which clearly indicate the presence of one (I) or two (II) preferred conformations at the carbon-carbon bonds in the polymer chain.

For both I and II the backbone hydrogen atoms separated into three regions of absorption, 5.8-6.3 τ , 6.3-6.85 τ , and 6.85-7.15 τ in the ratio of

TABLE VII
Comparison of Crystalline Polymers from *t*-BuEO

| | Crystal I | Crystal II |
|---------------------------|---|--|
| Catalyst | Coordination | <i>t</i> -BuOK |
| \bar{M}_n | 20 000-170 000 | 1200-2000 |
| $[\eta]$ | 0.42-3.8 | 0.025-0.038 |
| Melting point, °C | 130-150 | 42-53 |
| X-ray <i>d</i> spacing, Å | 7.81, 5.39, 4.86, 4.64, 3.89, 3.49 | 5.43, 5.10, 4.76, 3.65 |
| NMR, τ | 6.0, 6.6, 7.0 | 6.0, 6.65, 7.0, 6.25, 6.5, 7.0 |
| Solubility | | |
| Soluble in | Tetralin at 90°C | C ₆ H ₆ , CHCl ₃ , CCl ₄ , C ₆ H ₁₂ , CH ₃ COCH ₃ |
| Swollen by | C ₆ H ₆ , CHCl ₃ , CCl ₄ , C ₆ H ₁₂ | CH ₃ OH |
| Insoluble in | CH ₃ OH, CH ₃ COCH ₃ , Et ₂ O, H ₂ O, DMSO, DMF | H ₂ O, DMSO |

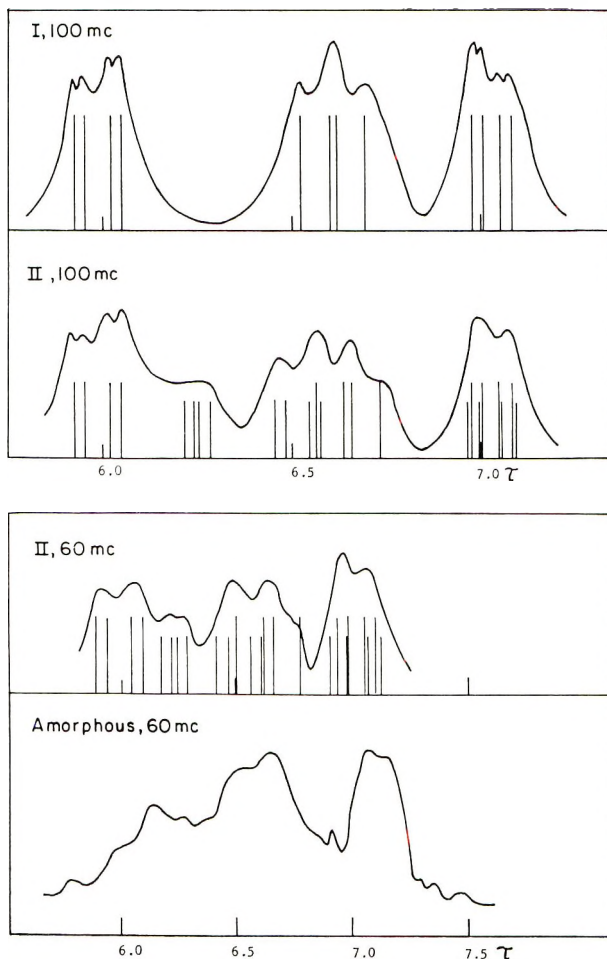
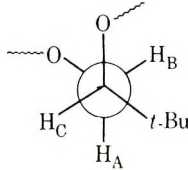
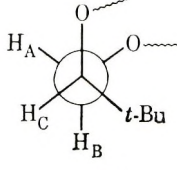
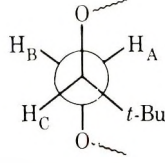


Fig. 2. NMR spectra of poly(*t*-BuEO): (*I*) isotactic; (*II*) syndiotactic and curve for amorphous polymer from triisobutylaluminum–water catalysis. The vertical lines represent absorption predicted by the chemical shifts and splitting constants in Table VIII. The experimental curves represent data in CCl_4 at 50°C . In chlorobenzene at 120°C the curves for syndiotactic and amorphous polymer were essentially unchanged, while the curve for isotactic in polymer the peaks were much sharper.

1:1:1. The three backbone hydrogens in the polymer consist of two secondary (H_A and H_B) and one tertiary hydrogen (H_C). The latter should be shifted further downfield than the former, as is indicated in Table VIII. One secondary hydrogen in both skew 1 and skew 2 is remote from oxygen and shifts upfield to 7.0τ , while in the *trans* conformer both secondary hydrogens are adjacent to the β -oxygen. In skew 2, the tertiary hydrogen is similarly remote from oxygen and shifted upfield. For the isotactic polymer, the NMR spectra at 60 or 100 Mcps can be readily explained by a single skew conformation (skew 1), as indicated in Figure 2 and Table VIII.

TABLE VIII
Conformations, τ Values, and Coupling Constants J for Poly(*t*-BuEO)^a

| Conformation | τ | J , cps |
|---|--------------|---|
|  | skew 1 | H_A 7.0 H_B 6.6 (6.65) ^b H_C 6.0 J_{AB} 7.5 J_{AC} 3 J_{BC} 9.5 |
|  | skew 2 | H_A 6.5 H_B 7.0 H_C 6.2-6.3 J_{AB} 9 J_{AC} 3 J_{BC} 4 |
|  | <i>trans</i> | H_A 6.6 H_B 6.5 H_C 6.0 J_{AB} 7.5-9 J_{AC} 9.5 J_{BC} 3 |

^a The values are those estimated to give the best fit to the experimental NMR curves.

^b The figure in parenthesis is for syndiotactic isomer, the other for isotactic.

For the syndiotactic polymer, the NMR spectra at 60 and 100 Mcps require, in addition to skew 1, the presence of skew 2 in an approximate 60:40 ratio (see Fig. 2 and Table VIII).

For the amorphous polymer from isobutylaluminum-water catalysis, the NMR spectrum was less resolved, and the ratio of absorbance in the three regions was in the approximate ratio 1:1:0.7. These relative intensities indicate that, in the amorphous polymer, about half the backbone carbon bonds are in the *trans* conformation, with chemical shifts and splitting constants about as indicated in Table VIII. Such a distribution of conformers would predict the ratio of 1:1.5:0.5.

The NMR spectra of the samples made in DMSO (Table III) most closely resembled the spectrum of II, suggesting that the low molecular weight oils formed under these circumstances contained mainly syndiotactic sequences.

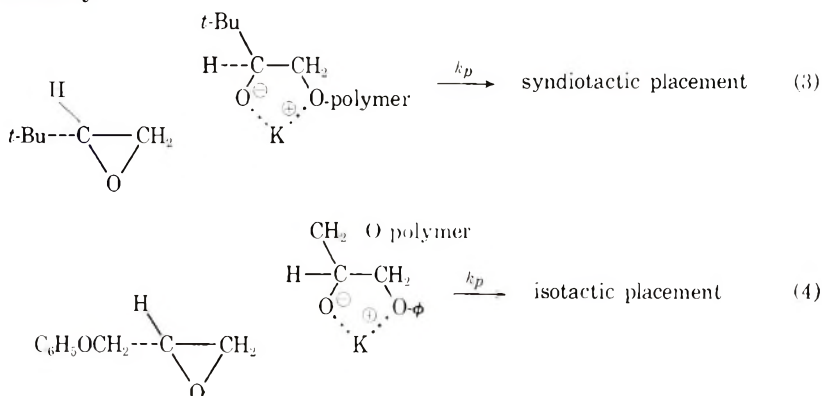
In contrast to a statement from an earlier publication,² indicating that models of syndiotactic poly(*t*-BuEO) could not be made without straining bond angles or distances, we found the skew 1 and skew 2 conformations were essentially strainless. For the isotactic models, skew 1 and *trans* were easily assembled with no major strain.

In view of earlier reports on the formation of isotactic poly(phenyl glycidyl ether) by bases,^{13,15} we have prepared PPGE by reaction in bulk catalyzed by *t*-BuOK. The polymer was of relatively low molecular weight ($[\eta] = 0.1$) but 16% was insoluble in acetone, mp 90°C, and showed an

x-ray pattern identical with that of isotactic polymer prepared by coordination catalysts.^{12,14}

Tsuruta¹⁶ has shown that steric control of isotactic polymer formed by coordination catalysts is the result of "catalyst site" control, rather than "polymer end" control.

For the case of PGE and *t*-BuEO we wish to suggest a mechanism involving polymer end control and chelation of the countercations by adjacent ether groups.* In the case of the polymer of *t*-BuEO, the only ether group eligible for chelation is that of the adjacent backbone unit. For the case of PPGE, the oxygen of the phenoxyl is available for this purpose. The proposed geometry of the transition states is indicated by eqs. (3) and (4), respectively.



There are three important steric conditions indicating the preferred nature of the geometry proposed.

(1) The S_N2 inversion occurring at each step in epoxide ring-opening¹⁸ requires that the epoxide oxygen, the oxirane methylene carbon and the chain-end oxyanion be essentially linear.

(2) The importance of the newly formed oxyanion associating as easily as possible with the counter cation requires that the substituted oxirane carbon be oriented away from the chain-end cation. This will favor the bending of the newly formed oxyanion on the oxirane oxygen so that it may chelate with the cation.

(3) The bulky groups, i.e., *tert*-butyl, $C_6H_5OCH_2^-$, and polymer, on the chelate and oxirane rings should be on opposite sides of the common plane containing the chelate and oxirane rings.

This scheme requires that once the propagation has occurred for PGE, the chelate ring prefers to rearrange from backbone ether to side-chain phenyl ether oxygen.

We have further work under way to determine the structure of amorphous polymer from coordination catalysis and to test the hypothesis advanced above for polymer end control in base-catalyzed systems.

* The ability of cyclic ethers to coordinate with alkali metal ions has been recently reported by Pedersen.¹⁷

EXPERIMENTAL

Materials

tert-Butylethylene oxide (*t*-BuEO) was prepared from pinacolone by bromination¹⁹ to yield the bromoketone in 80% yield, bp 58.5–61°C/3.5 mm. Reduction with sodium borohydride²⁰ gave the bromoalcohol in 60% yield, bp 55–58°C/8 mm, which was cyclized with KOH²⁰ to *tert*-butylethylene oxide in 75% yield, bp 96–97.5°C. The NMR spectrum showed a singlet at 9.1 τ and a multiplet centered at 7.45 τ in the proper 3:1 ratio. The purity was > 99% by vapor phase chromatography.

Phenyl glycidyl ether (PGE) was dried and distilled, bp 99°C/4 mm. DMSO was refluxed over calcium hydride and distilled, bp 88.5–89°C/25 mm. Benzene, heptane, and diglyme were also dried and distilled before use.

Polymerizations

In NMR Tubes. For the small-scale runs, 0.1 g of *t*-BuEO, 0.3 g of ²H₆-DMSO and 2×10^{-5} mole of *t*-BuOK (Aceto Chemical Co.) were heated under nitrogen. At specified times, CCl₄ was added to stop the reactions; this gave homogeneous solutions for NMR measurement.

Larger-Scale Experiments. Solvent, monomer, and catalyst were introduced into 20 ml Pyrex tubes, flushed with nitrogen and capped with rubber serum stoppers; these were cooled in an ice bath and sealed with an oxygen flame. After heating for a specified time, the tubes were cooled in Dry Ice, opened, neutralized with Dry Ice and extracted with cyclohexane. The solution was washed, dried, and evaporated to give polymer.

By Coordination Catalysts. The procedure was similar to that above. The polymer, swollen in benzene, was precipitated and washed with methanol and HCl in methanol. The polymer was separated into fractions soluble and insoluble in benzene at room temperature.

Polymerization of Phenyl Glycidyl Ether. The same procedure as described for larger-scale experiments on *t*-BuEO was used. The PPGI₂ was precipitated by methanol and separated into fractions soluble and insoluble in acetone at room temperature by centrifugation.

Characterization

Number-average molecular weights were measured at 30°C in benzene solution by a Mechrolab vapor pressure osmometer, Model 301A.

Viscosity measurements were run in an Ubbelohde viscometer in benzene solution at 30°C, except for high melting poly(*t*-BuEO) (I) which was run in tetralin at 90°C.

Melting points of polymers were determined by the capillary method. NMR spectra were determined on Varian instruments, Models HA-60 or A-60-A. We are indebted to Dr. Kermit C. Ramey, Atlantic-Richfield Refining Co., for the 100 Mcps NMR spectra. The x-ray powder spectra were obtained with nickel-filtered CuK α radiation by Mr. Henry Katz.

References

1. J. M. Bruce and S. J. Hurst, *Polymer*, **7**, 1 (1966).
2. G. Allen, C. Booth, and S. J. Hurst, *Polymer*, **8**, 385 (1967).
3. C. C. Price and D. Carmelite, *J. Amer. Chem. Soc.*, **88**, 4039 (1966).
4. E. J. Vandenberg, U. S. Pat. 3,285,861 (November 15, 1966).
5. E. C. Steiner, R. R. Pelletier, and R. O. Trucks, *J. Amer. Chem. Soc.*, **86**, 4678 (1964).
6. W. H. Snyder, private communication.
7. G. Gee, W. C. E. Higginson and G. T. Merrail, *J. Chem. Soc.*, **1959**, 1345.
8. G. Gee, W. C. E. Higginson, K. J. Taylor, and M. W. Trenholme, *J. Chem. Soc.*, **1961**, 4298.
9. W. H. Snyder, J. Parascandola, and M. Wolfinger, *J. Org. Chem.*, **31**, 2037 (1966).
10. F. E. Bailey and R. W. Callard, *J. Appl. Polym. Sci.*, **1**, 56 (1959).
11. G. Allen, C. Booth, and M. N. Jones, *Polymer*, **5**, 195 (1964).
12. A. Noshay and C. C. Price, *J. Polym. Sci.*, **34**, 165 (1959).
13. C. C. Price and R. Yamamoto, unpublished data.
14. A. Takahashi and S. Kambara, *Makromol. Chem.*, **72**, 92 (1964).
15. Y. Tanaka and H. Kakuichi, *J. Polym. Sci. A-1*, **4**, 109 (1966).
16. T. Tsuruta, S. Inoue, M. Yokota, and N. Yoshida, *Kogyo Kagaku Zasshi*, **68**, 896 (1965); *Makromol. Chem.*, **90**, 131 (1966); *Internatl. Sci. Technol.*, **71**, 66 (Nov. 1967).
17. C. L. Pedersen, *J. Amer. Chem. Soc.*, **87**, 7017 (1967).
18. C. C. Price and R. Spector, *J. Amer. Chem. Soc.*, **87**, 2069 (1965).
19. M. Jackman, M. Klenk, J. Fishburn, B. F. Tuller, and S. Archer, *J. Amer. Chem. Soc.*, **70**, 2884 (1948).
20. S. J. Hurst and J. M. Bruce, *J. Chem. Soc.*, **1963**, 1321.

This work was supported in part by the General Tire and Rubber Co. and in part by Mitsubishi Chemical Industries.

Received January 25, 1968

Revised March 6, 1968

Calorimetric Investigation of Polymerization Reactions. I. Diffusion-Controlled Polymerization of Methyl Methacrylate and Styrene

KAZUYUKI HORIE, ITARU MITA, and HIROTARO KAMBE,
*Institute of Space and Aeronautical Science, University of Tokyo, Komaba,
Tokyo, Japan*

Synopsis

The rate of bulk polymerization of methyl methacrylate and styrene was determined directly, continuously and over the whole range of conversion with a differential scanning calorimeter (DSC) operated isothermally. At the later stages of the accelerated polymerization of methyl methacrylate, a previously unknown inflection or peak in the rate of polymerization was observed. The variation of the rate after the onset of the gel effect, including this peculiar inflection, was interpreted on the basis of the diffusion behavior of monomer molecules and polymeric radicals in the polymer-monomer system, their diffusion rates being predicted from the free volume theory. The final conversion at which no further polymerization proceeds was determined for both monomers. It was affirmed quantitatively that the final conversion has a close relation with the transition of the polymer-monomer system from a viscous liquid to a glassy state.

INTRODUCTION

The gel effect in free-radical polymerization has been studied by many investigators since Schulz¹ and Trommsdorff.² A sudden increase in the rate of polymerization observed in the later stages of polymerization was shown to be due to the diffusion control of the termination process.

For the bulk polymerization of methyl methacrylate, which shows a marked gel effect, Hayden and Melville³ have evaluated apparent rate constants for the termination and propagation reactions up to 80% conversion by a thermocouple method. North and Reed⁴ have suggested that the rate-controlling process in termination is not a translational diffusion of macroradicals but a segmental diffusion of the radical chain end in the coiled polymeric free radical. Burnett and Duncan⁵ have explained the autoacceleration effect of the polymerization rate as a radical accumulation phenomenon. For the polymerization of styrene, a little acceleration in the rate has been observed by several investigators.⁶⁻⁸ In recent years several efforts have been devoted to the application of the theory of Kuhn and Kuhn on the diffusion of polymeric chain ends⁹ to the termination mechanism of diffusion-controlled polymerization.^{10,11} However, there has been no quantitative discussion as to the diffusion-controlled propagation step at very high conversion.

Rabinowitch¹² derived the rate constant of a second-order reaction in the viscous system as a function of diffusion coefficients of the two reactants. The diffusion coefficient of polymeric segments in the system consisting of polymer-diluent mixture was successfully formulated by Kelley and Bueche¹³ on the basis of the free volume theory with the assumption of additivity of the free volume of each constituent. As to the diffusion behavior of penetrant molecules in the polymer, several efforts have been devoted to relate the diffusion coefficient of the penetrant with its volume fraction in the mixture.^{14,15} In order to apply these results to a quantitative discussion on the mechanism of the whole process of diffusion-controlled polymerization, it was necessary to eliminate the experimental difficulties in determining the rate of polymerization and other parameters over the whole range of the conversion.

For the measurement of the rate of diffusion-controlled polymerization, several methods have been proposed. A disk-shaped dilatometer or other modified dilatometers^{5,6,16} is convenient for following the rate of polymerization in a liquid phase. A thermocouple method³ is applicable for the measurement of the rate of exothermic polymerization even in a soft solid phase. The former method, however, gives a change in polymerization rate with conversion indirectly through the differentiation of the time-conversion curve, and therefore it is impossible to detect delicate variations of the rate of polymerization. In fact, Anderson,¹⁷ using an isothermal kinetic calorimeter method, has revealed several previously overlooked changes in the rate of polymerization in emulsion polymerization. By the thermocouple method it is impossible to get a continuous relationship between the rate of polymerization and time, since the method consists of the measurement of a small temperature rise at a certain instant. Differential scanning calorimeter (DSC),¹⁸ differing from the above methods, may be used to determine the rate of polymerization directly, continuously and even in a gel or solid state. It has been already reported that DSC is useful for investigating the curing reaction of diallyl phthalate resin.¹⁹

The present paper is concerned with the kinetics of the diffusion-controlled bulk polymerization of methyl methacrylate and styrene throughout the whole conversion. It was found that the DSC is very effective for such a study. By isothermal operation a previously unknown feature in the rate of polymerization of methyl methacrylate was observed, and it was interpreted in relation to the diffusion behavior of monomer molecules and polymeric radicals in the polymer-monomer system. Values of the final conversion at which no further polymerization occurs were determined and discussed in connection with the glass transition temperature of the system.

EXPERIMENTAL

Materials

Methyl methacrylate was freed of inhibitor, dried, and purified by rectification under nitrogen at a reduced pressure. The middle fraction was

collected and stored in an icebox. Styrene was purified and stored in the same way. Benzoyl peroxide (BPO) and 2,2'-azobisisobutyronitrile (AIBN) were of guaranteed reagent quality.

Procedure

Polymerization of methyl methacrylate or styrene was carried out in a modified sample pan of a Perkin-Elmer differential scanning calorimeter (DSC-1) operated isothermally.

The modified sample pan was made of two standard aluminum pans, bonded face-to-face by a heat-resistant adhesive, Araldite AV-8. The sample was injected into the closed pan with a syringe, then the hole produced by the syringe was closed with a cellophane tape. The weight loss of the sample due to vaporization of liquid monomer was held to several per cent by the use of the modified sample pan, while with the standard open pan it amounted to 20-30%.

It was found that the baseline of the DSC charts obtained in the isothermal operation did not show a substantial drift in spite of a small change in the specific heat of the sample due to its transformation from liquid monomer to solid polymer. By addition of a trace of benzoquinone to the sample it was possible to obtain a baseline during the induction period, namely, before the onset of polymerization. This is shown in Figure 1. This

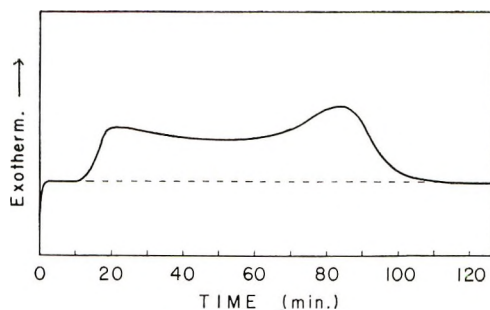


Fig. 1. DSC thermogram of bulk polymerization of styrene at 100°C with 0.10 mole/l BPO and 8.4×10^{-3} mole/l benzoquinone.

initial baseline coincided perfectly with that after the polymerization had finished. Therefore in subsequent experiments, the baseline was established by the extrapolation of the asymptotic flat line at the final stage of polymerization. The deflection of the curve from the baseline corresponds to the rate of polymerization. For the calibration of exothermic energy the transition at 125°C. of ammonium nitrate (1.01 kcal/mole)²⁰ was used as a standard.

Determination of Residual Monomer Content

The content of a residual monomer was determined both calorimetrically (by DSC) and spectrometrically.

After an isothermal polymerization, the sample was heated from ambient to 200°C at a constant heating rate. An exothermic peak due to the polymerization of the residual monomer appeared in the case of methyl methacrylate.

The residual monomer content was determined also by ultraviolet spectrometry. A Shimadzu IV-50A type spectrophotometer was used for determining the absorbance at 212 m μ for methyl methacrylate monomer in ethanol-acetone (99:1) mixture and at 282 m μ for styrene monomer in chloroform.

Molecular Weight Measurements

Intrinsic viscosities of poly(methyl methacrylate) in chloroform at 30°C and polystyrene in benzene at 30°C were measured, and the average molecular weights were obtained from the Mark-Houwink equation,

$$[\eta] = K\bar{M}^\alpha$$

where $K \times 10^3$ and α for poly(methyl methacrylate) were 0.62 and 0.80, and for polystyrene 1.78 and 0.71, respectively.⁸

RESULTS AND DISCUSSION

DSC Thermograms

Figure 2 shows DSC charts of methyl methacrylate polymerization. The gel effect in bulk polymerization of methyl methacrylate is clearly observed. As the polymerization proceeds, the rate of polymerization R_p increases up to eightfold the initial rate of polymerization R_{p0} . Subsequently it decreases and finally becomes practically zero. In the course of its decrease, a previously unknown shoulder in the rate curve is noticed in every experiment. This shoulder increases with the decrease in polymerization temperature and in a run at 70°C appears as large as the main peak.

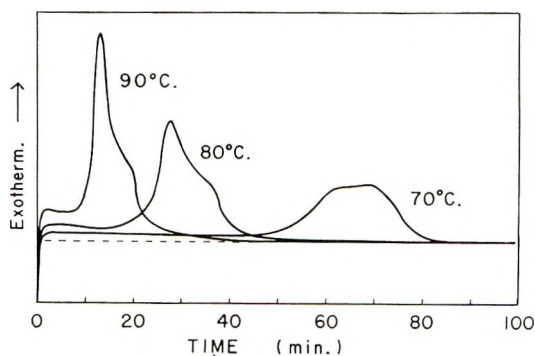


Fig. 2. DSC thermograms of isothermal bulk polymerization of methyl methacrylate. Polymerization temperatures are indicated beside the curves.

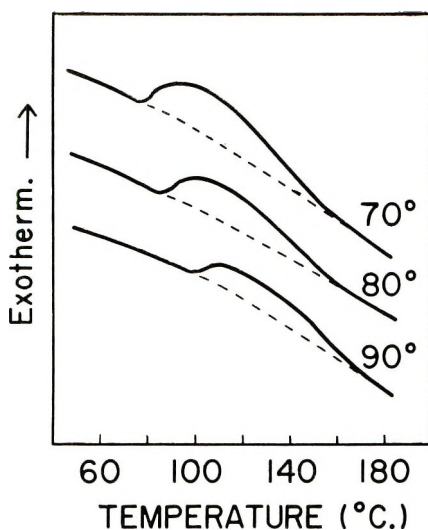


Fig. 3. DSC thermograms at rising temperature scanning of poly(methyl methacrylate) polymerized isothermally at the temperatures indicated beside the curves.

When the isothermal polymerization was completed, a scan at $8^{\circ}\text{C}/\text{min}$ was carried out, the temperature being increased to 180°C . This is illustrated in Figure 3. The exothermic peak due to the polymerization of the residual monomer began just when the temperature of the system exceeded the temperature of isothermal polymerization. No exothermic peak was observed during increased temperature scanning of polystyrene. This suggests that styrene polymerizes completely under isothermal conditions.

The values of reduced initial rate of polymerization ($R_{p0}/[I]_0^{1/2}[M]_0$) and heat of polymerization (ΔH) are given in Table I. The Arrhenius' plots of the reduced initial rate of polymerization against reciprocal temperature are shown in Figure 4 together with the data recalculated from the literature values.²¹⁻²⁵ The values obtained from the DSC data are a little smaller than those from the literature values. It may be due to the higher concentrations of the initiator used and to the influence of oxygen because of the difficulty of getting rid of air in the sample pan. The heat of polymerization calculated from DSC data shows a fairly good coincidence with values in the literature,²⁶ which are 13.0–13.9 kcal/mole for methyl methacrylate and 16.1–16.7 kcal/mole for styrene. It is clear from the above results that the polymerization reaction can be successfully followed by DSC.

Final Conversion

The final conversion (X_f) in an isothermal polymerization was calculated as a fraction of the exothermic energy at the isothermal run to the sum of the energies at the isothermal and rising temperature runs. The calculation is based on the assumption that during the rising temperature scanning the residual monomer polymerizes completely. As shown in Table I, this

TABLE I
Bulk Polymerization of Methyl Methacrylate (MMA) and Styrene (St) Followed by DSC

| Monomer | Polymer- ization temperature, °C | Initiator | Initiator concentration, mole/l | Weight loss, % | $R_p/([I]^{1/2} [M]_0),$ $l^{1/2}/(\text{mole}^{1/2} \text{-sec})$ $\times 10^4$ | $\Delta H,$ kcal/mole | Final conversion | |
|---------|---|-----------|---------------------------------------|-------------------|--|--------------------------|------------------|-------------|
| | | | | | | | By DSC, % | By UV, % |
| MMA | 70 | AIBN | 0.05 | 3.0 | 5.4 ± 0.5 | 12.7 ± 0.4 | 89 | 92 |
| MMA | 80 | AIBN | 0.05 | 3.0 | 9.8 ± 0.6 | 13.3 ± 0.2 | 93 | 94 |
| MMA | 90 | AIBN | 0.05 | 5.9 | 17.9 ± 1.0 | 13.1 ± 0.4 | 95 | 95 |
| St | 90 | BPO | 0.10 | 5.8 | 3.1 ± 0.4 | 15.9 ± 0.4 | 100 | 98 |
| St | 100 | BPO | 0.10 | 6.3 | 7.4 ± 0.6 | 16.1 ± 0.3 | 100 | 98 |

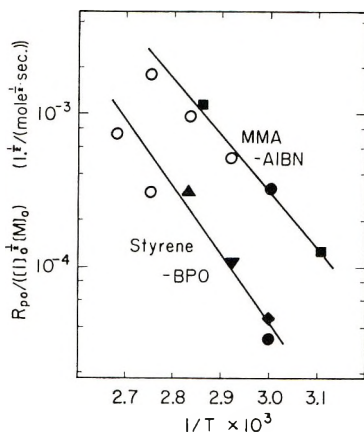


Fig. 4. $\log (R_{p0}/[I]_0^{1/2}[M]_0)$ vs. $1/T$ for the polymerization of methyl methacrylate and styrene: (O) results by DSC; other results recalculated from the data of (●) Baysal et al.,²¹ (■) Arnett,²² (▲) Horikx et al.,²³ (▼) Lowell et al.,²⁴ (◆) Mayo et al.²⁵

assumption is confirmed by the spectroscopic measurements of the residual monomer. The final conversion in the polymerization of methyl methacrylate comes near by to completion for the isothermal polymerization at higher temperatures. This fact must be related to the glass transition phenomenon of the system.

According to Fox and Flory,²⁷ the effect of molecular weight of a polymer (\bar{M}) on its glass transition temperature (T_{gp}) can be represented by eq. (1),

$$T_{gp} = T_{g\infty} - 2\rho N\theta/(\alpha_p \bar{M}) \quad (1)$$

where $T_{g\infty}$ is the glass transition temperature of the polymer with infinite molecular weight, ρ is the density of the polymer, N is Avogadro's number, α_p is the difference between the volume expansion coefficients of the polymer in melt and in a glassy state, and θ is the contribution of a chain end to the free volume. T_{gp} values listed in Table II were obtained by substituting \bar{M} values calculated from the viscosity data and setting $\rho = 1.1$ g/cm³, $\theta = 80 \text{ \AA}^3$, $\alpha_p = 0.48 \times 10^{-3}/^\circ\text{C}$ according to Bueche.²⁸ $T_{g\infty}$ for

TABLE II
Glass Transition of the Polymer-Monomer Systems

| Polymerization temperature, | | $[\eta]$, | \bar{M} | T_{gp} , | $(\phi_p)r_g$, | $(X_t)_{obs}$, |
|-----------------------------|------------------|------------|------------------|------------------|-----------------|-----------------|
| Monomer | $^\circ\text{C}$ | dl/g | $\times 10^{-4}$ | $^\circ\text{C}$ | $\%$ | $\%$ |
| MMA | 70 | 1.82 | 38.3 | 113.4 | 89.6 | 89 |
| MMA | 80 | 1.18 | 22.3 | 113.0 | 92.6 | 93 |
| MMA | 90 | 0.64 | 10.3 | 111.9 | 95.2 | 95 |
| St | 90 | 0.173 | 1.52 | 87 | | |
| St | 100 | 0.158 | 1.37 | 85 | | |

poly(methyl methacrylate) was evaluated as 114°C²⁹ and for polystyrene as 100°C.²⁷ The calculated T_{gp} values for polystyrene were lower than their polymerization temperatures; in other words, in our experimental conditions the polymerization of styrene proceeded at temperatures higher than T_{gp} of the final polystyrene. This is the reason for the complete conversion of styrene in isothermal polymerization. On the other hand, the calculated T_{gp} 's of poly(methyl methacrylate) were all higher than the experimental temperatures; therefore, the polymerization of methyl methacrylate did not reach 100% conversion. In this case, however, there must be a proper composition where the glass temperature of the polymer-monomer mixture is just equal to the polymerization temperature.

The glass transition temperature of a polymer-monomer mixture can be calculated by eq. (2) derived by Kelley and Bueche,¹³ assuming the additivity of the free volumes of each constituent,

$$T_g = \{ \alpha_p \phi_p T_{gp} + \alpha_m (1 - \phi_p) T_{gm} \} / \{ \alpha_p \phi_p + \alpha_m (1 - \phi_p) \} \quad (2)$$

where ϕ is the volume fraction in the system and the subscripts p and m represent polymer and monomer, respectively. On setting T_g in eq. (2) equal to the polymerization temperature and using a value of $T_{gm} = -106^\circ\text{C}$.³⁰ together with $\alpha_m = 1 \times 10^{-3}/^\circ\text{C}$,²⁸ the volume fraction of the polymer at which the system shows a transition from viscous liquid to glass $\{(\phi_p)_{T_g}\}$ was calculated. The calculated values of $(\phi_p)_{T_g}$ agree quite well with the final conversion values obtained from the DSC data, as is shown in Table II.

Thus it is concluded that the diffusion-controlled polymerization of methyl methacrylate ceases at a conversion where any translational diffusion of monomers and segmental diffusion of the polymeric chain ends are suppressed because of the transition of the polymer-monomer system from a viscous liquid to a glassy state.

Rate of Polymerization

The ratio of polymerization rate to its initial value (R_p/R_{p0}) at various conversions X is illustrated in Figure 5. In the polymerization of methyl methacrylate, the gel effect due to the diffusion-controlled termination reaction appears at a 15–20% conversion and reaches a maximum at the onset of the diffusion control of the propagation reaction, i.e., at ca. 40% conversion. The rate curve shows a shoulder at the later stage of conversion. In the polymerization of styrene, the gel effect is also observed clearly, but the shoulder observed in methyl methacrylate is not seen in this case.

In order to discuss the change in polymerization rate with conversion, it is convenient to express R_p/R_{p0} by eq. (3), which holds good both in stationary and in nonstationary state throughout the whole polymerization process,

$$R_p/R_{p0} = k_p [P^\cdot] [M] / (k_{p0} [P^\cdot]_0 [M]_0) \quad (3)$$

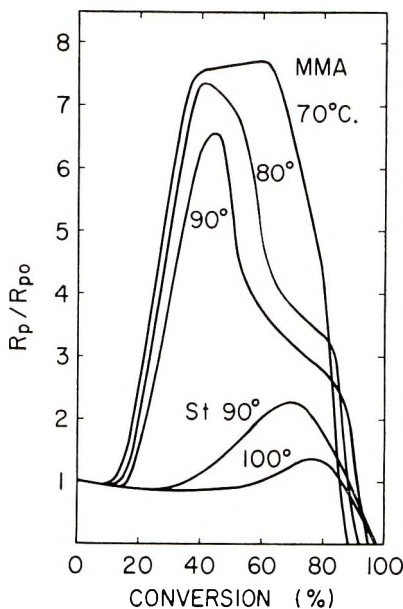


Fig. 5. Dependence of polymerization rate on conversion for the polymerization of methyl methacrylate and styrene. Polymerization temperatures are indicated beside the curves.

where k_p is the propagation rate constant which, however, is not a true constant but affected by diffusion; $[P\cdot]$ and $[M]$ are the concentrations of polymeric radicals and monomer, and the subscript zero indicates the initial state. As $[M]$ is easily calculated from conversion and $[M]_0$ is known, $k_p[P\cdot]/(k_{p0}[P\cdot]_0)$ is calculated from R_p/R_{p0} by reducing the factors concerning the concentration of monomer. In Figure 6, the logarithms of this value are plotted against conversion, the variables are k_p and $[P\cdot]$, since k_{p0} and $[P\cdot]_0$ are constants. Between 20 and 40% conversion $\log(k_p[P\cdot])$ increases by unity; its behavior between 40 and 80% conversion depends on the polymerization temperature, and its value suddenly drops at 80% conversion. A minimum is observed at 55% conversion in a polymerization at 90°C and becomes less distinguishable for the lower polymerization temperatures.

The mechanism of these remarkable changes in polymerization rate with conversion may be explained tentatively by means of the diffusion-controlled changes in $\log k_p$ and $\log [P\cdot]$ with conversion.

Rabinowitch's equation for the rate constant of a second-order reaction in a viscous system is given as follows,¹²

$$k = P \exp \left\{ -E/RT \right\} / [1 + Q \exp \left\{ -E/RT \right\} / (D_a + D_b)] \quad (4)$$

where P and Q are constants, D_a and D_b are the diffusion coefficients of the reactants A and B, and E is the activation energy of the reaction. In the case when $D_a + D_b$ is much greater than $Q \exp \left\{ -E/RT \right\}$, k becomes equal

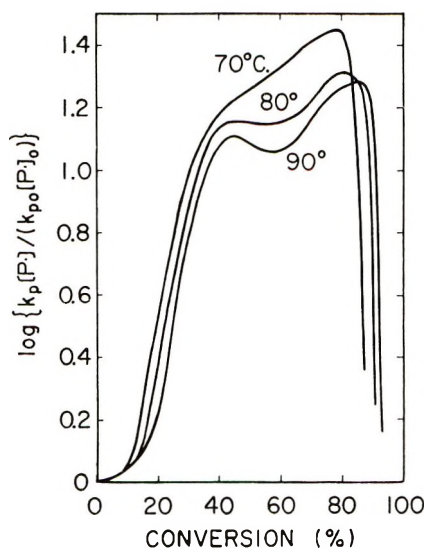


Fig. 6. The observed dependence of $\log k_p[P\cdot]/(k_{p0}[P\cdot]_0)$ on conversion for methyl methacrylate polymerized at various temperatures.

to $P \exp \{-E/RT\}$ the rate of reaction depending only on P and E . However, when $D_a + D_b$ becomes much smaller than the exponential factor, the rate of reaction is proportional to $D_a + D_b$ and the reaction is controlled by diffusion. As far as the propagation rate constant k_p is concerned, the diffusion coefficient of propagating polymeric radicals (D_p) is much smaller than that of monomer (D_m), and therefore, k_p is proportional to D_m .

The self-diffusion coefficient of the penetrant such as solvent or monomer in the polymer (D_m) was given empirically to be proportional to $\exp \{\phi_v\}$, where ϕ_m is the volume fraction of the monomer.¹⁴ In recent years Fujita et al. derived the self-diffusion coefficient of penetrant in the polymer as eq. (5) on the basis of the free volume theory,¹⁵

$$D_m = D_{m0} \exp \{B_d \beta' \phi_m / (v_f^2 + v_f \beta' \phi_m)\} \quad (5)$$

where D_{m0} is D_m in pure polymer, v_f is the free volume of pure polymer, β' is related to the free volume increment due to the penetrant, and B_d is of the same nature as the parameter B in the WLF equation.³¹ The validity of eq. (5) was supported at temperatures above the T_g of the pure polymer by Fujita et al. for various poly(methyl acrylate)-penetrant systems¹⁵ and by Moor and Ferry for a polyisobutylene-cetane mixture system.³² However, for the diffusion coefficient of penetrants in a polymer at temperatures below the T_g of the pure polymer, eq. (5) becomes invalid, since the excess local free volume in the immediate vicinity of the penetrant molecule cannot be disregarded.³² Though a suitable formulation for the diffusion coefficient of this range has not yet been provided, a tendency of the change in D_m with ϕ_p is estimated approximately from the graphical data (Fig. 7)

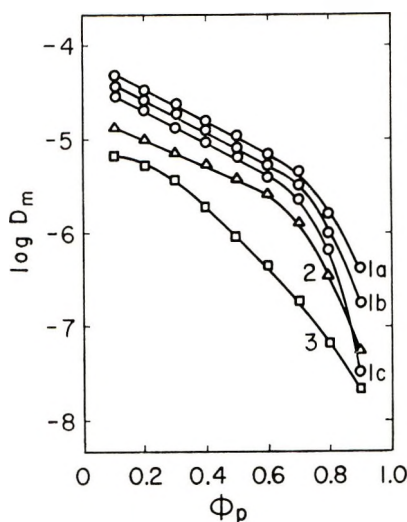


Fig. 7. Changes in self-diffusion coefficient of solvents with volume fraction in the polymer-solvent system:³³ (1a) polystyrene-benzene, 50°C.; (1b) polystyrene-benzene, 35°C.; (1c) polystyrene-benzene, 20°C.; (2) poly(vinyl chloride)-methyl ethyl ketone, 30°C.; (3) polyisobutylene-benzene, 20°C.

according to Chalykh and Vasenin.³³ From Figure 7 it is affirmed that $\log D_m$ changes linearly with ϕ_p in the range of $\phi_p = 0.3-0.7$ and decreases significantly at $\phi_p > 0.8$. The gradient of the linear range is reported to be independent of the temperature.³³ This is consistent with the constancy of the apparent activation energy observed for the self-diffusion of cetane in the same range of volume fraction.³² As k_p is proportional to D_m , the $\log k_p$ versus conversion curve shown in Figure 9 in a dotted line is obtained from the above estimates together with the fact that the propagation reaction is not controlled by diffusion up to 40% conversion.

The change in the logarithmic concentration of polymeric radical ($\log [P\cdot]$) with conversion X is evaluated as follows.

The polymerization behavior is expressed both in stationary and non-stationary states by eqs. (6) and (7),

$$R_p = k_p[P\cdot][M] \quad (6)$$

$$d[P\cdot]/dt = fk_d[I] - k_t[P\cdot]^2 \quad (7)$$

where k_t and k_d are the rate constants of termination and initiator decomposition and f is the initiator efficiency. In the range of $X < 80\%$, where the bimolecular termination process of polymeric radicals is predominant, $d[P\cdot]/dt$ is much smaller than each of the two terms in the right side of eq. (7); in consequence, the quasi-steady state holds, and $[P\cdot]$ is reciprocally proportional to a half power of k_t . In diffusion-controlled polymerization it is derived from eq. (4) that k_t is proportional to the diffusion coefficient of the polymeric radicals (D_p).

D_p in a highly viscous system is inversely proportional to the bulk viscosity of the system (η) and is related to the free volume of the system (v_f) by eq. (8),²⁸

$$D_p = C/\eta = (\Phi_0 \delta^2 / 6N^*) \exp \{-\beta^* v^* / v_f\} \quad (8)$$

where v^* is the critical amount of free volume for a segment to jump, Φ_0 is the jump frequency, δ is the jump distance, N^* is the number of segments, and β^* is considered as unity. For the system consisting of polymer-monomer mixture v_f is expressed by eq. (9), assuming the additivity of the free volumes of each constituent,¹³

$$v_f = \{0.025 + \alpha_p(T - T_{gp})\} \phi_p + \{0.025 + \alpha_m(T - T_{gm})\} (1 - \phi_p) \quad (9)$$

where the notation is similar to eq. (2). By substituting eq. (9) in eq. (8) and using suitable values for the parameters according to Bueche,²⁸ $\log D_p$ for the poly(methyl methacrylate)-methyl methacrylate system can be calculated as a function of ϕ_p and is graphically shown in Figure 8.

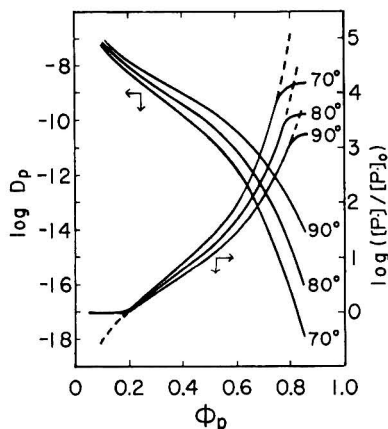


Fig. 8. Calculated dependence at various temperatures of diffusion coefficient and concentration of polymeric radicals on volume fraction for the poly(methyl methacrylate)-methyl methacrylate system.

The $\log D_p$ - ϕ_p curves are converted to $\log([P\cdot]/[P\cdot]_0)$ - ϕ_p curves since $[P\cdot]$ is reciprocally proportional to the one-half power of D_p at an intermediate range of the conversion. At 0-20% conversion the rate of polymerization is not controlled by diffusion, and therefore $\log [P\cdot]$ is kept constant. On the other hand, as the conversion proceeds over 80%, the diffusion coefficient of primary radicals of the initiator significantly decreases similarly to the case of D_m . Thus, the recombination of the primary radicals becomes predominant, which results in the decrease in the initiator efficiency³⁴ and the concentration of the polymeric radical does not increase. The change of $\log [P\cdot]$ with X is shown in Figure 8. The gradient of the curves at 30-80% conversion grows sharper as the temperature decreases. The values of $\log([P\cdot]/[P\cdot]_0)$ at the later stage of polymerization, namely,

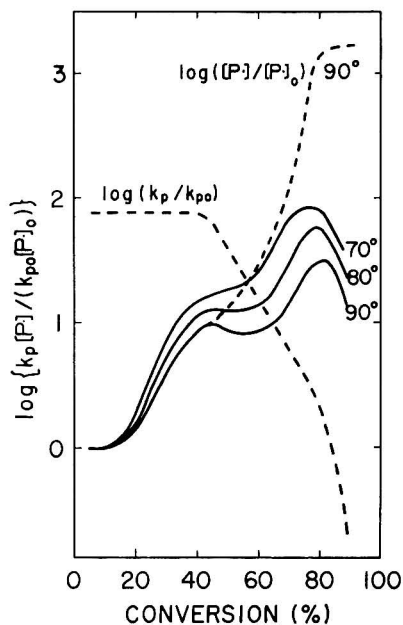


Fig. 9. Synthesized curves showing the dependence of $\log k_p[P\cdot]/(k_{p0}[P\cdot]_0)$ on conversion for methyl methacrylate polymerization at various temperatures. $\log(k_p/k_{p0})$ and $\log([P\cdot]/[P\cdot]_0)$ curves at 90°C are also shown to explain the depression in the synthesized curve at 40–60% conversion.

radical concentrations increased by a factor of 10^3 – 10^4 , are consistent in order with those presumed from the ESR measurements.³⁵

Thus, the graphical summation of the $\log[P\cdot]$ curves obtained from the diffusion behavior of the polymer segments and the $\log k_p$ curve obtained from the diffusion data of the monomer in the polymer yields the synthesized curves of $\log(k_p[P\cdot]/k_{p0}[P\cdot]_0)$ against conversion shown in Figure 9. The synthesized curves have two peaks at 40% and 80% conversions and a minimum between them. As the polymerization temperature is lowered, the minimum becomes less pronounced because of the sharper increase in the gradient of $\log[P\cdot]$ curve.

The synthesized curves are compared with the experimental curves obtained from DSC (Fig. 6). The agreement between them is considered to be satisfactory despite the rough approximations made. The calculated curves are a little greater at the later stages of conversion than the observed ones. This may have been caused by the overestimation of $\log[P\cdot]$ in the calculated curves.

It is concluded from the above results that the mechanism of diffusion-controlled polymerization can be explained by dividing the polymerization rate into k_p and $[P\cdot]$ factors and relating them to the diffusion behaviors of monomer molecules and polymeric radicals in the system. The free volume theory, especially the assumption of linear additivity of the free volumes of each component of the mixture, is successfully applied to the explanation of

the final conversion and to the diffusion behavior of polymeric radicals, but the effect of excess local free volume in the immediate vicinity of a monomer must be considered in the case of the diffusion behavior of monomers in the polymer-monomer system. This effect causes the previously unknown change in the rate of polymerization in the course of bulk polymerization of methyl methacrylate.

References

1. G. V. Schulz and G. Harborth, *Makromol. Chem.*, **1**, 106 (1947).
2. E. Trommsdorff, H. Köhler, and P. Lagally, *Makromol. Chem.*, **1**, 169 (1947).
3. P. Hayden and H. Melville, *J. Polym. Sci.*, **43**, 201 (1960).
4. A. M. North and G. A. Reed, *J. Polym. Sci. A*, **1**, 1311 (1963).
5. G. M. Burnett and G. L. Duncan, *Makromol. Chem.*, **51**, 154 (1962).
6. M. F. Vaughan, *Trans. Faraday Soc.*, **48**, 576 (1952).
7. S. Fujii, *Bull. Chem. Soc. Japan*, **27**, 216 (1954).
8. E. R. Robertson, *Trans. Faraday Soc.*, **52**, 426 (1956).
9. W. Kuhn and H. Kuhn, *Helv. Chim. Acta*, **29**, 1533 (1945).
10. S. W. Benson and A. M. North, *J. Amer. Chem. Soc.*, **84**, 935 (1962).
11. R. D. Burkhart, *J. Polym. Sci. A*, **3**, 883 (1965).
12. E. Rabinowitch, *Trans. Faraday Soc.*, **33**, 1225 (1937).
13. F. N. Kelley and F. Bueche, *J. Polym. Sci.*, **50**, 549 (1961).
14. G. S. Park, *Trans. Faraday Soc.*, **46**, 684 (1950).
15. H. Fujita, A. Kishimoto, and K. Matsumoto, *Trans. Faraday Soc.*, **56**, 424 (1960).
16. J. Hughes and A. M. North, *Trans. Faraday Soc.*, **60**, 960 (1964).
17. H. M. Anderson, *J. Polym. Sci. A-1*, **4**, 783 (1966).
18. E. S. Watson, M. J. O'Neill, J. Justin, and N. Brenner, *Anal. Chem.*, **36**, 1233 (1964).
19. H. Kambe and Y. Shibasaki, *Kogyo Kagaku Zasshi*, **69**, 1808 (1966).
20. Landolt-Börnstein, *Tabellen, Kalorische Zustandsgrößen*, Vol. II, Part 4, Springer-Verlag, Berlin, 1961.
21. B. Baysal and A. V. Tobolsky, *J. Polym. Sci.*, **8**, 529 (1952).
22. L. M. Arnett, *J. Amer. Chem. Soc.*, **74**, 2027 (1952).
23. M. M. Horikx and J. J. Hermans, *J. Polym. Sci.*, **11**, 325 (1953).
24. A. I. Lowell and J. R. Price, *J. Polym. Sci.*, **43**, 1 (1960).
25. F. R. Mayo, R. A. Gregg, and M. S. Matheson, *J. Amer. Chem. Soc.*, **73**, 1691 (1951).
26. C. T. Mortimer, *Reaction Heats and Bond Strengths*, Pergamon Press, London, 1962, p. 87.
27. T. G. Fox and P. J. Flory, *J. Appl. Phys.*, **21**, 581 (1950).
28. F. Bueche, *Physical Properties of Polymers*, Interscience, New York, 1962, pp. 85, 112.
29. R. B. Beevers and E. F. T. White, *Trans. Faraday Soc.*, **56**, 744 (1960).
30. A. Chapiro and S. Nakashio, *J. Chim. Phys.*, **63**, 1031 (1966).
31. M. L. Williams, R. F. Landel, and J. D. Ferry, *J. Amer. Chem. Soc.*, **77**, 3701 (1955).
32. R. S. Moor and J. D. Ferry, *J. Phys. Chem.*, **66**, 2699 (1962).
33. A. E. Chalykh and R. M. Vasenin, *Vysokomol. Soedin.*, **8**, 1908 (1966).
34. F. De Schrijver and G. Smets, *J. Polym. Sci. A-1*, **4**, 2201 (1966).
35. N. M. Atherton, H. Melville, and D. H. Whiffen, *J. Polym. Sci.*, **34**, 199 (1959).

Received February 5, 1968

NOTES

*Observation of Gel Formation in Penton
with Low-Energy X-Rays*

The accepted mechanism for radiation degradation of Penton (Hercules Inc., Wilmington, Del.) is chain scission¹ with absorbed radiation doses to above the equivalent of 1000 cal/g.¹ Gel formation has been observed recently in the surface disk, 0.0458 cm thick, of a stack of Penton disks irradiated with 50-pkV x-rays at several total energy levels. These levels were 5 cal/cm², 10 cal/cm², 25 cal/cm², and an aluminum-filtered 20 cal/cm² with average absorbed doses of 35.0, 70.1, 131.7, and 111.7 cal/g, respectively. The amount of gel formed is approximately 10% by weight (slightly less in the aluminum-filtered specimen). No gel was found in the subsurface disks of exposures up to 100 cal/cm² total incident energy except for perhaps a trace in the second disk. The gel formation does not appear to be dose-dependent, therefore, but rather position-dependent, which means spectrum-dependent. (The surface disk preferentially absorbs the lower-energy x-rays which are closer to the chlorine K-edge.) The gel formation appears to be a function of more intense excitation than is caused by higher energy x-rays or γ -rays.

The intrinsic viscosity of the dissolved portion of the sample was measured, and a plot of $(1/[\eta])^{1/\alpha}$ as a function of absorbed dose was found to bear the same linear relationship as had been obtained for specimens with no observable gel formation (see Fig. 3 of the previous work²). This indicates that chain scission proceeds independently of gel formation, as is suggested by Charlesby's data on polyethylene.³ Melting point measurements^{2,4} do bear the same linear relationship with absorbed dose with or without gel formation. The observation that heats of fusion of annealed samples have a linear relationship with absorbed dose in both surface and lower disks^{2,4} suggests that this amount of gel formation does not interfere, to an observable extent, with the ability of Penton to crystallize.

This work was performed under the auspices of the U.S. Atomic Energy Commission.

References

1. J. H. Golden and E. A. Hazell, *J. Polym. Sci. A*, **2**, 4017 (1964).
2. B. J. Mallon, *J. Polym. Sci. A-1*, **6**, 2637 (1968).
3. A. Charlesby, *Proc. Roy. Soc. (London)*, **A222**, 60 (1954).
4. B. J. Mallon, *J. Polym. Sci. B*, **5**, 977 (1967).

BARBARA J. MALLON

University of California
Lawrence Radiation Laboratory
Livermore, California 94550

Received March 22, 1968

Ozonolysis of Natural Rubber

A paper by Chakravarty and Sircar¹ repeated their finding² that ozonolysis of natural rubber yielded 23% of levulinic acid, together with breakdown products accounting for 86% of the original hydrocarbon chain. The classical work of Harries³ and Pummerer⁴ described levulinic acid yields of 26% and 46%, respectively. A recent note by Bevilacqua⁵ emphasized that inferences regarding structure based on ozonolysis and oxidative hydrolysis should be derived only from products formed in high yield. It seems, therefore, appropriate to draw attention to a method of rubber ozonolysis that has been successfully used in these laboratories for a number of years and which gives a high yield (up to 85%) of levulinic acid as its 2,4-dinitrophenylhydrazone (LADNP).

The method is based on that of Bailey,⁶ who prevented the formation of intractable polymeric peroxides and ozonides during the ozonolysis of cyclohexene by including alcohol in the ozonization solvent. The method to be described involves dissolution or suspension of the raw rubber in dry chloroform and the addition of ethyl alcohol, usually the maximum amount possible while still avoiding precipitation of the rubber. The resultant ozonization products are submitted to oxidative degradation with performic acid.

Control experiments, in which levulinic acid itself was submitted to the oxidative hydrolysis and subsequent treatment, gave an 86% yield of LADNP, indicating that the ozonolysis is virtually stoichiometric but that some of the levulinic acid formed is simultaneously decomposed.

A few experiments have shown that sulfur-vulcanized and peroxide-cured rubber can be ozonolyzed, giving LADNP yields of 52 and 75%. The method is capable of being used on milligram amounts of rubber, with a decrease in yield (e.g., 0.020 g. rubber gave 50% yield).

EXPERIMENTAL

The apparatus was a simplified form of that described by Barnard.⁷

Oxygen was passed via a tube of self-indicating silica gel through a Rotameter flowmeter at a constant flow rate of about 5 l/hr and thence through a Towers silent-discharge ozonizer. The emergent stream of ozonized oxygen was directed by a three-way tap to a potassium iodide analyzer (in which liberated iodine was titrated with sodium thiosulfate), to waste, or to the ozonolysis vessel.

Raw Rubber

A solution of rubber (0.1 g) in AR chloroform (dried over Linde molecular sieve) was transferred to the vessel, and ethyl alcohol (10 ml) was added dropwise with stirring. If the rubber precipitated, addition of alcohol was stopped and sufficient chloroform added to effect dissolution. The vessel was cooled to -30°C and ozonized oxygen passed through. It was found that ozone could be detected in the exit stream at precisely the theoretical end point of the reaction.

The theoretical time is given by the equation:

$$\text{Time} = \frac{2000 \times \text{wt. rubber sample (g)}}{68V \times \text{Normality of Na thiosulfate}}$$

where V is volume of Na thiosulfate required to titrate the iodine liberated by passage of ozone for 1 min. In practice, ozone passage was continued for a further 10% of the theoretical time. The solution was allowed to warm to room temperature, transferred

to a 100-ml round-bottomed flask, and evaporated at about 40°C/15 mm. The resultant syrup was treated with 90% formic acid (1 ml), and completely wetted by rotation of the flask. Hydrogen peroxide solution (30%, 0.3 ml) was added and the solution allowed to stand for 1/4 hr. A small amount of polymeric material was occasionally apparent at this stage.

The mixture was heated under reflux on a water bath, the temperature of which was slowly raised to 100°C and held at this value for 3/4 hr. The level of the water was kept about the same as that of the flask contents. Occasionally the latter became dark in color, in which case heating was stopped.

After refluxing, the solution was allowed to cool, and a crystal of ferrous sulfate was added to destroy any remaining peroxide. The condenser and flask were washed down with a little water and a solution of 2,4-dinitrophenylhydrazine (DNP) in 2*N* HCl (30 ml) added. [Reagent was prepared by dissolution of 2,4-DNP (1.5 g) in 2*N* HCl (100 ml) at 100°C with filtration immediately after cooling.]

The orange precipitate was allowed to stand 1 hr or more and collected in a sintered-glass Gooch crucible. The precipitate was dissolved in 5*N* ammonium hydroxide and the dark-colored solution filtered through the crucible, any residue being washed with a little water. Acidification of the filtrate with hydrochloric acid produced pure levulinic acid 2,4-dinitrophenylhydrazone, which was collected in a weighed sintered-glass Gooch crucible and washed well to remove ammonium chloride. The yield was 75–85% of the theoretical.

The product was recrystallized from dimethylformamide–water to give needles (mp and mixed mp 205°C).

The unrecrystallized product was substantially pure as shown by paper chromatography and thin-layer chromatography (TLC) on silica gel. The solvent for paper chromatography was *n*-butanol/ethanol/0.5*N* ammonium hydroxide, 70/20/10, and for TLC, benzene/methanol, 85/15.

Vulcanized Rubber

The sulfur- or peroxide-cured rubber was milled (five passes, tight nip), extracted overnight in cold AR acetone and dried at 0.1 mm. About 0.1 g. was weighed, cut into small (0.1 × 0.5 cm) pieces, and allowed to swell overnight in chloroform (30 ml) in the ozonolysis cell. Ethyl alcohol (30 ml) was added, and the stream of ozone was passed through until about 90% of the rubber had dissolved (about 1 hr). Unreacted rubber was removed by filtration through a weighed sintered-glass filter and the solution evaporated and treated as above. In one experiment, ozone passage was prolonged (3 hr) in an attempt to bring the residual material into solution. Two layers were apparent in the ozonization solution and on evaporation of the chloroform/ethanol mixture to a syrup, a violent explosion occurred. This may have been due to reaction between the ozone and the alcohol, yielding explosive peroxides.

This work forms part of the research program of the Natural Rubber Producers' Research Association.

Thanks are due to Dr. D. Barnard for helpful discussion and criticism and to Miss V. Bate for technical assistance.

References

1. S. N. Chakravarty and A. K. Sircar, *J. Appl. Polym. Sci.*, **11**, 37 (1967).
2. S. N. Chakravarty, D. Banerjee, and A. K. Sircar, *Trans. I.R.I.*, **38**, T226 (1962).
3. C. D. Harries, *Untersuchungen über die natürlichen und Künstlichen Kautschukarten*, Springer, Berlin, 1919, p. 191.

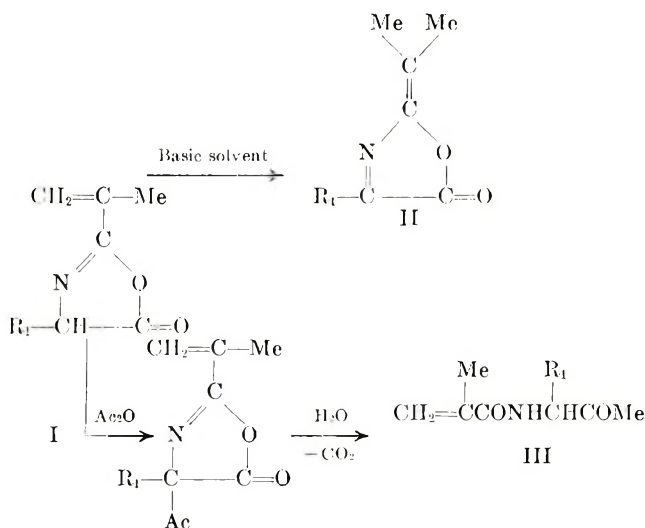
4. R. Pummerer and H. Richtzenhain, *Ann.*, **529**, 33 (1937).
5. E. M. Bevilacqua, *J. Polym. Sci. B*, **5**, 601 (1967).
6. P. S. Bailey, *Ind. Eng. Chem.*, **50**, 993 (1958).
7. D. Barnard, *J. Chem. Soc.*, **1957**, 4547.

G. P. McSWEENEY

The Natural Rubber Producers' Research Association
Welwyn Garden City
Herts, England
Received February 2, 1968

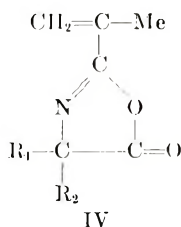
Copolymerization of 2-Isopropenyl-4,4-dialkyl-5-oxazolones with Styrene

In our preceding paper,¹ the synthesis and the copolymerization of 2-isopropenyl-5-oxazolone (2-isopropenyl-4-isopropyl-2-oxazolin-5-one, I) with styrene was reported in connection with the study of preparation of heterocyclic isopropenyl monomers,^{2,3} which are reactive towards nucleophilic reagents. However, compound I, which has a hydrogen in the C₄ position, was unstable on storage, and several side reactions were proved to be involved in preparation: (a) isomerization to pseudoxazolone (II) by proton abstraction with basic solvents;⁴ (b) acylation at the C₄ position with acetic anhydride to give *N*-acyl- α -amino ketone (III) through the 4-acetyl-5-oxazolone derivative;⁵ (c) equilibration of the 5-oxazolones with mesoionic oxazoles which may be regarded as azomethine ylides. Azomethine ylides were known to take part in cycloaddition of 1,3-dipoles with alkene evolving carbon dioxide.⁶



Moreover, the active methinyl hydrogen at C₄ would participate in chain transfer in radical polymerization.

In this paper, in order to obtain more information about the copolymerizability of 2-isopropenyl-5-oxazolone derivatives which have no hydrogen at the C₄ position, synthesis and radical copolymerization of 2-isopropenyl-4,4-dialkyl-2-oxazolin-5-ones (IV) with styrene and methyl methacrylate were accomplished.



α -Aminoisobutyric acid was prepared from acetone, sodium cyanide, and ammonium chloride.⁷ α -Amino- α -methyl-*n*-butyric acid, α -amino- α,γ -dimethyl-*n*-valeric acid, and α -amino- α,α -pentamethyleneacetic acid were obtained via hydantoin⁸ from the corresponding ketones, potassium cyanide, and ammonium carbonate. α,α -Disubstituted

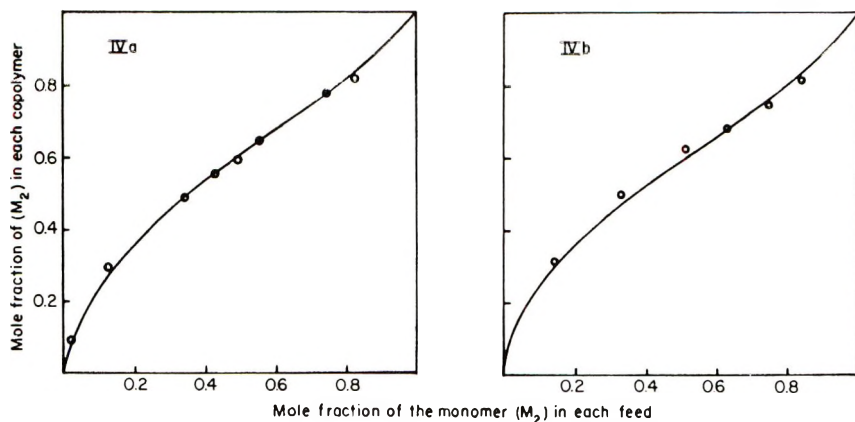


Fig. 1. Composition curves for styrene copolymers.

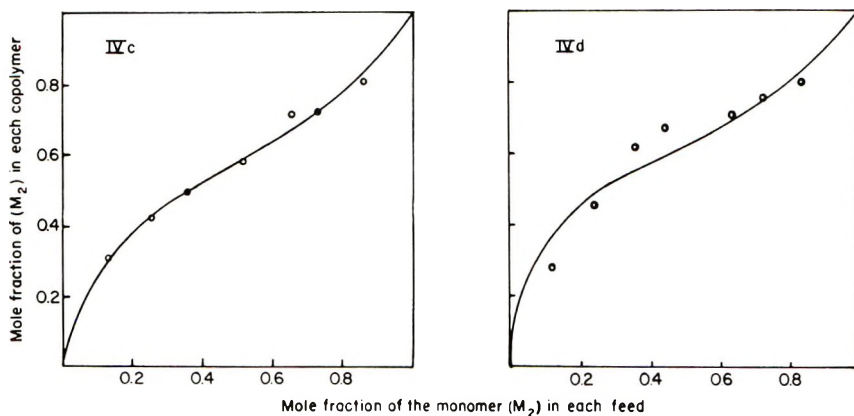


Fig. 2. Composition curves for styrene copolymers.

α -amino acids⁹ were acylated by methacryloyl chloride.¹⁰ The melting points and elemental analyses of *N*-methacryloyl derivatives are shown in Table I. These *N*-methacryloyl- α,α -dialkyl- α -amino acids were treated at 100–110°C. with an excess of acetic anhydride, and then the reaction mixtures were fractionated *in vacuo*. The structure of these new reactive monomers were confirmed by elemental analyses and infrared spectra. The principal characteristics of the infrared spectra are given in Table II; the yields, physical properties, and elemental analyses are summarized in Table III.

Bulk copolymerization of these monomers with styrene and MMA was carried out at 60°C. Monomer reactivity ratios were determined from the general copolymerization equation by using the method of Fineman and Ross plots.¹¹ The results are summarized in Table III and composition curves for the copolymers are shown in Figures 1–3. IV was well incorporated into the copolymers with styrene at the region rich in charged styrene monomer. The Alfrey-Price equations were used to calculate Q and e values listed in Table IV. From the results reported here, it can be seen that 5-oxazolone ring is electron-attracting in the copolymerization reaction as well as 2-isopropenyl-4,5-dimethyl-oxazole.¹² The copolymers of IVd with MMA have a larger amount of IVd than that originally charged as can be seen from the high r_2 (3.22) and low r_1 (0.05) values (Fig. 3).

The copolymers were soluble in benzene, tetrahydrofuran, dioxane, chloroform, ace-

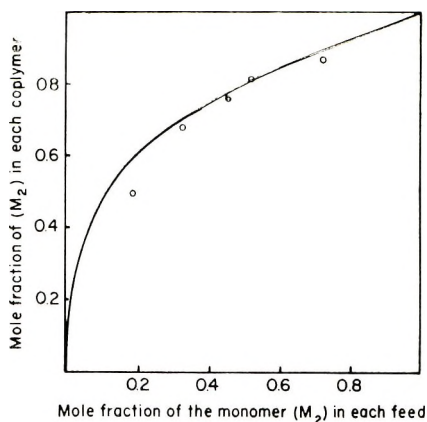


Fig. 3. Composition curves for copolymer of MMA and IVd.

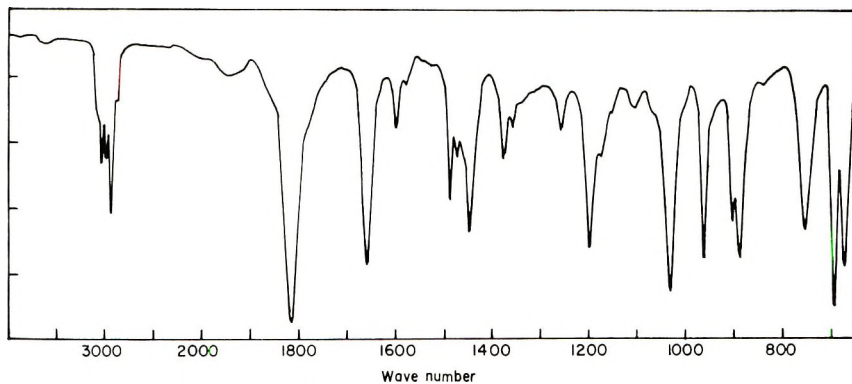


Fig. 4. Infrared spectrum of styrene-IVa copolymer.

tone, and ethyl acetate, but were insoluble in methanol, *n*-hexane, carbon tetrachloride and water. The infrared spectrum of the copolymer obtained from IVa and styrene is shown in Figure 4. Absorption bands which were assigned to the carbonyl and the C=N groups appeared at 1820 and 1660 cm^{-1} , respectively, and a band assigned to the phenyl group also appeared at 1600 cm^{-1} .

The copolymers reacted readily in solution with nucleophilic reagents such as *n*-butylamine. Increase in absorption intensity of the infrared spectrum of the reacted copolymer at 1660 cm^{-1} and disappearance of $\nu_{\text{C}=\text{O}}$ at 1820 cm^{-1} would indicate the change of copolymer structure in the course of polymer reaction as shown in eq. (1).

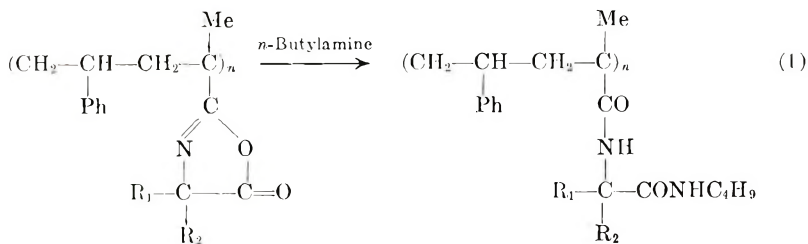


TABLE I
N-Methacryloyl- α,α -dialkyl- α -amino Acids



| R ₁ | R ₂ | Yield, % | m.p., °C. | Formula | Calcd. | | | Found | | |
|----------------|-------------------------------------|-------------|----------------------|---|--------|------|------|-------|------|------|
| | | | | | C, % | H, % | N, % | C, % | H, % | N, % |
| Me | Me | 37 | 15-160 ^a | C ₈ H ₁₂ NO ₂ | 56.12 | 7.65 | 8.18 | 56.29 | 7.67 | 8.01 |
| Me | Et | 25 | 88-90 ^b | C ₉ H ₁₂ NO ₂ | 58.36 | 8.16 | 7.56 | 58.70 | 8.28 | 7.56 |
| Me | (CH ₂) ₅ -Bu | 53 | 87-89 ^c | C ₁₁ H ₁₆ NO ₂ | 61.77 | 8.98 | 6.86 | 61.94 | 8.98 | 6.57 |
| | | 53 | 177-178 ^d | C ₁₁ H ₁₇ NO ₂ | 62.54 | 8.11 | 6.63 | 62.35 | 8.11 | 6.79 |

^a Recrystallized from H₂O.

^b Recrystallized from toluene.

^c Recrystallized from H₂O-EtOH.

^d Recrystallized from H₂O-EtOH.

TABLE II
2-Isopropenyl-4,4-dialkyl-2-oxazolin-5-ones (IV)

| R ₁ | R ₂ | Yield, % | b.p., °C./mm. Hg | m.p., °C. | Formula | Calcd. | | | Found | | |
|----------------|----------------|-------------|---------------------|--------------|---|--------|------|------|-------|------|------|
| | | | | | | C, % | H, % | N, % | C, % | H, % | N, % |
| IVa | Me | 56 | 75-76/19 | — | C ₈ H ₁₁ NO ₂ | 62.72 | 7.24 | 9.14 | 62.66 | 7.31 | 8.77 |
| IVb | Me | 51 | 68-70/8 | — | C ₉ H ₁₃ NO ₂ | 64.65 | 7.84 | 8.38 | 64.01 | 7.82 | 8.06 |
| IVc | Me | 64 | 75-76/5 | — | C ₁₁ H ₁₇ NO ₂ | 67.66 | 8.78 | 7.17 | 67.69 | 8.75 | 7.63 |
| IVd | | 74 | 118-120/5 | 52-54 | C ₁₁ H ₁₅ NO ₂ | 68.37 | 7.82 | 7.25 | 68.12 | 7.68 | 7.26 |

TABLE II
Assignment of Infrared Spectrum of IV

| Absorption band, cm.^{-1} | Assignment |
|------------------------------------|------------------------|
| 1825 | $\nu\text{C}=\text{O}$ |
| 1660 | $\nu\text{C}=\text{N}$ |
| 1610 | $\nu\text{C}=\text{C}$ |

TABLE IV
Copolymerization Data of 2-Isopropenyl-5-oxazolones with Styrene

| Compound | r_1 | r_2 | e_2 | Q_2 |
|---|-----------------|-----------------|-------|-------|
| IVa | 0.31 ± 0.06 | 1.00 ± 0.09 | 0.28 | 1.35 |
| IVb | 0.27 | 0.70 | 0.49 | 1.31 |
| IVc | 0.24 | 0.69 | 0.54 | 1.42 |
| IVd | 0.12 | 0.82 | — | — |
| 2-Isopropenyl- 4,5-dimethyl- oxazole ^a | 0.15 | 2.20 | 0.24 | 2.83 |

^a Data of Iwakura et al.¹²

EXPERIMENTAL

N-Methacryloyl- α,α -dialkyl- α -amino Acids

N-Methacryloyl- α,α -dialkyl- α -amino acids were prepared by the same method described in the literature.¹⁰

2-Isopropenyl-4,4-dialkyl-2-oxazolin-5-ones

A solution of *N*-methacryloyl- α,α -dialkyl- α -amino acids in acetic anhydride was added to acetic anhydride heated previously to 100–110°C. and the mixture was kept for 5–10 min. at the same temperature.¹ After removal of excess acetic anhydride and acetic acid under reduced pressure, the products were obtained by vacuum distillation. The crude monomers were distilled again giving pure product in yields shown in Table II.

The NMR spectra showed for IVa: 4,4-Me₂, τ 7.87; =C—Me, τ 8.51; CH₂=, τ 3.70, 3.98; for IVb: 4-Me, τ 7.99; 4-MeCH₂, τ 9.19 (t); 4-MeCH₂—, τ 8.21 (q); =C—Me, τ 8.50; CH₂=, τ 4.07, 4.38.

Copolymerization

Polymerization experiments were carried out at 60°C. in sealed tubes under nitrogen atmosphere. All experiments were initiated by AIBN (0.01 g.). The experimental methods of copolymerization were essentially those described by Mayo and Lewis.¹³ About 3 g. of a mixture of precisely weighed styrene (or MMA, M₁) and 2-isopropenyl-5-oxazolones (M₂) was kept at 60°C. for 1–3 hr. Conversions were below 15%. The copolymers obtained were reprecipitated twice, benzene being used as a solvent and methanol as a nonsolvent. The purified polymers were dried *in vacuo*, and the composition of the copolymers was determined by nitrogen analyses.

Reaction of Copolymer with Amine

A sample (440 mg.) of copolymer of IVc with styrene (content of IVc = 57.6 mole-%, $\eta_{inh} = 0.55$ at 30°C., $c = 0.2$ g./dl. in THF) was dissolved in 5 ml. of dioxane. After addition of five times the equimolar amount of *n*-butylamine, the polymer solution was kept at 80°C. for 12 hr. The reaction mixture was poured into petroleum ether and the precipitated polymer was collected by filtration and subjected to nitrogen analysis. Inherent viscosity of the reacted polymer was 0.46 (in THF at 30°C. at the concentration of 0.2 g./dl.), $N_{found} = 7.79\%$, ring-opening 89%. Reacted polymer was soluble in methanol and ethanol, but insoluble in benzene.

References

1. Y. Iwakura, F. Toda, and Y. Torii, *J. Polymer Sci. A-1*, **4**, 2649 (1966).
2. P. L. DeBenneville, L. S. Luskin, and H. J. Sims, *J. Org. Chem.*, **23**, 1355 (1958).
3. T. Kagiya, S. Narisawa, T. Maeda, and K. Fukui, *Kogyo Kagaku Zasshi*, **69**, 732 (1966).
4. Y. Iwakura, F. Toda, and Y. Torii, *Tetrahedron*, **23**, 3363 (1967).
5. Y. Iwakura, F. Toda, and H. Suzuki, *J. Org. Chem.*, **32**, 440 (1967).
6. R. Huisgen, R. Grashey, and J. Sauer, in *The Chemistry of Alkenes*, S. Patai, Ed., Interscience, New York, 1964, p. 739.
7. A. H. Blatt, Ed., *Organic Syntheses Coll.*, Vol. II, Wiley, New York, 1943.
8. H. R. Henze and C. B. Holder, *J. Am. Chem. Soc.*, **63**, 1943 (1941).
9. S. D. Upham and O. C. Dermer, *J. Org. Chem.*, **22**, 799 (1957).
10. Y. Iwakura, F. Toda, and H. Suzuki, *J. Polymer Sci. A-1*, **5**, 1599 (1967).
11. M. Fineman and S. D. Ross, *J. Polymer Sci.*, **5**, 269 (1950).
12. Y. Iwakura, F. Toda, H. Suzuki, and N. Kusakawa, *J. Polymer Sci. B*, **6**, 5 (1968).
13. F. R. Mayo and F. M. Lewis, *J. Am. Chem. Soc.*, **66**, 1594 (1944).

YOSHIO IWAKURA
FUJIO TODA
YOSHINORI TORII
REIKO SEKII

Department of Synthetic Chemistry
Faculty of Engineering
University of Tokyo
Bunkyo-ku, Tokyo, Japan

Received January 25, 1968

BOOK REVIEW

Progress in Physical Organic Chemistry. Volume 4. Andrew Streitwieser, Jr. and Robert W. Taft, Eds., Interscience, 1967. 303 + ix pp. \$15.50.

The opinion that physical organic chemistry has become more "physical" as the field has matured can be amply documented. The array of sophisticated physical methods for investigating structure and reaction mechanism continues to grow rapidly, and the typical investigator must devote much of his time to learning the new techniques. At the same time this field has become more "organic," as judged by the willingness of present-day physical organic chemists to tackle complex reactions and large molecules, including enzymes. In short, the field has grown in many directions until, today, very little of chemistry is outside the province of the physical organic chemist. He refuses to recognize limits on either the chemical systems he will study or the physical techniques he will use.

The volumes of this Interscience series reflect the diversity to be expected. Some chapters are devoted principally to a specific physical method, with illustrations of its use in widely different chemical systems. Other chapters review a particular reaction or group of reactions without detailed discussion of the many techniques involved. The present volume contains five chapters: (1) Mechanism and Catalysis for the Hydrolysis of Acetals, Ketals, and Ortho Esters, by E. H. Cordes; (2) Ionic Reactions in Acetonitrile, by J. F. Coetzee; (3) Nucleophilic Displacements on Peroxide Oxygen and Related Reactions, by E. J. Behrman and John O. Edwards; (4) Conformation and Structure as Studied by Electron Spin Resonance Spectroscopy, by David H. Geske; and (5) Solvolysis in Water, by R. E. Robertson. In a number of passages throughout the book the reader would have been assisted by more critical editing, but the quality of the writing is generally satisfactory.

Like many recent volumes, the present one contains numerous references to unpublished results, usually from the laboratory of the author. The temptation must always be great for an author who is active in the field to use such data to support his arguments and to enhance the up-to-date nature of the book. One regrettable incident in this volume may illustrate some of the hazards associated with reviewing work in progress. On pages 106-108 there is a discussion of the oxidation of nitrite by peroxydisulfate, based upon unpublished data which support a rather complicated mechanism, the novelty of which is emphasized. At the end of the chapter the authors have appended (or should one say hidden?) a note to say that additional experiments by the same investigators (also unpublished) have shown that the mechanism proposed earlier in the chapter cannot be correct. Surely the authors, editors, and publishers might have found a better way to dispose of the problem! If it was really impossible to alter the text to conform to the latest progress report, then a disclaiming footnote on page 108 would have been far better than the existing one.

Progress in Physical Organic Chemistry is a useful series of which some chapters will be valuable chiefly for reference, others as convenient summaries of current developments. Any good reference library will want to own the series. Individuals may prefer to consider the volumes one at a time, because of the amount of ground covered.

Martin Stiles

Department of Chemistry
University of Michigan
Ann Arbor, Michigan 48104